

Cover Page



Universiteit Leiden



The handle <http://hdl.handle.net/1887/28538> holds various files of this Leiden University dissertation

Author: Schimmel, Joost

Title: Regulation of genome stability and cell cycle progression by SUMOylation

Issue Date: 2014-09-09

Regulation of genome stability and cell cycle progression by SUMOylation

Joost Schimmel

Copyright © 2014 by J. Schimmel. All rights reserved.

Copyright of the individual chapters rests with the authors with the following exceptions:

Chapter 1: John Wiley & Sons, Inc

Chapter 2: the American Society for Biochemistry and Molecular Biology

Chapter 4 and 5: Elsevier - Cell Press (Molecular Cell)

Regulation of genome stability and cell cycle progression by SUMOylation

proefschrift

ter verkrijging van

de graad van Doctor aan de Universiteit Leiden,

op gezag van Rector Magnificus Prof. mr. C.J.J.M. Stolker,

volgens besluit van het College voor Promoties

te verdedigen op dinsdag 9 september 2014

klokke 13.45 uur

door

Joost Schimmel

geboren te Lopik

op 17 april 1984

Promotiecommissie:

Promotor: Prof. dr. P. ten Dijke

Copromotor: Dr. A.C.O Vertegaal

Overige leden: Prof. dr. T.K.Sixma (NKI, Amsterdam)
Prof. dr. G.J.P.L. Kops (UMC, Utrecht)
Dr. P. Knipscheer (Hubrecht Instituut, Utrecht)

The studies described in this thesis were performed at the department of Molecular and Cellular Biology, Leiden University Medical Center and was financed by the Nederlandse Organisatie voor Wetenschappelijk Onderzoek (NWO).

Cover: Painting by Hiroyuki Kimura. Photographed by Naosuke ii
With kind permission of both artist and photographer.

Printed by: Proefschriftmaken.nl || Uitgeverij BOXPress

Published by: Uitgeverij BOXPress, 's-Hertogenbosch

ISBN: 978-90-8891-919-0

The printing of this thesis was financially supported by the J.E. Jurriaanse Stichting and Greiner Bio-One.

*"I was just guessing at numbers and figures,
pulling the puzzles apart.
Questions of science, science and progress
do not speak as loud as my heart."*

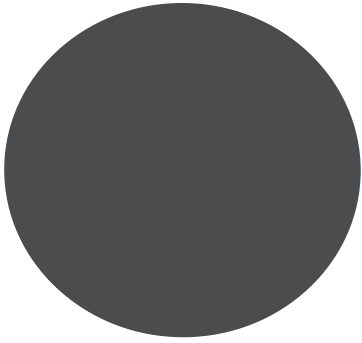
- Coldplay, The Scientist -

aan mijn familie

voor Karin

Table of contents

Aim and outline of the thesis	9
Chapter 1 Introduction	13
Chapter 2 The ubiquitin-proteasome system is a key component of the SUMO-2/3 cycle	41
Chapter 3 USP11 Counteracts RNF4 and Stabilizes PML Nuclear Bodies	63
Chapter 4 Site-Specific Identification of SUMO-2 Targets in Cells Reveals an Inverted SUMOylation Motif and a Hydrophobic Cluster SUMOylation Motif	87
Chapter 5 Uncovering SUMOylation Dynamics During Cell Cycle Progression Reveals FoxM1 as a Key Mitotic SUMO Target Protein	117
Chapter 6 The Cockayne Syndrome-B protein is SUMOylated upon UV induced DNA damage	155
Chapter 7: Summary and discussion	181
Chapter 8: Nederlandse samenvatting	195
List of abbreviations	201
Curriculum Vitae	207
List of publications	209



Aim and outline of the thesis

Aim and outline of the thesis

It has been well established that SUMOylation regulates a wide variety of cellular processes, either on its own or in coordination with other post translational modifications such as ubiquitination. Currently, little is known about the cooperative actions of different PTMs and quite often we lack knowledge on how global SUMOylation contributes to cellular processes. Therefore, the main aims of this thesis are to study the crosstalk between SUMOylation and ubiquitin, identify SUMO target proteins and their acceptor sites and to obtain more insight in the role that SUMOylation plays in maintaining genome stability.

The current concepts in SUMOylation are summarized and reviewed in **Chapter 1**. An overview of the SUMOylation machinery is given and several examples of crosstalk between SUMOylation and other PTMs are presented. Furthermore, the role of SUMOylation in cell cycle progression and DNA repair is discussed as well as the current state of SUMO based proteomic studies.

In **Chapter 2** we have investigated the crosstalk between SUMOylation and ubiquitination. Using proteasome inhibition we identified a subset of SUMO2 target proteins that are subsequently ubiquitinated and degraded. Furthermore we have found that the ubiquitin-proteasome system is essential for the recycling of unconjugated SUMO2 proteins and that SUMO2 is a direct target for ubiquitination.

Chapter 3 describes the identification of a protein that can reverse the ubiquitination of SUMOylated proteins. The ubiquitin specific protease protein USP11 was identified to interact with the SUMO targeted ubiquitin ligase RNF4. *In vitro* assays revealed that USP11 can counteract RNF4 activity by removing ubiquitin proteins from SUMO-ubiquitin hybrid chains; this activity depends on four SUMO interacting motifs in USP11. Functionally, USP11 stabilizes PML nuclear bodies by preventing RNF4 mediated ubiquitination and degradation.

Studying SUMOylation is often challenging due to a lack of information on the modified lysines in proteins. Therefore we have developed a strategy to map SUMO acceptor sites in cells; this is described in **Chapter 4**. Site specific identification of SUMO2 target proteins enabled the discovery of an inverted SUMO consensus site and the identification of a hydrophobic cluster SUMOylation motif. Furthermore, we found direct evidence for crosstalk between phosphorylation and SUMOylation on several proteins.

In **Chapter 5** we have analyzed global SUMOylation dynamics during cell cycle progression. Cell cycle synchronization experiments enabled us to identify and quantify SUMOylation of proteins at different phases of the cell cycle. Bioinformatics revealed that transcription

Aim and outline of the thesis

factors belong to the largest SUMO regulated group of proteins, including transcription factor Forkhead box protein M1 (FoxM1). Follow-up studies showed that FoxM1 SUMOylation mainly takes place during G2 and M phase. During these phases, SUMOylation enhances transcriptional activity of FoxM1 by counteracting autorepression. Functionally, FoxM1 SUMOylation contributes to the maintenance of genome stability by reducing the risk of developing polyploidy.

Chapter 6 focuses on the SUMOylation of the Cockayne Syndrome B protein (CSB). Mass spectrometry based experiments showed that CSB is specifically and rapidly SUMOylated upon UV induced DNA damage. Although this process is dispensable for cells to survive after DNA damage, global SUMOylation events seem to contribute to efficient DNA repair. We show that the recruitment of the Cockayne Syndrome A (CSA) E3 ubiquitin ligase complex to sites of DNA damage induces the destabilization of SUMOylated CSB, potentially via the ubiquitination and degradation of RNA polymerase II.

The work presented in this thesis is summarized and discussed in **Chapter 7**.





Introduction

Adapted from:

Schimmel, Joost; and Vertegaal, Alfred CO
(December 2009) SUMOylation. In: Encyclopedia of Life
Sciences (ELS). John Wiley & Sons, Ltd: Chichester. DOI:
10.1002/9780470015902.a0021849

Chapter 1. Introduction

Cells are the main building block of living organisms. All cells contain the genetic blueprint, known as DNA that harbors the information needed to execute all cellular processes that eventually results in proper cell division. The 'central dogma of molecular biology', first stated by Francis Crick (1), describes the transfer of this information in cells. It starts with the cell making an exact copy of its own DNA, a process known as replication. Subsequently, this DNA is transcribed into messenger RNA (mRNA) by enzymes and the unique code on this mRNA is translated by ribosomes into a specific order of amino acids that finally forms a protein. The unique code on a particular segment of DNA, also known as a 'gene', determines which protein is made. On estimate, the human genome spans between 20.000 and 25.000 genes (2); theoretically resulting in the same amount of proteins. However, mechanisms like genomic recombination, alternative splicing and alternative start and stop sites for transcription generate different mRNA transcripts from one unique gene (3). The total set of proteins expressed by the genome (the proteome) is thus significantly higher than the amount of genes.

The functional diversity of the proteome is further expanded by post-translational modifications (PTMs) of proteins. PTMs are chemical alterations to amino acids in proteins ranging from small chemical modifications to modifications by small proteins. Conjugation of these modifications is most often regulated by enzymatic activities and they can be reversible by the action of deconjugating enzymes. Due to its dynamic nature, PTMs are used by the cell to quickly alter the function of protein groups to regulate cellular processes (4). Deregulation of PTMs can cause genome instability and as a consequence lead to cancer due to uncontrolled cellular processes (5-7). Consequently, PTMs are believed to be interesting potential biomarkers or therapeutic targets in cancer; global identification of protein modifications and the biological repercussion of PTMs in all cellular processes therefore is an interesting and expanding field in scientific research.

1.1 SUMOylation

The activity of many proteins is controlled by post-translational modifications such as phosphorylation, acetylation and methylation. Small proteins like ubiquitin can also be used as post-translational modifiers of target proteins. Covalent binding of ubiquitin polymers to substrate proteins is well known for its role in regulating protein stability. These poly-ubiquitinated proteins are recognized by the proteasome and degraded. In addition, ubiquitin regulates target proteins in stability-independent ways. Several ubiquitin-like proteins exist including Neural precursor cell Expressed Developmentally Down-regulated protein 8 (NEDD8), Interferon-Stimulated Gene 15 (ISG15), HLA-F Adjacent Transcript 10 (FAT10), Histone monoubiquitination 1

(HUB1) and Small ubiquitin-like Modifiers (SUMOs) (8). SUMOs are also covalently attached to extensive sets of target proteins to regulate their function mainly in a degradation-independent way. The process of SUMO conjugation to a target protein is termed SUMOylation and requires three enzymatic activities known as E1, E2 and E3, analogous to the ubiquitin system. SUMOylation is reversible; SUMO-specific proteases (SENPs) can remove SUMOs from target proteins (9).

SUMOs were first discovered in the mid-1990s, where researchers observed a larger, modified form of the Ran GTPase-Activating Protein 1 (RanGAP1) (10, 11). These studies revealed that RanGAP1 was covalently modified by a so far unknown ubiquitin-like modifier, SUMO. Functionally, SUMOylation of RanGAP1 targets the protein to the nuclear pore complex (NPC) to facilitate nuclear import of proteins. RanGAP1 turned out to be a unique SUMO target since the modified form of the protein is often observed as the predominant form. For most other SUMO target proteins the stoichiometry of SUMOylation is low and often not detectable without pre-enrichment of SUMOylated proteins (12, 13).

Despite limited sequence identity (18%) between SUMOs and ubiquitin, the structures of SUMOs and ubiquitin are very similar. Three functional SUMO family members have been identified in vertebrates, SUMO-1, SUMO-2 and SUMO-3. SUMO-2 and SUMO-3 share 95% sequence identity and are therefore often referred to as SUMO-2/3, since it is difficult to discriminate between the two proteins. SUMO-2/3 are significantly different from SUMO-1 (+/- 50% sequence identity)(14). SUMOylation can affect the activity and subcellular localization of target proteins. More recently, it has been shown that SUMOylation can also affect the stability of a subset of target proteins. Furthermore, SUMOs are regulators of non-covalent protein-protein interactions via SUMO Interaction Motifs (SIMs).

SUMOs are mainly found throughout the nucleus and regulate virtually all nuclear processes such as transcription, DNA repair, replication, mitosis, transport and ribosome biogenesis (15,16). However, SUMOs are not restricted to the nucleus and also affect cytoplasmic processes including signaling and translation. Hundreds of target proteins and interacting proteins have been uncovered via proteomic approaches and the functional analysis of these SUMO targets will help us to understand in detail how SUMOs contribute to eukaryotic life. A second challenge for the future is to learn more about cooperation between SUMOylation and other post-translational modifications.

1.2 The SUMOylation Machinery

SUMOs are covalently attached to lysines in target proteins via an enzymatic cascade (Figure 1A). The cycle of SUMO conjugation begins with the expression of a precursor protein. This SUMO precursor protein is cleaved by SUMO specific proteases, exposing the C-terminal di-glycine motif. The resulting mature SUMO

Chapter 1

1

protein is subsequently activated by the dimeric E1 enzyme in an ATP-dependent reaction. Activated SUMO is transferred to the SUMOylation specific E2 enzyme Ubc9 and subsequently attached to lysines in target proteins. Several E3 enzymes have been identified that can catalyze this conjugation and provide target protein specificity. SUMOylation is a reversible process; SUMO specific proteases are also capable of removing SUMO proteins from target substrates.

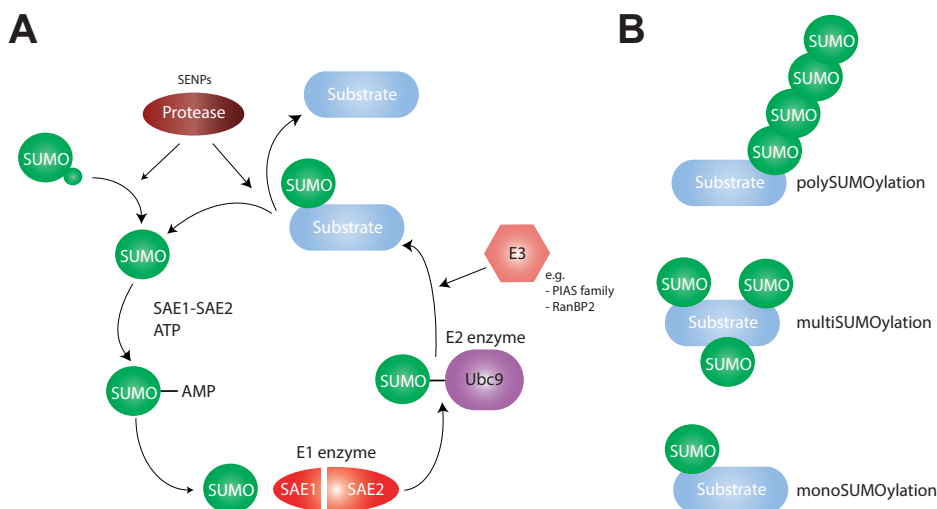


Figure 1. The SUMOylation machinery. (A) SUMO precursor proteins are cleaved by SUMO specific proteases (SENPs). The mature SUMO protein can be conjugated to target substrates via an ATP-dependent E1, E2 and E3 enzymatic cascade. SUMOylation is a reversible process; SENPs can deconjugate SUMO modified substrates. (B) Targets can be modified by a single SUMO protein (monoSUMOylation), by multiple SUMOs on different lysines (multiSUMOylation) and by SUMO chains (polySUMOylation)

E1 enzyme

The SUMO E1 protein was first identified as a heterodimeric enzyme consisting of Ubiquitin Activating enzyme E1-like (Uba2) and Activation of Smt3 (Aos1), activating the SUMO homologue in yeast, Smt3 (17). The human E1 protein comprises the 38 kDa SUMO Activating Enzyme subunit 1 (SAE1) subunit and the 72 kDa SAE2 subunit (18). The small subunits of these heterodimers are similar to the N-terminus of classical ubiquitin E1s, whereas the large subunits resemble the C-terminus of ubiquitin E1s. The SUMO E1 forms a high-energy thioester bond between a catalytic cysteine residue in its large subunit and the C-terminal part of a mature SUMO protein. This formation requires the adenylation of the C-terminus of SUMO (19).

E2 enzyme

An E1-activated SUMO protein is subsequently transferred to the SUMO specific E2, Ubiquitin carrier protein 9 (Ubc9). In contrast to the multiple E2 proteins that regulate ubiquitination, Ubc9 has been identified as the single SUMO E2 and Ubc9 is incapable of conjugating ubiquitin to target proteins (20, 21). Interaction between SAE1/SAE2 and Ubc9 initiates the transfer of an activated SUMO protein to the active cysteine in Ubc9, forming a SUMO-E2 thioester complex. In the final step of SUMOylation, Ubc9 covalently couples SUMO to a target substrate via an isopeptide bond formed by the C-terminal glycine of SUMO and the ϵ -amino group of a lysine residue in the target protein.

Consensus SUMOylation site

The acceptor lysine for SUMO conjugation is commonly located in a consensus SUMOylation site, ψ KxE/D, where ψ represents a large hydrophobic amino acid and x can be any amino acid (22). Although a significant number of published SUMO target proteins are modified on a lysine located in the consensus site, many exceptions have been found. Furthermore, many proteins that contain a SUMOylation consensus motif are not detectably SUMOylated possibly due to limited accessibility of these lysines in folded proteins (23). Thus, the presence of a SUMO consensus site is not sufficient for SUMO conjugation and other target protein features are also important for target selection. Ubc9 can directly bind to the SUMO consensus site which is sufficient for SUMOylation *in vitro* (24). However, there are several SUMO E3 proteins that can catalyze this conjugation and provide target specificity.

E3 enzymes

The Protein Inhibitor of Activated STAT (PIAS) protein family and the closely related yeast proteins SAP and Miz-finger domain-containing proteins (Siz) 1 and 2 are SUMO E3 ligases (25, 26). These proteins contain the catalytically important Siz/PIAS-RING (SP-RING) domain that resembles the Really Interesting New Gene (RING) motif found in ubiquitin E3 ligases. PIAS proteins can interact with the SUMO-Ubc9 complex and thereby act as an adapter protein between this complex and a target substrate for SUMOylation. PIAS-regulated or -enhanced SUMOylation has been shown for several transcription factors. SUMOylation of transcription factors can influence their activity; therefore, PIAS can act as a regulator of transcription (27-29). However, this regulating function is not only due to its SUMO E3 ligase activity; PIAS proteins can also regulate the activity of substrates independent of SUMOylation (30).

A second type of SUMO E3 ligase is the nuclear pore complex protein Ran Binding Protein 2 (RanBP2). RanBP2 forms a stable complex with SUMOylated RanGAP1 at the cytoplasmic fibrils of the NPC. This protein lacks a RING-like

structure; its SUMO ligase activity could be explained by stable binding to Ubc9 and by providing an optimal orientation of the SUMO-Ubc9 complex (31). Indeed, it was recently found that the complex formation between RanBP2/RanGAP1 and SUMO-1/Ubc9 induces activation of a catalytic site in RanBP2 which results in its E3 ligase activity (32). *In vitro*, RanBP2 can enhance the SUMOylation of several proteins (33). In cells, RanBP2 mediates SUMOylation of topoisomerase II α (Topo II α) (34) and Borealin (32, 35).

Another SUMO E3 ligase, the Polycomb group (PcG) Chromobox Protein Homolog 4 (CBX4, also known as Pc2), is localized at polycomb bodies in the nucleus. Potentially this restricts the SUMO ligase activity of CBX4 to substrates that are also localized at these nuclear bodies. CBX4 also lacks a RING-like structure and is not related to RanBP2 (36), it acts as a SUMO E3 ligase by recruiting Ubc9 to polycomb bodies (37). CBX4 mediated SUMOylation has been linked to the DNA damage response (38, 39).

The Methyl methanesulfonate sensitive 2/ Non-structural maintenance of chromosomes element 2 homolog (MMS21/NSE2) SUMO E3 ligase that is part of the Structural maintenance of chromosomes protein 5 and 6 (SMC5/6) complex is important for genome stability (40-42). Interestingly, one protein was identified that can act as a dual SUMO and ubiquitin E3 ligase. The C3HC4-type RING finger protein topoisomerase I-binding, arginine/serine-rich (TOPORS) can enhance both the ubiquitination and the SUMOylation of p53 (43).

SUMO proteases

Several proteins are involved in processing of the SUMO precursor proteins and in deconjugating SUMOylated substrates. The best studied SUMO proteases belong to the Ulp/SENPs family and comprises six SUMO specific protease- 1, 2, 3, 5, 6 and 7 (SENPs) in humans and Ubiquitin-like-specific protease (Ulp) 1 and 2 in yeast (44). SENPs recognize precursor SUMO proteins and remove C-terminal residues to expose the di-glycine motif. Deconjugation of a SUMOylated target protein is initiated by cleavage of the isopeptide bond between the ϵ -amino group of the target lysine and the C-terminus of SUMO (45). The SENP family members have different preferences for processing and deconjugating SUMO-1, -2 and -3 proteins. SENP1 preferentially processes and deconjugates SUMO-1 and shows less activity towards SUMO-2/3. SUMO-2/3 conjugated lysines are preferentially deconjugated by SENP -2, -3 and -5. In addition, SENP2 efficiently processes SUMO-2/3 precursor proteins. SENP6 and SENP7 appear to be SUMO-2/3 chain specific SUMO proteases.

SENPs are localized at specific sites in cells that presumably restricts their activity to local subsets of target proteins. SENP1 is located in the nucleoplasm, SENP2 is located at the nuclear pore and in nuclear speckles, SENP3 and SENP5 are present in nucleoli and are required for ribosome biogenesis and SENP6 and

SEN7 are nucleoplasmic components. Yeast expresses only two SUMO proteases, the nuclear envelope component Ulp1 and the nucleoplasmic component Ulp2.

DeSUMOylating Isopeptidase 1 (DeSI-1) was identified as a second class of SUMO proteases. DeSI-1 shows almost no activity towards SUMO-1 and SUMO-2 precursor proteins, but can deSUMOylate the transcriptional repressor Zinc finger and BTB-containing protein 46 (BZEL) (46, 47). Finally, the catalytic domain of Ubiquitin-specific protease-like 1 (USPL1) proteins can cleave SUMOs from targets *in vitro* and deconjugate SUMO conjugates when overexpressed in cells; however, no endogenous target proteins for USPL1 activity were identified so far (48).

1.3 SUMOylation is essential for eukaryotic life

Several studies have shown that reversible SUMOylation is essential for eukaryotic life. Mice deficient for the SUMO E2 enzyme Ubc9 die after embryonic day 3.5 and prior to embryonic day 7.5. Cells derived from these Ubc9-deficient embryos show major defects in chromosome condensation and segregation and defects in nuclear organization (49). Ubc9-deficiency leads to either embryonic lethality or severe cell-cycle defects in other eukaryotic organisms. Both SUMO E1 subunits are essential for proper cell-cycle progression in budding yeast (17) and E1-deficiency leads to embryonic lethality in *C.elegans* (50). Heterozygous Uba2 (part of the SUMO E1 dimer) mutant mice showed decreased body length and a decreased number of lumbar and sacral vertebrae. Homozygous mutant embryos were not identified during gestation, suggesting that they are not viable (51)(the International Mouse Phenotyping Consortium (IMPC)). Furthermore, the SUMO E3 enzyme RanBP2 is essential for embryonic development (34). Similar to Ubc9-deficiency, mice with low amounts of RanBP2 develop severe aneuploidy due to anaphase-bridge formation. Mechanistically, this is linked to reduced Topoisomerase II α SUMOylation during mitosis.

Contradictory results have been published about SUMO-1 deficient mice; Alkuraya and coworkers proposed that SUMO-1 plays a role in palatogenesis whereas Zhang and coworkers and Evdokimov and coworkers found that SUMO-1 is not essential for normal mouse development due to compensation by SUMO-2 and SUMO-3 (52-54). It is currently unclear whether SUMO-2 and SUMO-3 are required for viability. Interestingly, loss of SENP1 also results in embryonic lethality in mice due to reduced Hypoxia-inducible factor 1-alpha (HIF1 α) stability (55, 56), and loss of SENP2 resulted in embryonic lethality in mice due to a deficiency in cell cycle progression (57), indicating that a finely balanced SUMOylation / deSUMOylation system is required for eukaryotic life.

1.4 Noncovalent SUMO-binding

The SUMO-interaction motif

In addition to covalent attachment of SUMO proteins to lysines in target substrates via peptide-bonds, several proteins are able to interact with SUMO non-covalently via SUMO-interaction motifs (SIMs). It is known that a hydrophobic core in a target protein mediates SUMO binding, and the Val/Ile-X-Val/Ile-Val/Ile sequence has been proposed as a consensus SIM domain. This hydrophobic core is preferentially flanked by acidic residues. Hydrophobic and aromatic amino acids located in a SIM-binding groove of a SUMO protein can interact with the hydrophobic core of a SIM in binding proteins. Acidic amino acids surrounding the hydrophobic core can promote electrostatic interaction between SUMO and a binding protein. Furthermore, phosphorylation of residues surrounding a SIM can introduce a negative charge resulting in an interaction between these residues and lysines located in SUMO. SIMs have been identified in many proteins, including SUMO enzymes to increase their SUMOylation activity (58, 59).

PML nuclear bodies

SIM-mediated protein interactions are important for the formation of PML nuclear bodies (PML-NBs) (60). PML-NBs act as repositories for many proteins and these nuclear domains are important in processes such as DNA repair, transcription and tumor suppression. PML proteins form SIM-containing SUMOylated homodimers. SUMO proteins that are conjugated to lysines of PML homodimers interact non-covalently with SIMs on other PML homodimers, forming a complex network of PML proteins. Mutant PML proteins in which the SUMO accepting lysines or the SIM have been mutated fail to form PML-NBs. Thus, covalent and non-covalent interactions between PML and SUMO are required for the formation of nuclear bodies. Interestingly, several proteins that are recruited to PML-NBs also contain SIMs and can be SUMOylated. Recruitment of these proteins could also depend on covalent and non-covalent interaction with SUMO. A good example for SUMO-dependent recruitment of proteins to PML-NBs is Death Domain-Associated Protein 6 (Daxx). The Daxx protein can interact non-covalently with SUMOylated transcription factors and thereby repress transcriptional activity. Daxx can also interact with SUMOylated PML, resulting in the recruitment of Daxx to PML-NBs and relief of its transcriptional repression (61).

Noncovalent interactions and Ubc9

Non-covalent interaction with SUMO also influences target protein preferences of Ubc9. Ubc9 can be auto-SUMOylated on a non-consensus lysine in its N-terminus. Ubc9 SUMOylation enhances the SUMOylation of the SIM-containing proteins

Speckled 100 kDa protein (Sp100) and IE2 *in vitro* in a SIM-dependent manner, whereas the SUMOylation of several other targets is not affected or impaired (62, 63). SIMs have other important functions in several cellular processes such as DNA repair, protein stability and SUMO chain formation; these functions will be discussed hereafter.

1.5 SUMOs in chains

Ubiquitin chains attached to target proteins play important roles in many cellular processes in a chain architecture-dependent manner. Initially it was believed that SUMO target proteins are usually conjugated to one or more SUMO monomers. However, research on SUMOylation over the years showed that SUMOs are also able to form chains on target proteins. Mammalian SUMO-2 and SUMO-3 contain an internal consensus SUMOylation site located in their unstructured N-terminal protrusion. Interestingly, this site is missing in SUMO-1 (64). The yeast SUMO homologue Smt3 contains two SUMOylation consensus sites (65).

SUMO polymer formation in cells

Polymeric SUMO chains were initially identified *in vitro*. Using a recombinant SUMOylation system, it was first found that SUMO-2 and -3 multimerize very efficiently *in vitro* (64). Efficient chain formation occurs on lysine 11 (K11) located in a consensus site on SUMO-2 and SUMO-3, however chain formation has also been observed on non-consensus lysines in SUMO-1, -2 and -3 *in vitro*. Furthermore it has been shown that SUMO chains can be anchored to recombinant targets (e.g. PML, HIF-1 α) *in vitro*. Previously we showed that SUMO chain formation also occurs in cells. Using a mass spectrometry approach, we found evidence for SUMO polymerization *in vivo* by detecting the SUMO-2/3 branched peptide that is SUMOylated on K11. This study also showed that SUMO-1 can be conjugated to K11 in SUMO-2/3 and thereby limit SUMO-2 chain formation *in vitro* (66).

Ubc9 regulates SUMO chain formation

The observation that Ubc9 can interact with SUMO in a non-covalent manner has provided mechanistic insight into SUMO chain formation. Ubc9 binds SUMO non-covalently on a site that is located distal to the active cysteine that is used for the formation of a SUMO-Ubc9 thioester complex. This non-covalent interaction is important for SUMO multimerization since mutating the binding site in Ubc9 strongly reduced SUMO chain formation *in vitro*. Mechanistically, it is not completely clear how this non-covalent interaction induces chain formation. One possibility is that Ubc9 can dimerize and that a non-covalently bound SUMO on one Ubc9 moiety is SUMOylated on K11 by another SUMO-Ubc9 thioester complex (67). SUMO E3 ligases can enhance SUMO chain formation *in vitro*, probably also via lysines in

SUMO that are not situated in SUMOylation consensus sites. The SUMO specific proteases Ulp2 in yeast and SENP6 and SENP7 in mammals are very efficient in disassembling SUMO chains both *in vitro* and *in vivo* (68, 69). Research has provided insight into some biological functions of SUMO chain formation in cells, some examples can be found in the following sections.

1.6 Crosstalk between SUMOylation and other PTMs

In addition to SUMOylation, proteins are regulated by a diverse set of other post-translational modifications. Orchestration of these different modifications is important for full control of protein activity. Antagonistic and cooperative forms of crosstalk have been reported between SUMOylation and other types of post-translational modifications including phosphorylation, acetylation and ubiquitination (Figure 2).

Crosstalk between SUMOylation and phosphorylation

Phosphorylation events that occur in the vicinity of SUMOylation consensus sites can positively enhance SUMOylation. A specific Phosphorylation-dependent SUMOylation Motif (PDSM) was discovered, ψ KxExxSP, that mediates phosphorylation-dependent SUMOylation of target proteins such as heat-shock factors, GATA-1 and myocyte enhancer factor 2 (70). The local negative charge is important for enhancing SUMOylation since clusters of negatively charged amino acids can also enhance SUMOylation via increased binding of Ubc9 (71). The precise spacing between phosphorylation sites and SUMOylation sites might be critical for phosphorylation-mediated SUMOylation. Phosphorylation of residues that are not situated in PDSMs can also negatively influence SUMOylation. Interestingly, SUMO itself is a phosphoprotein, although the functional relevance of SUMO phosphorylation is currently unclear (72, 73).

Crosstalk between SUMOylation and acetylation

Other forms of crosstalk have been identified between SUMOylation and acetylation. A key function of SUMOs is repressing transcription factors (74). Interplay between SUMOylation and acetylation can explain the repressive activity of SUMO on the transcription factor Elk-1 (75). SUMOylation of Elk-1 promotes association with Histone Deacetylase 2 (HDAC2) to remove acetyl groups from histones in a local manner, thereby repressing transcription. Alternatively, HDACs can also promote SUMOylation of target proteins by deacetylation of lysines used for SUMO modification. SUMOylation and acetylation can also compete for the same lysine. SUMOylation of p53 blocks the acetylation of the same acceptor lysine and inhibits p53 binding to DNA (76). Furthermore it has been established that acetylation of SUMO proteins interferes with its binding to SIMs, thereby blocking the interaction between SUMO and SIM-containing proteins (77).

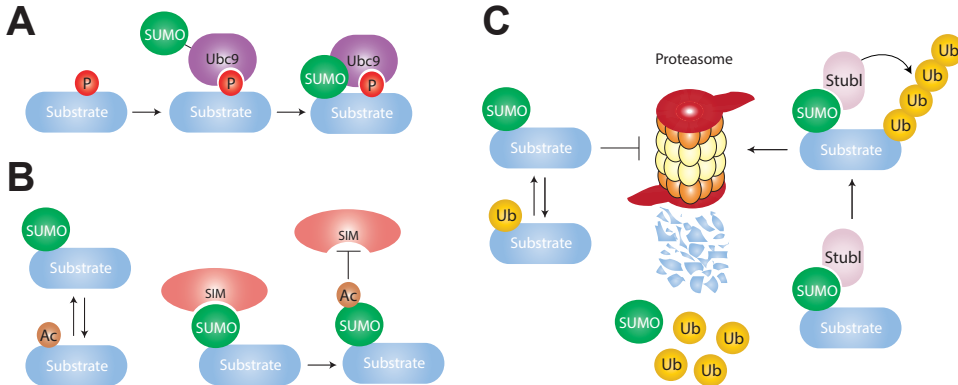


Figure 2. Crosstalk between SUMO and other PTMs. (A) Phosphorylation (P) downstream of a SUMO consensus site can induce SUMOylation by increased Ubc9 binding. (B) SUMOylation and acetylation (Ac) can compete for the same lysine. Acetylation of SUMOylated proteins blocks the interaction between SUMO and SIM-containing proteins. (C) SUMOylation can have both positive and negative effects on protein stability, by either blocking ubiquitination (Ub) of lysines or by targeting proteins for proteasomal degradation via the recruitment of SUMO targeted ubiquitin ligases (STUBLs)

Crosstalk between SUMOylation and ubiquitination

Although they were first seen as mutually exclusive events, extensive crosstalk between SUMOylation and ubiquitination has been uncovered by many studies. First of all, SUMOs and ubiquitin can compete for acceptor lysines in target proteins. For example, SUMOylation of the Nuclear Factor kappa-light-chain-enhancer of activated B cells (NF- κ B) inhibitor alpha (I κ B α) on a lysine that is also used for ubiquitination protects I κ B α from proteasomal degradation (78). Phosphorylation of I κ B α induces its ubiquitination and degradation, resulting in translocation of NF- κ B to the nucleus and activation of its target genes. Interestingly, phosphorylation inhibits the SUMOylation of I κ B α , indicating an antagonistic relation between SUMOylation and phosphorylation-dependent ubiquitination of I κ B α .

Another target for crosstalk between SUMO and ubiquitin in the NF- κ B pathway is the I κ B α kinase component Inhibitor of NF- κ B kinase subunit gamma/ NF-kappa-B essential modulator (IKK γ /NEMO) (79). Activation of this structural I κ B α kinase component depends on sequential modification of NEMO by SUMO and ubiquitin. Upon genotoxic stress, NEMO translocates to the nucleus and accumulates in a SUMOylated form. Upon deSUMOylation, NEMO gets phosphorylated and subsequently ubiquitinated on the same two lysines used for SUMOylation. Ubiquitin-modified NEMO translocates to the cytoplasm where it forms an active IKK kinase complex (80).

Originally it was understood that SUMOylation did not affect target protein stability. However, more recent studies have shown that SUMOylation of some proteins can act as an ubiquitination signal. This was uncovered via functional studies on the yeast Synthetic lethal of unknown function protein 5 and 8 (SLX5/8) complex and the mammalian RING finger protein 4 (RNF4) protein (81, 82). These ubiquitin E3 ligases can interact with SUMOylated proteins via internal SIMs and subsequently ubiquitinate these SUMOylated proteins and are therefore called SUMO-targeted ubiquitin ligases (STUBLs) (83). Yeast strains lacking SLX5/8 accumulate SUMOylated proteins and show genomic instability. PML was the first identified mammalian target protein for SUMO-dependent ubiquitination. It was shown that proteasomal degradation of PML and PML-retinoic acid receptor alpha (PML-RAR α) upon arsenic treatment depends on poly-SUMOylation of these proteins. Four internal SIMs in RNF4 are essential for targeting PML, most likely via binding to a SUMO chain on lysine 160 (84, 85). In another study, ubiquitin was found to co-purify with SUMO-2 target proteins. Quantitative proteomics was subsequently employed to identify a large set of proteins that are regulated by crosstalk between the ubiquitin-proteasome pathway and SUMOylation. It was shown that the SUMOylated fraction of several proteins strongly increased upon proteasome inhibition. This indicates that a subset of SUMO-2 modified proteins are subsequently degraded by the ubiquitin-proteasome system, possibly in an RNF4-dependent manner. Interestingly, this study identified a second set of SUMOylated proteins that were negatively affected by proteasome inhibition. The decrease in SUMOylation of these target proteins by proteasome inhibitors could potentially be explained by a lack of recycled SUMOs (86).

Two additional STUBLs were identified more recently; Ubiquitin ligase for SUMO conjugates protein 1 (Uls1) and RNF111. Uls1 is responsible for the ubiquitination and clearance of poly-SUMOylated Rap1 proteins to facilitate non-homologous end joining at telomeres (87). RNF111 is recruited to sites of DNA damage by SUMOylated Xeroderma Pigmentosum group C-complementing protein (XPC) to induce nonproteolytic ubiquitination (88). Like RNF4, RNF111 also seems to have an effect on PML stability (89). Crosstalk between SUMOylation and ubiquitination regulate several processes during the DNA damage response, this is further discussed in the section 'SUMOylation in DNA repair'.

1.7 SUMOylation and cell cycle progression

Cell cycle defects upon alterations in the SUMO landscape

Since its discovery, SUMO has been linked to cell cycle progression in many reports. A lot of these studies were based on interfering with expression levels of SUMO, SUMO conjugating enzymes or SUMO proteases. The first link was reported in

1995, when Seufert and coworkers found that knocking out Ubc9 expression in yeast caused an accumulation of large budded cells with a 4n DNA content due to an arrest at the G2 or M phase of the cell cycle (90). Similar defects on cell cycle progression in yeast were found upon interference with expression of the two SUMO E1 enzyme subunits, Uba2 and Aos1 (17, 91). Absence of Ubc9 or Smt3 (SUMO in yeast) expression in *S.cerevisiae* had an effect on the activity of the anaphase-promoting complex/cyclosome (APC/C), resulting in a metaphase block and defects in chromosome segregation (92). Furthermore, it has been shown that the formation of SUMO chains by Ubc9 plays an essential role in meiosis in *S.cerevisiae* (93).

Deletion of Ulp1 and Ulp2, the two SUMO specific proteases in yeast, also resulted in cell cycle defects. Deletion of Ulp1 expression caused a G2/M block, this was however partly unrelated to the effect on SUMO conjugation (44). Ulp2 expression is essential for the restart of cell division after checkpoint arrest by regulating mitotic spindle dynamics (94). These yeast studies revealed an emerging role for SUMOylation in cell cycle progression; this was further emphasized by studies in mammalian systems. Mouse embryonic fibroblast (MEFs) derived from Ubc9-deficient embryos displayed severe chromosome condensation and segregation defects, resulting in an increase in amount of cells that contain more than two paired sets of chromosomes (polyploidy) (49). Interestingly, although the total number of Ubc9 knockout MEFs was reduced compared to wild-type MEFs, the mitotic index was almost unchanged. Human fibroblasts with a decreased Ubc9 expression showed reduced proliferation without an arrest in a particular phase of the cell cycle, suggesting that Ubc9 knockdown induces a general growth arrest (95). Interestingly, knocking down the SUMO specific protease SENP5 in human HeLa cells, led to similar phenotypes. A strong reduction in proliferation rate was observed in cells with reduced SENP5 expression. In alignment with the results from the Ubc9 study, this could not be explained by an arrest during a specific phase of the cell cycle (96). Disruption of SENP2 expression in mice revealed an essential role for this SUMO specific protease in cell cycle progression rate and the transition from G1 to S phase (57). Together these studies showed that a dynamic SUMOylation/deSUMOylation system is essential for proper cell cycle progression.

SUMO targets at chromosomes

SUMO signals in fluorescence microscopy are often observed at centromeres and kinetochores of condensed chromosomes during the first stages of mitosis. Several centromere and kinetochore proteins that play essential roles during mitosis were identified as SUMO targets (97, 98). The SUMO E3 ligase RanBP2 SUMOylates Topo II α during mitosis. This is essential for the targeting of Topo II α to inner centromeres where it subsequently allows proper separation of sister chromosomes in anaphase (34). Dynamic SUMOylation of Topo II α seems to be important in this process;

Chapter 1

1

accumulation of the SUMOylated form of Topo II α in yeast after Ulp2 deletion results in prolonged metaphase and defects in centromeric cohesion (99).

Two other identified SUMO target proteins with a role in mitosis are members of the chromosomal passenger complex (CPC); this complex regulates the attachment of kinetochores to microtubules and cytokinesis. SUMOylation of the CPC member Aurora B during mitosis is needed for proper chromosome segregation, most likely by regulating the removal of CPC complexes from chromosomes during prometaphase (100, 101). Another member of the CPC, Borealin, was identified as a mitotic specific SUMO-2/3 target protein. The role of Borealin SUMOylation is currently unknown but does not affect CPC assembly and localization (35).

Centromere (CENP) protein family members form another group of SUMO regulated targets. SENP6 dependent deSUMOylation of CENP-I and CENP-H protects these proteins for proteasomal degradation during S phase, this is essential for the proper localization of kinetochore proteins (102, 103). The microtubule motor protein CENP-E specifically recognizes and binds to SUMO-2/3 chains which is essential for kinetochore localization of CENP-E. This is potentially regulated via non-covalent interactions between CENP-E and SUMO-2/3 chains on the centromere/kinetochore associated proteins Budding uninhibited by benzimidazoles 1 beta (BubR1) and Kinetochore protein Nuf2 (104); see also figure 3A.

SUMOylation and transcription

Besides regulating proteins directly involved in mitosis, SUMO also regulates cell cycle progression indirectly by affecting the expression of many genes. SUMOylation and its role in transcription is probably one of the most studied and best documented downstream consequence of SUMO modification and is extensively reviewed (105-107). Initially SUMOylation was mainly linked to transcription repression but now a growing number of studies report on examples where SUMOylation can also activate transcription. Genome-wide studies have uncovered a general link between SUMOylation and gene repression. It has been shown that targeting Ubc9 to a promoter decreases transcriptional activity (108) and that active SUMOylation at promoter regions represses expression of several classes of genes (95).

Several mechanisms can explain the regulation of transcription by SUMO. SUMOylation can induce or inhibit enzymatic activity of proteins and SUMOylation can directly affect the DNA binding capacity of transcription factors. Furthermore, SUMO can organize both the formation of repressive complexes as well as the formation of activation complexes on chromatin. A lot of studies report on how SUMOylation can either repress or activate the transcription of genes, one example for each case is given below (additional examples can be found in the section 'crosstalk between SUMOylation and acetylation'). SUMOylation of the maintenance methylase DNA (cytosine-5)-methyltransferase 1 (DNMT1) enhances the methylase activity of this

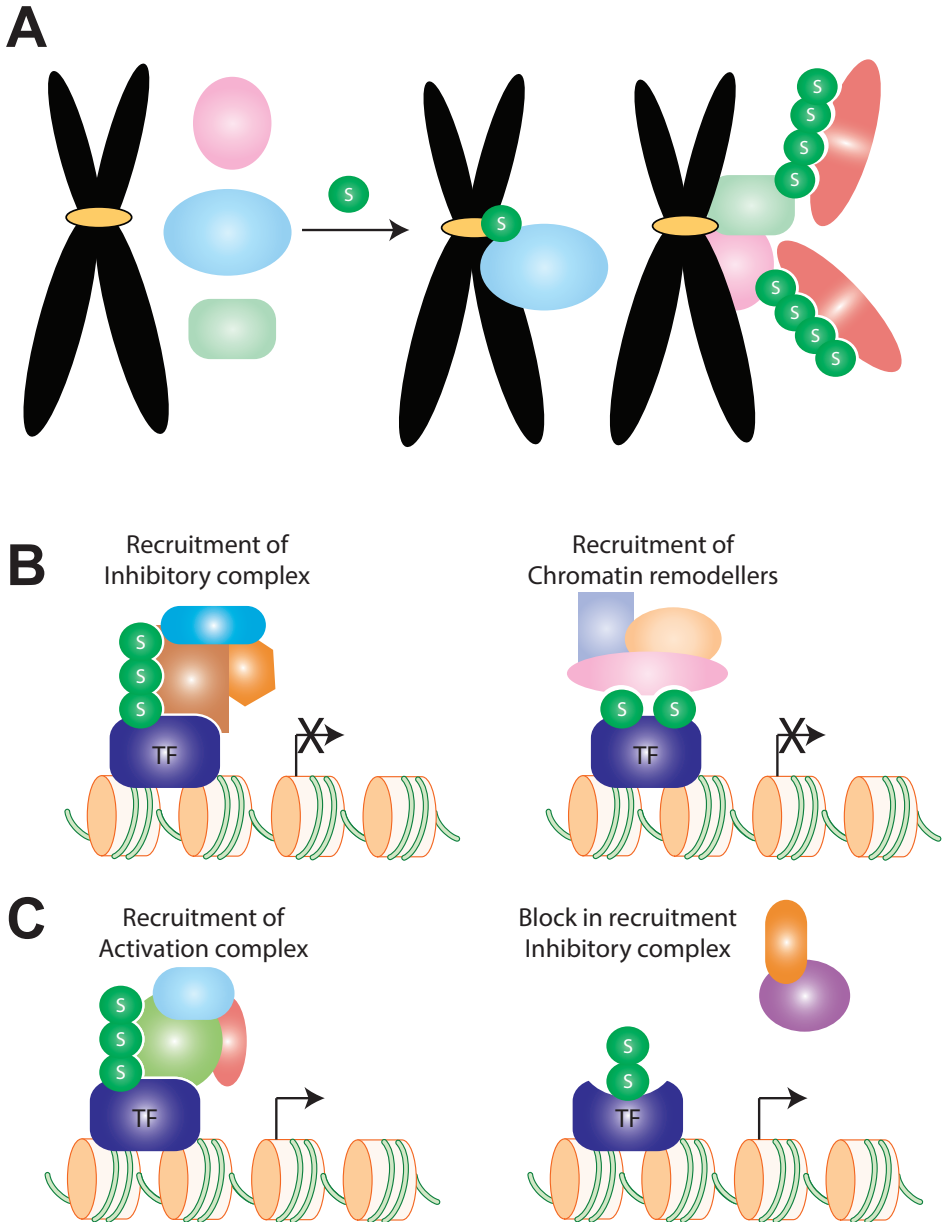


Figure 3. SUMOylation plays several roles during cell cycle progression. (A) SUMO (S) regulates the translocation of proteins to chromosomes and SUMOylation of chromosome interacting proteins induces the recruitment of SIM containing proteins. (B) SUMOylation has repressive effects on gene expression by recruiting inhibitory complexes or chromatin remodellers to transcription factors (TF). (C) SUMOylation has activating effects on gene expression by recruiting activation complexes to transcription factors and by blocking the interaction between transcription factors and inhibitory complexes. Figure 3B and 3C are based on figures in (15) and in (105).

protein on chromatin. Methylation of DNA physically blocks the binding of sequence specific transcriptional proteins and methylated DNA recruits chromatin remodeling proteins resulting in the formation of inactive chromatin. SUMO induced DNMT1 activity therefore results in repression of gene expression (109). One example where SUMOylation activates gene expression was reported for the transcriptional repressor Ikaros. SUMOylation of Ikaros hinders the interaction of Ikaros with the co-repressor complexes transcriptional regulatory protein Sin3 and Nucleosome Remodeling Deacetylase (NuRD), resulting in the release of repression (110). The effect of SUMOylation on transcription is thus substrate-dependent and can therefore not simply be described as 'repressive' or 'activating'; see also figure 3B and 3C.

1.8 SUMOylation and DNA repair

The genomic stability of cells is maintained by a variety of DNA repair pathways collectively called the DNA Damage Response (DDR). These DDRs consist of proteins that are responsible for the recognition, removal and repair of DNA lesions. These proteins are extensively regulated by dynamic post-translational modifications during the DDR. SUMOylation has been shown to play crucial roles during several DNA repair mechanisms, sometimes in coordination with ubiquitination (111, 112). Some of these roles are summarized in this section and in figure 4.

A role for SUMO in Base Excision Repair

The first link between SUMOylation and DNA repair was revealed in studies on Base Excision Repair (BER). During BER, base lesions are recognized by the Thymine-DNA glycosylase (TDG) protein, an enzyme that removes the damaged base. Removal of this base results in an abasic site, which in turn induces a strong interaction between TDG and the abasic site. This strong interaction has to be reduced to facilitate the subsequent steps in BER and to guarantee proper repair of the lesion. SUMO-1 modification on the C-terminus of TDG upon DNA binding induces a conformational change in the DNA bound N-terminus of this protein, leading to reduced binding of TDG to the abasic site. This initiates the next step in BER and is also needed for the enzymatic turnover of TDG (113, 114).

A SUMO – ubiquitin switch on PCNA

A good example of the cooperative regulation of DNA repair by SUMO and ubiquitin is the Proliferating Cell Nuclear Antigen (PCNA) protein, an essential cofactor for DNA polymerases (115, 116). PCNA encircles the DNA as a sliding clamp thereby acting as a docking platform for many proteins involved in DNA metabolism. Crosstalk between SUMO and ubiquitin on PCNA acts as a switch for different pathways of processing DNA lesions during replication. Monoubiquitination of PCNA on lysine 164 (K164) upon DNA damage induces translesion synthesis by recruiting the DNA

damage tolerant polymerase Pol η . In yeast, K63 ubiquitin chain formation on K164 of PCNA is somehow involved in error-free replication of the damaged DNA. Also in yeast, PCNA is SUMOylated in S phase on K164 as well as K127. SUMOylated PCNA recruits the antirecombinogenic helicase Srs2, thereby limiting recombination during replication (117, 118). Upon DNA damage, Srs2 bound to SUMOylated PCNA blocks the recombination machinery resulting in a stalled replication fork when it encounters a lesion. This Srs2 mediated block in replication results in damage avoidance. Crosstalk between SUMO and ubiquitin on PCNA has mainly been studied in yeast; PCNA SUMOylation is difficult to detect in human cells. More recently, PCNA-interacting partner (PARI) was identified as PCNA-interacting protein in human cells with a preferential binding to SUMOylated PCNA *in vitro* (119). This Srs2-like protein inhibits unwanted recombination at mammalian replication forks.

Coordinated SUMOylation and ubiquitination signals in DDR

The DDRs that regulate the repair of double strand breaks (DSBs) are broadly regulated by both SUMOylation and ubiquitination. Several members of the SUMOylation machinery were found to accumulate at sites of DSBs (120, 121). Accumulation of the SUMO E3 ligases PIAS1 and/or PIAS4 at DSBs induces a wave of SUMOylation which is needed for the recruitment of crucial repair factors such as RNF168, Tumor suppressor p53-binding protein 1 (53BP1), Receptor-associated protein 80 (RAP80) and Breast Cancer Type 1 Susceptibility Protein (BRCA1). This is regulated by the SUMOylation of several DSBs repair factors. SUMOylation of the ubiquitin E3 ligase BRCA1 at DSBs induces its ubiquitination activity *in vitro*, potentially by enhancing the interaction between SUMO-BRCA1 and target proteins that harbor SIMs. Other targets for PIAS1 / PIAS4 mediated, DSBs specific SUMOylation are the repair factors 53BP1 and RNF168. DNA damage- and PIAS4-dependent SUMOylation of Human epidermal growth factor receptor 2c (HERC2) is required for its binding to RNF8 at DSBs (122).

Another form of crosstalk between SUMO and ubiquitin at sites of DSBs is the recruitment of the STUBL RNF4 by SUMOylated DSB-response proteins. Interfering with RNF4 expression in human and chicken cells caused defects in the DSBs repair pathways homologous recombination (HR) and non-homologous end joining (NHEJ). RNF4 accumulates at sites of DNA damage through interactions between its SIMs and SUMOylated 53BP1, Mediator of DNA damage checkpoint protein 1 (MDC1) and Replication protein A (RPA). At DSBs, RNF4 mediates the ubiquitination and proteasomal degradation of DSB-repair proteins including MDC1, RPA and BRCA1. This is required for the rapid turnover of these proteins and for the efficient loading of Radiation sensitive 51 (RAD51) (123-126).

Another STUBL, RNF111, plays a critical role in nucleotide excision repair (NER). The DNA damage recognition factor XPC is SUMOylated upon UV induced DNA

Chapter 1

damage and subsequently recognized by RNF111. Together with the E2 enzyme Ubc13-Mms2, RNF11 promotes the nonproteolytic, K63-linked ubiquitination of SUMOylated XPC. This process is also regulating the recruitment of XPC to UV-damaged DNA; thereby facilitating efficient NER (88).

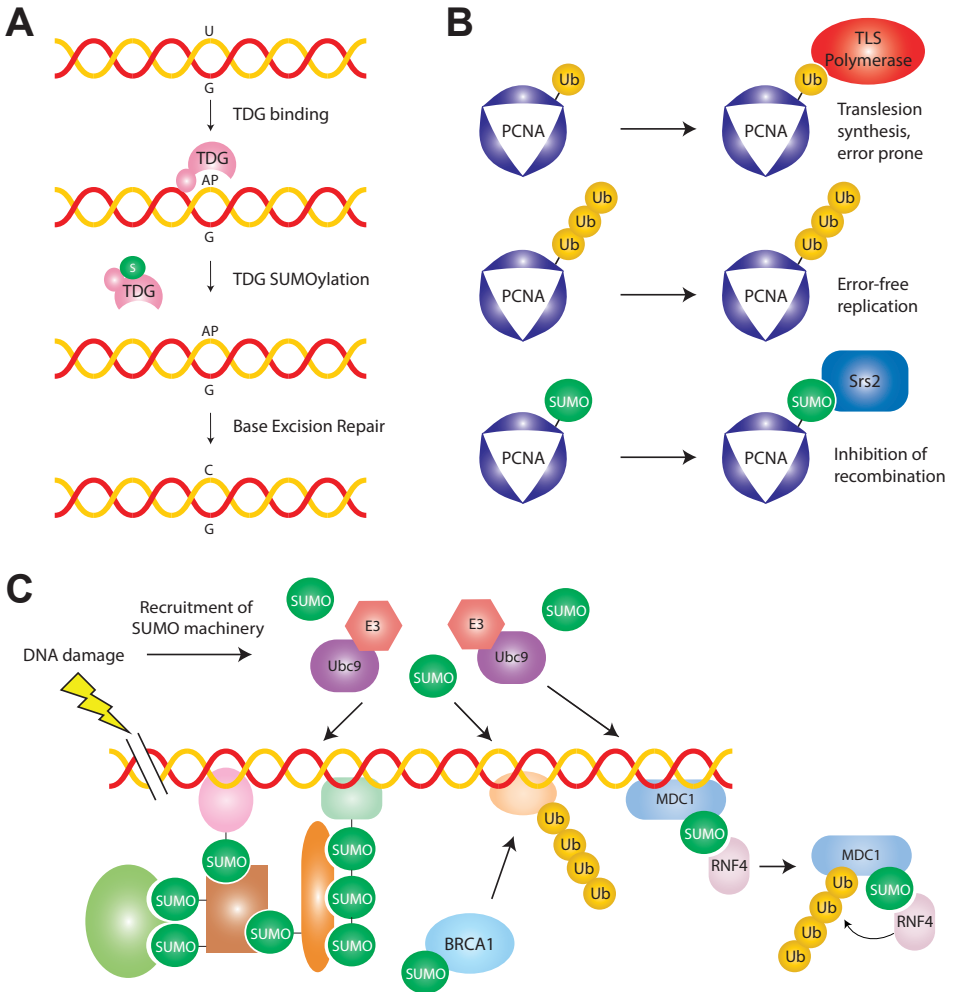


Figure 4. SUMOylation plays several roles in the DNA damage response. (A) SUMOylation (S) facilitates Base Excision Repair by inducing a conformational change in the Thymine-DNA glycosylase (TDG) protein. (B) The Proliferating Cell Nuclear Antigen (PCNA) protein is regulated by a SUMO – ubiquitin switchboard to process DNA lesions. (C) Recruitment of the SUMO machinery regulates different processes in double strand break repair. SUMOylation induces complex formation of repair proteins, enhances the ubiquitination activity of BRCA1 and initiates the recruitment of RNF4. Figures are based on figures in (111) (Figure 4A and 4C) and in (112) (Figure 4B).

Thus, DNA damage triggers SUMOylation of many proteins involved in DSBs repair. Interestingly, it was recently reported that only abolishing SUMOylation of several repair proteins significantly impairs HR pathway in yeast (127). The authors suggest that SUMOylation acts as a 'molecular glue' to enhance interactions between DNA repair proteins and that SUMO acts synergistically on protein groups to facilitate DNA repair. Protein group modification by SUMO was also found to be important for proper nucleotide excision repair in yeast (128).

1.9 SUMO proteomics

A revolution in understanding protein SUMOylation came with the introduction of mass-spectrometry (MS) based proteomics to study SUMO targets, SUMOylation dynamics and SUMO acceptor sites. MS based approaches are widely used for the systematic, quantitative and qualitative identification of post-translational modifications on proteins (129, 130). For ubiquitin-like modifications, these approaches are based on the purification of conjugated proteins using cells expressing tagged ubiquitin-like (UBL) proteins. These purified proteins are subjected to tryptic-digestion, the resulting peptide mixture is analyzed by MS and specific software is used to identify and quantify peptides. In addition, stable isotope labeling by amino acids in cell culture (SILAC), has enabled the metabolic labeling of endogenous proteins and subsequent quantification (131). SILAC can be used to study PTMs dynamics in response to different stimuli by labeling two or three sets of cells with distinct isotope variants, metabolic incorporation of the distinct amino acids results in a mass shift of labeled peptides. Cells that do not express tagged-UBL proteins are often included in SILAC experiments to discriminate between UBL target proteins and contaminants.

Studying SUMOylation by MS is challenging for different reasons. First of all, the low modification stoichiometry for many SUMOylated proteins requires the efficient and large scale purification of SUMO conjugates from cells. The activity of SUMO specific proteases in lysates during these purifications form another pitfall in SUMO based proteomics. Finally, site-specific identification of SUMO targets is very difficult due to the large SUMO peptide branch remaining after tryptic digestion (132). Nevertheless, SUMO proteomics has significantly increased our knowledge on SUMO target proteins and on SUMO dynamics during different cellular processes. By using denaturing buffers to inactivate SUMO proteases it has been revealed that SUMO-1 and SUMO-2/3 have both distinct and overlapping target proteins (133, 134).

So far hundreds of SUMO target proteins have been identified by MS-based studies in different organisms, revealing roles for SUMOylation in many cellular processes including transcription, DNA repair, growth control and RNA metabolism (135-140).

Furthermore, SILAC-based approaches are often used to study the changes

in SUMOylation patterns upon different cellular stress conditions such as heat shock (141, 142) and oxygen/glucose-deprivation (143). In these studies, it was not possible to discriminate between mono-SUMOylated and poly-SUMOylated target proteins. Interestingly, a method was developed that allowed the identification of polySUMO conjugates in cells (144). Although these studies shed light on which proteins are regulated by SUMOylation, they did not provide information on the exact acceptor lysines used for SUMO modification. This information is needed to be able to make SUMO-deficient mutants to study the effect of SUMOylation on individual target proteins. Mutating SUMO consensus sites only is often not sufficient to generate a SUMO-deficient mutant and quite often these consensus sites are not used since they are inaccessible for the SUMO machinery in folded proteins (145). Compared to other PTMs, mapping of SUMOylation sites by mass spectrometry is technically challenging since the long SUMO tryptic peptide conjugated to target lysines produces complex MS/MS spectra.

Despite its difficulties, several approaches were proven to be successful in mapping acceptor lysines for SUMO. Peptides modified by SUMO *in vitro* were successfully detected by a pattern recognition tool (SUMmOn) and low-resolution MS (146). In a previous study, we have used linearization of branched peptides in combination with targeted MS to identify SUMO polymerization sites (66). In other approaches, the tryptic SUMO remnant was shortened by mutating an amino acid close to the C-terminus of SUMO into a trypsin cleavable arginine. These mutations do not alter the conjugation efficiency of SUMOs to target proteins (147, 148). Utilizing these constructs, researchers identified 14 SUMO-1 sites in HeLa cells (149), 17 SUMO-3 sites in *A. thaliana* (150) and 17 SUMO-1 sites in HEK293 cells (151). Furthermore, the development of the database search tool “ChopNSpice” has enabled the identification of SUMO sites on endogenous proteins (152).

Despite the fact that SUMO proteomics has significantly contributed to our knowledge of SUMO's function, still a lot of targets and modified lysines remain to be identified. Improvement of proteomic based techniques will give us more detailed insight into SUMOylation dynamics in different cellular processes.

Reference List

1. CRICK, F. H. (1958) On protein synthesis. *Symp. Soc. Exp. Biol.* 12, 138-163
2. (2004) Finishing the euchromatic sequence of the human genome. *Nature* 431, 931-945
3. Vogel, C., and Marcotte, E. M. (2012) Insights into the regulation of protein abundance from proteomic and transcriptomic analyses. *Nat. Rev. Genet.* 13, 227-232
4. Walsh, C. T., Garneau-Tsodikova, S., and Gatto, G. J., Jr. (2005) Protein posttranslational modifications: the chemistry of proteome diversifications. *Angew. Chem. Int. Ed Engl.* 44, 7342-7372
5. Bettermann, K., Benesch, M., Weis, S., and Haybaeck, J. (2012) SUMOylation in carcinogenesis. *Cancer Lett.* 316, 113-125
6. Lopez-Otin, C., and Hunter, T. (2010) The regulatory crosstalk between kinases and proteases in cancer. *Nat. Rev. Cancer* 10, 278-292

7. Kirkin, V., and Dikic, I. (2011) Ubiquitin networks in cancer. *Curr. Opin. Genet. Dev.* 21, 21-28
8. Van der Veen, A. G., and Ploegh, H. L. (2012) Ubiquitin-like proteins. *Annu. Rev. Biochem.* 81, 323-357
9. Hay, R. T. (2005) SUMO: a history of modification. *Mol. Cell* 18, 1-12
10. Mahajan, R., Delphin, C., Guan, T., Gerace, L., and Melchior, F. (1997) A small ubiquitin-related polypeptide involved in targeting RanGAP1 to nuclear pore complex protein RanBP2. *Cell* 88, 97-107
11. Matunis, M. J., Coutavas, E., and Blobel, G. (1996) A novel ubiquitin-like modification modulates the partitioning of the Ran-GTPase-activating protein RanGAP1 between the cytosol and the nuclear pore complex. *J. Cell Biol.* 135, 1457-1470
12. Bossis, G., and Melchior, F. (2006) SUMO: regulating the regulator. *Cell Div.* 1, 13
13. Johnson, E. S. (2004) Protein modification by SUMO. *Annu. Rev. Biochem.* 73, 355-382
14. Saitoh, H., and Hinchev, J. (2000) Functional heterogeneity of small ubiquitin-related protein modifiers SUMO-1 versus SUMO-2/3. *J. Biol. Chem.* 275, 6252-6258
15. Geiss-Friedlander, R., and Melchior, F. (2007) Concepts in sumoylation: a decade on. *Nat. Rev. Mol. Cell Biol.* 8, 947-956
16. Flotho, A., and Melchior, F. (2013) Sumoylation: a regulatory protein modification in health and disease. *Annu. Rev. Biochem.* 82, 357-385
17. Johnson, E. S., Schwienhorst, I., Dohmen, R. J., and Blobel, G. (1997) The ubiquitin-like protein Smt3p is activated for conjugation to other proteins by an Aos1p/Uba2p heterodimer. *EMBO J.* 16, 5509-5519
18. Desterro, J. M., Rodriguez, M. S., Kemp, G. D., and Hay, R. T. (1999) Identification of the enzyme required for activation of the small ubiquitin-like protein SUMO-1. *J. Biol. Chem.* 274, 10618-10624
19. Lois, L. M., and Lima, C. D. (2005) Structures of the SUMO E1 provide mechanistic insights into SUMO activation and E2 recruitment to E1. *EMBO J.* 24, 439-451
20. Desterro, J. M., Thomson, J., and Hay, R. T. (1997) Ubc9 conjugates SUMO but not ubiquitin. *FEBS Lett.* 417, 297-300
21. Johnson, E. S., and Blobel, G. (1997) Ubc9p is the conjugating enzyme for the ubiquitin-like protein Smt3p. *J. Biol. Chem.* 272, 26799-26802
22. Rodriguez, M. S., Dargemont, C., and Hay, R. T. (2001) SUMO-1 conjugation in vivo requires both a consensus modification motif and nuclear targeting. *J. Biol. Chem.* 276, 12654-12659
23. Anckar, J., and Sistonen, L. (2007) SUMO: getting it on. *Biochem. Soc. Trans.* 35, 1409-1413
24. Bernier-Villamor, V., Sampson, D. A., Matunis, M. J., and Lima, C. D. (2002) Structural basis for E2-mediated SUMO conjugation revealed by a complex between ubiquitin-conjugating enzyme Ubc9 and RanGAP1. *Cell* 108, 345-356
25. Johnson, E. S., and Gupta, A. A. (2001) An E3-like factor that promotes SUMO conjugation to the yeast septins. *Cell* 106, 735-744
26. Sachdev, S., Bruhn, L., Sieber, H., Pichler, A., Melchior, F., and Grosschedl, R. (2001) PIASy, a nuclear matrix-associated SUMO E3 ligase, represses LEF1 activity by sequestration into nuclear bodies. *Genes Dev.* 15, 3088-3103
27. Roukens, M. G., Alloul-Ramdhani, M., Vertegaal, A. C., Anvarian, Z., Balog, C. I., Deelder, A. M., Hensbergen, P. J., and Baker, D. A. (2008) Identification of a new site of sumoylation on Tel (ETV6) uncovers a PIAS-dependent mode of regulating Tel function. *Mol. Cell Biol.* 28, 2342-2357
28. Palvimo, J. J. (2007) PIAS proteins as regulators of small ubiquitin-related modifier (SUMO) modifications and transcription. *Biochem. Soc. Trans.* 35, 1405-1408
29. Sharrocks, A. D. (2006) PIAS proteins and transcriptional regulation--more than just SUMO E3 ligases? *Genes Dev.* 20, 754-758
30. Rytinki, M. M., Kaikkonen, S., Pehkonen, P., Jaaskelainen, T., and Palvimo, J. J. (2009) PIAS proteins: pleiotropic interactors associated with SUMO. *Cell Mol. Life Sci.* 66, 3029-3041
31. Pichler, A., Knipscheer, P., Saitoh, H., Sixma, T. K., and Melchior, F. (2004) The RanBP2 SUMO E3 ligase is neither. *Nat. Struct. Mol. Biol.* 11, 984-991
32. Werner, A., Flotho, A., and Melchior, F. (2012) The RanBP2/RanGAP1*SUMO1/Ubc9 complex is a multisubunit SUMO E3 ligase. *Mol. Cell* 46, 287-298
33. Pichler, A., Gast, A., Seeler, J. S., Dejean, A., and Melchior, F. (2002) The nucleoporin RanBP2 has SUMO1 E3 ligase activity. *Cell* 108, 109-120
34. Dawlaty, M. M., Malureanu, L.,

- Jeganathan, K. B., Kao, E., Sustmann, C., Tahk, S., Shuai, K., Grosschedl, R., and van Deursen, J. M. (2008) Resolution of sister centromeres requires RanBP2-mediated SUMOylation of topoisomerase IIalpha. *Cell* 133, 103-115
35. Klein, U. R., Haindl, M., Nigg, E. A., and Muller, S. (2009) RanBP2 and SENP3 function in a mitotic SUMO2/3 conjugation-deconjugation cycle on Borealin. *Mol. Biol. Cell* 20, 410-418
 36. Wotton, D., and Merrill, J. C. (2007) Pc2 and SUMOylation. *Biochem. Soc. Trans.* 35, 1401-1404
 37. Yang, S. H., and Sharrocks, A. D. (2010) The SUMO E3 ligase activity of Pc2 is coordinated through a SUMO interaction motif. *Mol. Cell Biol.* 30, 2193-2205
 38. Ismail, I. H., Gagne, J. P., Caron, M. C., McDonald, D., Xu, Z., Masson, J. Y., Poirier, G. G., and Hendzel, M. J. (2012) CBX4-mediated SUMO modification regulates BMI1 recruitment at sites of DNA damage. *Nucleic Acids Res.* 40, 5497-5510
 39. Pelisch, F., Pozzi, B., Risso, G., Munoz, M. J., and Srebrow, A. (2012) DNA damage-induced heterogeneous nuclear ribonucleoprotein K sumoylation regulates p53 transcriptional activation. *J. Biol. Chem.* 287, 30789-30799
 40. Stephan, A. K., Kliszczak, M., and Morrison, C. G. (2011) The Nse2/Mms21 SUMO ligase of the Smc5/6 complex in the maintenance of genome stability. *FEBS Lett.* 585, 2907-2913
 41. Branzei, D., Sollier, J., Liberi, G., Zhao, X., Maeda, D., Seki, M., Enomoto, T., Ohta, K., and Foiani, M. (2006) Ubc9- and mms21-mediated sumoylation counteracts recombinogenic events at damaged replication forks. *Cell* 127, 509-522
 42. Zhao, X., and Blobel, G. (2005) A SUMO ligase is part of a nuclear multiprotein complex that affects DNA repair and chromosomal organization. *Proc. Natl. Acad. Sci. U. S. A* 102, 4777-4782
 43. Denuc, A., and Marfany, G. (2010) SUMO and ubiquitin paths converge. *Biochem. Soc. Trans.* 38, 34-39
 44. Li, S. J., and Hochstrasser, M. (1999) A new protease required for cell-cycle progression in yeast. *Nature* 398, 246-251
 45. Drag, M., and Salvesen, G. S. (2008) DeSUMOylating enzymes--SENPs. *IUBMB. Life* 60, 734-742
 46. Suh, H. Y., Kim, J. H., Woo, J. S., Ku, B., Shin, E. J., Yun, Y., and Oh, B. H. (2012) Crystal structure of DeSI-1, a novel deSUMOylase belonging to a putative isopeptidase superfamily. *Proteins* 80, 2099-2104
 47. Shin, E. J., Shin, H. M., Nam, E., Kim, W. S., Kim, J. H., Oh, B. H., and Yun, Y. (2012) DeSUMOylating isopeptidase: a second class of SUMO protease. *EMBO Rep.* 13, 339-346
 48. Schulz, S., Chachami, G., Kozaczekiewicz, L., Winter, U., Stankovic-Valentin, N., Haas, P., Hofmann, K., Urlaub, H., Ovaa, H., Wittbrodt, J., Meulmeister, E., and Melchior, F. (2012) Ubiquitin-specific protease-like 1 (USPL1) is a SUMO isopeptidase with essential, non-catalytic functions. *EMBO Rep.* 13, 930-938
 49. Nacerddine, K., Lehembre, F., Bhaumik, M., Artus, J., Cohen-Tannoudji, M., Babinet, C., Pandolfi, P. P., and Dejean, A. (2005) The SUMO pathway is essential for nuclear integrity and chromosome segregation in mice. *Dev. Cell* 9, 769-779
 50. Jones, D., Crowe, E., Stevens, T. A., and Candido, E. P. (2002) Functional and phylogenetic analysis of the ubiquitylation system in *Caenorhabditis elegans*: ubiquitin-conjugating enzymes, ubiquitin-activating enzymes, and ubiquitin-like proteins. *Genome Biol.* 3, RESEARCH0002
 51. van der Weyden, L., White, J. K., Adams, D. J., and Logan, D. W. (2011) The mouse genetics toolkit: revealing function and mechanism. *Genome Biol.* 12, 224
 52. Alkuraya, F. S., Saadi, I., Lund, J. J., Turbe-Doan, A., Morton, C. C., and Maas, R. L. (2006) SUMO1 haploinsufficiency leads to cleft lip and palate. *Science* 313, 1751
 53. Evdokimov, E., Sharma, P., Lockett, S. J., Luaidi, M., and Kuehn, M. R. (2008) Loss of SUMO1 in mice affects RanGAP1 localization and formation of PML nuclear bodies, but is not lethal as it can be compensated by SUMO2 or SUMO3. *J. Cell Sci.* 121, 4106-4113
 54. Zhang, F. P., Mikkonen, L., Toppari, J., Palvimo, J. J., Thesleff, I., and Janne, O. A. (2008) Sumo-1 function is dispensable in normal mouse development. *Mol. Cell Biol.* 28, 5381-5390
 55. Cheng, J., Kang, X., Zhang, S., and Yeh, E. T. (2007) SUMO-specific protease 1 is essential for stabilization of HIF1alpha during hypoxia. *Cell* 131, 584-595
 56. Yamaguchi, T., Sharma, P., Athanasiou, M., Kumar, A., Yamada, S., and Kuehn, M. R. (2005) Mutation of SENP1/SuPr-2

- reveals an essential role for desumoylation in mouse development. *Mol. Cell Biol.* 25, 5171-5182
57. Chiu, S. Y., Asai, N., Costantini, F., and Hsu, W. (2008) SUMO-specific protease 2 is essential for modulating p53-Mdm2 in development of trophoblast stem cell niches and lineages. *PLoS Biol.* 6, e310
 58. Kerscher, O. (2007) SUMO junction-what's your function? New insights through SUMO-interacting motifs. *EMBO Rep.* 8, 550-555
 59. Gareau, J. R., and Lima, C. D. (2010) The SUMO pathway: emerging mechanisms that shape specificity, conjugation and recognition. *Nat. Rev. Mol. Cell Biol.* 11, 861-871
 60. Matunis, M. J., Zhang, X. D., and Ellis, N. A. (2006) SUMO: the glue that binds. *Dev. Cell* 11, 596-597
 61. Lin, D. Y., Huang, Y. S., Jeng, J. C., Kuo, H. Y., Chang, C. C., Chao, T. T., Ho, C. C., Chen, Y. C., Lin, T. P., Fang, H. I., Hung, C. C., Suen, C. S., Hwang, M. J., Chang, K. S., Maul, G. G., and Shih, H. M. (2006) Role of SUMO-interacting motif in Daxx SUMO modification, subnuclear localization, and repression of sumoylated transcription factors. *Mol. Cell* 24, 341-354
 62. Knipscheer, P., Flotho, A., Klug, H., Olsen, J. V., van Dijk, W. J., Fish, A., Johnson, E. S., Mann, M., Sixma, T. K., and Pichler, A. (2008) Ubc9 sumoylation regulates SUMO target discrimination. *Mol. Cell* 31, 371-382
 63. Kim, E. T., Kim, K. K., Matunis, M. J., and Ahn, J. H. (2009) Enhanced SUMOylation of proteins containing a SUMO-interacting motif by SUMO-Ubc9 fusion. *Biochem. Biophys. Res. Commun.* 388, 41-45
 64. Tatham, M. H., Jaffray, E., Vaughan, O. A., Desterro, J. M., Botting, C. H., Naismith, J. H., and Hay, R. T. (2001) Polymeric chains of SUMO-2 and SUMO-3 are conjugated to protein substrates by SAE1/SAE2 and Ubc9. *J. Biol. Chem.* 276, 35368-35374
 65. Bencsath, K. P., Podgorski, M. S., Pagala, V. R., Slaughter, C. A., and Schulman, B. A. (2002) Identification of a multifunctional binding site on Ubc9p required for Smt3p conjugation. *J. Biol. Chem.* 277, 47938-47945
 66. Matic, I., van, H. M., Schimmel, J., Macek, B., Ogg, S. C., Tatham, M. H., Hay, R. T., Lamond, A. I., Mann, M., and Vertegaal, A. C. (2008) In vivo identification of human small ubiquitin-like modifier polymerization sites by high accuracy mass spectrometry and an in vitro to in vivo strategy. *Mol. Cell Proteomics* 7, 132-144
 67. Knipscheer, P., van Dijk, W. J., Olsen, J. V., Mann, M., and Sixma, T. K. (2007) Noncovalent interaction between Ubc9 and SUMO promotes SUMO chain formation. *EMBO J.* 26, 2797-2807
 68. Bylebyl, G. R., Belichenko, I., and Johnson, E. S. (2003) The SUMO isopeptidase Ulp2 prevents accumulation of SUMO chains in yeast. *J. Biol. Chem.* 278, 44113-44120
 69. Lima, C. D., and Reverter, D. (2008) Structure of the human SENP7 catalytic domain and poly-SUMO deconjugation activities for SENP6 and SENP7. *J. Biol. Chem.* 283, 32045-32055
 70. Hietakangas, V., Anckar, J., Blomster, H. A., Fujimoto, M., Palvimo, J. J., Nakai, A., and Sistonen, L. (2006) PDSM, a motif for phosphorylation-dependent SUMO modification. *Proc. Natl. Acad. Sci. U. S. A.* 103, 45-50
 71. Yang, S. H., Galanis, A., Witty, J., and Sharrocks, A. D. (2006) An extended consensus motif enhances the specificity of substrate modification by SUMO. *EMBO J.* 25, 5083-5093
 72. Olsen, J. V., Vermeulen, M., Santamaria, A., Kumar, C., Miller, M. L., Jensen, L. J., Gnad, F., Cox, J., Jensen, T. S., Nigg, E. A., Brunak, S., and Mann, M. (2010) Quantitative phosphoproteomics reveals widespread full phosphorylation site occupancy during mitosis. *Sci. Signal.* 3, ra3
 73. Matic, I., Macek, B., Hilger, M., Walther, T. C., and Mann, M. (2008) Phosphorylation of SUMO-1 occurs in vivo and is conserved through evolution. *J. Proteome. Res.* 7, 4050-4057
 74. Gill, G. (2005) Something about SUMO inhibits transcription. *Curr. Opin. Genet. Dev.* 15, 536-541
 75. Yang, S. H., and Sharrocks, A. D. (2004) SUMO promotes HDAC-mediated transcriptional repression. *Mol. Cell* 13, 611-617
 76. Wu, S. Y., and Chiang, C. M. (2009) Crosstalk between sumoylation and acetylation regulates p53-dependent chromatin transcription and DNA binding. *EMBO J.* 28, 1246-1259
 77. Ullmann, R., Chien, C. D., Avantaggiati, M. L., and Muller, S. (2012) An acetylation switch regulates SUMO-dependent protein interaction networks. *Mol. Cell* 46, 759-770
 78. Desterro, J. M., Rodriguez, M. S., and Hay, R. T. (1998) SUMO-1 modification of I κ B α inhibits NF- κ B

- activation. *Mol. Cell* 2, 233-239
79. Huang, T. T., Wuerzberger-Davis, S. M., Wu, Z. H., and Miyamoto, S. (2003) Sequential modification of NEMO/IKKgamma by SUMO-1 and ubiquitin mediates NF-kappaB activation by genotoxic stress. *Cell* 115, 565-576
 80. Mabb, A. M., and Miyamoto, S. (2007) SUMO and NF-kappaB ties. *Cell Mol. Life Sci.* 64, 1979-1996
 81. Prudden, J., Pebernard, S., Raffa, G., Slavin, D. A., Perry, J. J., Tainer, J. A., McGowan, C. H., and Boddy, M. N. (2007) SUMO-targeted ubiquitin ligases in genome stability. *EMBO J.* 26, 4089-4101
 82. Sun, H., Levenson, J. D., and Hunter, T. (2007) Conserved function of RNF4 family proteins in eukaryotes: targeting a ubiquitin ligase to SUMOylated proteins. *EMBO J.* 26, 4102-4112
 83. Perry, J. J., Tainer, J. A., and Boddy, M. N. (2008) A SIM-ultaneous role for SUMO and ubiquitin. *Trends Biochem. Sci.* 33, 201-208
 84. Lallemand-Breitenbach, V., Jeanne, M., Benhenda, S., Nasr, R., Lei, M., Peres, L., Zhou, J., Zhu, J., Raught, B., and De, T. H. (2008) Arsenic degrades PML or PML-RARalpha through a SUMO-triggered RNF4/ubiquitin-mediated pathway. *Nat. Cell Biol.* 10, 547-555
 85. Tatham, M. H., Geoffroy, M. C., Shen, L., Plechanovova, A., Hattersley, N., Jaffray, E. G., Palvimo, J. J., and Hay, R. T. (2008) RNF4 is a poly-SUMO-specific E3 ubiquitin ligase required for arsenic-induced PML degradation. *Nat. Cell Biol.* 10, 538-546
 86. Schimmel, J., Larsen, K. M., Matic, I., van, H. M., Cox, J., Mann, M., Andersen, J. S., and Vertegaal, A. C. (2008) The ubiquitin-proteasome system is a key component of the SUMO-2/3 cycle. *Mol. Cell Proteomics* 7, 2107-2122
 87. Lescasse, R., Pobięga, S., Callebaut, I., and Marcand, S. (2013) End-joining inhibition at telomeres requires the translocase and polySUMO-dependent ubiquitin ligase Uls1. *EMBO J.* 32, 805-815
 88. Poulsen, S. L., Hansen, R. K., Wagner, S. A., van, C. L., van Belle, G. J., Streicher, W., Wikstrom, M., Choudhary, C., Houtsmuller, A. B., Marteijn, J. A., Bekker-Jensen, S., and Mailand, N. (2013) RNF111/Arkadia is a SUMO-targeted ubiquitin ligase that facilitates the DNA damage response. *J. Cell Biol.* 201, 797-807
 89. Erker, Y., Neyret-Kahn, H., Seeler, J. S., Dejean, A., Atfi, A., and Levy, L. (2013) Arkadia, a novel SUMO-targeted ubiquitin ligase involved in PML degradation. *Mol. Cell Biol.* 33, 2163-2177
 90. Seufert, W., Futcher, B., and Jentsch, S. (1995) Role of a ubiquitin-conjugating enzyme in degradation of S- and M-phase cyclins. *Nature* 373, 78-81
 91. Dohmen, R. J., Stappen, R., McGrath, J. P., Forrova, H., Kolarov, J., Goffeau, A., and Varshavsky, A. (1995) An essential yeast gene encoding a homolog of ubiquitin-activating enzyme. *J. Biol. Chem.* 270, 18099-18109
 92. Dieckhoff, P., Bolte, M., Sancak, Y., Braus, G. H., and Irmiger, S. (2004) Smt3/SUMO and Ubc9 are required for efficient APC/C-mediated proteolysis in budding yeast. *Mol. Microbiol.* 51, 1375-1387
 93. Klug, H., Xaver, M., Chaugule, V. K., Koidl, S., Mittler, G., Klein, F., and Pichler, A. (2013) Ubc9 sumoylation controls SUMO chain formation and meiotic synapsis in *Saccharomyces cerevisiae*. *Mol. Cell* 50, 625-636
 94. Schwartz, D. C., Felberbaum, R., and Hochstrasser, M. (2007) The Ulp2 SUMO protease is required for cell division following termination of the DNA damage checkpoint. *Mol. Cell Biol.* 27, 6948-6961
 95. Neyret-Kahn, H., Benhamed, M., Ye, T., Le, G. S., Cossec, J. C., Lapaquette, P., Bischof, O., Ouspenskaia, M., Dasso, M., Seeler, J., Davidson, I., and Dejean, A. (2013) Sumoylation at chromatin governs coordinated repression of a transcriptional program essential for cell growth and proliferation. *Genome Res.*
 96. Di, B. A., Ouyang, J., Lee, H. Y., Catic, A., Ploegh, H., and Gill, G. (2006) The SUMO-specific protease SENP5 is required for cell division. *Mol. Cell Biol.* 26, 4489-4498
 97. Wan, J., Subramonian, D., and Zhang, X. D. (2012) SUMOylation in control of accurate chromosome segregation during mitosis. *Curr. Protein Pept. Sci.* 13, 467-481
 98. Dasso, M. (2008) Emerging roles of the SUMO pathway in mitosis. *Cell Div.* 3, 5
 99. Bachant, J., Alcasabas, A., Blat, Y., Kleckner, N., and Elledge, S. J. (2002) The SUMO-1 isopeptidase Smt4 is linked to centromeric cohesion through SUMO-1 modification of DNA topoisomerase II. *Mol. Cell* 9, 1169-1182
 100. Ban, R., Nishida, T., and Urano, T. (2011) Mitotic kinase Aurora-B is regulated by SUMO-2/3 conjugation/deconjugation

- during mitosis. *Genes Cells* 16, 652-669
101. Fernandez-Miranda, G., Perez, d. C., I, Carmena, M., Aguirre-Portoles, C., Ruchaud, S., Fant, X., Montoya, G., Earnshaw, W. C., and Malumbres, M. (2010) SUMOylation modulates the function of Aurora-B kinase. *J. Cell Sci.* 123, 2823-2833
 102. Cubenas-Potts, C., and Matunis, M. J. (2013) SUMO: a multifaceted modifier of chromatin structure and function. *Dev. Cell* 24, 1-12
 103. Mukhopadhyay, D., and Dasso, M. (2010) The fate of metaphase kinetochores is weighed in the balance of SUMOylation during S phase. *Cell Cycle* 9, 3194-3201
 104. Mukhopadhyay, D., Arnaoutov, A., and Dasso, M. (2010) The SUMO protease SENP6 is essential for inner kinetochore assembly. *J. Cell Biol.* 188, 681-692
 105. Zhang, X. D., Goeres, J., Zhang, H., Yen, T. J., Porter, A. C., and Matunis, M. J. (2008) SUMO-2/3 modification and binding regulate the association of CENP-E with kinetochores and progression through mitosis. *Mol. Cell* 29, 729-741
 106. Lyst, M. J., and Stancheva, I. (2007) A role for SUMO modification in transcriptional repression and activation. *Biochem. Soc. Trans.* 35, 1389-1392
 107. Ouyang, J., Valin, A., and Gill, G. (2009) Regulation of transcription factor activity by SUMO modification. *Methods Mol. Biol.* 497, 141-152
 108. Shiio, Y., and Eisenman, R. N. (2003) Histone sumoylation is associated with transcriptional repression. *Proc. Natl. Acad. Sci. U. S. A* 100, 13225-13230
 109. Lee, B., and Muller, M. T. (2009) SUMOylation enhances DNA methyltransferase 1 activity. *Biochem. J.* 421, 449-461
 110. Gomez-del, A. P., Koipally, J., and Georgopoulos, K. (2005) Ikaros SUMOylation: switching out of repression. *Mol. Cell Biol.* 25, 2688-2697
 111. Jackson, S. P., and Durocher, D. (2013) Regulation of DNA damage responses by ubiquitin and SUMO. *Mol. Cell* 49, 795-807
 112. Bergink, S., and Jentsch, S. (2009) Principles of ubiquitin and SUMO modifications in DNA repair. *Nature* 458, 461-467
 113. Baba, D., Maita, N., Jee, J. G., Uchimura, Y., Saitoh, H., Sugasawa, K., Hanaoka, F., Tochio, H., Hiroaki, H., and Shirakawa, M. (2005) Crystal structure of thymine DNA glycosylase conjugated to SUMO-1. *Nature* 435, 979-982
 114. Steinacher, R., and Schar, P. (2005) Functionality of human thymine DNA glycosylase requires SUMO-regulated changes in protein conformation. *Curr. Biol.* 15, 616-623
 115. Hoege, C., Pfander, B., Moldovan, G. L., Pyrowolakis, G., and Jentsch, S. (2002) RAD6-dependent DNA repair is linked to modification of PCNA by ubiquitin and SUMO. *Nature* 419, 135-141
 116. Stelter, P., and Ulrich, H. D. (2003) Control of spontaneous and damage-induced mutagenesis by SUMO and ubiquitin conjugation. *Nature* 425, 188-191
 117. Papouli, E., Chen, S., Davies, A. A., Huttner, D., Krejci, L., Sung, P., and Ulrich, H. D. (2005) Crosstalk between SUMO and ubiquitin on PCNA is mediated by recruitment of the helicase Srs2p. *Mol. Cell* 19, 123-133
 118. Pfander, B., Moldovan, G. L., Sacher, M., Hoege, C., and Jentsch, S. (2005) SUMO-modified PCNA recruits Srs2 to prevent recombination during S phase. *Nature* 436, 428-433
 119. Moldovan, G. L., Dejsuphong, D., Petalcorin, M. I., Hofmann, K., Takeda, S., Boulton, S. J., and D'Andrea, A. D. (2012) Inhibition of homologous recombination by the PCNA-interacting protein PARI. *Mol. Cell* 45, 75-86
 120. Galanty, Y., Belotserkovskaya, R., Coates, J., Polo, S., Miller, K. M., and Jackson, S. P. (2009) Mammalian SUMO E3-ligases PIAS1 and PIAS4 promote responses to DNA double-strand breaks. *Nature* 462, 935-939
 121. Morris, J. R., Boutell, C., Keppler, M., Densham, R., Weekes, D., Alamshah, A., Butler, L., Galanty, Y., Pangon, L., Kiuchi, T., Ng, T., and Solomon, E. (2009) The SUMO modification pathway is involved in the BRCA1 response to genotoxic stress. *Nature* 462, 886-890
 122. Danielsen, J. R., Povlsen, L. K., Villumsen, B. H., Streicher, W., Nilsson, J., Wikstrom, M., Bekker-Jensen, S., and Mailand, N. (2012) DNA damage-inducible SUMOylation of HERC2 promotes RNF8 binding via a novel SUMO-binding Zinc finger. *J. Cell Biol.* 197, 179-187
 123. Galanty, Y., Belotserkovskaya, R., Coates, J., and Jackson, S. P. (2012) RNF4, a SUMO-targeted ubiquitin E3 ligase, promotes DNA double-strand break repair. *Genes Dev.* 26, 1179-1195
 124. Luo, K., Zhang, H., Wang, L., Yuan, J., and Lou, Z. (2012) Sumoylation of MDC1

- is important for proper DNA damage response. *EMBO J.* 31, 3008-3019
125. Yin, Y., Seifert, A., Chua, J. S., Maure, J. F., Golebiowski, F., and Hay, R. T. (2012) SUMO-targeted ubiquitin E3 ligase RNF4 is required for the response of human cells to DNA damage. *Genes Dev.* 26, 1196-1208
 126. Vyas, R., Kumar, R., Clermont, F., Helfricht, A., Kalev, P., Sotiropoulou, P., Hendriks, I. A., Radaelli, E., Hochepped, T., Blanpain, C., Sablina, A., van, A. H., Olsen, J. V., Jochemsen, A. G., Vertegaal, A. C., and Marine, J. C. (2013) RNF4 is required for DNA double-strand break repair in vivo. *Cell Death Differ.* 20, 490-502
 127. Psakhye, I., and Jentsch, S. (2012) Protein group modification and synergy in the SUMO pathway as exemplified in DNA repair. *Cell* 151, 807-820
 128. Silver, H. R., Nissley, J. A., Reed, S. H., Hou, Y. M., and Johnson, E. S. (2011) A role for SUMO in nucleotide excision repair. *DNA Repair (Amst)* 10, 1243-1251
 129. Jensen, O. N. (2004) Modification-specific proteomics: characterization of post-translational modifications by mass spectrometry. *Curr. Opin. Chem. Biol.* 8, 33-41
 130. Choudhary, C., and Mann, M. (2010) Decoding signalling networks by mass spectrometry-based proteomics. *Nat. Rev. Mol. Cell Biol.* 11, 427-439
 131. Mann, M. (2006) Functional and quantitative proteomics using SILAC. *Nat. Rev. Mol. Cell Biol.* 7, 952-958
 132. Vertegaal, A. C. (2011) Uncovering ubiquitin and ubiquitin-like signaling networks. *Chem. Rev.* 111, 7923-7940
 133. Vertegaal, A. C., Andersen, J. S., Ogg, S. C., Hay, R. T., Mann, M., and Lamond, A. I. (2006) Distinct and overlapping sets of SUMO-1 and SUMO-2 target proteins revealed by quantitative proteomics. *Mol. Cell Proteomics* 5, 2298-2310
 134. Becker, J., Barysch, S. V., Karaca, S., Dittner, C., Hsiao, H. H., Berriel, D. M., Herzig, S., Urlaub, H., and Melchior, F. (2013) Detecting endogenous SUMO targets in mammalian cells and tissues. *Nat. Struct. Mol. Biol.* 20, 525-531
 135. Denison, C., Rudner, A. D., Gerber, S. A., Bakalarski, C. E., Moazed, D., and Gygi, S. P. (2005) A proteomic strategy for gaining insights into protein sumoylation in yeast. *Mol. Cell Proteomics* 4, 246-254
 136. Ganesan, A. K., Kho, Y., Kim, S. C., Chen, Y., Zhao, Y., and White, M. A. (2007) Broad spectrum identification of SUMO substrates in melanoma cells. *Proteomics* 7, 2216-2221
 137. Panse, V. G., Hardeland, U., Werner, T., Kuster, B., and Hurt, E. (2004) A proteome-wide approach identifies sumoylated substrate proteins in yeast. *J. Biol. Chem.* 279, 41346-41351
 138. Hannich, J. T., Lewis, A., Kroetz, M. B., Li, S. J., Heide, H., Emili, A., and Hochstrasser, M. (2005) Defining the SUMO-modified proteome by multiple approaches in *Saccharomyces cerevisiae*. *J. Biol. Chem.* 280, 4102-4110
 139. Westman, B. J., and Lamond, A. I. (2011) A role for SUMOylation in snoRNP biogenesis revealed by quantitative proteomics. *Nucleus* 2, 30-37
 140. Tirard, M., Hsiao, H. H., Nikolov, M., Urlaub, H., Melchior, F., and Brose, N. (2012) In vivo localization and identification of SUMOylated proteins in the brain of His6-HA-SUMO1 knock-in mice. *Proc. Natl. Acad. Sci. U. S. A* 109, 21122-21127
 141. Golebiowski, F., Matic, I., Tatham, M. H., Cole, C., Yin, Y., Nakamura, A., Cox, J., Barton, G. J., Mann, M., and Hay, R. T. (2009) System-wide changes to SUMO modifications in response to heat shock. *Sci. Signal.* 2, ra24
 142. Miller, M. J., and Vierstra, R. D. (2011) Mass spectrometric identification of SUMO substrates provides insights into heat stress-induced SUMOylation in plants. *Plant Signal. Behav.* 6, 130-133
 143. Yang, W., Thompson, J. W., Wang, Z., Wang, L., Sheng, H., Foster, M. W., Moseley, M. A., and Paschen, W. (2012) Analysis of oxygen/glucose-deprivation-induced changes in SUMO3 conjugation using SILAC-based quantitative proteomics. *J. Proteome. Res.* 11, 1108-1117
 144. Bruderer, R., Tatham, M. H., Plechanovova, A., Matic, I., Garg, A. K., and Hay, R. T. (2011) Purification and identification of endogenous polySUMO conjugates. *EMBO Rep.* 12, 142-148
 145. Jeram, S. M., Srikanth, T., Pedrioli, P. G., and Raught, B. (2009) Using mass spectrometry to identify ubiquitin and ubiquitin-like protein conjugation sites. *Proteomics* 9, 922-934
 146. Pedrioli, P. G., Raught, B., Zhang, X. D., Rogers, R., Aitchison, J., Matunis, M., and Aebersold, R. (2006) Automated identification of SUMOylation sites using mass spectrometry and SUMOn pattern recognition software. *Nat. Methods* 3,

- 533-539
147. Knuesel, M., Cheung, H. T., Hamady, M., Barthel, K. K., and Liu, X. (2005) A method of mapping protein sumoylation sites by mass spectrometry using a modified small ubiquitin-like modifier 1 (SUMO-1) and a computational program. *Mol. Cell Proteomics* 4, 1626-1636
 148. Wohlschlegel, J. A., Johnson, E. S., Reed, S. I., and Yates, J. R., III. (2006) Improved identification of SUMO attachment sites using C-terminal SUMO mutants and tailored protease digestion strategies. *J. Proteome. Res.* 5, 761-770
 149. Blomster, H. A., Imanishi, S. Y., Siimes, J., Kastu, J., Morrice, N. A., Eriksson, J. E., and Sistonen, L. (2010) In vivo identification of sumoylation sites by a signature tag and cysteine-targeted affinity purification. *J. Biol. Chem.* 285, 19324-19329
 150. Miller, M. J., Barrett-Wilt, G. A., Hua, Z., and Vierstra, R. D. (2010) Proteomic analyses identify a diverse array of nuclear processes affected by small ubiquitin-like modifier conjugation in Arabidopsis. *Proc. Natl. Acad. Sci. U. S. A* 107, 16512-16517
 151. Galisson, F., Mahrouche, L., Courcelles, M., Bonneil, E., Meloche, S., Chelbi-Alix, M. K., and Thibault, P. (2011) A novel proteomics approach to identify SUMOylated proteins and their modification sites in human cells. *Mol. Cell Proteomics* 10, M110
 152. Hsiao, H. H., Meulmeester, E., Frank, B. T., Melchior, F., and Urlaub, H. (2009) "ChopNSpice," a mass spectrometric approach that allows identification of endogenous small ubiquitin-like modifier-conjugated peptides. *Mol. Cell Proteomics* 8, 2664-2675

2

The ubiquitin-proteasome system is a key component of the SUMO-2/3 cycle

Joost Schimmel*, Katja M. Larsen*, Ivan Matic*,
Martijn van Hagen, Jürgen Cox, Matthias Mann,
Jens S. Andersen and Alfred C.O. Vertegaal

Molecular & Cellular Proteomics (2008), 7, 2107-2122

*These authors contributed equally to this work.

Additional figures are available at: <http://www.mcponline.org/content/7/11/2107/suppl/DC1>

Chapter 2. The ubiquitin-proteasome system is a key component of the SUMO-2/3 cycle

2

Abstract

Many proteins are regulated by a variety of post-translational modifications and orchestration of these modifications is frequently required for full control of activity. Currently, little is known about the combinatorial activity of different post-translational modifications. Here we show that extensive crosstalk exists between sumoylation and ubiquitination. We found that a subset of SUMO-2 conjugated proteins is subsequently ubiquitinated and degraded by the proteasome. In a screen for preferential SUMO-1 or SUMO-2 target proteins, we found that ubiquitin accumulated in purified SUMO-2 conjugates, but not in SUMO-1 conjugates. Upon inhibition of the proteasome, the amount of ubiquitin in purified SUMO-2 conjugates increased. In addition, we found that endogenous SUMO-2/3 conjugates, but not endogenous SUMO-1 conjugates, accumulated in response to proteasome inhibitors. Quantitative proteomics experiments enabled the identification of 73 SUMO-2 conjugated proteins that accumulated in cells treated with proteasome inhibitors. Crosstalk between SUMO-2/3 and the ubiquitin-proteasome system controls many target proteins that regulate all aspects of nucleic acid metabolism. Surprisingly, the relative abundance of 40 SUMO-2 conjugated proteins was reduced by proteasome inhibitors, possibly due to a lack of recycled SUMO-2. We conclude that SUMO-2/3 conjugation and the ubiquitin-proteasome system are tightly integrated and act in a cooperative manner.

Introduction

The ubiquitin-proteasome system plays a key role in virtually all cellular processes by tightly regulating the degradation of a large set of proteins (1). Proteins are targeted for degradation by lysine-48 linked polyubiquitin chains that are covalently conjugated to lysines in target proteins. Ubiquitination furthermore regulates target proteins in a degradation-independent manner, e.g. mono-ubiquitination is important for endocytosis (2). A significant part of the human genome encodes components of the ubiquitin-proteasome system, including E1, E2 and hundreds of E3 enzymes that mediate the conjugation of target proteins to ubiquitin, and ubiquitin proteases that remove ubiquitins from target proteins.

The ubiquitin family comprises ubiquitin-like proteins NEDD8, ISG15, SUMO-1, -2, -3, FAT10, FUB1, UBL5, URM1, ATG8 and ATG12 (3, 4). These proteins share the 3D structure of ubiquitin and are also conjugated to target proteins. Like ubiquitination, sumoylation is essential for eukaryotic life (5). The largest functional group of SUMO targets are transcription factors (6) and in general, sumoylation inhibits their transcriptional activity (7). Sumoylation also regulates other cellular

processes including DNA-repair, RNA metabolism, protein transport, translation and replication (8-10). Whereas mature SUMO-2 and SUMO-3 are nearly identical (~95% identity), they differ significantly from SUMO-1 (~50% identity). Previously, we have shown that SUMO-1 and SUMO-2 are conjugated to preferential sets of target proteins (6). Furthermore, SUMO-2 and SUMO-3 contain an internal sumoylation site that is used for SUMO chain formation *in vivo* (11-13).

Sumoylation is not linked to the degradation of target proteins, although some exceptions have been reported. The SUMO-accepting lysine 160 in PML and in the oncogenic PML-RAR α protein is required for the degradation of this fusion protein upon arsenic-trioxide treatment (14). Furthermore, it has been published that sumoylation might be important for the degradation of DNA Topoisomerase II α in response to a catalytic inhibitor (15).

Different kinds of crosstalk between ubiquitination and sumoylation have currently been reported (16). SUMO and ubiquitin were shown to counteract each other by competing for the same acceptor lysine in I κ B α (17). NF- κ B signaling is furthermore affected by the ubiquitination and sumoylation of NEMO/IKK γ , a structural component of the IKK complex (18). In this case, SUMO-1 and ubiquitin do not directly compete for the same acceptor lysine, but are conjugated in a sequential manner in response to genotoxic stress. PCNA is also modified by SUMO and ubiquitin on the same acceptor lysine (K164) (16, 19). Sumoylation enables the interaction between PCNA and the helicase Srs2, whereas monoubiquitination enables translesion synthesis by Pol η , a DNA damage-tolerant polymerase and polyubiquitination is needed for DNA repair.

In a screen for preferential SUMO-1 and preferential SUMO-2 conjugates, we found that ubiquitin specifically co-enriched with SUMO-2. The amount of ubiquitin in SUMO-2 purified fractions significantly increased upon inhibition of the proteasome. Quantitative proteomics enabled us to study the crosstalk between sumoylation and the ubiquitin-proteasome system at the target protein level. We show here that the conjugation of a large set of target proteins to SUMO-2 is tightly connected to the ubiquitin-proteasome system and conclude that the ubiquitin-proteasome system is a key component of the SUMO-2/3 cycle in cells.

Results

Ubiquitin co-purifies preferentially with SUMO-2 conjugates

The quantitative proteomics experiment that we previously described to show that SUMO-1 and SUMO-2 are conjugated to preferential sets of target proteins (6) was repeated using lysine encoding instead of arginine encoding (Fig. 1A). Control HeLa cells were labeled with Lys0, HeLa cells stably expressing His6-SUMO-1 were labeled with Lys4 and HeLa cells stably expressing His6-SUMO-2 were labeled with Lys8. Cells were harvested and nuclear lysates from the three different populations

Chapter 2

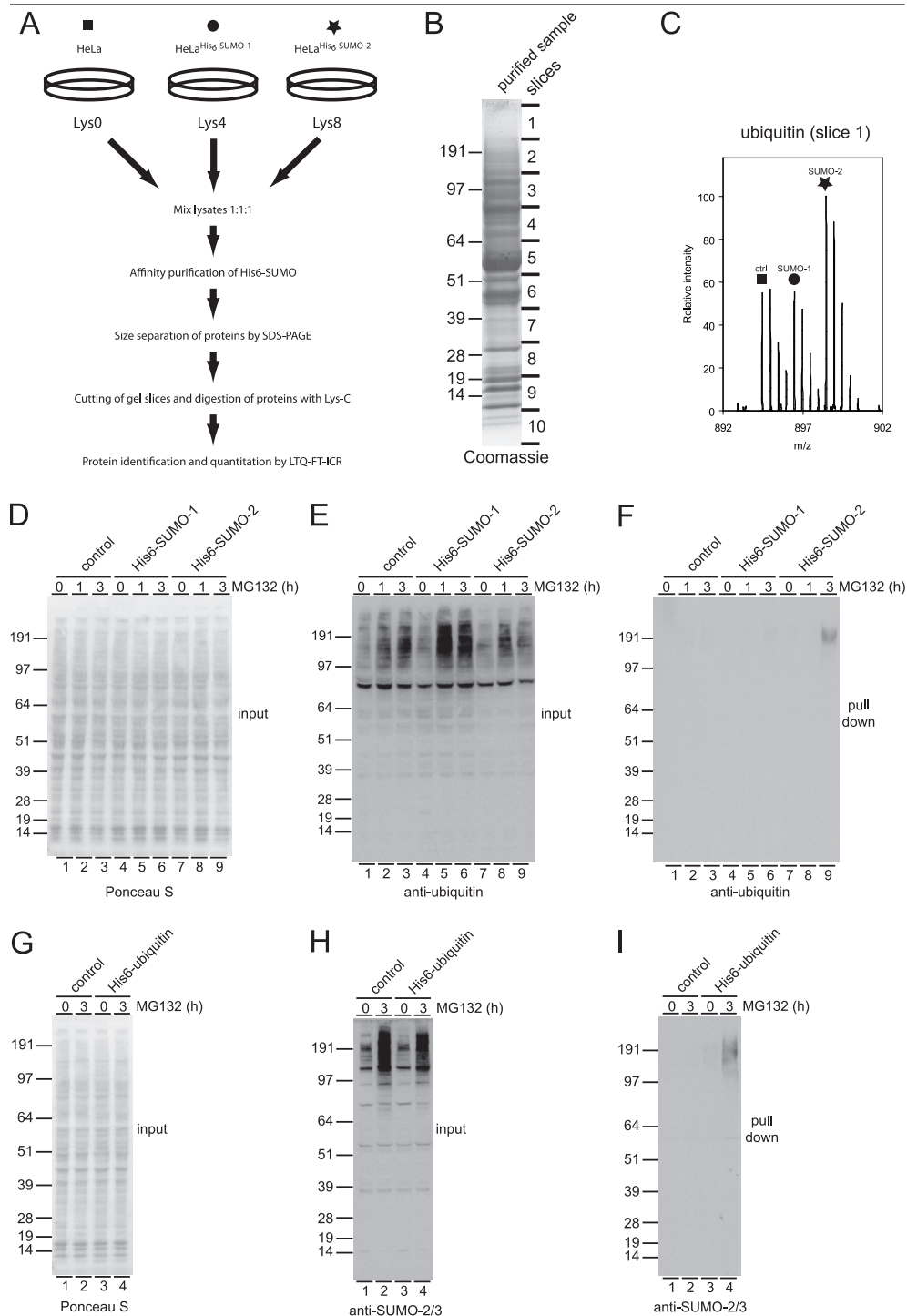


Fig. 1. SUMO-2 conjugates are enriched for ubiquitin. A, a quantitative proteomics strategy to identify SUMO-1 and SUMO-2 conjugates. B, HeLa cells were labeled with Lys0, HeLa^{His6-SUMO-1} cells were labeled

with Lys4 and HeLa^{His6-SUMO-2} cells were labeled with Lys8. Equal amounts of nuclear lysates from the three different populations were mixed and proteins conjugated to His6-SUMO were purified. The SUMO enriched fraction was separated by SDS-PAGE, proteins were visualized by Coomassie staining, the gel lane was cut in slices and the proteins present in these slices were digested by Lys-C and identified by mass spectrometry. Peptide mass spectra were quantified to identify proteins potentially conjugated to SUMO-1 and/or SUMO-2. C, the His6-SUMO-2 purified fraction is specifically enriched for ubiquitin. Two different ubiquitin peptides (aa MQIFVK and TITLEVEPSDTIENVK) were found to be enriched in His6-SUMO-2 conjugates but not in His6-SUMO-1 conjugates in the top part of the gel lane. The peptide mass spectra of the ubiquitin peptide TITLEVEPSDTIENVK is shown. D-F, the proteasome inhibitor MG132 increases the amount of ubiquitin in His6-SUMO-2 conjugates. HeLa cells, HeLa^{His6-SUMO-1} cells and HeLa^{His6-SUMO-2} cells were treated for 1 or 3 hours with MG132 or were treated with DMSO for 3 hours. Whole cell lysates were prepared, size-separated by SDS-PAGE and transferred to a membrane. Total protein was visualized by Ponceau S staining (D) and the membrane was probed using antibody SC-8017 to detect ubiquitin (E). His6-SUMO conjugates from whole cell lysates were purified, size-separated by SDS-PAGE, transferred to a membrane and probed to detect ubiquitin (F). G-I, the proteasome inhibitor MG132 increases the amount of SUMO-2/3 in His6-ubiquitin conjugates. HeLa cells were transfected with a plasmid that encodes His6-ubiquitin, or with an empty control plasmid and cells were subsequently treated with MG132 or DMSO for 3 hours. Whole cell lysates were prepared, size-separated by SDS-PAGE and transferred to a membrane. Total protein was visualized by Ponceau S staining (G) and the membrane was probed using antibody AV-SM23-0100 to detect SUMO-2/3 (H). His6-ubiquitin conjugates were purified from whole cell lysates, size-separated by SDS-PAGE, transferred to a membrane and probed to detect SUMO-2/3 (I).

were mixed in a 1:1:1 ratio. His6-SUMO conjugates were subsequently purified and separated on a one-dimensional gel (Fig. 1B). The gel lane was cut in slices and proteins were in-gel digested by Lys-C and analyzed by mass spectrometry. Interestingly, we identified two different ubiquitin peptides from the top slices of the gel lane that were preferentially enriched in the Lys8 encoded form, indicating that endogenous ubiquitin co-purified with large His6-SUMO-2 conjugates but not with large His6-SUMO-1 conjugates (Fig. 1C and Supplementary Fig. S1). The amount of ubiquitin that co-purified with His6-SUMO-2 conjugates significantly increased upon inhibition of the proteasome (Fig. 1D-F). The reverse experiment showed that endogenous SUMO-2/3 co-purified with His6-ubiquitin conjugates (Fig. 1G-I).

Endogenous SUMO-2/3 conjugates accumulate in cells treated with proteasome inhibitors

To study the effect of proteasome inhibition on endogenous SUMO-1 and endogenous SUMO-2/3, HeLa cells were treated with MG132 or epoxomicin for up to eight hours (Fig. 2). These inhibitors caused rapid accumulation of ubiquitin in cells (Fig. 2A and E) and in addition caused the accumulation of SUMO-2/3 conjugates, albeit with slower kinetics (Fig. 2C and G). Simultaneously, the amount of non-conjugated SUMO-2/3 was significantly reduced by these inhibitors (Fig. 2M). The total amount of SUMO-1 conjugates in cells was not affected by MG132 or epoxomicin treatments, although the pattern of SUMO-1 conjugates slightly changed (Fig. 2B and F). Control DMSO treatments did not affect ubiquitination or sumoylation (Fig. 2I-K).

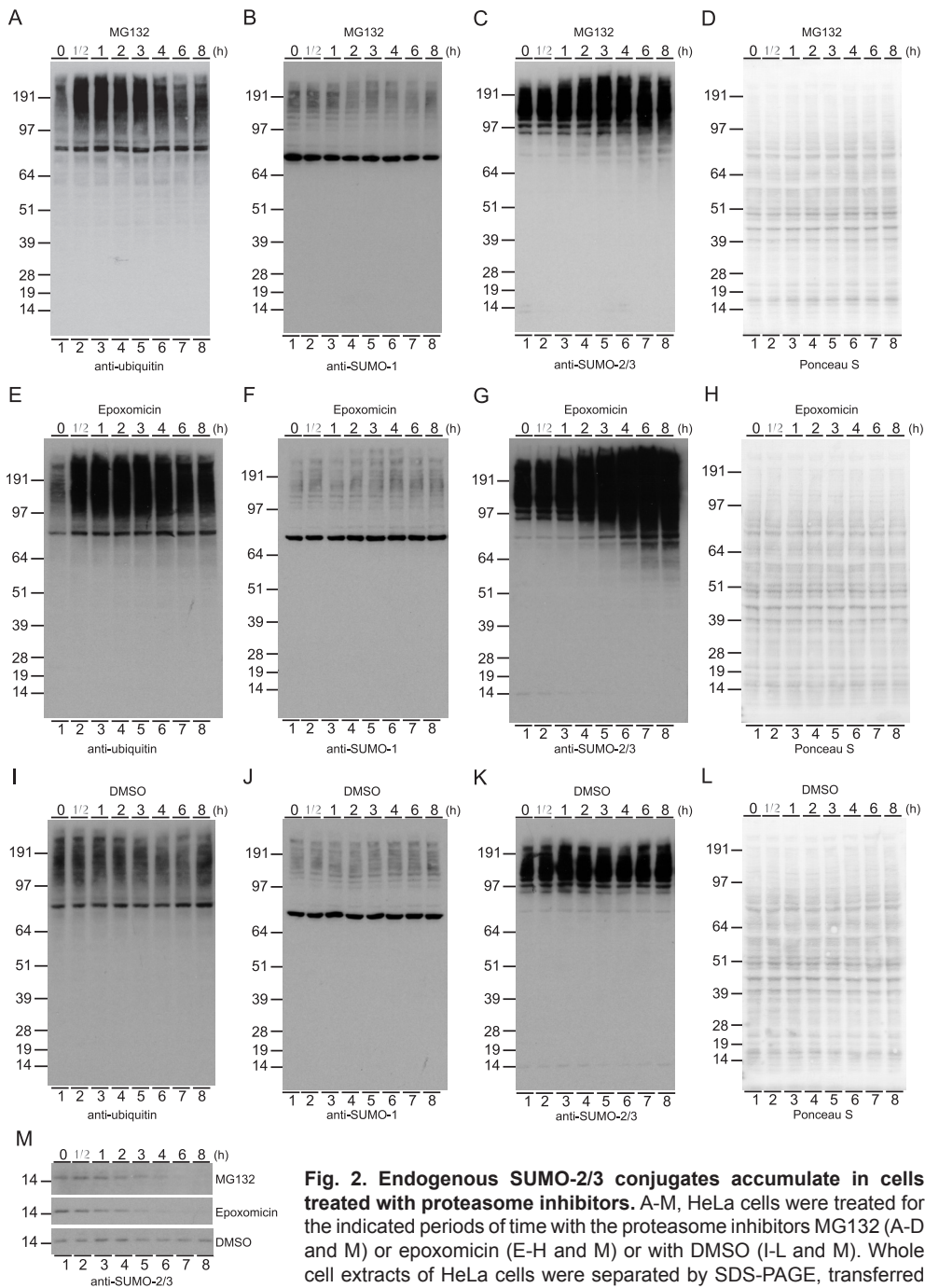


Fig. 2. Endogenous SUMO-2/3 conjugates accumulate in cells treated with proteasome inhibitors. A-M, HeLa cells were treated for the indicated periods of time with the proteasome inhibitors MG132 (A-D and M) or epoxomicin (E-H and M) or with DMSO (I-L and M). Whole cell extracts of HeLa cells were separated by SDS-PAGE, transferred to membranes, stained with Ponceau S to visualize total protein (D, H and L) and probed using antibody SC-8017 to detect ubiquitin (A, E and I), antibody 21C7 to detect SUMO-1 (B, F and J) or antibody AV-SM23-0100 to detect SUMO-2/3 (C, G, K and M).

Identification of SUMO-2 target proteins that are affected by the proteasome inhibitor MG132

To identify individual SUMO-2 target proteins that are sensitive to proteasome inhibition, quantitative proteomics was employed (Fig. 3A). Two pools of HeLa^{His6-SUMO-2} cells were used for this experiment, the first pool of cells was labeled with Arg0 and Lys0 and treated with DMSO and the second pool of cells was labeled with Arg10 and Lys8 and treated with MG132. It is important to note that this strategy was optimal for identifying SUMO-2 conjugates that were sensitive to proteasome inhibition, but it is likely that contaminating non-sumoylated proteins were co-purified. Especially the group of purified proteins with an unaltered ratio might contain a significant percentage of contaminants. Cells were harvested and whole cell lysates were mixed in a 1:1 ratio. His6-SUMO-2 conjugates were subsequently purified, digested in solution with trypsin, and analyzed by mass spectrometry. A summary of the results is depicted in Fig. 3B. 847 proteins were identified by at least two unique peptides (Supplementary Table 1 Proteins Sheet) and in total 7643 peptides were identified by mass spectrometry (Supplementary Table 1 Peptides Sheet). Interestingly, two different subsets of MG132-sensitive SUMO-2 target proteins were identified, 73 target proteins showed a significant increase in sumoylation upon inhibition of the proteasome (Supplementary Table 3) and 40 target proteins showed a significant decrease in sumoylation in response to MG132 (Supplementary Table 4). The MG132 mediated increase in SUMO-2 conjugation was consistent with the immunoblot experiments (Fig. 2) whereas the MG132 mediated decrease in SUMO-2 conjugation of other target proteins was unexpected. The decrease in sumoylation of these target proteins might potentially be explained by a reduction in free SUMO-2 (Fig. 2M).

The largest functional group of MG132-regulated SUMO-2 conjugated proteins control nucleic acid metabolism (Supplementary Fig. S2). This group constitutes 47% of all MG132-upregulated targets and 40% of all MG132-downregulated targets and includes DNA repair factors, replication factors, helicases, basal transcription machinery components, transcription factors, chromatin modifiers and RNA binding and processing factors (Supplementary Fig. S2). In addition, both MG132 sensitive subsets contain a variety of other proteins, implicating that crosstalk between SUMO-2 and ubiquitin has a broad impact on cellular processes.

To confirm our findings independently, His6-SUMO-2 conjugates were purified from DMSO or MG132 treated cells and immunoblotting experiments were carried out (Fig. 4). These experiments confirmed the accumulation of SUMO-2 conjugated forms of hnRNP M, MCM-7 and PIAS1 upon proteasome inhibition (Fig. 4A-C) and a decrease of SUMO-2 conjugated forms of SAFB and SART1 (Fig. 4E and F). We noticed a slight decrease in SUMO-2 conjugation of RanGAP1 in this experiment (Fig. 4D). Strikingly, the total pools of these proteins were not affected by MG132,

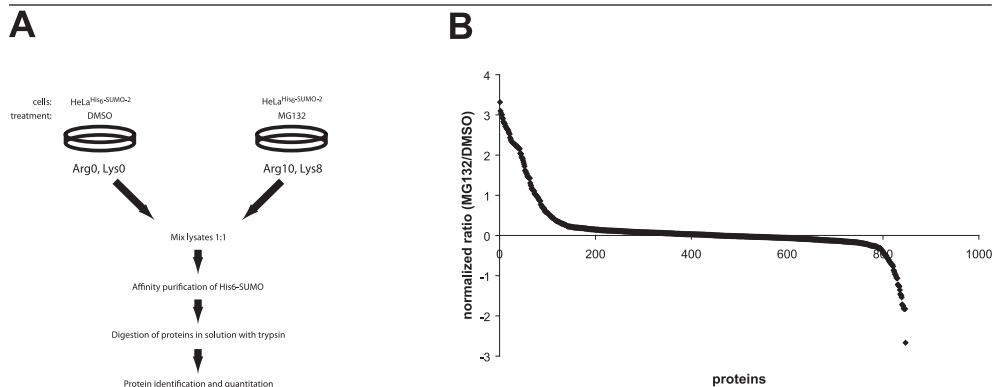


Fig. 3. Dynamic alterations in the SUMO-2 conjugated proteome in response to the proteasome inhibitor MG132. A, a quantitative proteomics strategy to study the effect of MG132 on the SUMO-2 conjugated proteome. HeLa^{His6-SUMO-2} cells were labeled with Arg0 and Lys0 and treated with DMSO for three hours and a second pool of HeLa^{His6-SUMO-2} cells were labeled with Arg10 and Lys8 and treated with MG132 for 3 hours. Equal amounts of whole cell lysates from the two different populations were mixed and proteins conjugated to His6-SUMO-2 were purified, digested by trypsin and identified by mass spectrometry. Peptide mass spectra were quantified to identify MG132-induced changes in the SUMO-2 conjugated proteome. B, In total 847 proteins were identified by at least two unique peptides, including 73 proteins that were preferentially enriched upon MG132 treatment and 40 proteins that were significantly reduced in response to MG132. The natural logarithm of the SILAC ratio for each protein is depicted in order to visualize upregulated- and downregulated proteins.

indicating that the ubiquitin-proteasome system specifically regulates SUMO-2 conjugated forms of these proteins (Fig. 4A-F, inputs).

The most obvious explanation for our results would be that a subset of SUMO-2/3 target proteins is subsequently ubiquitinated and degraded by the proteasome. Inhibition of the proteasome system could then lead to proteins accumulating in the sumoylated and ubiquitinated form. To study the ubiquitination status of hnRNP M, MCM-7, PIAS1, SAFB and SART1, similar experiments were carried out using His6-ubiquitin instead of His6-SUMO-2 (Fig. 5). As expected, hnRNP M, MCM-7 and PIAS1 were indeed ubiquitinated in an MG132-sensitive manner. PIAS1 (30) was also previously reported to be ubiquitinated. In contrast, ubiquitinated forms of SAFB or SART1 could not be detected in these experiments.

SUMO-2/3 chains accumulate in cells treated with MG132

Previously, we have shown that SUMO-2 and SUMO-3 are able to multimerize in cells in an ubiquitin-like manner (11). To investigate whether SUMO-2/3 chains accumulated in cells treated with proteasome inhibitors, we searched for tryptic SUMO-SUMO peptides in purified His6-SUMO-2 conjugates from our quantitative proteomics experiments. Interestingly, both SUMO2-SUMO2 and SUMO2-SUMO3 peptides were shown to accumulate upon MG132 treatment (Fig. 6A and B).

In order to determine whether these SUMO polymers are functionally important for the processing of SUMO-2 targets by the proteasome, plasmids were generated that

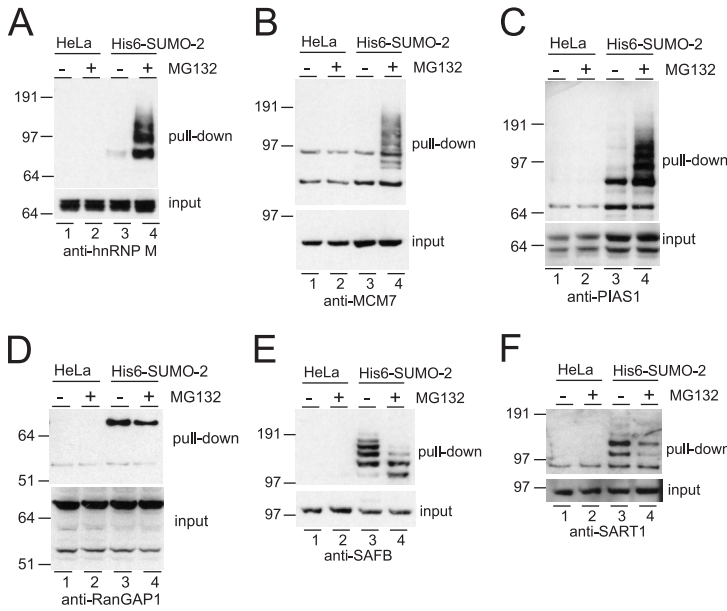


Fig. 4. Dynamic alterations in the SUMO-2 conjugated proteome in response to the proteasome inhibitor MG132 detected by immunoblotting. A-F, HeLa cells and HeLa^{His6-SUMO-2} cells were treated with MG132 or DMSO for 3 hours and His6-SUMO-2 conjugates were purified from equal amounts of whole cell lysates. His6-SUMO-2 conjugates or equal amounts of whole cell extracts were size-separated by SDS-PAGE, transferred to membranes and probed using antibodies to detect hnRNP M (A), MCM-7 (B), PIAS1 (C), RanGAP1 (D), SAFB (E), or SART1 (F). Note that the PIAS levels are slightly higher in the HeLa^{His6-SUMO-2} cells compared to the HeLa cells.

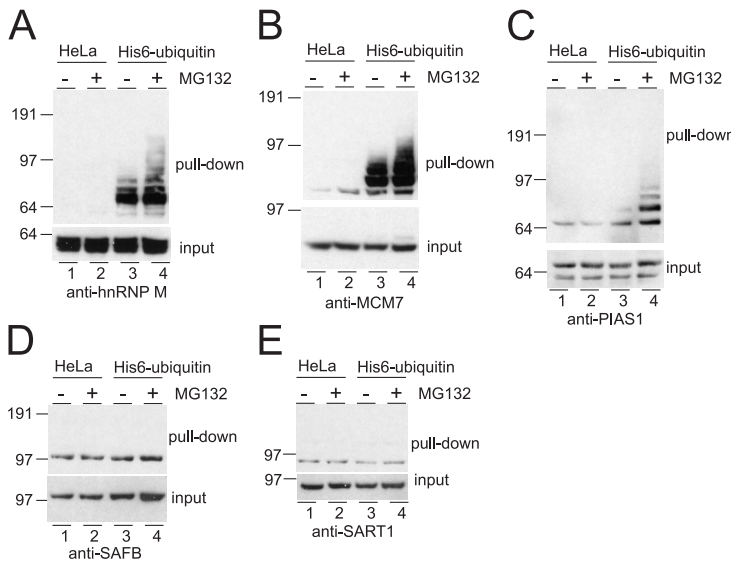


Fig. 5. hnRNP M, MCM7 and PIAS1 are conjugated to ubiquitin. A-E, HeLa cells were transfected with a plasmid that encodes His6-ubiquitin, or with an empty control plasmid and cells were treated with MG132 or DMSO for 3 hours. His6-ubiquitin conjugates were subsequently purified from equal amounts of whole cell lysates. His6-ubiquitin conjugates or equal amounts of whole cell extracts were size-separated by SDS-PAGE, transferred to membranes and probed using antibodies to detect hnRNP M (A), MCM-7 (B), PIAS1 (C), SAFB (D) or SART1 (E).



Chapter 2

encode SUMO-2 mutants reduced for chain formation. HeLa cells were transiently transfected, treated with DMSO or MG132 and proteins conjugated to wild-type or mutant SUMOs were purified and analyzed by immunoblotting. The SUMO-2 mutants accumulated in MG132-treated cells similarly to wild-type SUMO-2 (Fig. 6C) and ubiquitin still co-purified with the SUMO-2 mutants (Fig. 6D). Furthermore, both wild-type- and mutant SUMO-2-conjugated forms of hnRNP M, MCM-7 and PIAS1 accumulated upon inhibition of the proteasome (Fig. 6E-G). We conclude that SUMO chain formation is not required for the processing of SUMO-2 targets by the proteasome.

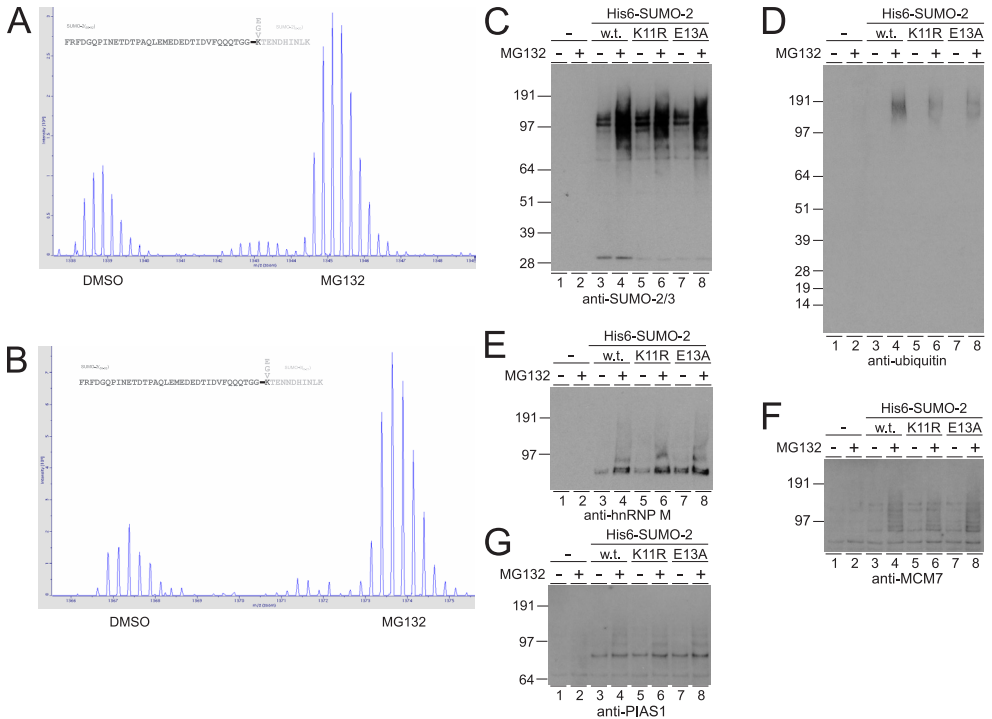


Fig. 6. SUMO chains accumulate in cells treated with MG132. A and B, a quantitative proteomics experiment was performed to identify changes in SUMO chains induced by MG132. HeLa^{His6-SUMO-2} cells were labeled with Arg0 and Lys0 and treated with DMSO for 3 hours and a second set of HeLa^{His6-SUMO-2} cells were labeled with Arg10 and Lys8 and treated with MG132 for 3 hours. Equal amounts of whole cell lysates from the two different populations were mixed and proteins conjugated to His6-SUMO-2 were purified, digested by trypsin in solution and identified by mass spectrometry. A, MS spectrum of a tryptic peptide consisting of aa 59-92 of SUMO-2 and aa 8-20 of another molecule of SUMO-2 (m/z 1338.1246 (4+); mass deviation - 1.21 ppm). B, MS spectrum of a tryptic peptide consisting of aa 59-92 of SUMO-2 and aa 8-21 of SUMO-3 (m/z 1366.6353 (4+); mass deviation - 1.65 ppm). C-G, HeLa cells were transfected with plasmids that encode His6-tagged forms of wild-type (w.t.), K11R- or E13A SUMO-2 mutants that are reduced for SUMO chain formation. Cells were treated with MG132 or DMSO for 5 hours and His6-SUMO-2 conjugates were purified from equal amounts of whole cell lysates. Purified fractions were size-separated by SDS-PAGE, transferred to membranes and probed using antibodies to detect SUMO-2/3 (C), ubiquitin (D) hnRNP M (E), MCM-7 (F) or PIAS1 (G).

Ubiquitination of SUMO-2/3

The accumulation of ubiquitin in SUMO-2 conjugates could potentially be explained by the formation of mixed SUMO-2 / ubiquitin chains and also by the conjugation of SUMO-2 and ubiquitin to independent lysines in target proteins. To test the formation of mixed chains, His6-ubiquitin was purified from cells, digested and analyzed by mass spectrometry to investigate the ubiquitination of endogenous SUMO-2/3. A high quality MS/MS spectrum was obtained showing the ubiquitination of endogenous SUMO-2 on lysine 32 or the ubiquitination of endogenous SUMO-3 on lysine 33 (Fig. 7A).

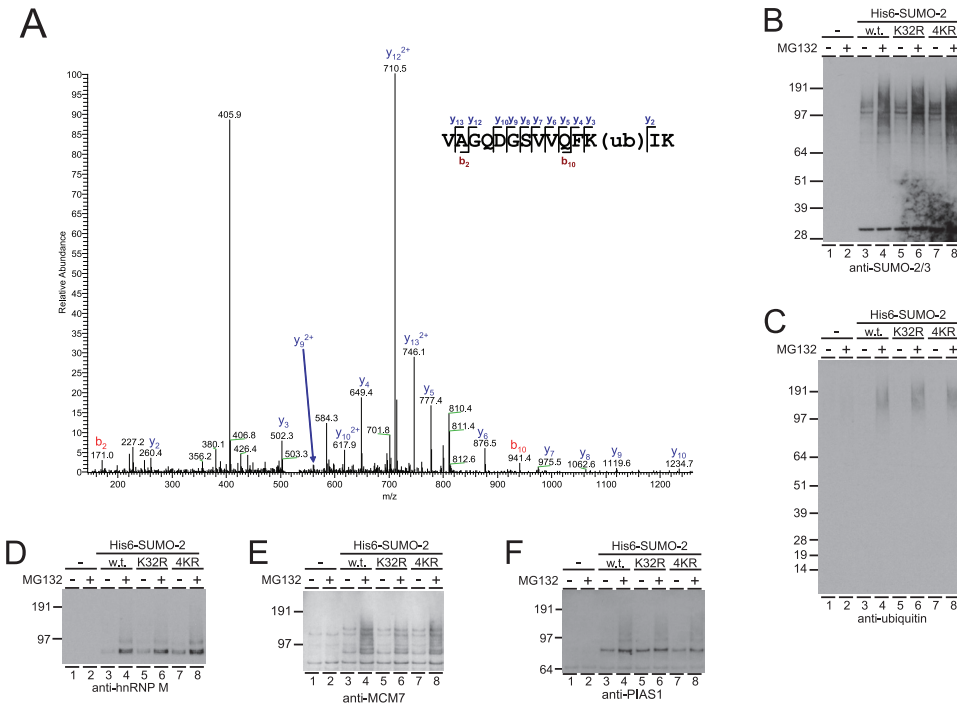


Fig. 7. SUMO-2 is ubiquitinated in cells. A, HeLa cells were transfected with a plasmid that encodes a His6-tagged lysine-deficient ubiquitin mutant. Cells were lysed and His6-ubiquitin conjugates were purified and digested by trypsin. The digest was analyzed by mass spectrometry and a peptide was identified that corresponds to ubiquitinated SUMO-2/3. The MS/MS fragmentation spectrum of this tryptic peptide consisting of aa 21-34 of SUMO-2 and the diglycine fragment of ubiquitin attached to lysine 32 of SUMO-2 is shown. This tryptic peptide is identical to a tryptic peptide consisting of aa 22-35 of SUMO-3 and the diglycine fragment of ubiquitin attached to lysine 33 of SUMO-3. Precursor ion mass was measured in the orbitrap mass spectrometer (m/z 530.6264 (3+); mass deviation - 1.12 ppm) and the peptide was fragmented and acquired in the LTQ mass spectrometer (Mascot Score 49.73; Mascot Delta 3.28; false positive rate: 1.765E-20). B-F, His6-SUMO-2 plasmids were generated that encode K32R- or K32, 34, 41 and 44R (4KR) mutants. HeLa cells were transfected with plasmids that encode His6-tagged forms of wild-type (w.t.), K32R- or 4KR SUMO-2 mutants. Cells were treated with MG132 or DMSO for 5 hours and His6-SUMO-2 conjugates were purified from equal amounts of whole cell lysates. Purified fractions were size-separated by SDS-PAGE, transferred to membranes and probed using antibodies to detect SUMO-2/3 (B), ubiquitin (C) hnRNP M (D), MCM-7 (E) or PIAS1 (F).

In order to determine whether mixed chains are functionally important for the processing of SUMO-2 targets by the proteasome, a plasmid was generated that encoded a SUMO-2 K32R mutant and a second mutant was generated that lacked other adjacent lysines 34, 41 and 44 (4KR). HeLa cells were transiently transfected, treated with DMSO or MG132 and proteins conjugated to wild-type or mutant SUMOs were purified and analyzed by immunoblotting. The SUMO-2 mutants accumulated in MG132-treated cells similarly to wild-type SUMO-2 (Fig. 7B) and ubiquitin co-purified efficiently with the SUMO-2 mutants (Fig. 7C). Both wild-type- and mutant SUMO-2-conjugated forms of hnRNP M, MCM-7 and PIAS1 all accumulated upon inhibition of the proteasome (Fig. 7D-F). Moreover, a lysine-deficient SUMO-2 mutant accumulated in MG132-treated cells similarly to wild-type SUMO-2 and both wild-type- and mutant SUMO-2-conjugated forms of hnRNP M, MCM-7 and PIAS1 all accumulated upon inhibition of the proteasome (Fig. 8A-E)

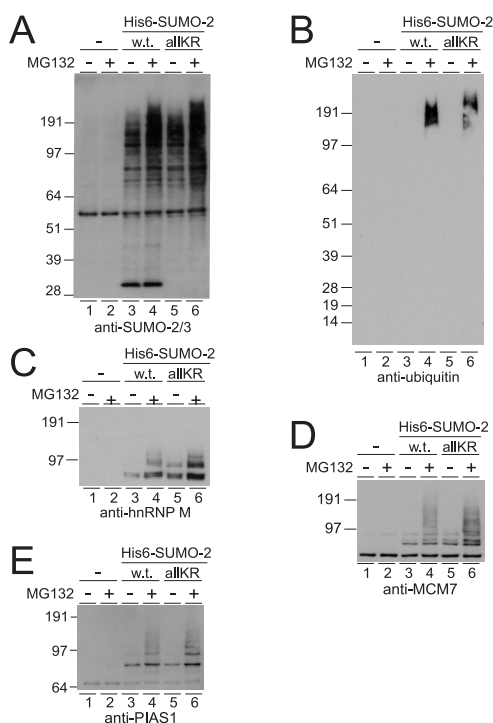


Fig. 8. A lysine-deficient SUMO-2 mutant is sensitive to proteasome inhibition. A-E, a His6-SUMO-2 plasmid was generated that encodes a lysine-deficient mutant (allKR). HeLa cells were transfected with plasmids that encode His6-tagged forms of wild-type (w.t.) or the allKR SUMO-2 mutant. Cells were treated with MG132 or DMSO for 5 hours and His6-SUMO-2 conjugates were purified from equal amounts of whole cell lysates. Purified fractions were size-separated by SDS-PAGE, transferred to membranes and probed using antibodies to detect SUMO-2/3 (A), ubiquitin (B) hnRNP M (C), MCM-7 (D) or PIAS1 (E).

We conclude that SUMO-2 / ubiquitin mixed chain formation and SUMO-SUMO chain formation are not required for the processing of SUMO-2 targets by the proteasome. In principle, it is still possible that these SUMO-2 mutants form residual polymers with endogenous SUMO-2/3. However, dimers consisting of the lysine-deficient SUMO-2 mutant and endogenous SUMO-2/3 could not be detected by immunoblotting (Fig. 8A lanes 5 and 6). Our data are compatible with consecutive

sumoylation and ubiquitination of a significant subset of SUMO-2 target proteins via independent lysines in these target proteins (Fig. 9). Upon ubiquitination, SUMO-2/3 conjugated proteins are degraded by the proteasome, which enables the recycling of SUMO-2/3.

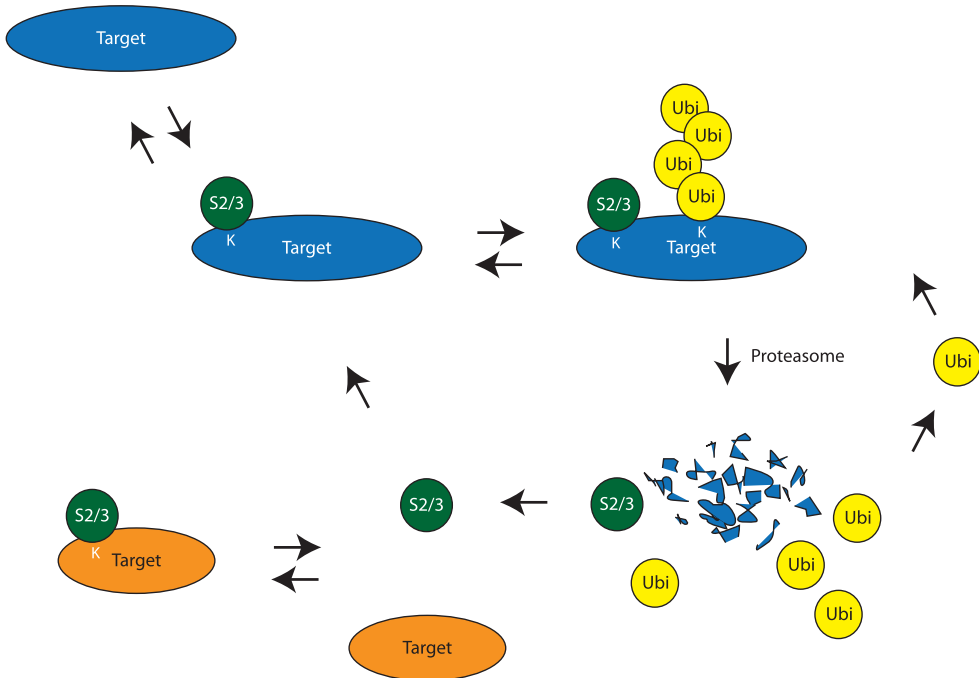


Fig. 9. The ubiquitin-proteasome system is a component of the SUMO-2/3 cycle. Our data indicate that the turn-over of a subset of SUMO-2/3 conjugates is regulated by the ubiquitin-proteasome system. Target proteins that are conjugated to a single monomer of SUMO-2 or SUMO-3 or to multiple monomers can subsequently be ubiquitinated and degraded by the proteasome. This process enables the recycling of SUMOs to provide sufficient amounts of free SUMOs for new rounds of conjugation. In addition, mixed SUMO / ubiquitin chains are formed and SUMO-SUMO chains.

Discussion

Ubiquitination and sumoylation are generally considered to be independent protein modifications. We have shown here that extensive crosstalk exists between ubiquitin and SUMO-2/3 conjugation of target proteins (Fig. 9). This crosstalk regulates selected SUMO-2/3 targets either directly or indirectly. A substantial percentage of SUMO-2/3 conjugates is directly regulated by subsequent ubiquitination and processing by the proteasome. A second subset of target proteins is indirectly dependent on the ubiquitin-proteasome system to provide a sufficiently large pool of free recycled SUMO-2/3 for subsequent rounds of conjugation.

The recent identification of the SLX5/8 complex in yeast and RNF4 in mammals (also known as SNURF) provides mechanistic insight in the ubiquitination of

Chapter 2

2

sumoylated proteins (31-36). These proteins contain both a RING domain and SUMO Interaction Motifs (SIMs) and act as ubiquitin E3 ligases that are targeted to sumoylated proteins via these SIMs (32-34, 36-38). SLX5 and SLX8 are required for maintenance of the genome (32-35, 39-43). The identification of a large subset of nucleic acid binding proteins that are sumoylated in a proteasome inhibitor sensitive manner provides an important framework for further detailed analysis of the regulation of nucleic acid metabolism by SUMO-2/3 and the ubiquitin-proteasome system.

The precise roles of SUMO-SUMO chains as shown in Fig. 6A and B and of mixed SUMO-2/3 ubiquitin chains as shown in Fig. 7A is currently unclear. Since mutants that lack acceptor lysines still accumulate in cells treated with proteasome inhibitors and ubiquitin still co-purified similarly to wild-type SUMO forms, these chains are not required for targeting the majority of SUMO-2/3 targets to the proteasome. Nevertheless, it is possible that certain proteins are targeted to the proteasome via these chains (37, 38). Alternatively, these chains could regulate degradation-independent processes.

The conjugation of another subset of SUMO-2 target proteins was unaffected by the inhibition of the proteasome, including RanGAP1. Interestingly, a very large fraction of RanGAP1 exists in a sumoylated form, mainly conjugated to SUMO-1 (6). It seems likely that sumoylated forms of RanGAP1 are very stable and have a very slow turnover compared to most other known target proteins. The half-life of the sumoylated forms of a subset of target proteins is regulated by ubiquitination and degradation by the proteasome as shown here, but also via SUMO proteases (SENPs) (44). Sumoylated RanGAP1 is localized at the cytoplasmic surface of the nuclear pore complex (45, 46), which might positively contribute to its stability since the majority of SUMO proteases are nuclear proteins (44).

Although the sumoylated forms of hnRNP M, MCM7 and PIAS1 and the ubiquitinated forms of these proteins are strongly stabilized by MG132, the total pools of these proteins were unaffected by this inhibitor. It is therefore likely that only a small fraction of these proteins are modified within the three hour time frame of the experiment.

Transiently sumoylated proteins with short half-lives of the sumoylated forms due to the activity of SUMO proteases are likely to show the strongest decrease in sumoylation upon inhibition of the proteasome due to insufficient amounts of free SUMO-2/3. Therefore, the relative reduction in sumoylation of SUMO-2/3 target proteins upon inhibition of the proteasome is likely to reflect the relative instability of the sumoylated forms of these proteins.

Currently, it is unclear why some SUMO-2/3 targets are subsequently ubiquitinated and degraded whereas sumoylated forms of other SUMO-2/3 targets such as SART1 and SAFB are not subjected to detectable amounts of ubiquitination. Most likely, RNF4 plays a critical role and binds preferentially to a subset of SUMO-

2/3 target proteins. Alternatively, the localization of RNF4 in the cell might limit its activity to a subset of SUMO-2/3 target proteins in a manner similar to the SUMO proteases (44). It is interesting to note that RNF4 specifically localizes to PML-bodies (47), sites that are significantly enriched in SUMOs (23, 48). These nuclear bodies have also been shown to contain ubiquitin and proteasomal proteins (49), suggesting that the ubiquitination and degradation of sumoylated proteins can occur in PML-bodies (37, 38).

The total levels of SUMO-1 were not affected by inhibition of the proteasome (Fig. 2), in contrast to a previous publication (50), nevertheless SUMO-1 accumulated in purified SUMO-2 in a manner similar to ubiquitin. Currently, the role of SUMO-1 attached to SUMO-2 conjugates is unclear. Previously, we have shown that SUMO-1 can directly be attached to lysine 11 of SUMO-2 (11). These mixed SUMO chains are unlikely to play a role in targeting proteins to the proteasome, since SUMO-2 K11R or E13A mutants still accumulated upon proteasome inhibition and ubiquitin efficiently co-purified with these mutants (Fig. 6).

In summary, we have shown here that the ubiquitin-proteasome system is an important component of the cellular SUMO-2/3 cycle that is required for the processing of a subset of SUMO-2/3 targets and the recycling of SUMO-2/3. The identification of other components of this pathway and the detailed dissection of the regulated target proteins will be an important step towards uncovering the connection between SUMO-2/3 and the ubiquitin-proteasome system in detail.

Materials and methods

Cell culture and transfections

HeLa cells stably expressing His6-SUMO-1 or His6-SUMO-2 were previously described (6). HeLa cells were grown in Dulbecco's modified Eagle's medium (DMEM), supplemented with 10% FCS and 100 U/ml penicillin and streptomycin (Invitrogen). Stable isotope labeling was carried out essentially as described (6, 20), using $^{12}\text{C}_6\text{ }^{14}\text{N}_4$ -Arginine (referred to as Arg0), $^{13}\text{C}_6\text{ }^{14}\text{N}_4$ -Arginine (referred to as Arg6), $^{13}\text{C}_6\text{ }^{15}\text{N}_4$ -Arginine (referred to as Arg10), $^{12}\text{C}_6\text{ }^{14}\text{N}_2$ -Lysine (referred to as Lys0), $^2\text{H}_4\text{ }^{12}\text{C}_6\text{ }^{14}\text{N}_2$ -Lysine (referred to as Lys4) or $^{13}\text{C}_6\text{ }^{15}\text{N}_2$ -Lysine (referred to as Lys8) as indicated. Transfections were carried out using 25kDa linear polyethyleneimine (Brunschwig-Chemie) essentially as described (21).

Plasmids, Mutagenesis, Antibodies, Protein Electrophoresis and Immunoblotting

The plasmids encoding His6-ubiquitin wild-type or 7KR and the plasmid encoding wild-type His6-SUMO-2 were previously described (22, 23). The His6-SUMO-2 K11R, E13A, K32R, K32,34,41,44R and allKR plasmids were generated by site-directed mutagenesis using the QuikChange II kit according to the instructions of the manufacturer (Stratagene). Mutants were confirmed by DNA sequencing.

The amino acid sequence of the mature protein that we refer to as SUMO-2 is MSEEKPKEGVKTEND-HINLKVAGQDGSVVQFKIKRHTPLSKLMKAYCERQGLSMRQIRFRFDGQPINETDTPAQLEMEDEDTI-

DVFQQQTGG (12). Peptide antibody AV-SM23-0100 against SUMO-2/3 was generated in rabbit using the peptide MEDEDTIDVFQQQTG (Eurogentec) (6, 23). Peptide antibody 1607 against SART1 was also generated in rabbit by Eurogentec using peptides CSLSIEETNKLRAKLGKPLEV and CNLD-EEKQQQDFSSASSTT as described previously (6). Monoclonal antibodies 21C7 against SUMO-1 and 19C7 against RanGAP1 were obtained from Zymed, monoclonal antibodies HIS-1 against polyHistidine, R-3902 against hnRNP M and M-7931 against MCM-7 were obtained from Sigma, monoclonal antibody SC-8017 against ubiquitin and polyclonal antibody SC-8152 against PIAS1 were obtained from Santa-Cruz Biotechnology, monoclonal antibody ab8060 against SAFB was obtained from Abcam. This antibody also recognizes SAFB2. Secondary antibodies used were anti-rabbit HRP and anti-mouse HRP (1:5000, Pierce Chemical Co.) and anti-goat HRP (1:5000, Sigma).

Protein samples were size fractionated on Novex 4-12% Bis-TRIS gradient gels using 4-morpholinepropanesulfonic acid buffer (Invitrogen). For immunoblotting experiments, size fractionated proteins were subsequently transferred onto Hybond-C extra membranes (Amersham Biosciences) using a submarine system (Invitrogen). The membranes were incubated with specific antibodies as indicated. Bound antibodies were detected via chemiluminescence with ECL Plus (Amersham Biosciences).

Purification of His6-SUMO and His6-ubiquitin conjugated proteins

His6-SUMO conjugates and His6-ubiquitin conjugates were purified essentially as previously described (24). Cells were scraped in ice-cold PBS. Two small aliquots of each sample were lysed in LDS protein sample buffer (Invitrogen) as input control, or in 8 M Urea, 100 mM $\text{Na}_2\text{HPO}_4/\text{NaH}_2\text{PO}_4$, 10 mM Tris/HCl, pH 7.0 to determine the protein concentration. The remaining cells were solubilized in lysis buffer (6 M Guanidinium-HCl, 100 mM $\text{Na}_2\text{HPO}_4/\text{NaH}_2\text{PO}_4$, 10 mM Tris/HCl, pH 8.0, 20 mM Imidazole, 10 mM β mercapto-ethanol) and sonicated to reduce the viscosity. His6-SUMO conjugates or His6-ubiquitin conjugates were enriched on Ni-NTA Agarose beads (Qiagen) and washed using wash buffers A-D. (Buffer A: 6 M Guanidinium-HCl, 100 mM $\text{NaH}_2\text{PO}_4/\text{Na}_2\text{HPO}_4$, 10 mM Tris/HCl pH 8.0 and 0.2% Triton-X-100. Buffer B: 8 M Urea, 100 mM $\text{NaH}_2\text{PO}_4/\text{Na}_2\text{HPO}_4$, 10 mM Tris/HCl pH 8.0 and 0.2% Triton-X-100. Buffer C: 8 M Urea, 100 mM $\text{NaH}_2\text{PO}_4/\text{Na}_2\text{HPO}_4$, 10 mM Tris/HCl pH 6.3 and 0.2% Triton-X-100. Buffer D: 8 M Urea, 100 mM $\text{NaH}_2\text{PO}_4/\text{Na}_2\text{HPO}_4$, 10 mM Tris/HCl pH 6.3 and 0.1% Triton-X-100. These wash buffers also contained 10 mM β mercapto-ethanol. Samples were eluted in 6.4 M Urea, 80 mM $\text{NaH}_2\text{PO}_4/\text{Na}_2\text{HPO}_4$, 8 mM Tris/HCl pH 7.0, 200 mM imidazole.

For the experiment described in Fig. 1A-C, a previously described method was used (6). For the experiments described in Fig. 3A and B and 6A and B His6-SUMO conjugates were immunoprecipitated using monoclonal antibody HIS-1 (Sigma) as described previously (24). For the experiment described in Fig. 7A HeLa cells were transfected with the His6-ubiquitin 7KR encoding plasmid. Cells were lysed in 6 M Guanidinium-HCl, 100 mM $\text{NaH}_2\text{PO}_4/\text{Na}_2\text{HPO}_4$, 10 mM Tris/HCl pH 8.0 and proteins were digested with endopeptidase Lys-C. His6-ubiquitin conjugates were subsequently purified on Talon beads (BD Biosciences), washed 2x with lysis buffer and 4x with 8 M Urea, 100 mM $\text{NaH}_2\text{PO}_4/\text{Na}_2\text{HPO}_4$, 10 mM Tris/HCl pH 8.0 and eluted in 6.4 M Urea, 80 mM $\text{NaH}_2\text{PO}_4/\text{Na}_2\text{HPO}_4$, 8 mM Tris/HCl pH 7.0, 200 mM imidazole. His6-ubiquitin and conjugated peptides were digested with trypsin in solution and identified by mass spectrometry.

Mass spectrometry and data analysis

Mass spectrometric analysis was performed by nanoscale liquid chromatography-tandem mass spectrometry (LC MS/MS) using a linear ion trap Fourier-transform ion-cyclotron resonance mass spectrometer (LTQ-FT-ICR, Thermo-Finnigan, Bremen). Eluates were analyzed by 1-dimensional gel electrophoresis. Gel lanes were cut in slices and subjected to in-gel digestion with Lys-C. The resulting peptides were extracted, concentrated, and then loaded onto a fused silica capillary with a 75 μm ID and an 8 μm tip opening (New Objective, Woburn, MA) filled with Reprosil 3 μm reverse phase material (Dr. Maisch, Ammerbuch, Germany). Peptides were eluted with a 140 min linear gradient of 95% buffer A (0.5% acetic acid in H_2O) to 50% buffer B (80% acetonitrile, 0.5% acetic acid in H_2O). The LTQ-FT-ICR instrument was operated in the data dependent mode to acquire high-resolution precursor ion spectra (from m/z 300-1500, $R=50,000$, and ion accumulation to a target value of 5,000,000) in the ICR cell. The three most intense ions were sequentially isolated for accurate mass measurements by SIM scans (10 Da mass window, $R=50,000$, and a target accumulation value of 90,000). The ions were simultaneously fragmented in the linear ion trap with a normalized collision energy setting of 27 % and a target value of 10,000.

Peak list-generating software was DTA supercharge (release date April 20, 2006). Combined peak list were searched in the International Protein Index (IPI) database (<http://www.ebi.ac.uk/IPI/IPIhelp.html>; release date April 21, 2006; total of 66279 sequences) using the Mascot program (Matrix Science, London). The enzyme specificity was set to Lys-C, allowing for cleavage N-terminal of proline and between aspartic acid and proline. Cysteine carbamidomethylation was selected as fixed modification, and methionine oxidation, protein N-acetylation, Lysine D4 and Lysine- $^{13}\text{C}_6^{15}\text{N}_2$ were searched as variable modifications. LTQ-FT-ICR data were searched with a peptide mass tolerance of 10 ppm and a fragment mass tolerance of 0.6 Da. Iterative calibration algorithms on the basis of identified peptides resulted in an average absolute peptide mass accuracy of better than 1 ppm. A maximum of 1 missed cleavage was allowed. Stringent criteria were required for protein identification based on the LTQ-FT-ICR data: at least two matching peptides per protein, a mass accuracy within 3 ppm, a Mascot score for individual ions of better than 20, and a delta score of better than 5.

Protein ratios were calculated for each peptide and peptide ratios were averaged for all quantified peptides sequenced for each protein. MSQuant, an in-house developed software program was used to extract information from the Mascot HTML database search files and to manually validate the certainty in peptide identification and in peptide abundance ratio. The quantitation was based on relative intensities from combined scans. The program is available as open source at <http://msquant.sourceforge.net/>.

For the experiments described in Fig. 3A and B and 6A and B mass spectrometric analysis was performed by nanoscale liquid chromatography-tandem mass spectrometry (LC-MS/MS) using a LTQ-Orbitrap mass spectrometer (LTQ-FT-ICR, Thermo Fisher Scientific, Bremen, Germany) equipped with a nanoelectrospray ion source (Proxeon Biosystems, Odense, Denmark) and coupled to an Agilent 1200 nano-HPLC system (Agilent Technologies), fitted with an in-house made 75 μm reverse phase C_{18} column, as described previously (25). In-solution digestion was performed essentially as in (26). The resulting peptides were desalted on RP- C_{18} STAGE tips (27). Peptides were eluted with a 140 min linear gradient of 98% solvent A (0.5% acetic acid in H_2O) to 50% solvent B (80% acetonitrile, 0.5% acetic acid

Chapter 2

in H₂O).

Data were acquired in the data dependent mode: full scan spectra (*m/z* 300-2000, *R*=60000 and ion accumulation to a target value of 1,000,000), were acquired in the orbitrap. The ten most intense ions were fragmented and recorded in the ion trap, as described in (25). Raw files were processed with our in-house quantitative proteomics software MaxQuant (version 1.0.7.5) which performs peak list generation, SILAC-based quantitation, false discovery rate determination, peptide to protein assembly and data filtration, essentially as described in (28, 29). The quantitation was based on relative intensities from combined scans. The data were searched against a target/decoy human IPI database (version 3.24) supplemented with frequently observed contaminants (total of 66948 forward) using Mascot (Matrix Science, version 2.1.04). The enzyme specificity was set to trypsin, allowing for cleavage N-terminal of proline and between aspartic acid and proline. Cysteine carbamidomethylation was selected as fixed modification, and methionine oxidation and protein N-acetylation and deamidation of asparagine and glutamine were searched as variable modifications. Spectra determined to be heavy-labeled in the pre-search MaxQuant detection of SILAC pairs were searched with the fixed modifications Arg10 and Lys8; for MS/MS spectra with a SILAC state not determinable before the database search Arg10 and Lys8 were taken as variable modifications. Initial maximum allowed mass deviation was set to 7 ppm for peptide masses and 0.5 for MS/MS peaks. The minimum peptide length was set to 6 amino acids and a maximum of 3 missed cleavages and 3 labeled amino acids were allowed. Two proteins were grouped together if the peptide sequence set of one protein was equal to or a subset of the second protein's set.

A false discovery rate of 1% at both the protein and peptide level was used. Peptide false positive rates were calculated by deriving with the Bayes theorem the probability of a false identification for a top-scoring peptide from Mascot score and peptide sequence length dependent histograms. Protein group false positive rates were calculated by multiplying the contained peptide sequences' false positive rates. Each distinct peptide sequence contributed only one factor, the false positive rate of the MS/MS spectrum for a given peptide sequence with the best false positive rate value. All MS/MS spectra associated with a peptide sequence, which might consist of re-sequencing events on the same peak, sequencing on different isotopic peaks in the same isotope pattern, sequencing of different charge states, different SILAC or modification states, were entering the protein false discovery rate only with one single peptide false positive rate. Protein groups were then sorted by the false positive rate and a given false discovery rate was ensured by terminating a list of proteins so that a given percentage of reverse proteins were contained. The used FDR of 1% ensured that at most one percent of the proteins were wrongly identified. Peptides that lost all containing proteins after this procedure were also removed from the peptide list. In addition to the protein false discovery rate threshold, proteins were considered identified by at least two unique-sequence peptides; quantified with at least one quantifiable SILAC pair. No outliers were removed due to the use of median instead of average values.

Significance of protein ratios was calculated in two different ways. Significance A was calculated by first estimating the variance of the distribution of all protein ratios in a non-parametric way and then reporting the error function for the z-score corresponding to the given ratio. A robust and asymmetrical estimate of the standard deviation was obtained by calculating the 15.87, 50 and 84.13 percentiles r_{-} , r_0 and r_{+} , which correspond to one sigma in each direction from the average. $r_{+}-r_0$ was defined as the right-

and r_0-r_{-1} as left-sided robust standard deviations. In case of normally distributed data, r_1-r_0 and r_0-r_{-1} would be equal to each other (conventional definition of standard deviation). The distance of a ratio $r>r_0$ from the main distribution is measured in terms of the right standard deviation as follows.

$$Z = \frac{r - r_0}{r_1 - r_0} \quad (\text{Eq. 1})$$

An analogous calculation is defined for $r<r_0$. Significance A is the value of the complementary error function for the z above, which for a normal distribution corresponds to the probability of obtaining a value this large or larger by chance. Significance B was calculated using the same strategy, but in addition it is based on the dependence of the distribution on the summed protein intensity. We consider a protein as upregulated if its significance B was below 0.001 and the ratio higher than 1; downregulated with the significance B below 0.001 and the ratio lower than 1; not regulated if the significance B was higher than 0.001.

Raw mass spectrometric files are stored at Tranche (<http://tranche.proteomecommons.org/>), a public repository for sharing scientific data. From this link (<http://www.proteomecommons.org/dev/dfs/GetFileTool.jnlp>) files can be downloaded with the following hash: 51ebd8yrJijxprwSrYlms0w9M4ZhR-6rwulAmelGyGs4WgqWQ4e8vcMgaqspuaRcEwBJ4I1pFV6ZILZBVLdEMWQJO5oAAAAAAAAAFjA==

To address the reproducibility of the data, independent control immunoblotting experiments were performed (Fig 4). We have used antibodies directed against six different proteins identified by mass spectrometry and confirmed increases and decreases in sumoylation of these proteins upon inhibition of the proteasome, showing the reproducibility of the data.

Acknowledgments

This work was supported by the Netherlands Organisation for Scientific Research (NWO) to ACOV as part of the Innovational Research Incentives Scheme, by a generous grant from the Danish National Research Foundation to JSA and MM and by a grant from the The European Community (RUBICON, VI Framework) to MM.

* The costs of publication of this article were defrayed in part by the payment of page charge. This article must therefore be hereby marked “*advertisement*” in accordance with 18 U.S.C. Section 1734 solely to indicate this fact.

* The online version of this article (available at <http://www.mcponline.org>) contains supplemental material.

Reference List

1. Goldberg, A. L. (2007) Functions of the proteasome: from protein degradation and immune surveillance to cancer therapy. *Biochem. Soc. Trans.* 35, 12-17
2. Mukhopadhyay, D., and Riezman, H. (2007) Proteasome-independent functions of ubiquitin in endocytosis and signaling. *Science* 315, 201-205
3. Kerscher, O., Felberbaum, R., and Hochstrasser, M. (2006) Modification of Proteins by Ubiquitin and Ubiquitin-Like Proteins. *Annu. Rev. Cell Dev. Biol.*
4. Welchman, R. L., Gordon, C., and Mayer, R. J. (2005) Ubiquitin and ubiquitin-like proteins as multifunctional signals. *Nat. Rev. Mol. Cell Biol.*

- Biol. 6, 599-609
5. Nacerddine, K., Lehenbre, F., Bhaumik, M., Artus, J., Cohen-Tannoudji, M., Babinet, C., Pandolfi, P. P., and Dejean, A. (2005) The SUMO pathway is essential for nuclear integrity and chromosome segregation in mice. *Dev. Cell* 9, 769-779
 6. Vertegaal, A. C., Andersen, J. S., Ogg, S. C., Hay, R. T., Mann, M., and Lamond, A. I. (2006) Distinct and overlapping sets of SUMO-1 and SUMO-2 target proteins revealed by quantitative proteomics. *Mol. Cell Proteomics* 5, 2298-2310
 7. Gill, G. (2005) Something about SUMO inhibits transcription. *Curr. Opin. Genet. Dev.* 15, 536-541
 8. Wilson, V. G., and Heaton, P. R. (2008) Ubiquitin proteolytic system: focus on SUMO. *Expert. Rev. Proteomics* 5, 121-135
 9. Geiss-Friedlander, R., and Melchior, F. (2007) Concepts in sumoylation: a decade on. *Nat. Rev. Mol. Cell Biol.* 8, 947-956
 10. Meulmeester, E., and Melchior, F. (2008) Cell biology: SUMO. *Nature* 452, 709-711
 11. Matic, I., van Hagen, M., Schimmel, J., Macek, B., Ogg, S. C., Tatham, M. H., Hay, R. T., Lamond, A. I., Mann, M., and Vertegaal, A. C. (2008) In vivo identification of human SUMO polymerization sites by high accuracy mass spectrometry and an in-vitro to in vivo strategy. *Mol. Cell Proteomics* 7, 132-144
 12. Tatham, M. H., Jaffray, E., Vaughan, O. A., Desterro, J. M., Botting, C. H., Naismith, J. H., and Hay, R. T. (2001) Polymeric chains of SUMO-2 and SUMO-3 are conjugated to protein substrates by SAE1/SAE2 and Ubc9. *J. Biol. Chem.* 276, 35368-35374
 13. Vertegaal, A. C. (2007) Small ubiquitin-related modifiers in chains. *Biochem. Soc. Trans.* 35, 1422-1423
 14. Lallemand-Breitenbach, V., Zhu, J., Puvion, F., Koken, M., Honore, N., Doubekovsky, A., Duprez, E., Pandolfi, P. P., Puvion, E., Freemont, P., and de The, H. (2001) Role of promyelocytic leukemia (PML) sumolation in nuclear body formation, 11S proteasome recruitment, and As2O3-induced PML or PML/retinoic acid receptor alpha degradation. *J. Exp. Med.* 193, 1361-1371
 15. Isik, S., Sano, K., Tsutsui, K., Seki, M., Enomoto, T., Saitoh, H., and Tsutsui, K. (2003) The SUMO pathway is required for selective degradation of DNA topoisomerase IIbeta induced by a catalytic inhibitor ICRF-193(1). *FEBS Lett.* 546, 374-378
 16. Ulrich, H. D. (2005) Mutual interactions between the SUMO and ubiquitin systems: a plea of no contest. *Trends Cell Biol.* 15, 525-532
 17. Desterro, J. M., Rodriguez, M. S., and Hay, R. T. (1998) SUMO-1 modification of IkkappaAlpha inhibits NF-kappaB activation. *Mol. Cell* 2, 233-239
 18. Huang, T. T., Wuerzberger-Davis, S. M., Wu, Z. H., and Miyamoto, S. (2003) Sequential modification of NEMO/IKKgamma by SUMO-1 and ubiquitin mediates NF-kappaB activation by genotoxic stress. *Cell* 115, 565-576
 19. Moldovan, G. L., Pfander, B., and Jentsch, S. (2007) PCNA, the maestro of the replication fork. *Cell* 129, 665-679
 20. Andersen, J. S., Lam, Y. W., Leung, A. K., Ong, S. E., Lyon, C. E., Lamond, A. I., and Mann, M. (2005) Nucleolar proteome dynamics. *Nature* 433, 77-83
 21. Durocher, Y., Perret, S., and Kamen, A. (2002) High-level and high-throughput recombinant protein production by transient transfection of suspension-growing human 293-EBNA1 cells. *Nucleic Acids Res.* 30, E9
 22. van der Horst, A., Vries-Smits, A. M., Brenkman, A. B., van Triest, M. H., van den, B. N., Colland, F., Maurice, M. M., and Burgering, B. M. (2006) FOXO4 transcriptional activity is regulated by monoubiquitination and USP7/HAUSP. *Nat. Cell Biol.* 8, 1064-1073
 23. Vertegaal, A. C., Ogg, S. C., Jaffray, E., Rodriguez, M. S., Hay, R. T., Andersen, J. S., Mann, M., and Lamond, A. I. (2004) A proteomic study of SUMO-2 target proteins. *J. Biol. Chem.* 279, 33791-33798
 24. Jaffray, E. G., and Hay, R. T. (2006) Detection of modification by ubiquitin-like proteins. *Methods* 38, 35-38
 25. Olsen, J. V., de Godoy, L. M., Li, G., Macek, B., Mortensen, P., Pesch, R., Makarov, A., Lange, O., Horning, S., and Mann, M. (2005) Parts per million mass accuracy on an Orbitrap mass spectrometer via lock mass injection into a C-trap. *Mol. Cell Proteomics* 4, 2010-2021
 26. Foster, L. J., de Hoog, C. L., and Mann, M. (2003) Unbiased quantitative proteomics of lipid rafts reveals high specificity for signaling factors. *Proc. Natl. Acad. Sci. U. S. A.* 100, 5813-5818
 27. Rappsilber, J., Ishihama, Y., and Mann, M. (2003) Stop and go extraction tips for matrix-assisted laser desorption/ionization, nanoelectrospray, and LC/MS sample pretreatment in proteomics. *Anal. Chem.* 75, 663-670
 28. Cox, J., and Mann, M. (2007) Is proteomics the new genomics? *Cell* 130, 395-398
 29. Graumann, J., Hubner, N. C., Kim, J. B., Ko, K., Moser, M., Kumar, C., Cox, J., Schoeler,

- H., and Mann, M. (2007) SILAC-labeling and proteome quantitation of mouse embryonic stem cells to a depth of 5111 proteins. *Mol. Cell Proteomics*
30. Depaux, A., Regnier-Ricard, F., Germani, A., and Varin-Blank, N. (2007) A crosstalk between hSiah2 and Pias E3-ligases modulates Pias-dependent activation. *Oncogene* 26, 6665-6676
 31. Wang, Z., Jones, G. M., and Prelich, G. (2006) Genetic analysis connects SLX5 and SLX8 to the SUMO pathway in *Saccharomyces cerevisiae*. *Genetics* 172, 1499-1509
 32. Prudden, J., Pebernard, S., Raffa, G., Slavin, D. A., Perry, J. J., Tainer, J. A., McGowan, C. H., and Boddy, M. N. (2007) SUMO-targeted ubiquitin ligases in genome stability. *EMBO J.* 26, 4089-4101
 33. Uzunova, K., Gottsche, K., Miteva, M., Weisshaar, S. R., Glanemann, C., Schnellhardt, M., Niessen, M., Scheel, H., Hofmann, K., Johnson, E. S., Praefcke, G. J., and Dohmen, R. J. (2007) Ubiquitin-dependent proteolytic control of SUMO conjugates. *J. Biol. Chem.* 282, 34167-34175
 34. Sun, H., Leveson, J. D., and Hunter, T. (2007) Conserved function of RNF4 family proteins in eukaryotes: targeting a ubiquitin ligase to SUMOylated proteins. *EMBO J.* 26, 4102-4112
 35. Kosoy, A., Calonge, T. M., Outwin, E. A., and O'Connell, M. J. (2007) Fission yeast Rnf4 homologs are required for DNA repair. *J. Biol. Chem.* 282, 20388-20394
 36. Xie, Y., Kerscher, O., Kroetz, M. B., McConchie, H. F., Sung, P., and Hochstrasser, M. (2007) The yeast Hex3.Slx8 heterodimer is a ubiquitin ligase stimulated by substrate sumoylation. *J. Biol. Chem.* 282, 34176-34184
 37. Tatham, M. H., Geoffroy, M. C., Shen, L., Plechanovova, A., Hattersley, N., Jaffray, E. G., Palvimo, J. J., and Hay, R. T. (2008) RNF4 is a poly-SUMO-specific E3 ubiquitin ligase required for arsenic-induced PML degradation. *Nat. Cell Biol.* 10, 538-546
 38. Lallemand-Breitenbach, V., Jeanne, M., Benhenda, S., Nasr, R., Lei, M., Peres, L., Zhou, J., Zhu, J., Raught, B., and de The, H. (2008) Arsenic degrades PML or PML-RARalpha through a SUMO-triggered RNF4/ubiquitin-mediated pathway. *Nat. Cell Biol.* 10, 547-555
 39. Burgess, R. C., Rahman, S., Lisby, M., Rothstein, R., and Zhao, X. (2007) The Slx5-Slx8 complex affects sumoylation of DNA repair proteins and negatively regulates recombination. *Mol. Cell Biol.* 27, 6153-6162
 40. Azam, M., Lee, J. Y., Abraham, V., Chanoux, R., Schoenly, K. A., and Johnson, F. B. (2006) Evidence that the *S. cerevisiae* Sgs1 protein facilitates recombinational repair of telomeres during senescence. *Nucleic Acids Res.* 34, 506-516
 41. Zhang, C., Roberts, T. M., Yang, J., Desai, R., and Brown, G. W. (2006) Suppression of genomic instability by SLX5 and SLX8 in *Saccharomyces cerevisiae*. *DNA Repair (Amst)* 5, 336-346
 42. Mullen, J. R., Nallaseth, F. S., Lan, Y. Q., Slagle, C. E., and Brill, S. J. (2005) Yeast Rmi1/Nce4 controls genome stability as a subunit of the Sgs1-Top3 complex. *Mol. Cell Biol.* 25, 4476-4487
 43. Mullen, J. R., Kaliraman, V., Ibrahim, S. S., and Brill, S. J. (2001) Requirement for three novel protein complexes in the absence of the Sgs1 DNA helicase in *Saccharomyces cerevisiae*. *Genetics* 157, 103-118
 44. Mukhopadhyay, D., and Dasso, M. (2007) Modification in reverse: the SUMO proteases. *Trends Biochem. Sci.* 32, 286-295
 45. Mahajan, R., Delphin, C., Guan, T., Gerace, L., and Melchior, F. (1997) A small ubiquitin-related polypeptide involved in targeting RanGAP1 to nuclear pore complex protein RanBP2. *Cell* 88, 97-107
 46. Matunis, M. J., Coutavas, E., and Blobel, G. (1996) A novel ubiquitin-like modification modulates the partitioning of the Ran-GTPase-activating protein RanGAP1 between the cytosol and the nuclear pore complex. *J. Cell Biol.* 135, 1457-1470
 47. Hakli, M., Karvonen, U., Janne, O. A., and Palvimo, J. J. (2005) SUMO-1 promotes association of SNURF (RNF4) with PML nuclear bodies. *Exp. Cell Res.* 304, 224-233
 48. Muller, S., Matunis, M. J., and Dejean, A. (1998) Conjugation with the ubiquitin-related modifier SUMO-1 regulates the partitioning of PML within the nucleus. *EMBO J.* 17, 61-70
 49. Wojcik, C., and DeMartino, G. N. (2003) Intracellular localization of proteasomes. *Int. J. Biochem. Cell Biol.* 35, 579-589
 50. Bailey, D., and O'Hare, P. (2005) Comparison of the SUMO1 and ubiquitin conjugation pathways during the inhibition of proteasome activity with evidence of SUMO1 recycling. *Biochem. J.* 392, 271-281



2



USP11 counteracts RNF4 and stabilizes PML Nuclear Bodies

Ivo A. Hendriks*, Joost Schimmel*, Jesper V. Olsen
and Alfred C.O. Vertegaal

Manuscript submitted

*These authors contributed equally to this work.

Chapter 3. USP11 counteracts RNF4 and stabilizes PML Nuclear Bodies

Abstract

RNF4 is a SUMO-targeted ubiquitin E3 ligase, with a pivotal function in the DNA damage response (DDR). We identified the deubiquitylating enzyme USP11, a known DDR-component, as an interactor of RNF4. USP11 can deubiquitylate hybrid SUMO-ubiquitin chains to counteract RNF4. Four closely spaced SUMO Interacting Motifs (SIMs) in USP11 are required for its activity, revealing USP11 as a SUMO-targeted ubiquitin protease. SUMO-enriched nuclear bodies are stabilized by USP11, which functions downstream of RNF4 as a counterbalancing mechanism. In response to DNA damage induced by methyl methanesulfonate, USP11 counteracts RNF4 to block the dissolution of nuclear bodies. Thus, we provide novel insight into crosstalk between ubiquitin in SUMO, and uncover USP11 and RNF4 as a balanced SUMO-targeted ubiquitin ligase/protease pair with a role in the DDR.

Introduction

Small Ubiquitin-like Modifiers (SUMOs) are predominantly located in the nucleus and play key roles in all nuclear processes including transcription, chromatin modification and maintenance of genome stability (1). Analogous to the ubiquitin system, a set of E1, E2 and E3 enzymes mediate the conjugation of SUMO to target proteins, and a set of SUMO-specific proteases is responsible for the reversible nature of this post-translational modification (2, 3). Mouse models have shown that the SUMOylation system is essential for embryonic development. Mice deficient for the single SUMO E2 enzyme Ubc9 die at the early post-implantation stage as a result of hypocondensation and other chromosomal aberrancies (4).

Large sets of target proteins have been identified for the different SUMO family members, involved in all different nuclear processes (5-7). About half of the SUMO acceptor lysines in these target proteins are located in short stretches that fit the SUMOylation consensus motif Ψ KxE (7, 8), a motif that is directly recognized by Ubc9 (9, 10). SUMO signal transduction furthermore includes proteins that bind non-covalently to SUMOylated proteins via SUMO-Interaction Motifs (SIMs) (11), including the novel SUMO-binding Zinc finger identified in HERC2 (12).

Interestingly, extensive crosstalk exists between the SUMOylation system and the ubiquitylation system (13, 14). This crosstalk includes competition between SUMO and ubiquitin for the same acceptor lysines (15), or sequential modification by SUMO and ubiquitin of a target protein (16). Moreover, the SUMO system is tightly connected to the ubiquitin-proteasome pathway since a significant subset of SUMO-2/3 target proteins is subsequently ubiquitylated and degraded by the proteasome

(17, 18). Inhibition of the proteasome led to accumulation of SUMO-2/3 conjugates and the depletion of the pool of non-conjugated SUMO-2/3, indicating that this biochemical pathway is required for SUMO-2/3 recycling. SUMO and ubiquitin can form hybrid chains, including via lysine 32 of SUMO-2 or lysine 33 of SUMO-3 (17).

The SUMO system and the ubiquitin system are linked together via the SUMO-targeted ubiquitin ligases (STUbLs), responsible for ubiquitylating SUMOylated proteins. They were first identified in *Schizosacharomyces pombe* as Rfp1 and Rfp2 and in *Saccharomyces cerevisiae* as the Slx5-Slx8 complex (19, 20). Rfp1 and -2 each have an N-terminal SIM and a C-terminal RING-finger domain to enable interaction with SUMOylated proteins. Ubiquitin E3 ligase activity is obtained by RING-RING-mediated recruitment of the active RING-finger protein Slx8. RNF4 is a major mammalian STUbL containing four N-terminal SIMs and a C-terminal RING domain that enables homodimerization (21). More recently, RNF111/Arkadia was identified as a second mammalian STUbL (22, 23).

STUbLs play key roles in the DNA damage response (24). *Schizosacharomyces pombe* strains deficient for STUbLs display genomic instability and are hypersensitive to different DNA damaging agents including hydroxyurea (HU), methylmethane sulfonate (MMS), camptothecin (CPT) and ultraviolet (UV) light (19, 20). RNF4 knockdown in human cells also results in increased sensitivity to DNA-damaging agents (25). Moreover, RNF4 accumulates at DNA damage sites induced by laser micro-irradiation (25-27). SUMOylated target proteins for RNF4 include MDC1 and BRCA1 (27, 28) and furthermore HIF-2 α (29). Mice deficient for RNF4 die during embryogenesis (27, 30). Mice expressing strongly reduced levels of RNF4 are born alive, albeit at a reduced Mendelian ratio, and showed an age-dependent impairment in spermatogenesis (27). MEFs derived from these mice exhibit increased sensitivity to genotoxic stress.

A key feature of ubiquitin-like modification systems is their reversible nature to carefully balance cellular systems (2, 31). Deubiquitylating enzymes (DUBs) play a pivotal role in the regulation of cellular ubiquitylation levels, essentially controlling all cellular processes. There are around 100 DUBs, with different substrate specificity, subcellular localization, and protein-protein interactions (31, 32). Currently, it is not clear how the activity of the STUbLs is balanced. Here, we report the identification of a ubiquitin-specific protease with the ability to counteract RNF4.

Results

Purification of FLAG-tagged Ring Finger Protein 4 (RNF4) from MCF7 cells

SUMO-targeted ubiquitin ligase RNF4 specifically recognizes targets that are modified by multiple SUMOs, through recognition of the SUMO-fold with its SUMOylation Interacting Motifs (SIMs) (11, 33). Subsequently, these SUMOylated targets are

ubiquitylated by RNF4, which can lead to the degradation of these proteins by the proteasome (21, 34, 35). Poly-SUMOylated targets of RNF4 have been identified employing a trap consisting of the RNF4 SIM-domain (36).

We were interested in identifying SIM-independent RNF4 interactors. In order to facilitate this study, an MCF7 cell line stably expressing C-terminally FLAG-tagged RNF4 was generated, and a biological triplicate experiment comparing the parental MCF7 cell line versus the RNF4-FLAG cell line was performed. The levels of RNF4-FLAG in all experiments were investigated following lysis of the cells (Figures 1A and 1B). Relative to the endogenous RNF4, there is a moderate overexpression of RNF4-FLAG. Considering the highly specific nature of the FLAG antibody, and the exploratory nature of our experiment, such expression levels are acceptable. The subcellular localization of RNF4-FLAG was inspected by confocal fluorescent microscopy, demonstrating the fusion protein to be located correctly and exclusively in the nucleus (Figure 1C). Some of the RNF4-FLAG localized into nuclear bodies, which likely correspond to PML nuclear bodies. The non-fused and co-expressing Green Fluorescent Protein (GFP) was included as a control.

We performed FLAG-immunoprecipitation (IP), and found that RNF4-FLAG is very efficiently purified, with no other signal other than RNF4-FLAG being detectable by immunoblot (Figure 1D). Lysis of the cells and IP of FLAG was performed under relatively stringent conditions, but mild enough for the robust SUMO-specific proteases (SENPs) to still be able to cleave SUMO off all target proteins. Finally, prior to in-gel digestion and LC-MS/MS analysis, Coomassie analysis of the purified RNF4-FLAG and its potential interactors revealed a singular and very clear band corresponding to RNF4-FLAG, indicative of a clean and highly stringent purification of RNF4-FLAG (Figure 1E).

Identification of Ubiquitin-Specific Protease 11 (USP11) as an Interactor of RNF4

The RNF4-FLAG IP was performed in biological triplicate, and the gel lanes were cut in five separate slices and analyzed by mass spectrometry experiments. Over 800 proteins were identified in the FLAG-IP samples, with nearly all of these proteins being background proteins equally identified in the RNF4-FLAG line and the parental control. Only a few proteins were specifically and significantly enriched in the RNF4-FLAG line, indicative of the stringent purification conditions. Strikingly, we did not detect free or conjugated forms of SUMO in the IP, proving that our lysis and IP conditions were sufficiently harsh to yield a clean IP, yet mild enough to allow the highly robust SENPs to cleave SUMO off virtually all proteins. Unsurprisingly, RNF4 itself was detected as the highest enriching protein after RNF4-FLAG IP. Furthermore, we identified the ubiquitin carboxyl-terminal hydrolase 11 (USP11) as an important RNF4 interactor (Figure 2A), as USP11's innate function as a ubiquitin protease

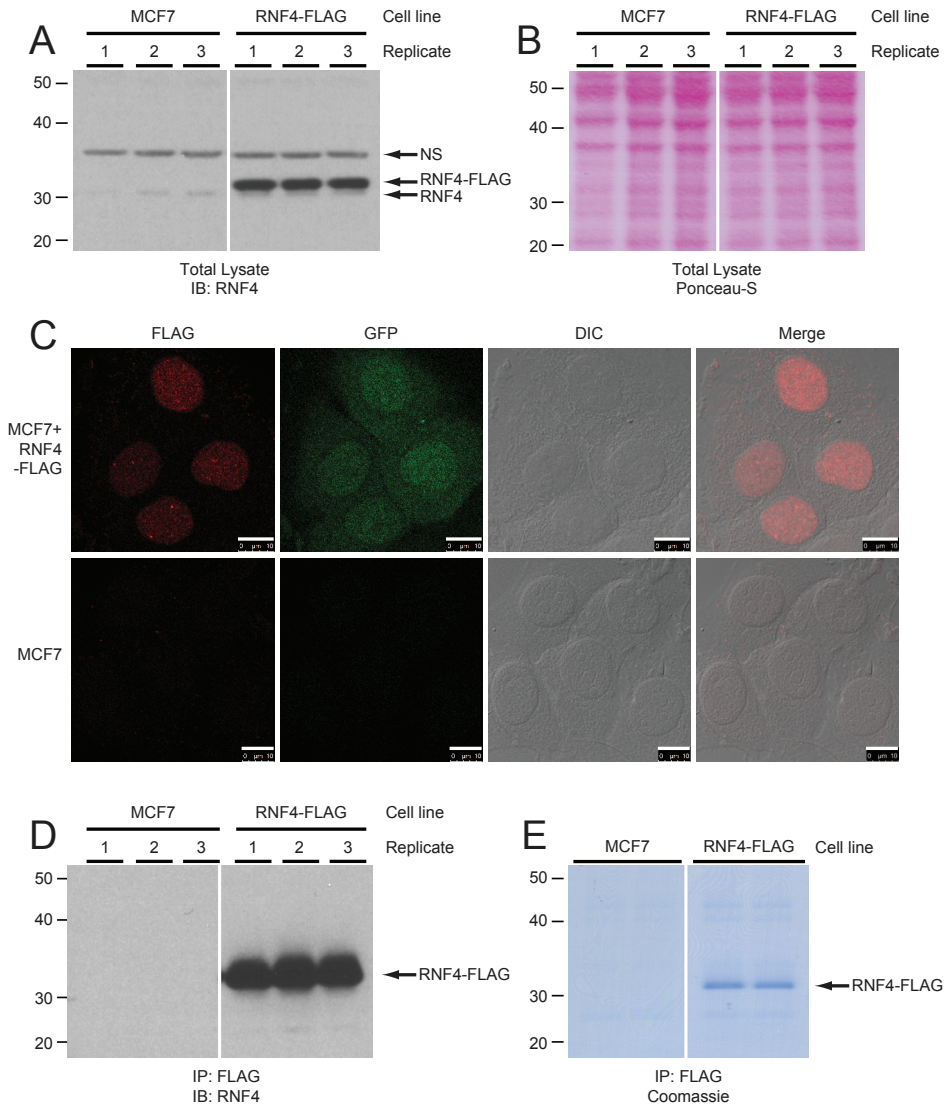


Figure 1. Generation of a cell line stably expressing RNF4-FLAG. A) MCF7 cells were infected with a bicistronic lentivirus encoding RNF4-FLAG and GFP separated by an Internal Ribosome Entry Site (IRES). Cells stably expressing low levels of the transgene were selected by flow cytometry. Total lysates were analyzed by immunoblotting to confirm expression of RNF4-FLAG relative to endogenous RNF4. The experiment was performed in biological triplicate for mass spectrometric analysis. B) Ponceau-S loading control for section A. C) Stable cell lines were investigated by confocal fluorescent microscopy to confirm the nuclear localization of RNF4-FLAG. GFP was visualized as an expression control, and differential interference contrast (DIC) was used to localize the cellular nuclei. Scale bars represent 10 μm . D) RNF4 complexes were purified by immunoprecipitation (IP), and three biological replicates were analyzed by immunoblotting (IB) for the presence of RNF4. Parental cells were included as a negative control. E) Coomassie analysis of one replicate of the FLAG-IP, loaded over two lanes, prior to in-gel digestion and analysis by LC-MS/MS.

is directly opposing of RNF4's function as a ubiquitin ligase. USP11 was found to be enriched over the control with a Log_2 ratio of 5.1, and eleven MS/MS spectral identifications matching USP11 were made in the RNF4-FLAG IP as opposed to zero in the control IP.

After finding USP11 as an interactor of RNF4 through mass spectrometry analysis, the experiment was repeated, and samples were analyzed by immunoblotting (Figure 2B). Additionally, a potential effect of the DNA damaging agent methyl methanesulfonate (MMS) on the interaction between RNF4 and USP11 was investigated, as MMS is known to cause disassembly of the PML nuclear bodies harboring RNF4 (37). After RNF4-FLAG IP, immunoblot analysis with an antibody against endogenous USP11 shows a very clear and specific interaction with RNF4, with no signal detectable in the parental control (Figure 2B). There was no indication that the interaction between RNF4 and USP11 is disrupted upon treating the cells with MMS. A small decrease in both RNF4 and USP11 levels was observed after DNA damage, indicative of their function in the DNA damage response, which may eventually lead to their degradation. Even though input levels of both RNF4-FLAG and USP11 dropped slightly after MMS treatment, the detectable level of USP11 co-immunoprecipitating with RNF4 remains identical. Finally, equal protein loading was validated through Ponceau-S staining, and immunoblot analysis with an antibody against SUMO-2 was performed to investigate the SUMOylation state of proteins in the total lysate and the IP fractions (Figure 2C). In agreement with the mass spectrometry findings, free SUMO was detected only in the total lysates, a direct result of the SENPs removing all SUMO from target proteins following lysis, indicating that the interaction between USP11 and RNF4 is SUMOylation-independent.

USP11 deubiquitylates SUMO-2-ubiquitin hybrid chains *in vitro* in a SIM-dependent manner

To test whether USP11 can counteract RNF4 *in vitro*, a hybrid SUMO-2-ubiquitin polymer was generated as a potential USP11 substrate, using a recombinant linear SUMO-2 polymer, composed of four SUMO proteins which was ubiquitylated *in vitro* by RNF4 (21). Subsequently, recombinant USP11 was added to the reaction to analyze the deubiquitylation activity of USP11. Adding wild type USP11 resulted in the deubiquitylation of SUMO-2-ubiquitin hybrid chains while adding a catalytic inactive USP11 mutant (C318A) had no effect on these chains (Figure 3A). Since USP11 and RNF4 were simultaneously present in the reaction mixture, a limited amount of ubiquitylated SUMO-2 polymer was still detected, probably representing multiple mono-ubiquitylated forms. We conclude that USP11 could indeed counteract the activity of RNF4 on a SUMO-2 polymer *in vitro*.

Analysis of the USP11 sequence revealed four potential SIMs located in an undefined domain between the DUSP and UCH domains of USP11 (Figure

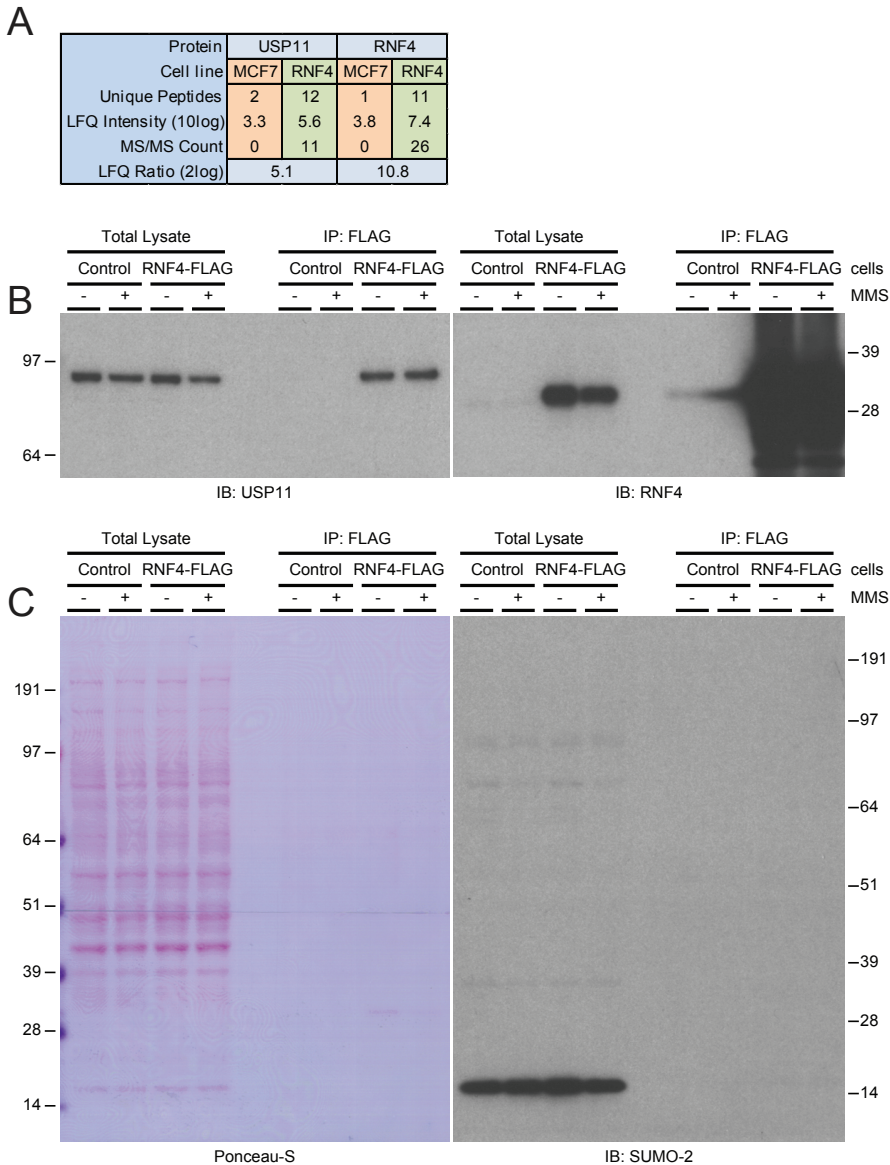


Figure 2. Identification of USP11 as an RNF4-interacting ubiquitin protease. A) Overview of the mass spectrometry results pertaining to USP11 and RNF4. USP11 was found to be significantly enriched after FLAG-IP from the RNF4-FLAG stable cell line, with 0/0/0 USP11 MS/MS counts in the parental line versus 8/14/11 USP11 MS/MS counts in the RNF4-FLAG line, respectively. USP11 was found to be enriched after RNF4-FLAG IP with a Label-Free Quantification (LFQ) Log_2 ratio of over 5. B) MCF7 cell lines expressing RNF4-FLAG and parental controls were treated with methyl methanesulfonate (MMS), lysed, and FLAG-IP was performed. Total lysates and IP fractions were analyzed by immunoblotting against USP11 to confirm the co-immunoprecipitation of endogenous USP11 with RNF4-FLAG. Immunoblotting for RNF4 was performed as an immunoprecipitation control. C) Ponceau-S loading control for section B. Additionally, total lysates and IP fractions were analyzed by immunoblotting against SUMO-2 to investigate potential co-immunoprecipitation of SUMO-2 with RNF4 through its SUMO-interacting motifs (SIMs).

Chapter 3

3B). To further establish confidence in these SIMs, PHYRE2 (38) was used to generate a structural model of USP11 (Figure S1A). Using homology modeling and superimposition of multiple homologous known structural elements, a USP11

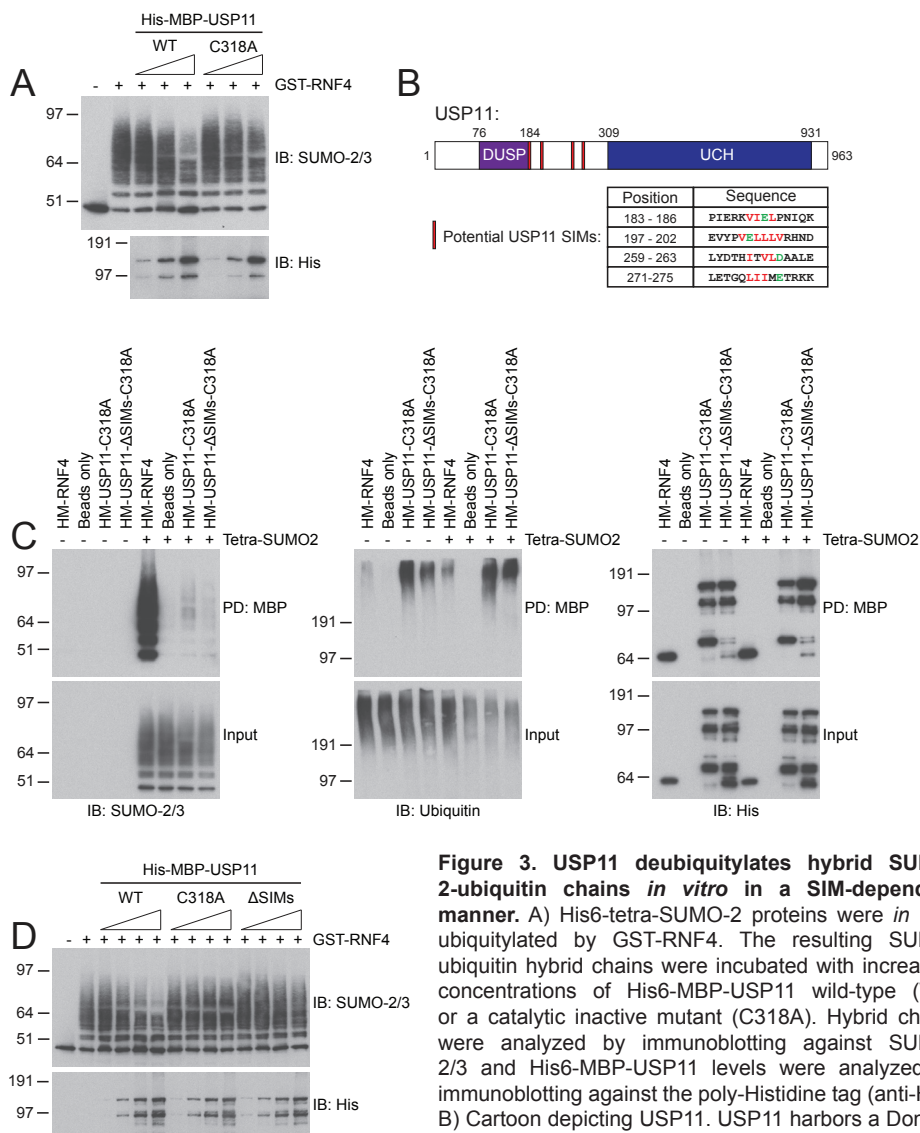


Figure 3. USP11 deubiquitylates hybrid SUMO-2-ubiquitin chains *in vitro* in a SIM-dependent manner. A) His6-tetra-SUMO-2 proteins were *in vitro* ubiquitylated by GST-RNF4. The resulting SUMO-ubiquitin hybrid chains were incubated with increasing concentrations of His6-MBP-USP11 wild-type (WT) or a catalytic inactive mutant (C318A). Hybrid chains were analyzed by immunoblotting against SUMO-2/3 and His6-MBP-USP11 levels were analyzed by immunoblotting against the poly-Histidine tag (anti-His). B) Cartoon depicting USP11. USP11 harbors a Domain present in Ubiquitin-Specific Proteases (DUSP) and an

Ubiquitin Carboxyl-terminal Hydrolase domain (UCH). USP11 contains four potential SUMO interacting motifs (SIMs), located in between the DUSP and UCH domains. Hydrophobic residues depicted in red were incubated replace by alanines to generate a USP11 Δ SIM mutant. C) Ubiquitin chains only (-) or SUMO-2-Ubiquitin mixed chains (+) were incubated with His6-MBP(HM)-RNF4, His6-MBP(HM)-USP11-C318A, or His6-MBP(HM)-USP11-C318A proteins where the four potential SIMs were mutated (Δ SIMs-C318A). His6-MBP proteins were subsequently purified with amylose beads to enrich for the MBP tag. Amylose beads-only samples were used as a negative control. Inputs and bound proteins were analyzed by immunoblotting with the indicated antibodies. D) The experiment described in section A was repeated and the His-MBP-USP11- Δ SIMs protein was included to study the contribution of the SIMs.

structure was generated with 65% of residues modeled at 90% or greater confidence. 283 out of 931 residues could not be aligned to existing structures, and were modeled *ab initio*. These residues were mainly located within the center of the UCH. The four potential SIMs in USP11 (Figure 3B and S1B) were observed to be located on a “bridge” connecting the DUSP with the UCH domains in a clustered manner to enable synergistic binding to SUMO polymers (Figure S1C). All of the SIMs were solvent-exposed, and located in a region of USP11 accessible for small proteins such as SUMO or ubiquitin.

A USP11 mutant lacking SIMs (Δ SIMs) was generated by mutating the large hydrophobic residues in the SIMs to alanines. Note that this mutant was made in the background of the C318A mutant to prevent deubiquitylation activity on the chains during the interaction experiments. To analyze the interaction between USP11 and SUMO-2 and/or ubiquitin, the SUMO-Ubiquitin mixed chains described above or unanchored ubiquitin chains made by RNF4 were used. SUMO-2/3 immunoblot analysis confirmed the strong interaction between RNF4 and SUMO-2-Ubiquitin mixed chains. Compared to RNF4, USP11 displayed a weak but visible interaction with these mixed chains and this interaction was reduced by mutating the SIMs of USP11 (Figure 3C). In contrast, USP11 had more affinity for binding unanchored ubiquitin chains as compared to RNF4 (Figure 3C).

Interestingly, mutating these four SIMs in USP11 prevented the processing of these hybrid chains, indicating that USP11 deubiquitylates SUMO-ubiquitin hybrids in a SIM-dependent manner (Figure 3D).

USP11 counterbalances RNF4 and controls stability of nuclear bodies

Since RNF4 is known to ubiquitylate SUMOylated PML, which in turn leads to degradation of PML and the destabilization of nuclear bodies (21), we set out to study the role of endogenous USP11 in nuclear body integrity. Lentiviral shRNA-mediated depletion of endogenous USP11 or RNF4, or depletion of both proteins was performed in U2OS cells, prior to analysis of the cells by confocal Z-stacked fluorescent microscopy (Figure 4A). The effect on PML bodies and additionally the effect on other SUMO nuclear bodies was investigated. Although SUMO and PML can co-localize in nuclear bodies, the overlap is limited.

Strikingly, after depletion of endogenous USP11, a significant reduction in PML and SUMO nuclear bodies was observed (Figure 4A). Accordingly, depletion of endogenous RNF4 led to significant increases in PML bodies and SUMO bodies. Multiple fields of cells were recorded, and at least 400 cells per experimental condition were quantified, by counting several thousands of nuclear bodies. Ultimately, a 25% reduction in PML bodies and a 50% reduction in SUMO bodies was found upon USP11 depletion, and a 35% increase in PML bodies and a 50% increase in SUMO bodies upon RNF4 depletion (Figure 4B). Efficient depletion of both USP11 and

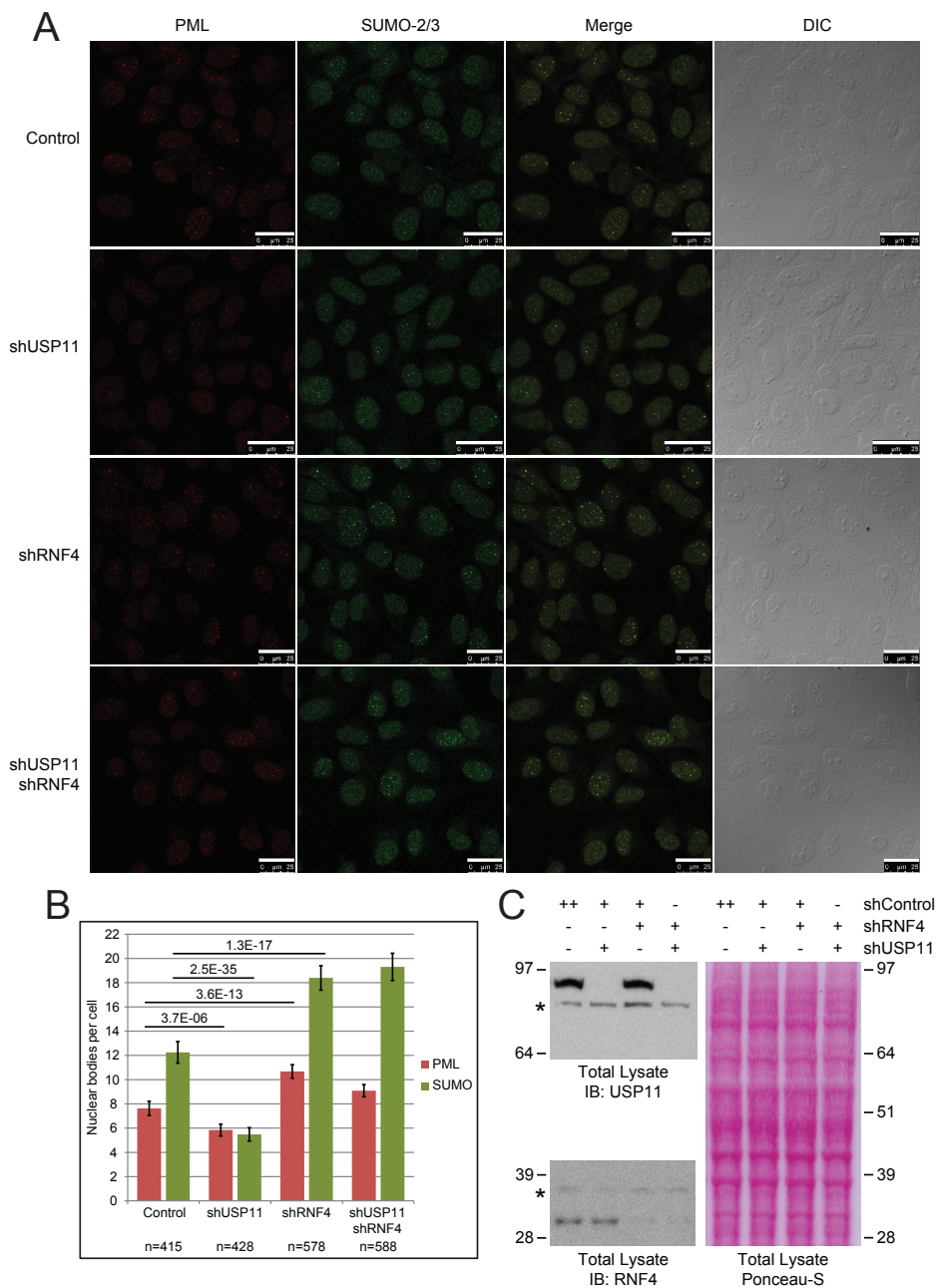


Figure 4. USP11 stabilizes PML and SUMO nuclear bodies, counteracting the destabilizing effect of RNF4. A) U2OS cells were depleted for endogenous USP11, RNF4, or both, by infection with lentiviral knockdown constructs. As a control, an untargeted lentiviral knockdown construct was used. Following depletion of proteins, cells were fixed, immunostained and subsequently analyzed by confocal fluorescence microscopy for the presence of PML and SUMO-2/3 positive nuclear bodies. Images represent maximum projections of Z-stacks. DIC was used to visualize the nuclei. Depletion of USP11 destabilizes PML and

SUMO-2/3 nuclear bodies, whereas depletion of RNF4 stabilizes PML and SUMO-2 nuclear bodies. Scale bars represent 25 μm . B) Multiple maximum projected fields of cells were recorded as in section A. Cells were counted, and PML and SUMO-2/3 nuclear bodies were quantified per cell. At least 400 cells were counted for each experimental condition, with the exact number of cells shown below each experiment. Error bars represent 2x SEM. Student's t-test p-values are indicated over their respective experiments. C) Total cell lysates were analyzed by immunoblotting to confirm the depletion of USP11 and RNF4.

RNF4 was confirmed through immunoblot analysis (Figure 4C). Similar results were obtained in MCF7 cells (data not shown).

Interestingly, when combining depletion of both USP11 and RNF4, a somewhat intermediate phenotype was observed (Figures 4A and 4B). Whereas the increase in PML bodies resulting from depletion of RNF4 was modestly countered by additional knockdown of USP11, there was no clear effect on SUMO positive nuclear bodies. Thus, it is likely that USP11 acts downstream of RNF4, providing an important counterbalancing mechanism to the ubiquitin ligase activity of RNF4 to establish an important equilibrium characteristic of ubiquitin signaling and generally characteristic for post-translational modifications.

USP11 modulates the level of SUMOylated PML

In addition to cellular analysis by microscopy, the SUMOylation state of the PML protein after depletion of endogenous USP11 in HeLa cells was investigated. In order to facilitate the experiment, HeLa cell lines stably expressing His-tagged SUMO-2 were used to allow for efficient purification of SUMOylated proteins. Additionally, a similar cell line stably expressing lysine-deficient His-tagged SUMO-2 was used in order to investigate a potential effect of inhibited SUMO-2 chain formation on the SUMOylation of PML, and any cumulative result in combination with USP11 depletion. Parental HeLa cells, and the two cell lines expressing the His-tagged SUMO-2 wild-type or lysine-deficient mutant, were all treated with either a lentiviral shRNA targeted against USP11 or a non-targeted shRNA. After depletion of USP11 and enrichment of SUMOylated proteins, total lysates and SUMO-enriched fractions were analyzed by immunoblotting using an antibody against PML (Figure 5A).

Similar to observations made with counting PML bodies, a significant decrease in SUMOylated PML was found after depletion of USP11, in both total lysate and SUMO-enriched fractions. Interestingly, in the cell line expressing lysine-deficient SUMO-2, PML was found to be SUMOylated at a somewhat lower base level as compared to the cell line expressing wild-type SUMO-2 (Figure 5A). However, a further decrease in SUMOylated PML upon additional USP11 depletion was still observed. Thus, while SUMO-2 deficient in chain-formation reduced the overall levels of SUMOylation on PML, RNF4 was still able to ubiquitylate SUMOylated PML, and USP11 was still able to counteract RNF4 and protect SUMOylated PML from degradation.

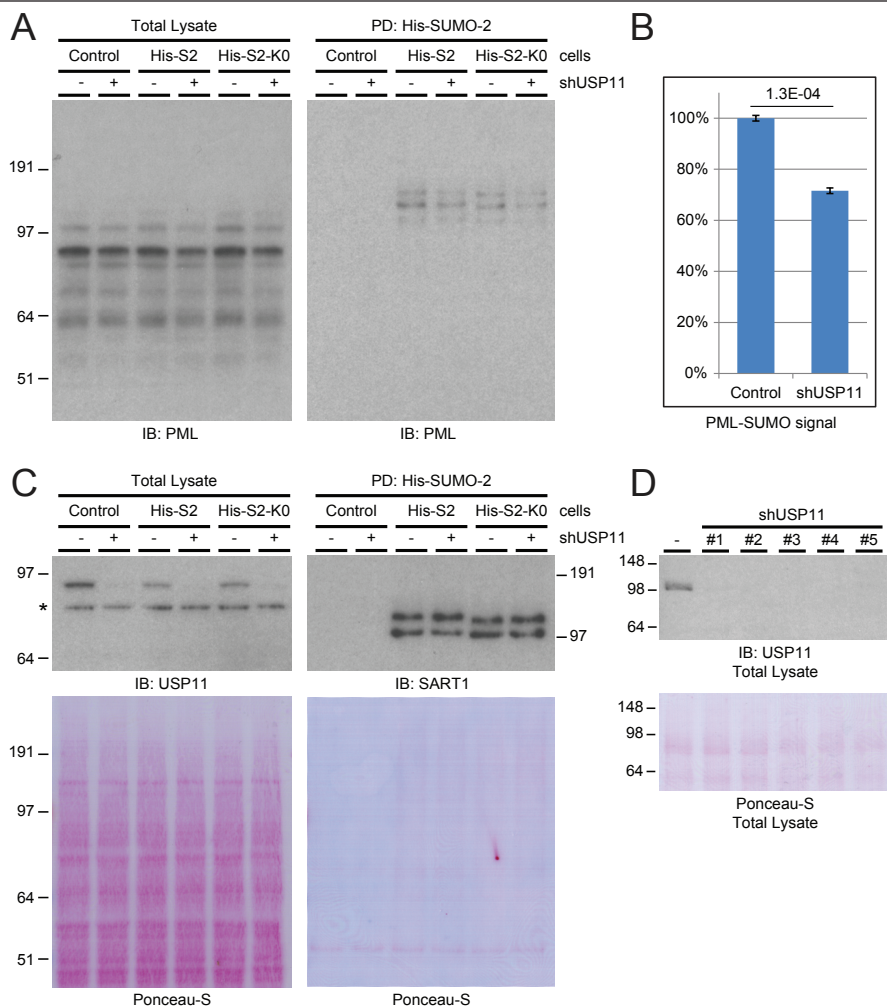


Figure 5. USP11 stabilizes SUMOylated PML. A) HeLa cells expressing His-tagged SUMO-2, HeLa cells expressing His-tagged lysine-deficient SUMO-2, and parental HeLa cells were either depleted of USP11 by infection with lentiviral knockdown constructs, or treated with an untargeted knockdown construct. After depletion of USP11 cells were lysed, and His-pull-down was performed to enrich SUMOylated proteins. Total lysates and SUMO-enriched fractions were analyzed by immunoblotting using an antibody against PML. Note that PML modified with lysine-deficient SUMO has slightly different migration behavior due to lysine-to-arginine substitutions. B) Quantification of the PML-SUMO signal in the total lysate and SUMO-enriched lanes corresponding to the His-SUMO cell lines, comparing the PML-SUMO signal in the control versus USP11-depleted cells. Error bars represent standard deviation. Student's t-test p-value is indicated. C) Total lysates from section A were analyzed by immunoblotting with an antibody versus USP11 as a knockdown control, and Ponceau-S staining was used as a loading control. SUMO-enriched fractions from section A were analyzed by immunoblotting with an antibody versus SART1 as a SUMO-level control, and Ponceau-S staining was used as a pull-down control. Note that SART1 modified with lysine-deficient SUMO has slightly different migration behavior due to lysine-to-arginine substitutions. D) HeLa cells were depleted of USP11 by infection with five different lentiviral knockdown constructs, or treated with an untargeted knockdown construct. Subsequently, cells were lysed, and total lysates were analyzed by immunoblotting using an antibody against USP11. All five viruses were found to be efficient, and a low-concentration mixture of all viruses was used for all other USP11 depletion experiments to provide an effective knockdown.

The decrease in SUMOylated PML signal was found to be 30% (Figure 5B); highly similar to the 25% decrease in PML nuclear bodies observed through confocal microscopy (Figure 4B). Efficient depletion of endogenous USP11 was validated by immunoblotting (Figures 5C and 5D), and additionally the well-known SUMOylation target protein SART1 (39) was investigated as a control for equal SUMO-enrichment (Figure 5C). The SUMOylation state of SART1 was virtually identical regardless of USP11 depletion, indicating that the effect on PML SUMOylation was specific. Note that the slight shift in migration behavior visible between the wild-type SUMO-2 and the lysine-deficient SUMO-2 is a direct effect of lysine-to-arginine substitutions. Equal total lysate loading and equal pulldown efficiency and loading were confirmed by Ponceau-S staining (Figures 5C and 5D).

USP11 prevents the disintegration of nuclear bodies in response to DNA damage

In order to investigate the extent of protection USP11 offers to SUMOylated PML and their associated nuclear bodies, an overexpression experiment was performed where U2-OS cells were transfected with V5-tagged USP11. Subsequently, the cells were treated with MMS, which is known to cause degradation of SUMOylated PML and instigate a disassembly of nuclear bodies (37). The treatment dose and time chosen for the experiment was sufficient to completely abolish all PML nuclear bodies. Confocal fluorescence microscopy was used to investigate mock treated cells, as well as cells treated with MMS for an extended period of time. Antibodies directed against the V5 tag and against PML were used to detect exogenous V5-USP11 and PML nuclear bodies, respectively. Differential interference contrast (DIC) was used to visualize the nuclei (Figure 6).

In untreated cells, nuclear bodies were observed to be distributed fairly equally between cells expressing V5-USP11 and untransfected cells. However, upon MMS treatment, all untransfected cells completely lost their nuclear bodies, whereas many cells overexpressing V5-USP11 were able to retain some PML nuclear bodies, and in some cases these cells even retained all PML bodies (Figure 6). Thus, an increased presence of USP11 within the cell was able to counteract the ubiquitylation and degradation of SUMOylated PML, and could counteract the disassembly of the PML nuclear bodies in response to DNA damage.

DISCUSSION

Using a proteomic screen, we have identified USP11 as a ubiquitin protease that co-purified with RNF4, possessing the ability to process hybrid SUMO-ubiquitin polymers. This USP family member contains a DUSP domain with the ability to bind ubiquitin, as well as a catalytic UCH domain. Furthermore, four putative SIMs are harboured between the DUSP and UCH domains. Combined, these domains

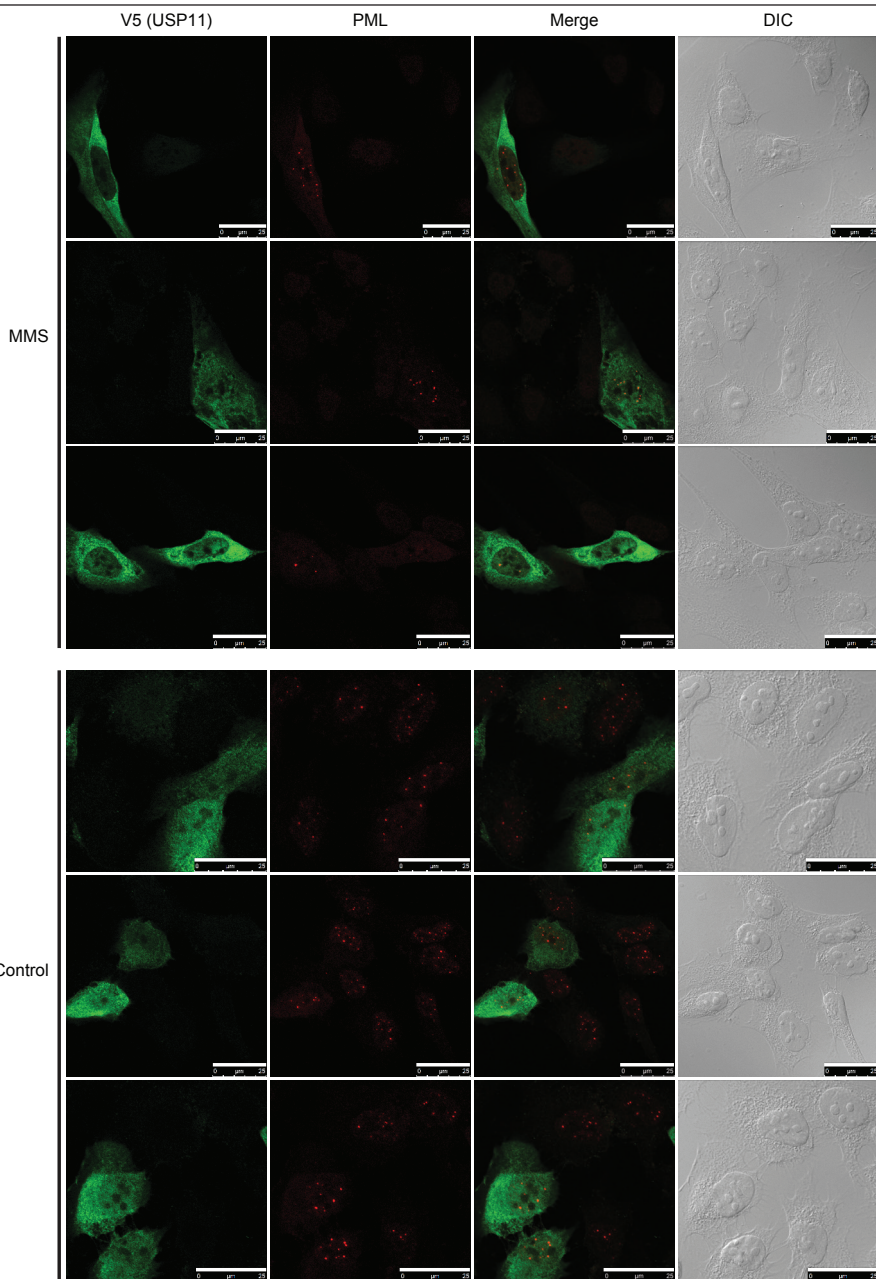


Figure 6. USP11 counteracts RNF4-mediated degradation of nuclear bodies in response to treatment the DNA damaging agent methyl methanesulfonate. U2OS cells were transfected with a construct encoding V5-USP11, and subsequently mock treated or treated with 0.02% MMS for 135 minutes. Following treatment, cells were fixed, and immunostained. Confocal fluorescence microscopy was used to visualize V5 (USP11 - green) and PML (red). DIC was used to visualize nuclei. Three separate fields of cells are shown for each experimental condition. Upon treatment with MMS, cells overexpressing USP11 retain PML bodies, whereas PML bodies disintegrate in all other cells. Scale bars represent 25 μm .

enabled the processing of hybrid SUMO-ubiquitin chains that were synthesized by RNF4. USP11 was able to deubiquitylate these hybrid chains via its catalytically active C-terminal hydrolase domain. A USP11 mutant lacking the four SIMs between the DUSP domain and the UCH domain was found to be deficient in deubiquitylating hybrid SUMO-ubiquitin chains.

USP11 possesses the ability to counteract RNF4 during regular growth conditions. Depletion of USP11 led to a decrease in the amount of nuclear bodies, whereas depletion of RNF4 led to the exact opposite. Furthermore, we observed cells containing a far-above-average amount of PML and SUMO bodies even with the double knockdown, analogous to RNF4-only knockdown (Figure 4A and 4B). This could be indicative of USP11 primarily functioning downstream of RNF4. If SUMOylated proteins were not ubiquitylated in the first place, USP11 would logically not have SUMOylated proteins to deubiquitylate. We also noted that USP11 knockdown led to a decrease in the SUMOylated form of PML, indicative of a more rapid degradation through the mechanistic action of RNF4. We did not note a large effect of USP11 on total PML levels overall, as compared to the SUMOylated form (Figure 5A).

Moreover, we found that USP11 could counteract RNF4's role in the DNA damage response by blocking the dissociation of PML bodies in response to MMS. We also observed a slight decrease in USP11 levels after MMS treatment in MCF7 cells (Figure 2B), suggesting that USP11 may be degraded or otherwise inactivated. The dissociation of PML bodies enables proper progression of the DNA damage response (40) or induction of apoptosis (41, 42).

USP11 was previously found to be involved in repair of double-stranded breaks by homologous recombination, where knockdown of USP11 resulted in spontaneous activation of DNA damage response pathways, rendering cells hypersensitive to PARP inhibition, ionizing radiation and other genotoxic stresses (43). This finding coincides with our findings, as a loss of PML bodies could prohibit cells from properly responding to DNA damage, and could ambiguously initiate the DNA damage response or cause induction of apoptosis. Similarly, the ability to rescue PML bodies by overexpression of USP11 would thus serve to block the DNA damage response from proceeding efficiently. Furthermore, USP11 has been shown to interact with BRCA2, a key component of the homologous recombination pathway, where BRCA2 was shown to be a target for deubiquitylation by USP11 (44). Treatment of cells by Mitomycin C led to a degradation of BRCA2, which could be countered by USP11 overexpression, and inhibition of USP11's function increased cellular sensitivity to Mitomycin C (44). BRCA2 is not known to be SUMOylated. Similar to USP11, RNF4 is also required for homologous recombination (25-27), indicating that balanced ubiquitylation and deubiquitylation of SUMOylated proteins is required for efficient DNA repair via homologous recombination.

Chapter 3

The function of USP11 in the DNA damage response makes it a potential clinical target, as inhibition of USP11 would render cancer cells susceptible to apoptosis, especially combined with other treatments such as PARP inhibition. Accordingly, some progress has been made on compounds targeting and counteracting USP11, displaying the ability to inhibit pancreatic cancer cells (45).

More recently, USP11 has been found to interact directly with PML (46). Contrarily, we found USP11 to interact with the SUMO-targeted ubiquitin ligase RNF4, and a set of SIMs in USP11 potentiated its activity towards hybrid SUMO-ubiquitin chains. Wu et al. further reported that USP11 depletion leads to a decrease in PML bodies, which is consistent with our findings. USP11 overexpression was shown by Wu et al. to be able to counteract arsenic-induced degradation of PML, but a role in the DNA damage response was not investigated by Wu et al. USP11 was found to be transcriptionally repressed in human glioma, with upregulation of the Hey1/Notch pathway resulting in downregulation of USP11 and correspondingly PML (46). Interestingly, this was found to increase cellular malignancy as well as potentiate survival and resistance to therapeutic treatment, which is directly opposing findings where antagonizing USP11 leads to inhibition of pancreatic cancer (45), and general findings where USP11 depletion leads to cellular hypersensitivity to DNA damage (43, 44).

We propose that USP11 keeps RNF4 in check, and is able to reverse RNF4's ubiquitylation of SUMOylated proteins (Figure 4B). Under certain stress conditions, such as DNA damage, USP11 loses its ability to effectively counteract RNF4, allowing the cellular stress response to proceed efficiently. Thus, our results provide novel insight in crosstalk between SUMOylation and ubiquitylation, and further elucidate the function of USP11 in the DNA damage response.

Materials and methods

Plasmids

The cDNA encoding the USP11 protein was a kind gift from Dr. Long Zhang. The cDNA encoding the RNF4 protein was obtained from the Mammalian Gene Collection (Image ID 4824114; supplied by Source Bioscience). Both cDNAs were amplified by a two-step PCR reaction using the following primers: 5'-AAAAAGCAGGCTATATGGCAGTAGCCCCGCGACTG-3' and 5'-AGAAAGCTGGGTGTCAATTAACATCCATGAATC-3' (USP11), 5'-AAAAAGCAGGCTCAATGAGTACAAGAAAGC-3' and 5'-AGAAAGCTGGGTTTCATATATAAATGGGGT-3' (RNF4) for the first reaction and 5'-GGGGACAAGTTTGTACAAAAAAGCAGGCT-3' and 5'-GGGGACCACTTTGTACAAGAAAGCTGGGT-3' for the second reaction. RNF4 was cloned in between the *SpeI* and *XhoI* sites of the plasmid pLV-CMV-X-FLAG-IRES-GFP (kind gift from Dr. R.C. Hoeben). Additionally, RNF4 and USP11 cDNAs were inserted into pDON207 employing standard Gateway technology (Invitrogen). The C318A mutation in USP11 was introduced by QuickChange site-directed mutagenesis (Stratagene) using oligonucleotides 5'-CAATCTGGGCAACACGGCCTTCATGAAGCTCGG-3'

and 5'-CCGAGTTCATGAAGGCCGTGTTGCCAGATTG-3'. pDON207-USP11-C318A-ΔSIMs was generated by a gene synthesis service (GenScript) by replacing residues V183, I184, L186, V197, L199, L200, L201, L202, V203, I259, V261, L262, L271, I272, I273 and M274 with alanines. These different cDNAs were subsequently transferred to the destination vector pDEST-T7-His6-MBP (a kind gift from Dr. L. Fradkin). RNF4 was cloned into pGEX-2T to obtain a construct encoding GST-tagged RNF4 by amplifying RNF4 cDNA using the following primers: 5'-ACAAACGGATCCATGAGTACAAGAAAGCGTCGTG-3' and 5'-GCCGCGGAAT TCTCATATATAAATGGGGTGGTAC-3'. Both the PCR product and the pGEX-2T vector were subsequently digested with *Bam*HI and *Eco*RI and the PCR product was ligated into the vector with T4 ligase (New England Biolabs). The His6-ΔN11-SUMO-2-Tetramer expression vector was a kind gift of Prof. Dr. R.T. Hay (Dundee, U.K.) (21).

Cell culture & cell line generation

MCF7, U2-OS and HeLa cells were cultured in Dulbecco's Modified Eagle's Medium (DMEM) supplemented with 10% FBS and 100 U/mL penicillin and streptomycin (Invitrogen). MCF7 cells stably expressing RNF4-FLAG were generated through lentiviral infection with a construct carrying RNF4-FLAG-IRES-GFP. The Internal Ribosome Entry Site (IRES) allowed the same mRNA to code for a non-fused GFP, in order to quantify RNF4-FLAG expression without adding a bulky fusion tag to RNF4. Similarly, MCF7 and HeLa cell lines stably expressing His-SUMO-2 were generated through lentiviral infection with a construct encoding His-SUMO-2-IRES-GFP. Two weeks after infection, cells were sorted for a low level of GFP by flow cytometry, using a FACSAria II (BD Biosciences). All cells were cultured in CELLSTAR flasks (175cm²) and petri dishes (145 x 20 mm) (both from Greiner Bio-One).

Treatments, transfection and lentiviral infection

Cells were treated with 0.02% MMS and 1 μM As₂O₃ (Sigma) for the indicated amounts of time. For transfection, cells were cultured in DMEM lacking penicillin and streptomycin. Transfections were performed using 2.5 μg of polyethylenimine (PEI) per 1 μg of plasmid DNA, using 1 μg of DNA per 1 million cells. Transfection reagents were mixed in 150 mL NaCl and allowed to rest for 15 minutes before adding it directly to the cells. Cells were split after 24 hours (if applicable) and investigated after 48 hours. Lentiviruses were generated essentially as described previously (47). Infections were performed with a multiplicity of infection of 2 and using a concentration of 8 μg/mL polybrene in the medium. 24 hours after infection the medium was replaced. Cells were split 72 hours after infection (if applicable) and investigated 96 hours after infection.

RNF4-FLAG purification

Parental MCF7 cells and MCF7 cells stably expressing RNF4-FLAG were grown in regular DMEM, until fully confluent in 10x 15-cm dishes (approximately 0.2 billion cells). Cells were washed 3 times in ice-cold PBS prior to addition of 3 mL of ice-cold Lysis Buffer to each plate (150 mM NaCl, 50 mM TRIS, 0.5% sodium deoxycholate, 1.0% N-P40, buffered at pH 7.5, with every 10 mL of Lysis Buffer supplemented by one tablet of protease inhibitors + EDTA (Roche)). Subsequently, cells were scraped in the Lysis Buffer, on ice, and collected in 50 mL tubes. The lysates were sonicated on ice for 10 seconds using a

Chapter 3

microtip sonicator at 30 Watts. Next, lysates were centrifuged at 4 °C and 10,000 RCF to clear debris from the soluble fraction. Lysates were equalized using the bicinchoninic acid assay (BCA, Pierce). 1 μ L (dry volume) of FLAG-M2 agarose beads (Sigma) were prepared per 1 mL of lysate, and equilibrated by washing 5 times in ice-cold Lysis Buffer. FLAG-M2 beads were added to the lysates and incubated while tumbling for 2 hours at 4 °C. Next, beads were pelleted by centrifugation at 250 RCF and washed 5 times with ice-cold Lysis Buffer. After every single wash step, the tubes were exchanged. RNF4-FLAG and interacting proteins were eluted off the beads by incubating them for 10 minutes with three bead volumes of Lysis Buffer supplemented with 1 mM FLAG-M2 peptide. Elution of the beads was repeated twice, and a fourth elution was performed with 2x LDS Sample Buffer (Novex). The primary three peptide elutions were pooled and concentrated. Culturing of cells, immunoprecipitation of RNF4-FLAG and subsequent steps leading to the LC-MS/MS analysis were performed in biological triplicate.

Purification of His-SUMO-2

Purification of His-SUMO-2-modified proteins was essentially performed as described previously (8).

Recombinant proteins

His6-MBP and His6- Δ N11-SUMO-2-Tetramer recombinant proteins were purified essentially as described previously (39). Briefly, BL21 cells were transformed with expression constructs. Cells were grown to an OD₆₀₀ of 0.6. Subsequently, cells were grown overnight at 24°C in the presence of 0.1 mM isopropyl- β -D-thiogalactopyranoside (IPTG), 20 mM HEPES pH 7.5, 1 mM MgCl₂ and 0.05% Glucose. Lysates were prepared and proteins were affinity-purified on TALON beads (BD Biosciences). GST-tagged RNF4 was produced in *E. coli* and purified as described previously (48).

In vitro ubiquitylation and deubiquitylation assay

15 ng of His6- Δ N11-SUMO-2-Tetramer was *in vitro* ubiquitylated using 8 μ M ubiquitin, 40 nM UBE1, 0.7 μ M UbcH5a (all from Boston Biochem), 0.5 μ M GST-RNF4 in 50 mM TRIS pH 7.5, 5 mM MgCl₂, 1 mM DTT, and 4 mM ATP. 5 μ L reactions were incubated at 37°C for three hours after which different concentrations (1 to 7.5 μ g) of His6-MBP-USP11 proteins were added to a final volume of 15 μ L. Reaction were incubated at 37°C for an additional three hours. Finally, reactions were stopped by adding 5 μ L 4X LDS Sample Buffer (Novex).

In vitro interaction assay

In vitro ubiquitylation reactions were performed as described above in the presence or absence of 250 ng His6- Δ N11-SUMO-2-Tetramer. Ubiquitin or SUMO-2-Ubiquitin chains were incubated with 5 μ g His6-MBP-RNF4, His6-MBP-USP11-C318A, His6-MBP-USP11- Δ SIMs-C318A or His6-MBP elution buffer in EBC buffer (50 mM TRIS pH 7.5, 150 mM NaCl, 1 mM EDTA, 1 mM DTT, 0.5 % NP-40) (23). Reactions were incubated at 4°C for 2 hours, and subsequently bound to 25 μ L of Amylose resin (New England Biolabs) for another 2 hours at 4°C. Beads were washed extensively with EBC buffer and finally eluted in 25 μ L 2X LDS sample buffer.

Electrophoresis and immunoblotting

Protein samples were size-fractionated on Novex 4-12% Bis-Tris gradient gels using MOPS as a running buffer (Invitrogen), or on regular SDS-PAGE gels with a Tris-Glycine running buffer. Size-separated proteins were transferred to Hybond-C membranes (Amersham Biosciences) using a submarine system (Invitrogen). Membranes were stained for total protein loading using Ponceau-S (Sigma). Membranes were blocked using PBS containing 0.1% Tween-20 (PBST) and 5% milk powder for one hour. Subsequently, membranes were incubated with primary antibodies as indicated, in blocking solution. Incubation with primary antibody was performed overnight at 4 °C. Subsequently, membranes were washed three times with PBST and briefly blocked again with blocking solution. Next, membranes were incubated with secondary antibodies (donkey-anti-mouse-HRP or rabbit-anti-goat-HRP) for one hour, before washing three times with PBST and two times with PBS. Membranes were then treated with ECL2 (Pierce) as per manufacturer's instructions, and chemiluminescence was captured using Biomax XAR film (Kodak).

Antibodies

The following antibodies were used in this study: mouse α FLAG (M2, Sigma), mouse α PML (5E10, kind gift from Prof. R. van Driel, University of Amsterdam (49)), rabbit α USP11 (A301-613A, Bethyl), mouse α SUMO-2/3 (8A2, Abcam), rabbit α SUMO-2/3 (raised against the C-terminus of SUMO-2), rabbit α RNF4 (raised against GST-RNF4), rabbit α SART1 (raised against GST-SART1), rabbit α V5 (V8137, Sigma), mouse α His (HIS-1, Sigma) and rabbit α Ubiquitin (9133, Santa Cruz).

Electrophoresis, Coomassie Staining and In-gel digestion

RNF4-FLAG IP samples were size-separated by SDS-PAGE using Novex 4-12% gradient gels and MES SDS running buffer (Invitrogen), followed by staining with Colloidal Blue Kit (Invitrogen). Gel lanes were excised as ten slices per eluted fraction, cut into 2-mm³ cubes and in-gel digested with sequencing-grade modified trypsin (Promega) as described before (Shevchenko et al., 2006). The peptides extracted from the gel after digestion were cleaned, desalted and concentrated on C18 reverse phase StageTips (50).

LC-MS/MS analysis and data processing

Experiments were performed in triplicate. The analysis of in-gel digested samples was performed as described previously (Schimmel et al. 2014, in press). Raw data were processed using MaxQuant (51, 52). RNF4-FLAG interactors were investigated through inspection of Label-Free Quantification (LFQ) intensities as well as MS/MS spectral counting.

Microscopy

Cells were seeded on glass coverslips, and fixed 24 hours later for 10 minutes in 3.7% paraformaldehyde in PHEM buffer (60 mM PIPES, 25 mM HEPES, 10 mM EGTA, 2 mM MgCl₂ pH 6.9) at 37 °C. After washing with PBS, cells were permeated with 0.1% Triton-X100 for 10 minutes, washed with PBST, and blocked using TNB (100 mM TRIS pH 7.5, 150 mM NaCl, 0.5% Blocking Reagent (Roche)) for 30 minutes. Cells were incubated with primary antibody as indicated, in TNB for one hour. Subsequently cells were washed five times with PBST, and incubated with secondary antibodies (Goat α Ms Alexa

Chapter 3

488 and Goat α Rb Alexa 594 (Invitrogen)) in TNB for one hour. Next, cells were washed five times with PBST and dehydrated using alcohol, prior to fixing them in DAPI solution (Citifluor) and sealing the slides with nail varnish. Images were recorded on a Leica SP5 confocal microscope system using 488 nm and 561 nm lasers for excitation, a 63X lens for magnification, and were analyzed with Leica confocal software. For quantification of PML bodies, groups of cells were recorded in similar-sized fields using Z-stacking with steps of 0.5 μ m to acquire 10 images ranging from the bottom to the top of the cells. Images were maximum projected, individual cells were localized and PML bodies were counted using in-house customized Stacks software (53).

3

Structural modeling of USP11

The structure of USP11 was modeled using the Protein Homology/analogy Recognition Engine V 2.0 (PHYRE2)(38). *Homo sapiens* USP11 (Uniprot ID P51784) was submitted to the PHYRE2 Protein Fold Recognition Server, and subjected to Intensive Modelling. 3D Molecule Viewer (Vector NTI Advance 11.5.1, Invitrogen), was used to highlight putative SIMs within the structure.

ACKNOWLEDGEMENTS

We are grateful to Drs. R. van Driel, R.T. Hay, R.C. Hoeben and L. Fradkin for providing critical reagents and to M. Verlaan – de Vries for technical assistance. This work was supported by the Netherlands Organization for Scientific Research (NWO) (A.C.O.V.), ZonMW (A.C.O.V.), the European Research Council (A.C.O.V) and the research career program FSS Sapere Aude (J.V.O.) from the Danish Research Council. The NNF Center for Protein Research is supported by a generous donation from the Novo Nordisk Foundation.

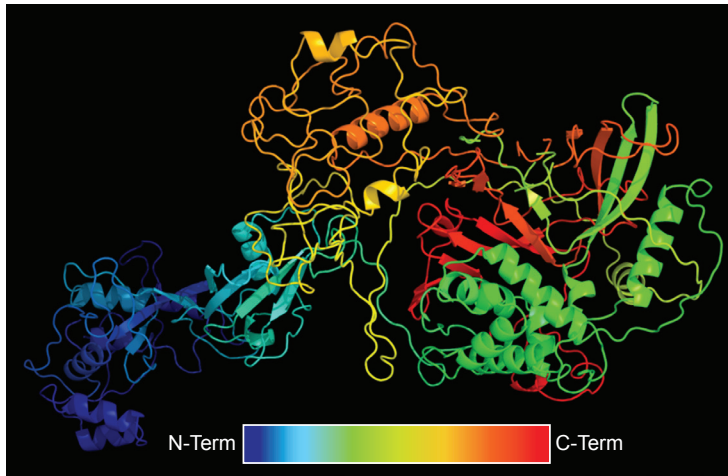
Reference List

1. Flotho, A., and Melchior, F. (2013) Sumoylation: a regulatory protein modification in health and disease. *Annu. Rev. Biochem.* 82, 357-385
2. Hickey, C. M., Wilson, N. R., and Hochstrasser, M. (2012) Function and regulation of SUMO proteases. *Nat. Rev. Mol. Cell Biol.* 13, 755-766
3. Hay, R. T. (2007) SUMO-specific proteases: a twist in the tail. *Trends Cell Biol.* 17, 370-376
4. Nacerddine, K., Lehembre, F., Bhaumik, M., Artus, J., Cohen-Tannoudji, M., Babinet, C., Pandolfi, P. P., and Dejean, A. (2005) The SUMO pathway is essential for nuclear integrity and chromosome segregation in mice. *Dev. Cell* 9, 769-779
5. Becker, J., Barysch, S. V., Karaca, S., Dittner, C., Hsiao, H. H., Berriel, D. M., Herzig, S., Urlaub, H., and Melchior, F. (2013) Detecting endogenous SUMO targets in mammalian cells and tissues. *Nat. Struct. Mol. Biol.* 20, 525-531
6. Golebiowski, F., Matic, I., Tatham, M. H., Cole, C., Yin, Y., Nakamura, A., Cox, J., Barton, G. J., Mann, M., and Hay, R. T. (2009) System-wide changes to SUMO modifications in response to heat shock. *Sci. Signal.* 2, ra24
7. Vertegaal, A. C. (2011) Uncovering ubiquitin and ubiquitin-like signaling networks. *Chem. Rev.* 111, 7923-7940
8. Matic, I., Schimmel, J., Hendriks, I. A., van Santen, M. A., van de Rijke, F., van, D. H., Gnad, F., Mann, M., and Vertegaal, A. C. (2010) Site-specific identification of SUMO-2 targets in cells reveals an inverted SUMOylation motif and a hydrophobic cluster SUMOylation motif. *Mol. Cell* 39, 641-652
9. Rodriguez, M. S., Dargemont, C., and Hay, R. T. (2001) SUMO-1 conjugation in vivo requires both a consensus modification motif and nuclear targeting. *J. Biol. Chem.* 276, 12654-12659
10. Bernier-Villamor, V., Sampson, D. A., Matunis, M. J., and Lima, C. D. (2002) Structural basis for E2-mediated SUMO

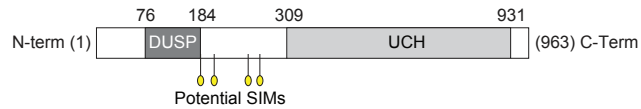
- conjugation revealed by a complex between ubiquitin-conjugating enzyme Ubc9 and RanGAP1. *Cell* 108, 345-356
11. Kerscher, O. (2007) SUMO junction-what's your function? New insights through SUMO-interacting motifs. *EMBO Rep.* 8, 550-555
 12. Danielsen, J. R., Povlsen, L. K., Villumsen, B. H., Streicher, W., Nilsson, J., Wikstrom, M., Bekker-Jensen, S., and Mailand, N. (2012) DNA damage-inducible SUMOylation of HERC2 promotes RNF8 binding via a novel SUMO-binding Zinc finger. *J. Cell Biol.* 197, 179-187
 13. Hunter, T., and Sun, H. (2008) Crosstalk between the SUMO and ubiquitin pathways. *Ernst. Schering. Found. Symp. Proc.*, 1-16
 14. Ulrich, H. D. (2005) Mutual interactions between the SUMO and ubiquitin systems: a plea of no contest. *Trends Cell Biol.* 15, 525-532
 15. Desterro, J. M., Rodriguez, M. S., and Hay, R. T. (1998) SUMO-1 modification of I κ B α inhibits NF- κ B activation. *Mol. Cell* 2, 233-239
 16. Huang, T. T., Wuerzberger-Davis, S. M., Wu, Z. H., and Miyamoto, S. (2003) Sequential modification of NEMO/I κ B γ by SUMO-1 and ubiquitin mediates NF- κ B activation by genotoxic stress. *Cell* 115, 565-576
 17. Schimmel, J., Larsen, K. M., Matic, I., van, H. M., Cox, J., Mann, M., Andersen, J. S., and Vertegaal, A. C. (2008) The ubiquitin-proteasome system is a key component of the SUMO-2/3 cycle. *Mol. Cell Proteomics* 7, 2107-2122
 18. Tatham, M. H., Matic, I., Mann, M., and Hay, R. T. (2011) Comparative proteomic analysis identifies a role for SUMO in protein quality control. *Sci. Signal.* 4, rs4
 19. Prudden, J., Pebernard, S., Raffa, G., Slavin, D. A., Perry, J. J., Tainer, J. A., McGowan, C. H., and Boddy, M. N. (2007) SUMO-targeted ubiquitin ligases in genome stability. *EMBO J.* 26, 4089-4101
 20. Sun, H., Leverson, J. D., and Hunter, T. (2007) Conserved function of RNF4 family proteins in eukaryotes: targeting a ubiquitin ligase to SUMOylated proteins. *EMBO J.* 26, 4102-4112
 21. Tatham, M. H., Geoffroy, M. C., Shen, L., Plechanovova, A., Hattersley, N., Jaffray, E. G., Palvimo, J. J., and Hay, R. T. (2008) RNF4 is a poly-SUMO-specific E3 ubiquitin ligase required for arsenic-induced PML degradation. *Nat. Cell Biol.* 10, 538-546
 22. Sun, H., and Hunter, T. (2012) Poly-small ubiquitin-like modifier (PolySUMO)-binding proteins identified through a string search. *J. Biol. Chem.* 287, 42071-42083
 23. Poulsen, S. L., Hansen, R. K., Wagner, S. A., van, C. L., van Belle, G. J., Streicher, W., Wikstrom, M., Choudhary, C., Houtsmuller, A. B., Marteijn, J. A., Bekker-Jensen, S., and Mailand, N. (2013) RNF111/Arkadia is a SUMO-targeted ubiquitin ligase that facilitates the DNA damage response. *J. Cell Biol.* 201, 797-807
 24. Heideker, J., Perry, J. J., and Boddy, M. N. (2009) Genome stability roles of SUMO-targeted ubiquitin ligases. *DNA Repair (Amst)* 8, 517-524
 25. Yin, Y., Seifert, A., Chua, J. S., Maure, J. F., Golebiowski, F., and Hay, R. T. (2012) SUMO-targeted ubiquitin E3 ligase RNF4 is required for the response of human cells to DNA damage. *Genes Dev.* 26, 1196-1208
 26. Galanty, Y., Belotserkovskaya, R., Coates, J., and Jackson, S. P. (2012) RNF4, a SUMO-targeted ubiquitin E3 ligase, promotes DNA double-strand break repair. *Genes Dev.* 26, 1179-1195
 27. Vyas, R., Kumar, R., Clermont, F., Helfricht, A., Kalev, P., Sotiropoulou, P., Hendriks, I. A., Radaelli, E., Hochepped, T., Blanpain, C., Sablina, A., van, A. H., Olsen, J. V., Jochemsen, A. G., Vertegaal, A. C., and Marine, J. C. (2013) RNF4 is required for DNA double-strand break repair in vivo. *Cell Death Differ.* 20, 490-502
 28. Luo, K., Zhang, H., Wang, L., Yuan, J., and Lou, Z. (2012) Sumoylation of MDC1 is important for proper DNA damage response. *EMBO J.* 31, 3008-3019
 29. van, H. M., Overmeer, R. M., Abolvardi, S. S., and Vertegaal, A. C. (2010) RNF4 and VHL regulate the proteasomal degradation of SUMO-conjugated Hypoxia-Inducible Factor-2 α . *Nucleic Acids Res.* 38, 1922-1931
 30. Hu, X. V., Rodrigues, T. M., Tao, H., Baker, R. K., Miraglia, L., Orth, A. P., Lyons, G. E., Schultz, P. G., and Wu, X. (2010) Identification of RING finger protein 4 (RNF4) as a modulator of DNA demethylation through a functional genomics screen. *Proc. Natl. Acad. Sci. U. S. A.* 107, 15087-15092
 31. Nijman, S. M., Luna-Vargas, M. P., Velds, A., Brummelkamp, T. R., Dirac, A. M., Sixma, T. K., and Bernards, R. (2005) A genomic and functional inventory of deubiquitinating enzymes. *Cell* 123, 773-786
 32. Reyes-Turcu, F. E., Ventii, K. H., and Wilkinson, K. D. (2009) Regulation and cellular roles of ubiquitin-specific deubiquitinating enzymes. *Annu. Rev. Biochem.* 78, 363-397
 33. Lin, D. Y., Huang, Y. S., Jeng, J. C., Kuo,

- H. Y., Chang, C. C., Chao, T. T., Ho, C. C., Chen, Y. C., Lin, T. P., Fang, H. I., Hung, C. C., Suen, C. S., Hwang, M. J., Chang, K. S., Maul, G. G., and Shih, H. M. (2006) Role of SUMO-interacting motif in Daxx SUMO modification, subnuclear localization, and repression of sumoylated transcription factors. *Mol. Cell* 24, 341-354
34. Weisshaar, S. R., Keusekotten, K., Krause, A., Horst, C., Springer, H. M., Gottsche, K., Dohmen, R. J., and Praefcke, G. J. (2008) Arsenic trioxide stimulates SUMO-2/3 modification leading to RNF4-dependent proteolytic targeting of PML. *FEBS Lett.* 582, 3174-3178
35. Lallemand-Breitenbach, V., Jeanne, M., Benhenda, S., Nasr, R., Lei, M., Peres, L., Zhou, J., Zhu, J., Raught, B., and De, T. H. (2008) Arsenic degrades PML or PML-RARalpha through a SUMO-triggered RNF4/ubiquitin-mediated pathway. *Nat. Cell Biol.* 10, 547-555
36. Bruderer, R., Tatham, M. H., Plechanovova, A., Matic, I., Garg, A. K., and Hay, R. T. (2011) Purification and identification of endogenous polySUMO conjugates. *EMBO Rep.* 12, 142-148
37. Conlan, L. A., McNees, C. J., and Heierhorst, J. (2004) Proteasome-dependent dispersal of PML nuclear bodies in response to alkylating DNA damage. *Oncogene* 23, 307-310
38. Kelley, L. A., and Sternberg, M. J. (2009) Protein structure prediction on the Web: a case study using the Phyre server. *Nat. Protoc.* 4, 363-371
39. Schimmel, J., Balog, C. I., Deelder, A. M., Drijfhout, J. W., Hensbergen, P. J., and Vertegaal, A. C. (2010) Positively charged amino acids flanking a sumoylation consensus tetramer on the 110kDa tri-snRNP component SART1 enhance sumoylation efficiency. *J. Proteomics* 73, 1523-1534
40. Dellaire, G., and Bazett-Jones, D. P. (2004) PML nuclear bodies: dynamic sensors of DNA damage and cellular stress. *Bioessays* 26, 963-977
41. Guo, A., Salomoni, P., Luo, J., Shih, A., Zhong, S., Gu, W., and Pandolfi, P. P. (2000) The function of PML in p53-dependent apoptosis. *Nat. Cell Biol.* 2, 730-736
42. Wang, Z. G., Ruggero, D., Ronchetti, S., Zhong, S., Gaboli, M., Rivi, R., and Pandolfi, P. P. (1998) PML is essential for multiple apoptotic pathways. *Nat. Genet.* 20, 266-272
43. Wiltshire, T. D., Lovejoy, C. A., Wang, T., Xia, F., O'Connor, M. J., and Cortez, D. (2010) Sensitivity to poly(ADP-ribose) polymerase (PARP) inhibition identifies ubiquitin-specific peptidase 11 (USP11) as a regulator of DNA double-strand break repair. *J. Biol. Chem.* 285, 14565-14571
44. Schoenfeld, A. R., Apgar, S., Dolios, G., Wang, R., and Aaronson, S. A. (2004) BRCA2 is ubiquitinated in vivo and interacts with USP11, a deubiquitinating enzyme that exhibits pro-survival function in the cellular response to DNA damage. *Mol. Cell Biol.* 24, 7444-7455
45. Burkhart, R. A., Peng, Y., Norris, Z. A., Tholey, R. M., Talbott, V. A., Liang, Q., Ai, Y., Miller, K., Lal, S., Cozzitorto, J. A., Witkiewicz, A. K., Yeo, C. J., Gehrmann, M., Napper, A., Winter, J. M., Sawicki, J. A., Zhuang, Z., and Brody, J. R. (2013) Mitoxantrone Targets Human Ubiquitin-Specific Peptidase 11 (USP11) and Is a Potent Inhibitor of Pancreatic Cancer Cell Survival. *Mol. Cancer Res.* 11, 901-911
46. Wu, H. C., Lin, Y. C., Liu, C. H., Chung, H. C., Wang, Y. T., Lin, Y. W., Ma, H. I., Tu, P. H., Lawler, S. E., and Chen, R. H. (2014) USP11 regulates PML stability to control Notch-induced malignancy in brain tumours. *Nat. Commun.* 5, 3214
47. Tiscornia, G., Singer, O., and Verma, I. M. (2006) Production and purification of lentiviral vectors. *Nat. Protoc.* 1, 241-245
48. Tatham, M. H., Jaffray, E., Vaughan, O. A., Desterro, J. M., Botting, C. H., Naismith, J. H., and Hay, R. T. (2001) Polymeric chains of SUMO-2 and SUMO-3 are conjugated to protein substrates by SAE1/SAE2 and Ubc9. *J. Biol. Chem.* 276, 35368-35374
49. Stuurman, N., de, G. A., Floore, A., Josso, A., Humbel, B., de, J. L., and van, D. R. (1992) A monoclonal antibody recognizing nuclear matrix-associated nuclear bodies. *J. Cell Sci.* 101 (Pt 4), 773-784
50. Rappsilber, J., Mann, M., and Ishihama, Y. (2007) Protocol for micro-purification, enrichment, pre-fractionation and storage of peptides for proteomics using StageTips. *Nat. Protoc.* 2, 1896-1906
51. Cox, J., Neuhauser, N., Michalski, A., Scheltema, R. A., Olsen, J. V., and Mann, M. (2011) Andromeda: a peptide search engine integrated into the MaxQuant environment. *J. Proteome. Res.* 10, 1794-1805
52. Cox, J., and Mann, M. (2008) MaxQuant enables high peptide identification rates, individualized p.p.b.-range mass accuracies and proteome-wide protein quantification. *Nat. Biotechnol.* 26, 1367-1372
53. Smeenk, G., Wiegant, W. W., Vrolijk, H., Solari, A. P., Pastink, A., and van, A. H. (2010) The NuRD chromatin-remodeling complex regulates signaling and repair of DNA damage. *J. Cell Biol.* 190, 741-749

A



B



C

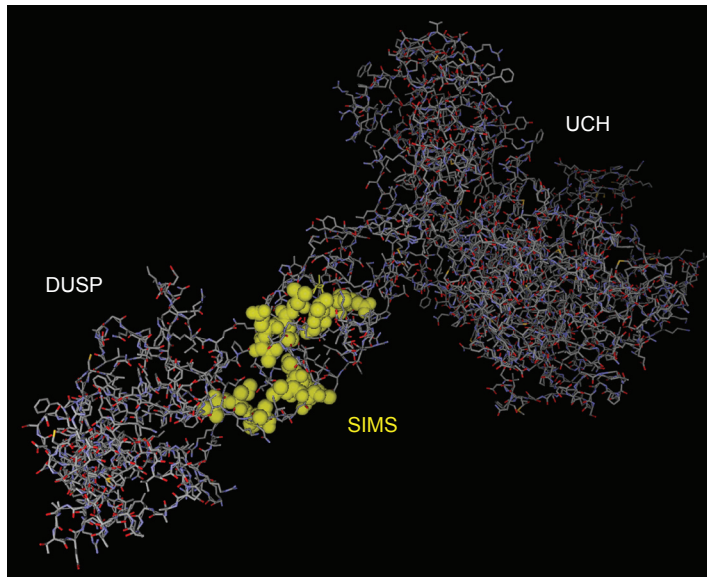


Figure S1. Structural modeling of USP11 reveals four putative SIMs to be located within the DUSP and UCH domains. A) A rainbow-ribbon model of USP11, using a gradual transition in color to indicate progression from N-terminus to C-terminus. Alpha helices and beta sheets are indicated. B) Cartoon depicting USP11. USP11 harbors a Domain present in Ubiquitin-Specific Proteases (DUSP) and an Ubiquitin Carboxyl-terminal Hydrolase domain (UCH). USP11 contains four potential SUMO interacting motifs (SIMs), located in between the DUSP and UCH domains. C) A structural skeleton model of USP11, with the SIMs indicated in yellow and using space-fill modelling for the respective molecules. The general location of the DUSP, UCH and SIMs are indicated.



3

4

Site-specific identification of SUMO-2 targets in cells reveals an Inverted SUMOylation Motif and a Hydrophobic Cluster SUMOylation Motif

Ivan Matic*, Joost Schimmel*, Ivo A. Hendriks*, Maria A. van Santen*, Frans van de Rijke, Hans van Dam, Florian Gnad, Matthias Mann, Alfred C.O. Vertegaal

Molecular Cell 2010 39(4):641-52

*These authors contributed equally to this work.

Supplemental data is available online at: <http://www.sciencedirect.com/science/article/pii/S1097276510005733>

Chapter 4. Site-specific identification of SUMO-2 targets in cells reveals an Inverted SUMOylation Motif and a Hydrophobic Cluster SUMOylation Motif

Abstract

Reversible protein modification by Small Ubiquitin-like Modifiers (SUMOs) is critical for eukaryotic life. Mass spectrometry-based proteomics has proven effective at identifying hundreds of potential SUMO target proteins. However, direct identification of SUMO acceptor lysines in complex samples by mass spectrometry is still very challenging. We have developed a generic method for the identification of SUMO acceptor lysines in target proteins. We have identified 103 SUMO-2 acceptor lysines in endogenous target proteins. 76 of these acceptor lysines are situated in the SUMOylation consensus site [VILMFPC]KxE. Interestingly, eight sites fit the inverted SUMOylation consensus motif [ED]xK[VILFP]. In addition, we found direct mass spectrometric evidence for crosstalk between SUMOylation and phosphorylation with a preferred spacer between the SUMOylated lysine and the phosphorylated serine of four residues. In 16 proteins we identified a Hydrophobic Cluster SUMOylation Motif (HCSM). SUMO conjugation of RanGAP1 and ZBTB1 via HCSMs is remarkably efficient.

4

Introduction

Ubiquitin (Ub) and ubiquitin-like proteins (Ubls) are covalently attached to other proteins via an isopeptide bond, which links the C-terminal glycine in these protein modifiers to the ϵ -amino group of lysines in substrate proteins. The Ubl family includes Nedd8, SUMO-1, -2, -3, ISG15, FAT10, FUB1, UBL5, URM1, ATG8 and ATG12. Reversible attachment of ubiquitin and Ubls to target proteins involves a set of enzymes (1-3). Components of the SUMO system play critical roles in regulation of fundamental cellular processes such as gene expression, cell cycle progression, DNA replication and DNA repair (1, 4).

A significant number of previously identified SUMOylated lysines in target proteins reside within the consensus motif Ψ KXE/D, where Ψ is a large hydrophobic amino acid and X is any amino acid. However, this motif also frequently occurs in non-SUMOylated proteins and many functionally important SUMO sites are known to be in non-consensus sequences. Therefore, bioinformatic analysis is not sufficient. Instead, SUMO sites need to be determined directly.

Mass spectrometry (MS)-based proteomics has established itself as the leading high-throughput proteomics technology and has become sufficiently mature to allow large scale studies of sub-proteomes and even entire proteomes (5, 6). One of the

main applications of MS is the direct mapping and quantitation of post-translational modifications (PTMs) of proteins. These modifications result in mass changes that can be detected by MS analysis (7). Although all PTMs can potentially be studied by MS, site-directed large scale proteomics analysis of a specific PTM requires efficient enrichment of modified peptides. For example, for phosphorylation it is possible to identify thousands of modification sites (8, 9).

MS is also well suited for the characterization of Ub/Ubls substrate proteomes. However, in contrast to phosphorylation, the application of MS to the Ub/Ubl field currently relies on purification at the protein level. In a typical Ub/Ubl proteomics experiment for the study of these PTMs, targets covalently attached to the Ub/Ubl of interest are purified from cells expressing a tagged form of the modifier, such as His6-Ub or TAP-SUMO-2. Although this approach has been successfully employed to identify and quantify proteins modified by Ub/Ubls (10-16), purification of intact modified species produces a peptide mixture that is too complex for efficient detection of Ub/Ubls modification sites. This is particularly problematic for SUMOylation since most SUMO substrates are low-abundant proteins and are modified at a small percentage.

In addition, the analysis of crosslinked peptides containing the large C-terminal SUMO sequence makes MS analysis challenging. Trypsin-digested SUMOs release large signature tags, such as 19 and 32 amino acids respectively for mammalian SUMO-1 and SUMO-2/3, which produce many fragment ions during MS/MS fragmentation. Although this makes the SUMO-crosslinked peptide identification unambiguous as compared to ubiquitin, it also makes identification challenging because the long modifying tryptic SUMO peptide leads to complex MS/MS fragmentation patterns. Several different approaches have been proposed for the identification of SUMOylated peptides. SUMmOn (17), a pattern recognition tool, in combination with low resolution mass spectrometry, has been successful in detecting peptides modified by SUMO *in vitro*. In a previous study we have applied a targeted mass spectrometric approach combined with the linearization of the branched peptides to detect SUMO polymerization sites *in vivo* (18). In another approach, a database containing “linearized branched” peptides is employed to detect SUMO modified lysines (19). Despite the validity and sophistication of these strategies, their application to *in vivo* samples has been limited by the much higher complexity of the peptide mixture and very low abundance of SUMO conjugates (20). Here we report a method for selective enrichment of SUMOylated peptides from complex cellular proteomes. We have used this method to map SUMO modification sites in endogenous target proteins purified from cell lysates to obtain insight into protein SUMOylation.

Results

A strategy to enrich SUMO modified peptides

In contrast to phosphorylation, direct identification of SUMO acceptor lysines in target proteins purified from cell lysates has remained very challenging. To selectively enrich SUMO modified peptides from cells, we employed a previously published His6-tagged SUMO-2 mutant in which internal lysines were replaced by arginines (13). In addition, arginines were introduced at positions 90 (mutant T90R) or 87 (mutant Q87R; Figure 1A) to shorten the SUMO branched peptide generated after tryptic digestion (21). The positions of these arginines correspond to the arginines that are present in ubiquitin or Smt3, respectively. Smt3 is the single SUMO family member found in *S. cerevisiae*. These mutants behave very similar to the wild-type counterpart (Figures 2 and S2) and related mutants have already been used successfully (22-24). These lysine-deficient SUMO mutants are sensitive to digestion by trypsin, but not by Lys-C, an enzyme that specifically cleaves after lysine residues. After Lys-C digestion, peptides from target proteins that are covalently attached to lysine-deficient SUMOs via their SUMOylated lysines were purified under denaturing conditions via the His6-Tag. Next, in solution or in gel tryptic digestion removed a large part of SUMO from the substrate peptides while leaving short SUMO remnants – namely GG for the T90R mutant and QQTGG in case of the Q87R mutant (Figure 1B). This is an efficient way to limit the complexity of the purified sample (Figure 1C).

4

Mass spectrometric mapping of SUMOylation sites

SUMOylated peptides were analyzed by nanoscale liquid chromatography coupled to high resolution hybrid mass spectrometers (LTQ-Orbitrap XL and LTQ-Orbitrap Velos) (see Materials and Methods). The LTQ Orbitrap Velos was operated in the higher-energy C-trap dissociation (HCD) mode, in which fragment ions are acquired with high resolution (25, 26). Samples were analyzed multiple times using different acquisition strategies. SUMOylated peptides identified by standard database search were manually validated to maximize the confidence of identification (see Supplementary Material and Methods for a description of the measurements and for manual validation criteria). This was beneficial especially for the Q87R experiments because fragmentation of the QQTGG tag produced peaks that are not assigned by the search engine. During manual inspection of high resolution MS/MS spectra, we noticed the presence of QQTGG signature fragment ions in the low mass region, namely m/z 257.125 (QQ), m/z 240.097 (QQ with loss of ammonia) and m/z 239.114 (QQ with loss of water) (Figure 3A and Figure S1). These ions were subsequently used as reporter ions for SUMOylated peptides.

Our strategy enabled the identification of 103 SUMOylated lysines from 82 endogenous target proteins (Table S1). This is significantly better than previous attempts (19, 22-24, 27). Among the identified SUMOylated peptides, 69 were

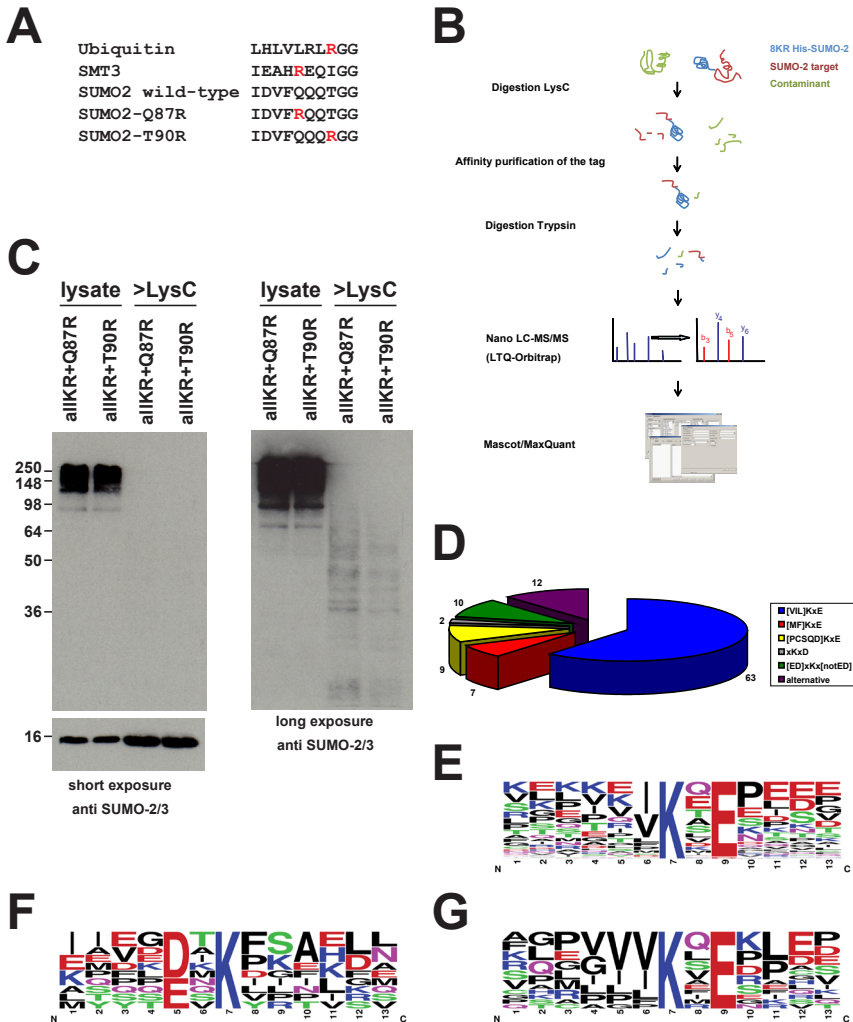


Figure 1. A method to identify SUMO acceptor lysines in endogenous target proteins purified from cell lysates. (A) The carboxyl-termini of mature ubiquitin, SMT3 and human SUMO-2 are depicted. Two SUMO-2 mutants were created, Q87R and T90R that contained arginines on positions corresponding to arginines in SMT3 or ubiquitin, respectively. (B) Purification Strategy. Lysine deficient His6-SUMO-2 mutants were expressed in HeLa cells and proteins in cell lysates were digested with endoprotease Lys-C that cleaves after lysine residues. His6-SUMO-2 and conjugated target protein fragments were purified by Immobilized Metal Affinity Chromatography (IMAC), digested with trypsin and analyzed by nano LC-MS/MS. Mascot and MaxQuant software were employed to identify SUMO-2 acceptor lysines in target proteins. (C) The SUMO-2 mutant proteins were efficiently conjugated to target proteins and conjugates were efficiently digested by Lys-C. Protein samples were analyzed by immunoblotting using an antibody directed against SUMO-2/3. (D) Out of the 103 SUMO-2 conjugated lysines that were detected in our screen 63 were situated in the SUMOylation consensus motif [VIL]KxE. Seven sites were situated in the consensus site [MF]KxE and nine were situated in [PCSQD]KxE sites. Ten SUMOylated lysines were situated in the inverted consensus site [ED]xKx[notED] and two contained aspartic acids at position +2. Twelve SUMOylated lysines were missing acidic residues at position +2 or -2. (E-G) Graphical representations of the local target protein contexts of SUMO-2 conjugated lysines situated in the consensus motif KxE/D (E), in the inverted consensus motif E/DxKx[notED] (F) and in the Hydrophobic Cluster SUMOylation Motif (G). See also Figure S1.

Chapter 4

detected in both T90R and Q87R experiments, additionally validating the accuracy of our approach.

Analysis of SUMOylation Sites

Among the identified SUMO sites, 69% conformed to the previously established consensus site for SUMOylation, ψ KxE/D, where ψ represents a large hydrophobic amino acid (Figure 1D and E). Remarkably, with the exception of the ψ KxD type site that we identified in H/ACA ribonucleoprotein complex subunit 2, all sites that fit the SUMOylation consensus contain a glutamic acid. SUMOylation of H/ACA ribonucleoprotein complex subunit 2 on lysine 5 was confirmed in the accompanying paper by Westman et al. The SUMOylated lysines were most frequently preceded by isoleucine, valine or leucine. Alternative amino acids that preceded the SUMOylated lysines were phenylalanine (4x), proline (4x), methionine (3x), cysteine (2x), aspartic acid (1x), glutamine (1x) and serine (1x) (Table S1). The validity of our approach was confirmed by the identification of previously published SUMO attachment sites in e.g. RanGAP1, PML, DNA topoisomerase I, PARP1, Sp1, Sp3 and SUMO-2 (Table S1).

The identification of SUMO attachment sites that are not situated in the SUMOylation consensus motif remains a challenge. Interestingly, we identified ten SUMO attachment sites that contained acidic residues two positions upstream of the SUMOylated lysine (Figure 1F and Figure S1B). The SUMOylated lysines were directly followed by phenylalanine (3x), proline (2x), isoleucine, leucine, valine, and also aspartic acid and tyrosine, so there is some preference for a hydrophobic residue. In contrast to the identified SUMO sites that matched the regular SUMOylation consensus motif, five of the inverted SUMOylation consensus sites contained an aspartic acid and the other five contained a glutamic acid at position -2. We have named this type of SUMOylation motif the inverted SUMOylation consensus motif E/DxK ψ . Surprisingly, SUMO-1 contains an inverted SUMOylation consensus site that was empirically identified in the present study, indicating unexpected atypical chain formation between SUMO-2 and SUMO-1 (18, 28).

We were intrigued by the identification of SUMO attachment sites in ACIN1, ADAR, AHNAK, APC4, BRD4, FOSL2, GRL, hnRNP-M, NUMA1, RanGAP1, RSF1, SAFB2, SNIP-1, YLPM1, ZBTB1 and ZNF280C on lysines that were preceded by hydrophobic clusters of at least three hydrophobic residues instead of the single hydrophobic residue that is usually present (Figure 1G and Table S1). We have named this type of SUMOylation site the Hydrophobic Cluster SUMOylation Motif (HCSM). These results will help to predict SUMO attachment sites in proteins. To facilitate the prediction of SUMOylation sites in proteins based on our results, we created a SUMOylation motif matcher in the Phosida database (<http://www.phosida.com>) (29).

Interestingly, SUMO-acceptor lysines in BRD4 (K1111), RanGAP1 (K526), SAFB2 (K293) and Treacle protein TCOF1 (K755) (Table S1) were previously identified as acetylated lysines (18, 30). Since SUMOylation and acetylation are mutually exclusive, this indicates competition between acetylation and SUMOylation for the same lysines.

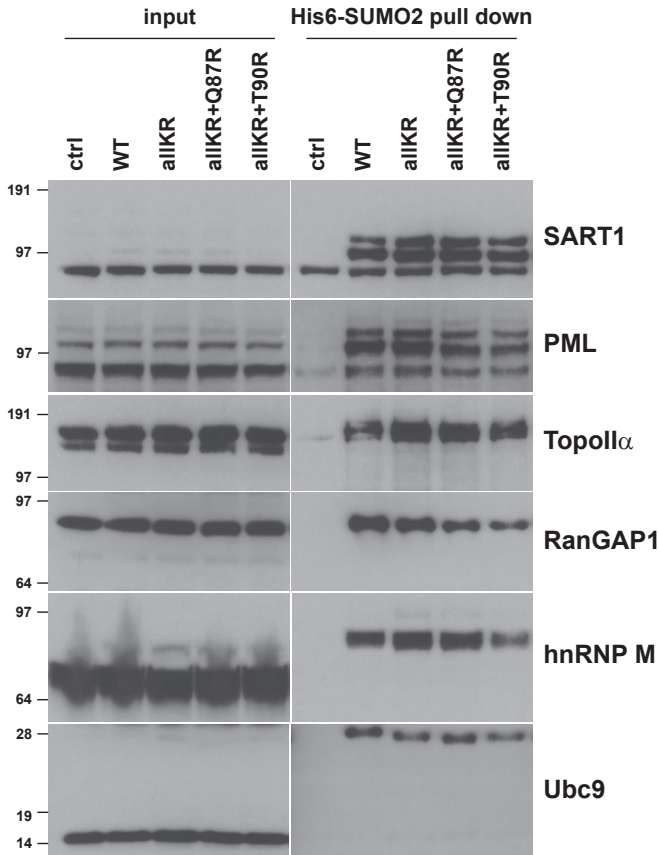


Figure 2. Verification of SUMO-2 mutants that were used for proteomics experiments. HeLa cells were transfected with plasmids expressing wild-type His6-SUMO-2 or the indicated lysine-deficient His6-SUMO-2 mutants. Cells were lysed and SUMOs were purified by IMAC. Input and SUMO-2 enriched fractions were size-separated by SDS-PAGE, blotted onto membranes and probed with antibodies directed against SART1, PML, DNA Topoisomerase II α , RanGAP1, hnRNP M or Ubc9. SUMO-2/3 probed immunoblots are depicted in Figure S2.

Crosstalk between SUMOylation and phosphorylation

Our mass spectrometry results revealed that the SUMOylated tryptic peptides of NOP5/58, RBM25, APC4, SNIP-1 and TOP2 contained downstream phosphorylated serines (Figure 3 and Figures S3). The spacing between the SUMOylated lysines and the downstream phosphorylated serines is remarkably consistent in NOP5/58, RBM25, SNIP-1 and APC4 with a preferred spacer of four amino acids between the SUMOylated lysine and the phosphorylated serine (Table S1, Figure S3). To establish the relevance of the phosphorylation of serine 502 in NOP5/58, we mutated this serine to alanine and studied the SUMOylation of this mutant (Figure 3C). Our results indicate that phosphorylation of NOP5/58 on serine 502 is a pre-requisite for the

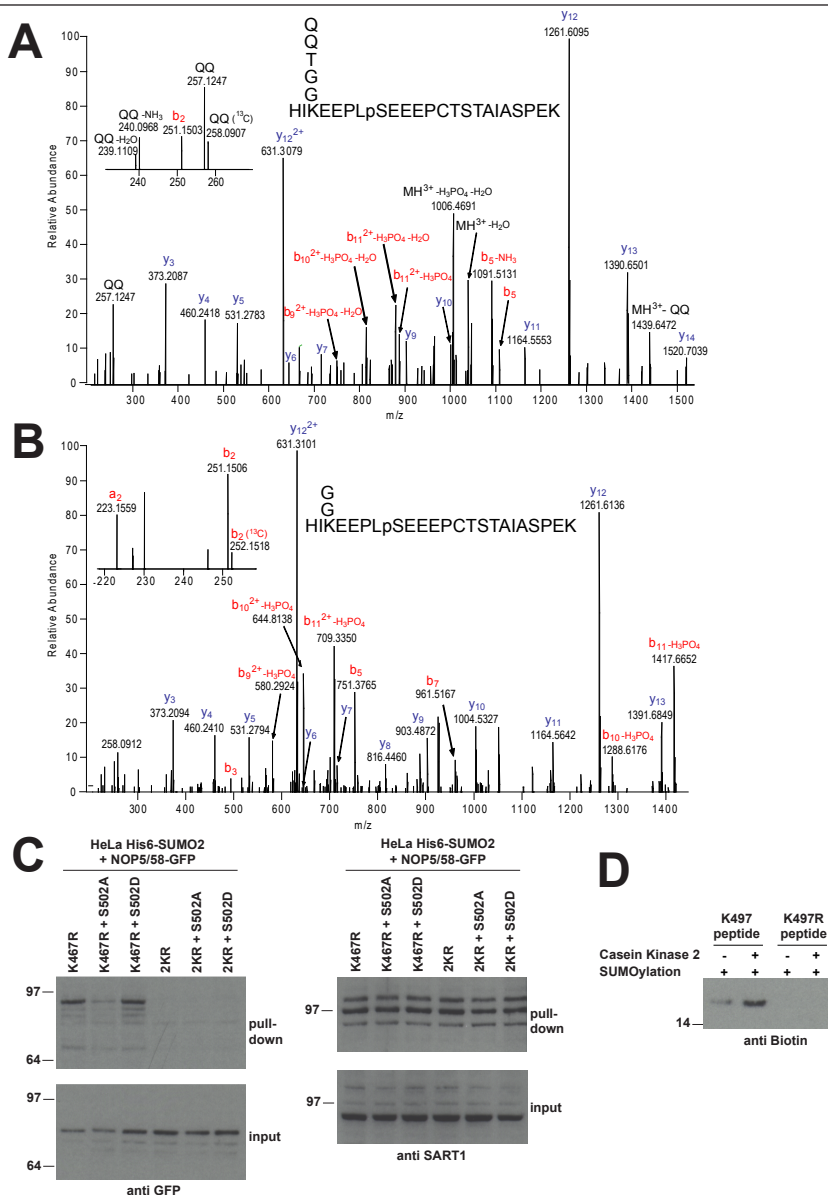


Figure 3. Phosphorylation-directed SUMOylation of NOP5/58. (A and B) Lysine 497 of NOP5/58 was identified as a SUMO-2 acceptor site in our screen using the SUMO-2 mutant Q87R (A) or the SUMO-2 mutant T90R (B). In both cases, the identified tryptic fragments contained phosphorylated serines on position 502. The doubly modified peptide was identified by high resolution tandem mass spectrometry using HCD fragmentation. Insets, magnifications of the low mass regions showing QQTGG signature fragment ions (A) and the a₂/b₂ pair (B). (C) Serine 502 of NOP5/58 was mutated to alanine to prevent phosphorylation or to aspartic acid to mimic phosphorylation using a plasmid encoding NOP5/58-GFP. In addition, lysine 467 of NOP5/58 was mutated to arginine to avoid SUMOylation on this lysine residue. A double mutant (2KR) in which lysines 467 and 497 were replaced for arginines was included as a negative control. HeLa cells expressing His6-SUMO-2 were transfected with these plasmids or with the wild-type control. Lysates were prepared and His6-SUMO-2 conjugates were purified by IMAC. Protein samples

were analyzed by immunoblotting using antibodies against GFP and against SART1 as a control. (D) A biotin-tagged NOP5/58 PDSM peptide (residues 495-505 Biotin-HIKEEPLSEEE) and control peptide (Biotin-HIREEPLSEEE) were synthesized, phosphorylated *in vitro* by Casein Kinase 2 and SUMOylated. After termination of the reaction with LDS sample buffer, samples were size-separated by SDS-PAGE and immunoblots were analyzed using an antibody against the Biotin-tag. See also Figure S3.

SUMO conjugation of lysine 497. Remarkably, the three glutamic acids on positions 503-505 were not able to compensate for the absence of the serine in the S502A mutant. Serine 502 is situated in the Casein Kinase II consensus phosphorylation site [ST]xx[ED]. Consistently, Casein Kinase II-mediated phosphorylation of a peptide matching the SUMO-phospho motif in NOP5/58 enhanced its SUMOylation (Figure 3D). Functionally, the SUMOylation of NOP5/58 is relevant for snoRNA binding (Westman et al. accompanying manuscript).

SUMOylation of ZBTB1 via an extended SUMOylation motif

The Hydrophobic Cluster SUMOylation Motif in ZBTB1 was studied in detail by mutagenesis (Figure 4). The ZBTB1 protein contains an amino-terminal BTB domain, eight Zinc fingers, two nuclear localization signals and two lysines situated in the SUMOylation consensus motif ψ KxE, lysines 265 and lysine 328 (Figure 4A). Lysine 328 was identified in our screen for SUMOylated lysines and is preceded by three consecutive isoleucines (Figure S4A). ZBTB1 was efficiently conjugated to SUMO-2 *in vitro* mainly via lysine 328 and to a lesser extent via lysine 265 (Figure 4B and C). Similar results were obtained for SUMOylation of ZBTB1 in cells, uncovering a remarkably efficient SUMOylation of this protein (Figure 4D and E and S4B). The hydrophobic cluster preceding lysine 328 enhanced the SUMOylation efficiency, since mutating the isoleucines to corresponding amino acids serine and asparagine that precede the less efficiently SUMOylated lysine 265 significantly reduced the SUMO conjugation of lysine 328 (Figure 4F). This strikingly efficient SUMOylation site does not consist of an integrated SUMO Interaction Motif (SIM) and a SUMOylation site, since mutating the isoleucines on position 325 and 326 to alanines did not affect the SUMOylation efficiency (Figure S4C) in contrast to SIM-mediated SUMO conjugation of USP25 (31).

The BTB domain regulates the SUMOylation level of ZBTB1

Four ZBTB family members were identified in our SUMOylation site screen, ZBTB1, ZBTB2, ZBTB9 and ZBTB38. Previously, the BTB domain has been shown to mediate protein ubiquitination via interaction with Cul-3 (32). Furthermore, the BTB-domain enables BTB-proteins to oligomerize. To test whether the BTB domain is involved in protein SUMOylation, we created a ZBTB1 mutant lacking the BTB domain (Figure 5A and B). As expected, this mutant lacked the capacity to form oligomers (Figure 5C). A striking decrease in SUMOylation was observed for the mutant protein compared to wild-type ZBTB1, indicating that an intact BTB domain is required for the

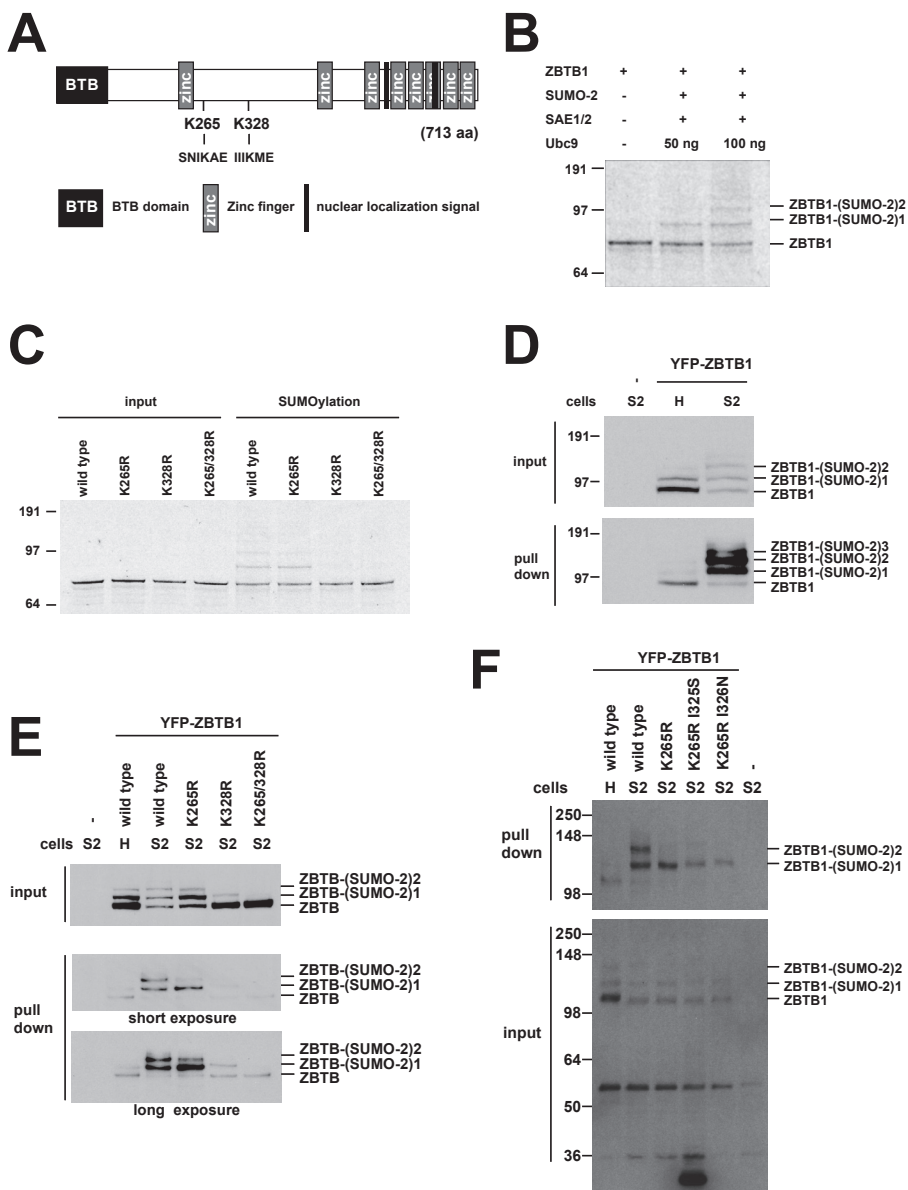


Figure 4. A Hydrophobic Cluster SUMOylation Motif mediates efficient conjugation of ZBTB1 to SUMO-2. (A) Cartoon depicting Zinc finger and BTB domain protein 1 (ZBTB1). ZBTB1 is composed of 713 amino acids and harbors a BTB domain, eight C₂H₂-type zinc fingers, two nuclear localization signals and two consensus SUMOylation sites (K265, K328). (B) ZBTB1 is SUMOylated *in vitro*. An *in vitro* SUMO-2 conjugation reaction was performed, containing SUMO-2, SAE1/2, and Ubc9 as indicated and *in vitro* transcribed and translated [³⁵S] labeled ZBTB1. The reaction was incubated for 3 hours at 37°C. After termination of the reaction by adding LDS sample buffer, samples were fractionated by SDS-PAGE, and dried gels were subjected to autoradiography. (C) The *in vitro* SUMOylation experiment was repeated including ZBTB1 mutants lacking one or two SUMOylation sites (K265R, K328R or double mutant). (D) ZBTB1 is SUMOylated *in vivo*. HeLa cells stably expressing His6-SUMO-2 (S2) and control HeLa (H) cells were transfected with an expression construct encoding YFP-ZBTB1. Cells were lysed 24 hours after

transfection in 8M Urea and His6-SUMO-2 conjugates were purified by IMAC. Total lysates (inputs) and purified fractions (pull down) were separated by SDS-PAGE, transferred to a membrane and probed using an antibody to detect YFP. (E) The experiment described in D was repeated including ZBTB1 mutants lacking one or two SUMOylation sites (K265R, K328R or double mutant). (F) Hydrophobic residues on position 325 and 326 of ZBTB1 affect the efficiency of ZBTB1 SUMOylation. The experiments described in D and E were repeated including ZBTB1 K265R mutants that are only SUMOylated on lysine 328. Hydrophobic residues on positions 325 or 326 were replaced for the corresponding amino acids preceding lysine 265. See also Figure S4.

efficient SUMOylation of ZBTB1 (Figure 5D). Subsequently, we tested whether the recombinant BTB domain can enhance SUMOylation in trans. GST-BTB(aa1-141) was produced in *E. coli*, purified and added to *in vitro* SUMOylation reactions (Figure 5E). Addition of recombinant BTB domain to these SUMOylation assays did not alter the SUMOylation efficiency of ZBTB1, indicating that the BTB domain functions in cis via oligomerization. Thus, the ZBTB1 oligomer is more efficiently SUMOylated compared to the monomer (33).

SUMOylation inhibits the repressive activity of ZBTB1.

Some ZBTB family members act as transcriptional repressors (Deweindt et al., 1995; Numoto et al., 1993; Li et al., 1997; Koh et al., 2009; Jeon et al., 2009). Since the target genes of ZBTB1 are currently unknown, we employed the Gal4 system (34) to study the transcriptional activity of ZBTB1. The thyroid hormone receptor fused to the Gal4 DNA binding domain was used as a control repressor in this experiment. In the absence of hormone, this receptor repressed the Gal4 binding site containing luciferase reporter 6.1 fold whereas ZBTB1 repressed this reporter construct 10.6 fold, indicating that ZBTB1 is a potent transcriptional repressor (Figure 6A). In general, SUMOylation inhibits transcription factors (35). Here, we show that SUMOylation of ZBTB1 via lysine 265 reduces its repressive activity (Figure 6B and C and S5A and B). The location of the SUMOylated lysine in the protein appears to be important since SUMOylation of lysine 328 did not affect the repressive activity of ZBTB1.

SUMOylation regulates subnuclear partitioning of ZBTB1

SUMOylation can affect the subcellular localization of proteins as demonstrated for RanGAP1, Sp3 and other proteins (1). Confocal microscopy was used to study the subcellular localization of YFP-ZBTB1 (Figure 6D). This revealed that ZBTB1 is a nuclear protein, which was expected since the protein harbors two nuclear localization signals (aa574-578 and aa645-652) (Fig 4A). ZBTB1 mainly localized to the nucleoplasm and accumulated in nuclear bodies. These ZBTB1 nuclear bodies did not colocalize with PML (data not shown) in contrast to the BTB domain containing protein Bach2 (36) but did colocalize with the transcriptional repressor SMRT (Figure 6E). Next, we compared the subcellular localization of wild-type and SUMOylation-deficient ZBTB1 (Figure 6F). Both proteins colocalize in the nucleoplasm and in

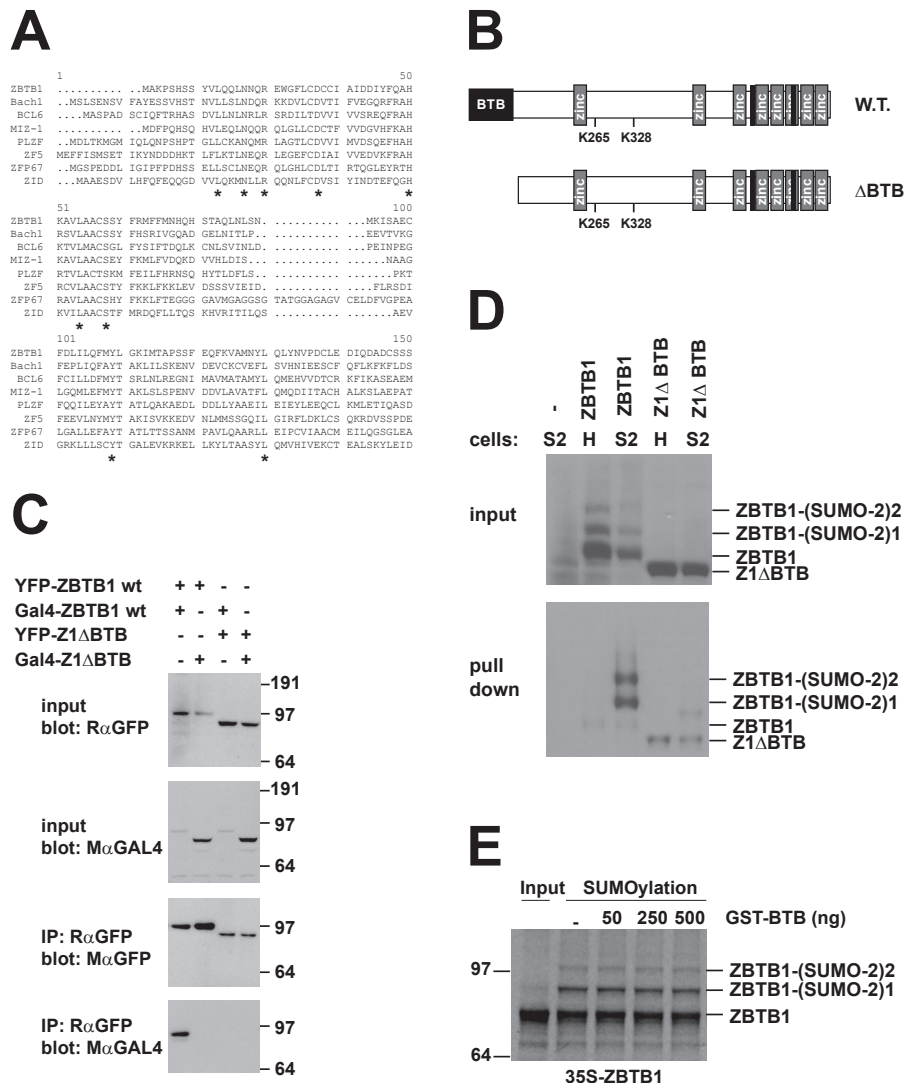


Figure 5. A role for the BTB domain in protein SUMOylation. (A) BTB domains of ZBTB1, Bach1, BCL6, MIZ-1, PLZF, ZV5, ZFP67 and ZID were aligned. (B) A ZBTB1 deletion construct was created that lacked the BTB domain. This Δ BTB mutant lacked the first 142 amino acids of the wild-type ZBTB1 protein. (C) Wild-type ZBTB1 and the Δ BTB mutant were fused to YFP or Gal4. These proteins were transiently expressed in HeLa cells and immunoprecipitated from lysates using rabbit anti GFP antibody. Inputs and immunoprecipitates were analyzed by immunoblotting using mouse anti GFP antibody and mouse anti Gal4 antibody. (D) HeLa cells stably expressing His6-SUMO-2 (S2) and control HeLa (H) cells were transfected with expression construct encoding YFP-ZBTB1 wild-type or Δ BTB mutant. His6-SUMO-2 conjugates were purified from a denaturing lysate and analyzed by immunoblotting to visualize SUMOylated ZBTB1. (E) Recombinant GST-BTB domain (aa1-141) was generated in *E. coli* and added to *in vitro* SUMOylation assays using [³⁵S] labeled ZBTB1 as a substrate. The reaction was incubated for 3 hours at 37°C. After termination of the reaction by adding LDS sample buffer, samples were fractionated by SDS-PAGE, and dried gels were subjected to autoradiography.

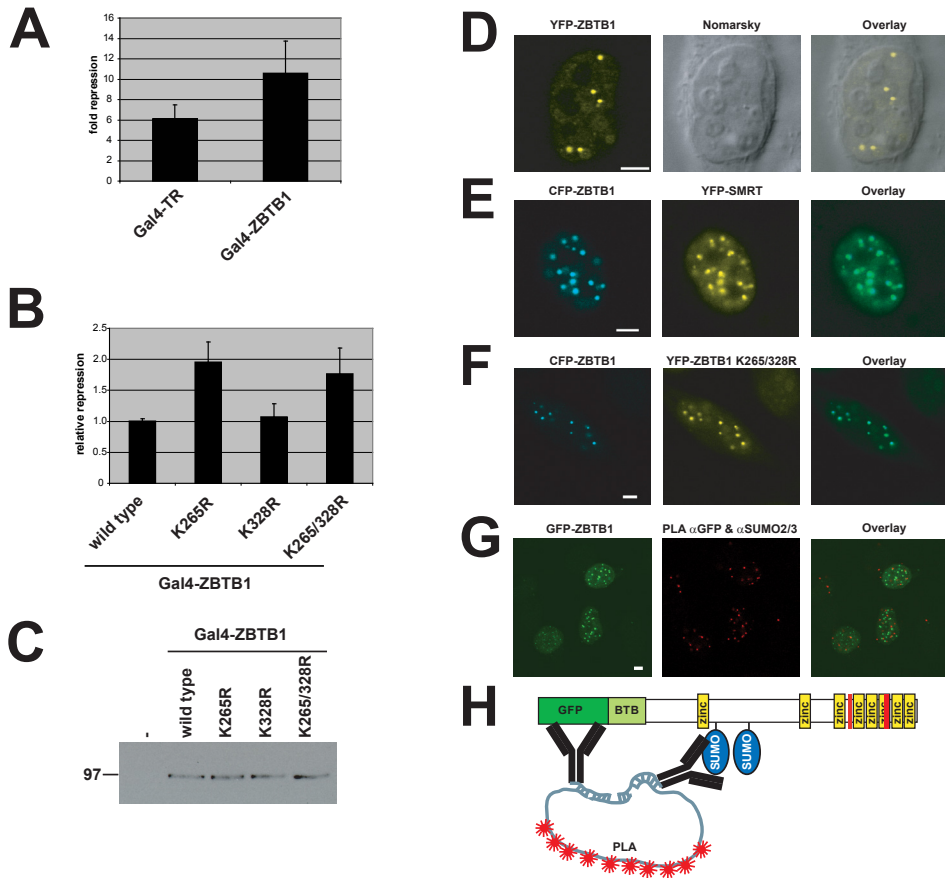


Figure 6. SUMOylation regulates the transcriptional activity and subcellular localization of ZBTB1. (A-C) HeLa cells were grown on 24-well dishes and transfected with 500 ng of Gal4(DBD)-fusion expression plasmids and 500 ng of the reporter construct 5xGal4-Tk-Pgl3. Cells were lysed in reporter lysis buffer 24 hours after transfection and luciferase activity was measured. Results are representative of four independent experiments; the error bars indicate one standard deviation from the average. (A) The transcriptional activity of Gal4-ZBTB1 was compared to the known transcriptional repressor thyroid hormone receptor (TR) fused to Gal4. (B) The transcriptional activities of Gal4-ZBTB1 wild type and SUMOylation mutants were determined. (C) Transfection mixtures were split and one set of wells was lysed in LDS sample buffer to verify the expression levels of the Gal4-ZBTB1 proteins by immunoblotting using an antibody directed against Gal4. (D-H) HeLa cells were (co)transfected with expression constructs encoding YFP-ZBTB1, CFP-ZBTB1, GFP-ZBTB1, YFP-ZBTB1 K265/328R or YFP-SMRT. Cells were fixed and analyzed by confocal microscopy. Scale bars are 4 μ m. (D) YFP-ZBTB1 localizes to the nucleoplasm and accumulates in nuclear bodies. (E) Colocalization of CFP-ZBTB1 and YFP-SMRT. (F) Colocalization of CFP-ZBTB1 and YFP-ZBTB1 K265/328R. (G) Proximal Ligation Assay (PLA) to detect SUMOylated ZBTB1. Cells were transfected with an expression construct encoding GFP-ZBTB1, fixed and the PLA was performed using affinity purified peptide anti SUMO-2/3 antibodies and a monoclonal antibody directed against GFP. Secondary antibodies were labeled with specific oligonucleotides. Oligonucleotide hybridization, ligation, amplification and detection were performed. (H) The cartoon briefly depicts the PLA technique. See also Figure S5.

Chapter 4

nuclear bodies. SUMOylation-deficient ZBTB1 can still interact with wild-type ZBTB1 via BTB-domain mediated oligomerization, therefore, this experiment does not reveal the specific subcellular localization of the SUMOylated form of ZBTB1. To positively identify the location of SUMOylated ZBTB1, we adapted the Proximal Ligation Assay (PLA) (37, 38) for protein SUMOylation. The PLA principle is depicted in the cartoon in Figure 6H. Primary antibodies directed against GFP and SUMO-2/3 and secondary antibodies labeled with oligonucleotides were employed to reveal the location of SUMOylated ZBTB1 (Figure 6G). The GFP signal represents the location of SUMOylated and non-SUMOylated ZBTB1. PLA signals were located in the nucleoplasm, but not in the nuclear bodies, indicating that SUMOylated ZBTB1 is located in the nucleoplasm outside the nuclear bodies. No detectable PLA signal was observed for the SUMOylation-deficient ZBTB1 mutant (Figure S5C). We conclude that SUMOylation regulates ZBTB1 via altering its subcellular localization.

4

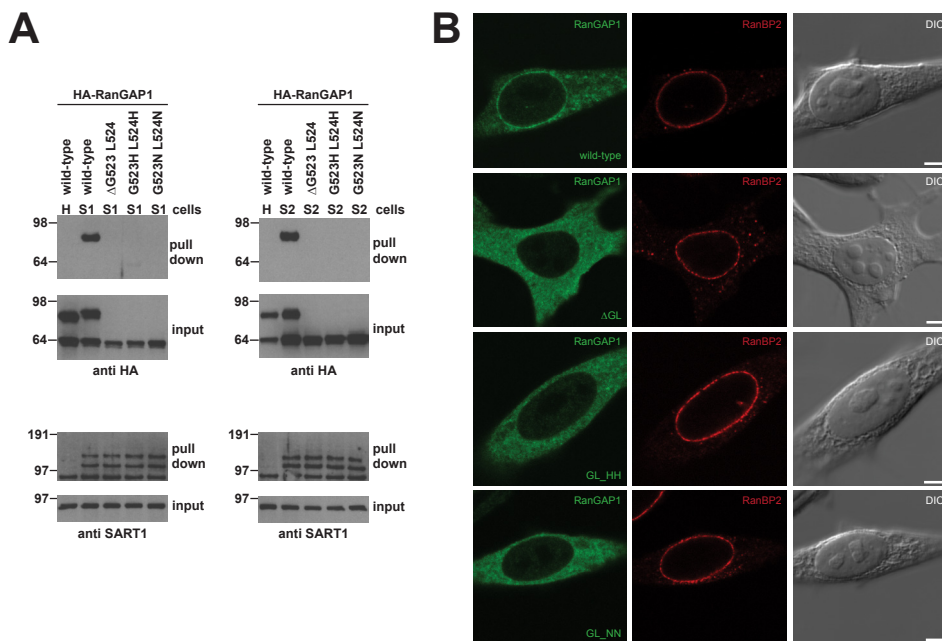


Figure 7. A Hydrophobic Cluster SUMOylation Motif mediates efficient conjugation of RanGAP1 to SUMO. (A) HeLa cells stably expressing His6-SUMO-1 (S1) or His6-SUMO-2 (S2) and control HeLa (H) cells were transfected with expression constructs encoding HA-RanGAP1 wild-type or the indicated HCSM mutants. Cells were lysed 24 hours after transfection and His6-SUMO conjugates were purified by IMAC. Total lysates (inputs) and SUMO purified fractions (pull down) were separated by SDS-PAGE, transferred to membranes and probed using antibodies against HA and against SART1 as a control. (B) HeLa cells were transfected with expression constructs encoding HA-RanGAP1 wild-type or the indicated HCSM mutants. Cells were fixed, co-stained with antibodies against the HA-tag (green) and against the nucleoporin RanBP2 (red) and analyzed by confocal microscopy. Scale bars are 4 μ m.

Efficient conjugation of RanGAP1 to SUMO is mediated by a HCSM.

RanGAP1 was the first identified SUMO substrate and is very efficiently conjugated to SUMO via lysine 526 (39, 40) that is situated in the Hydrophobic Cluster SUMOylation Motif GLLKSE. To verify whether this HCSM is involved in RanGAP1 SUMOylation, we deleted glycine 523 and leucine 524, or replaced these residues for the basic residue histidine or the polar residue asparagine. SUMOylation of these mutants was severely reduced compared to wild-type RanGAP1 indicating that glycine 523 and leucine 524 contribute to the efficient SUMOylation of RanGAP1 (Figure 7A). Consistently, RanGAP1 HCSM mutants failed to accumulate at nuclear pore complexes due to reduced SUMOylation (Figure 7B) (39, 40).

Discussion

Reversible post-translational modification of proteins by small chemical groups and small proteins enables tight control of protein activity. Recently, global analysis of protein phosphorylation dynamics by mass-spectrometry has enabled system-wide insight into signal transduction networks (9, 30, 41). Mass-spectrometric analysis of protein SUMOylation is currently very challenging (16). We have developed a MS-based method to map acceptor lysines for SUMOs in endogenous substrate proteins purified from cells. The majority of the identified SUMO acceptor lysines were situated in the SUMOylation consensus motif ψ KxE. In addition, we have uncovered an inverted SUMOylation consensus motif E/DxK ψ and an extended SUMOylation consensus motif, the HCSM, where the SUMOylated lysine is preceded by a cluster of at least three hydrophobic amino acids. Moreover, we uncovered crosstalk between SUMOylation and phosphorylation and competition between SUMOylation and acetylation.

Most SUMO acceptor lysines are currently identified using site-directed mutagenesis of potential SUMO acceptor sites. This method is very laborious and is unable to discriminate between SUMOylation sites and sites whose mutation changes the substrates and results in loss of SUMOylation at distal lysines (16). In studies on SUMOylation in yeast by the Gygi laboratory, six SUMOylation sites were identified (27) and in a study by the Yates laboratory, 22 sites were identified using the Smt3 I96R mutant and seven sites using wild-type Smt3 (23). In the most comprehensive study on protein SUMOylation in mammalian cells (10), five SUMOylation sites were identified. Recently, 14 SUMOylation sites were identified by Blomster et al. (2010) and a single SUMO site was identified by “ChopNspice” in endogenous proteins purified directly from cells and 17 sites including 8 sites on the SUMO E3 ligase RanBP2 by “ChopNspice” after incubation of a cellular extract with ATP (19). Our methodology enabled us to identify significantly more SUMOylation sites in endogenous target proteins purified directly from cells and yielded important insight into SUMOylation motifs.

Chapter 4

The identification of SUMO attachment sites in target proteins that lack classical SUMOylation consensus sites is very challenging and this has hampered progress in the field. The discovery of the inverted SUMOylation consensus sites E/DxK ψ in our study could be particularly useful to predict SUMOylation sites in these target proteins and enable direct follow up by mutagenesis of SUMO targets that contain these motifs.

The SUMO-phospho modified sites that we identified in our screen in NOP5/58, RBM25, APC4, SNIP-1 and TOP2 did not strictly fit the previously published Phosphorylation-Dependent SUMOylation Motif (PDSM) ψ KxE/DxxSP since the phosphorylation event was only proline-directed in SNIP-1 (42). This indicates more extensive crosstalk between phosphorylation and SUMOylation than previously anticipated. Interestingly, it has recently been shown that phosphorylation of the PDSM motif in Myocyte Enhancement Factor 2 and Heat-shock Transcription Factor 1 mediates the binding of this protein to a basic patch in the SUMO E2 ligase Ubc9, providing mechanistic insight into crosstalk between SUMOylation and phosphorylation (18, 43).

Phosphorylated residues downstream of SUMOylation sites that enhance protein SUMOylation can functionally be replaced by negatively charged residues in the Negatively charged amino acid-Dependent SUMOylation Motif (NDSM) (44). Consistently, we found that the most frequently occurring amino acids five positions downstream of the SUMOylated lysines are glutamic acid, aspartic acid and serine. Positively charged residues were frequently found upstream of SUMOylated lysines and can enhance SUMOylation efficiency (45).

We have identified an additional type of extended SUMOylation motif in our screen, the Hydrophobic Cluster SUMOylation Motif (HCSM). Mutagenesis experiments with the HCSMs in ZBTB1 and RanGAP1 indicated that these sites are very efficiently used for SUMO conjugation possibly due to enhanced binding to the SUMO E2 enzyme Ubc9 (46). Unexpectedly, the BTB domain was required for the efficient SUMOylation of ZBTB1. Previously, the BTB-domain was shown to function in protein ubiquitination as an adapter protein for Cul-3 (32, 47). Mechanistically, the BTB domain mediates oligomerization, therefore, we expect that the ZBTB1 oligomer is more efficiently SUMOylated due to Ubc9 hopping to the different moieties of the oligomer. SUMOylated ZBTB1 does no longer co-localize with the co-repressor SMRT in nuclear bodies, thus we expect that SUMOylation regulates ZBTB1 activity via altering its subcellular localization.

We present a strategy for selective enrichment of SUMO modified peptides in complex cellular proteomes. The identified SUMOylated lysines and the discovery of SUMOylation motifs will provide a useful resource for the increasingly important SUMO field.

Materials and methods

Plasmids

Plasmid constructs are described in Supplemental Experimental Procedures.

Cell lines, cell culture and transfection

HeLa cells and HeLa cells stably expressing His6-SUMO-2 (HeLa^{His6SUMO-2}) (14) were cultured in Dulbecco's modified Eagle's medium (DMEM) (Invitrogen), supplemented with 10% FCS and 100 U/ml penicillin and streptomycin (Invitrogen). Transfections were carried out using 2.5 μ l Polyethylenimine (PEI, 1 mg/ml, Alpha Aesar) per μ g DNA or using Lipofectamine 2000 (Invitrogen) according to the instructions of the manufacturer.

Antibodies

Peptide antibody AV-SM23-0100 (Eurogentec) against SUMO-2/3 and peptide antibody 1607 against SART1 were described previously (14, 15). Monoclonal antibody 5E10 against PML was a kind gift from Dr. Van Driel (Amsterdam, the Netherlands) and goat antibody against RanBP2 was a kind gift from Dr. Melchior (Heidelberg, Germany). Other antibodies that we used were mouse anti-HA, mouse anti-GFP (Roche), rabbit anti GFP (Invitrogen) mouse anti-Gal4 (Santa-Cruz Biotechnology), mouse anti Ubc9 and mouse anti DNA Topoisomerase II α (BD Biosciences), mouse anti RanGAP1 (Zymed) and mouse anti hnRNP M (Sigma).

Purification of SUMOylated proteins for mass spectrometry

Transfected cells were harvested in icecold PBS. Cells were lysed in 6M Guanidinium-HCl containing 0.1M NaHPO₄ and 0.01M Tris/HCl pH8.0. Samples were filtered 3 times over Qiashredders (Qiagen) to reduce the viscosity. After centrifugation for 5 minutes at 14K, proteins in the supernatants were reduced using 1 mM dithiothreitol and alkylated using 5 mM iodoacetamide at room temperature. Proteins were digested by endoprotease Lys-C and His₆-SUMO-2 conjugates were purified using Ni²⁺-NTA agarose beads. Beads were washed twice with lysis buffer and 5 times with 8M Urea containing 0.1M NaHPO₄ and 0.01M Tris/HCl pH 8.0. Samples were eluted in 6.4 M Urea pH 8.0 containing 200 mM imidazole. The eluted His₆-SUMO-2 conjugates were diluted 4 times with 10 mM ammonium bicarbonate and digested in solution with trypsin for 12 hours at room temperature. In a separate set of experiments, the His₆-SUMO-2 conjugates were separated by SDS-PAGE and the bands in the molecular weight range 15-38 kDa were excised from the gel and subjected to in-gel digestion (48).

Mass spectrometric analysis

The procedure is detailed in supplementary materials and methods. Briefly, the trypsin-digested peptides were purified on StageTips (49) and analyzed by nanoscale LC-MS/MS on a LTQ-Orbitrap XL or LTQ-Orbitrap Velos mass analyzer (Thermo Fisher Scientific, Germany) coupled to EASY-nLC system (Proxeon Biosystems, Denmark). Raw MS data were processed with MaxQuant (50, 51) and the Mascot search engine (Matrix Science, UK). MS/MS spectra of identified SUMO modified peptides were manually validated and are available upon request. The identified sites were aligned

Chapter 4

using WebLogo (Computational Genomics Research Group, University of California, Berkeley).

Microscopy and Proximity Ligation Assay

Cells were grown on glass coverslips and transfected with expression constructs encoding EGFP-, EYFP- ECFP- or HA-tagged proteins. Cells were fixed 24 hours after transfection for 10 minutes in 3.7% paraformaldehyde in PHEM buffer (60 mM PIPES, 25 mM HEPES, 10 mM EGTA, 2 mM MgCl₂, pH 6.9) at 37°C. After washing with PBS, cells were mounted in Vectashield (Vector Laboratories). Immunostaining was performed as previously described (Matunis et al., 1998). Secondary antibodies were rabbit anti goat Alexa 594 and rabbit anti mouse Alexa 488 (Invitrogen). Proximity Ligation was performed as previously described (37, 38). Images were recorded on a Leica TCS/SP2 confocal microscope system using a 100x NA 1.4PL APO lens and were analyzed with Leica confocal software.

Acknowledgments

This work was supported by the Netherlands Organisation for Scientific Research (NWO) (to A.C.O.V.) and the RUBICON EU Network of Excellence (to M.M.) I.M. is the recipient of a fellowship from RUBICON. We would like to thank Drs. A.I. Lamond and B. Westman for sharing unpublished data and reagents. We would like to thank Drs. F. Melchior, C. Lima, S. Zanivan and E. Meulmeester for helpful discussions. We are grateful to Drs. F. Melchior, G. Gill, N. Perkins, R. van Driel, M. Posch, E. Kalkhoven, E.J. Park and J.D. Chen for providing critical reagents and to Dr. M. Tatham for comparisons with previously published SUMO target proteomes.

4

Reference List

1. Geiss-Friedlander, R., and Melchior, F. (2007) Concepts in sumoylation: a decade on. *Nat. Rev. Mol. Cell Biol.* 8, 947-956
2. Hay, R. T. (2007) SUMO-specific proteases: a twist in the tail. *Trends Cell Biol.* 17, 370-376
3. Mukhopadhyay, D., and Dasso, M. (2007) Modification in reverse: the SUMO proteases. *Trends Biochem. Sci.* 32, 286-295
4. Bergink, S., and Jentsch, S. (2009) Principles of ubiquitin and SUMO modifications in DNA repair. *Nature* 458, 461-467
5. Cox, J., and Mann, M. (2007) Is proteomics the new genomics? *Cell* 130, 395-398
6. de Godoy, L. M., Olsen, J. V., Cox, J., Nielsen, M. L., Hubner, N. C., Frohlich, F., Walther, T. C., and Mann, M. (2008) Comprehensive mass-spectrometry-based proteome quantification of haploid versus diploid yeast. *Nature* 455, 1251-1254
7. Witze, E. S., Old, W. M., Resing, K. A., and Ahn, N. G. (2007) Mapping protein post-translational modifications with mass spectrometry. *Nat. Methods* 4, 798-806
8. Macek, B., Mann, M., and Olsen, J. V. (2009) Global and site-specific quantitative phosphoproteomics: principles and applications. *Annu. Rev. Pharmacol. Toxicol.* 49, 199-221
9. Olsen, J. V., Blagoev, B., Gnäd, F., Macek, B., Kumar, C., Mortensen, P., and Mann, M. (2006) Global, in vivo, and site-specific phosphorylation dynamics in signaling networks. *Cell* 127, 635-648
10. Golebiowski, F., Matic, I., Tatham, M. H., Cole, C., Yin, Y., Nakamura, A., Cox, J., Barton, G. J., Mann, M., and Hay, R. T. (2009) System-wide changes to SUMO modifications in response to heat shock. *Sci. Signal.* 2, ra24
11. Mayor, T., Graumann, J., Bryan, J., MacCoss, M. J., and Deshaies, R. J. (2007) Quantitative profiling of ubiquitylated proteins reveals proteasome substrates and the substrate repertoire influenced by the Rpn10 receptor pathway. *Mol. Cell Proteomics* 6, 1885-1895
12. Peng, J., Schwartz, D., Elias, J. E., Thoreen, C. C., Cheng, D., Marsischky, G., Roelofs, J., Finley, D., and Gygi, S. P. (2003) A

- proteomics approach to understanding protein ubiquitination. *Nat. Biotechnol.* 21, 921-926
13. Schimmel, J., Larsen, K. M., Matic, I., van Hagen, M., Cox, J., Mann, M., Andersen, J. S., and Vertegaal, A. C. (2008) The ubiquitin-proteasome system is a key component of the SUMO-2/3 cycle. *Mol. Cell Proteomics* 7, 2107-2122
 14. Vertegaal, A. C., Ogg, S. C., Jaffray, E., Rodriguez, M. S., Hay, R. T., Andersen, J. S., Mann, M., and Lamond, A. I. (2004) A proteomic study of SUMO-2 target proteins. *J. Biol. Chem.* 279, 33791-33798
 15. Vertegaal, A. C., Andersen, J. S., Ogg, S. C., Hay, R. T., Mann, M., and Lamond, A. I. (2006) Distinct and overlapping sets of SUMO-1 and SUMO-2 target proteins revealed by quantitative proteomics. *Mol. Cell Proteomics* 5, 2298-2310
 16. Wilson, V. G., and Heaton, P. R. (2008) Ubiquitin proteolytic system: focus on SUMO. *Expert. Rev. Proteomics* 5, 121-135
 17. Pedrioli, P. G., Raught, B., Zhang, X. D., Rogers, R., Aitchison, J., Matunis, M., and Aebersold, R. (2006) Automated identification of SUMOylation sites using mass spectrometry and SUMMoN pattern recognition software. *Nat. Methods* 3, 533-539
 18. Matic, I., van Hagen, M., Schimmel, J., Macek, B., Ogg, S. C., Tatham, M. H., Hay, R. T., Lamond, A. I., Mann, M., and Vertegaal, A. C. (2008) In vivo identification of human small ubiquitin-like modifier polymerization sites by high accuracy mass spectrometry and an in vitro to in vivo strategy. *Mol. Cell Proteomics* 7, 132-144
 19. Hsiao, H. H., Meulmeester, E., Frank, B. T., Melchior, F., and Urlaub, H. (2009) "ChopNspice", a mass-spectrometric approach that allows identification of endogenous SUMO-conjugated peptides. *Mol. Cell Proteomics*
 20. Makhnevych, T., Sydorsky, Y., Xin, X., Srikumar, T., Vizeacoumar, F. J., Jeram, S. M., Li, Z., Bahr, S., Andrews, B. J., Boone, C., and Raught, B. (2009) Global Map of SUMO Function Revealed by Protein-Protein Interaction and Genetic Networks. *Mol. Cell* 33, 124-135
 21. Jeram, S. M., Srikumar, T., Pedrioli, P. G., and Raught, B. (2009) Using mass spectrometry to identify ubiquitin and ubiquitin-like protein conjugation sites. *Proteomics* 9, 922-934
 22. Knuesel, M., Cheung, H. T., Hamady, M., Barthel, K. K., and Liu, X. (2005) A method of mapping protein sumoylation sites by mass spectrometry using a modified small ubiquitin-like modifier 1 (SUMO-1) and a computational program. *Mol. Cell Proteomics* 4, 1626-1636
 23. Wohlschlegel, J. A., Johnson, E. S., Reed, S. I., and Yates, J. R., III. (2006) Improved identification of SUMO attachment sites using C-terminal SUMO mutants and tailored protease digestion strategies. *J. Proteome Res.* 5, 761-770
 24. Blomster, H. A., Imanishi, S. Y., Siimes, J., Kastu, J., Morrice, N. A., Eriksson, J. E., and Sistonen, L. (2010) In vivo identification of sumoylation sites by a signature tag and cysteine-targeted affinity purification. *J. Biol. Chem.*
 25. Olsen, J. V., Macek, B., Lange, O., Makarov, A., Horning, S., and Mann, M. (2007) Higher-energy C-trap dissociation for peptide modification analysis. *Nat. Methods* 4, 709-712
 26. Olsen, J. V., Schwartz, J. C., Griep-Raming, J., Nielsen, M. L., Damoc, E., Denisov, E., Lange, O., Remes, P., Taylor, D., Splendore, M., Wouters, E. R., Senko, M., Makarov, A., Mann, M., and Horning, S. (2009) A dual pressure linear ion trap orbitrap instrument with very high sequencing speed. *Mol. Cell Proteomics* 8, 2759-2769
 27. Denison, C., Rudner, A. D., Gerber, S. A., Bakalarski, C. E., Moazed, D., and Gygi, S. P. (2005) A proteomic strategy for gaining insights into protein sumoylation in yeast. *Mol. Cell Proteomics* 4, 246-254
 28. Ikeda, F., and Dikic, I. (2008) Atypical ubiquitin chains: new molecular signals. 'Protein Modifications: Beyond the Usual Suspects' review series. *EMBO Rep.* 9, 536-542
 29. Gnad, F., Ren, S., Cox, J., Olsen, J. V., Macek, B., Oroshi, M., and Mann, M. (2007) PHOSIDA (phosphorylation site database): management, structural and evolutionary investigation, and prediction of phosphosites. *Genome Biol.* 8, R250
 30. Choudhary, C., Kumar, C., Gnad, F., Nielsen, M. L., Rehman, M., Walther, T. C., Olsen, J. V., and Mann, M. (2009) Lysine acetylation targets protein complexes and co-regulates major cellular functions. *Science* 325, 834-840
 31. Meulmeester, E., Kunze, M., Hsiao, H. H., Urlaub, H., and Melchior, F. (2008) Mechanism and consequences for paralog-specific sumoylation of ubiquitin-specific protease 25. *Mol. Cell* 30, 610-619
 32. Zhuang, M., Calabrese, M. F., Liu, J., Waddell, M. B., Nourse, A., Hammel, M.,

- Miller, D. J., Walden, H., Duda, D. M., Seyedin, S. N., Hoggard, T., Harper, J. W., White, K. P., and Schulman, B. A. (2009) Structures of SPOP-substrate complexes: insights into molecular architectures of BTB-Cul3 ubiquitin ligases. *Mol. Cell* 36, 39-50
33. Roukens, M. G., Alloul-Ramdhani, M., Vertegaal, A. C., Anvarian, Z., Balog, C. I., Deelder, A. M., Hensbergen, P. J., and Baker, D. A. (2008) Identification of a new site of sumoylation on Tel (ETV6) uncovers a PIAS-dependent mode of regulating Tel function. *Mol. Cell Biol.* 28, 2342-2357
 34. Ross, S., Best, J. L., Zon, L. I., and Gill, G. (2002) SUMO-1 modification represses Sp3 transcriptional activation and modulates its subnuclear localization. *Mol. Cell* 10, 831-842
 35. Gill, G. (2005) Something about SUMO inhibits transcription. *Curr. Opin. Genet. Dev.* 15, 536-541
 36. Tashiro, S., Muto, A., Tanimoto, K., Tsuchiya, H., Suzuki, H., Hoshino, H., Yoshida, M., Walter, J., and Igarashi, K. (2004) Repression of PML nuclear body-associated transcription by oxidative stress-activated Bach2. *Mol. Cell Biol.* 24, 3473-3484
 37. Soderberg, O., Leuchowius, K. J., Gullberg, M., Jarvius, M., Weibrecht, I., Larsson, L. G., and Landegren, U. (2008) Characterizing proteins and their interactions in cells and tissues using the in situ proximity ligation assay. *Methods* 45, 227-232
 38. Soderberg, O., Gullberg, M., Jarvius, M., Ridderstrale, K., Leuchowius, K. J., Jarvius, J., Wester, K., Hydbring, P., Bahram, F., Larsson, L. G., and Landegren, U. (2006) Direct observation of individual endogenous protein complexes in situ by proximity ligation. *Nat. Methods* 3, 995-1000
 39. Mahajan, R., Gerace, L., and Melchior, F. (1998) Molecular characterization of the SUMO-1 modification of RanGAP1 and its role in nuclear envelope association. *J. Cell Biol.* 140, 259-270
 40. Matunis, M. J., Wu, J., and Blobel, G. (1998) SUMO-1 modification and its role in targeting the Ran GTPase-activating protein, RanGAP1, to the nuclear pore complex. *J. Cell Biol.* 140, 499-509
 41. Daub, H., Olsen, J. V., Bairlein, M., Gnad, F., Oppermann, F. S., Korner, R., Greff, Z., Keri, G., Stemmann, O., and Mann, M. (2008) Kinase-selective enrichment enables quantitative phosphoproteomics of the kinome across the cell cycle. *Mol. Cell* 31, 438-448
 42. Hietakangas, V., Anckar, J., Blomster, H. A., Fujimoto, M., Palvimo, J. J., Nakai, A., and Sistonen, L. (2006) PDSM, a motif for phosphorylation-dependent SUMO modification. *Proc. Natl. Acad. Sci. U. S. A.* 103, 45-50
 43. Mohideen, F., Capili, A. D., Bilimoria, P. M., Yamada, T., Bonni, A., and Lima, C. D. (2009) A molecular basis for phosphorylation-dependent SUMO conjugation by the E2 UBC9. *Nat. Struct. Mol. Biol.* 16, 945-952
 44. Yang, S. H., Galanis, A., Witty, J., and Sharrocks, A. D. (2006) An extended consensus motif enhances the specificity of substrate modification by SUMO. *EMBO J.* 25, 5083-5093
 45. Schimmel, J., Balog, C. I., Deelder, A. M., Drijfhout, J. W., Hensbergen, P. J., and Vertegaal, A. C. (2010) Positively charged amino acids flanking a sumoylation consensus tetramer on the 110kDa tri-snRNP component SART1 enhance sumoylation efficiency. *J. Proteomics*
 46. Bernier-Villamor, V., Sampson, D. A., Matunis, M. J., and Lima, C. D. (2002) Structural basis for E2-mediated SUMO conjugation revealed by a complex between ubiquitin-conjugating enzyme Ubc9 and RanGAP1. *Cell* 108, 345-356
 47. Xu, L., Wei, Y., Reboul, J., Vaglio, P., Shin, T. H., Vidal, M., Elledge, S. J., and Harper, J. W. (2003) BTB proteins are substrate-specific adaptors in an SCF-like modular ubiquitin ligase containing CUL-3. *Nature* 425, 316-321
 48. Shevchenko, A., Tomas, H., Havlis, J., Olsen, J. V., and Mann, M. (2006) In-gel digestion for mass spectrometric characterization of proteins and proteomes. *Nat. Protoc.* 1, 2856-2860
 49. Rappsilber, J., Mann, M., and Ishihama, Y. (2007) Protocol for micro-purification, enrichment, pre-fractionation and storage of peptides for proteomics using StageTips. *Nat. Protoc.* 2, 1896-1906
 50. Cox, J., and Mann, M. (2008) MaxQuant enables high peptide identification rates, individualized p.p.b.-range mass accuracies and proteome-wide protein quantification. *Nat. Biotechnol.* 26, 1367-1372
 51. Cox, J., Matic, I., Hilger, M., Nagaraj, N., Selbach, M., Olsen, J. V., and Mann, M. (2009) A practical guide to the MaxQuant computational platform for SILAC-based quantitative proteomics. *Nat. Protoc.* 4, 698-705

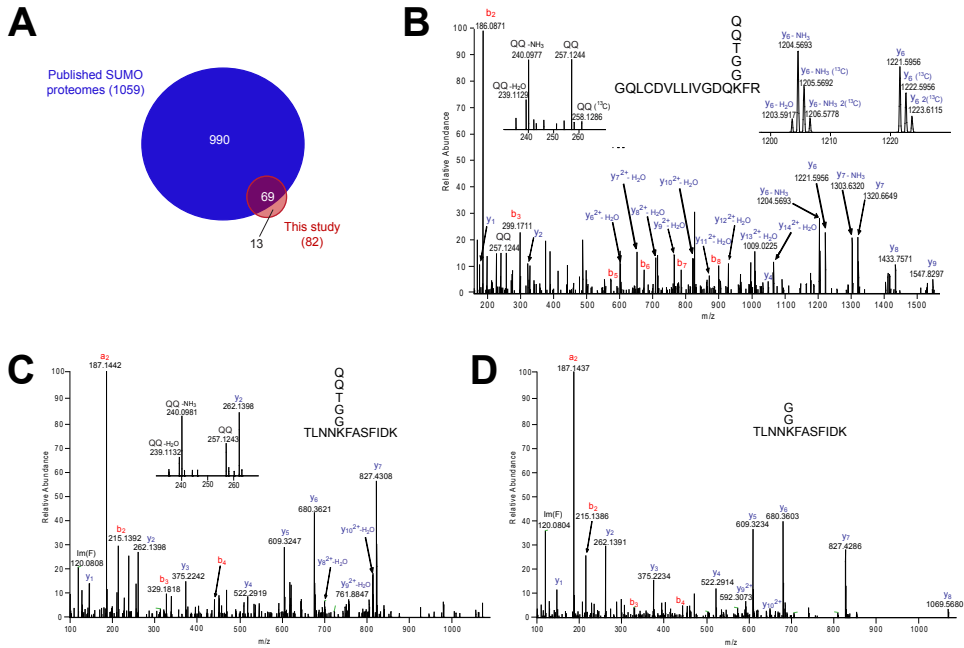


Figure S1 related to Figure 1 A. Overlap between our study and previous SUMO proteomics projects. We have identified 103 SUMOylation sites in 82 SUMO target proteins including 69 SUMO target proteins that were previously identified as potential human SUMO target proteins (1-14). Nine of the SUMO target proteins identified in this study have previously been identified as targets for Smt3; YFL039C, YKR092C, YKR008W, YJL148W, YEL026W, YLR335W, YDR390C, YOL006C and YNL088 (Denison et al., 2005; Panse et al., 2004; Wohlschlegel et al., 2004; Zhou et al., 2004). B. HCD MS/MS spectrum showing the SUMOylation of ZNF295 via an inverted SUMOylation consensus site. C and D. HCD MS/MS spectra showing the SUMOylation of type II cytoskeletal keratin 5.

His6-SUMO2 pull down

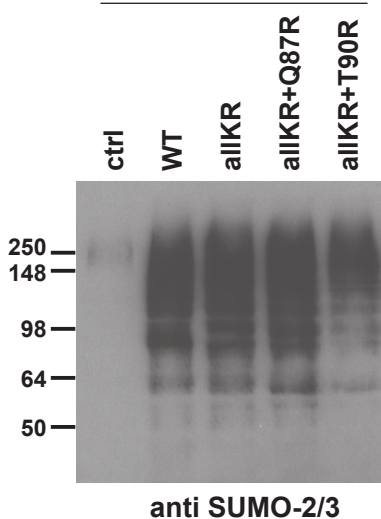


Figure S2 related to Figure 2. Control immunoblot for Figure 2 probed with anti SUMO-2/3 antibody.

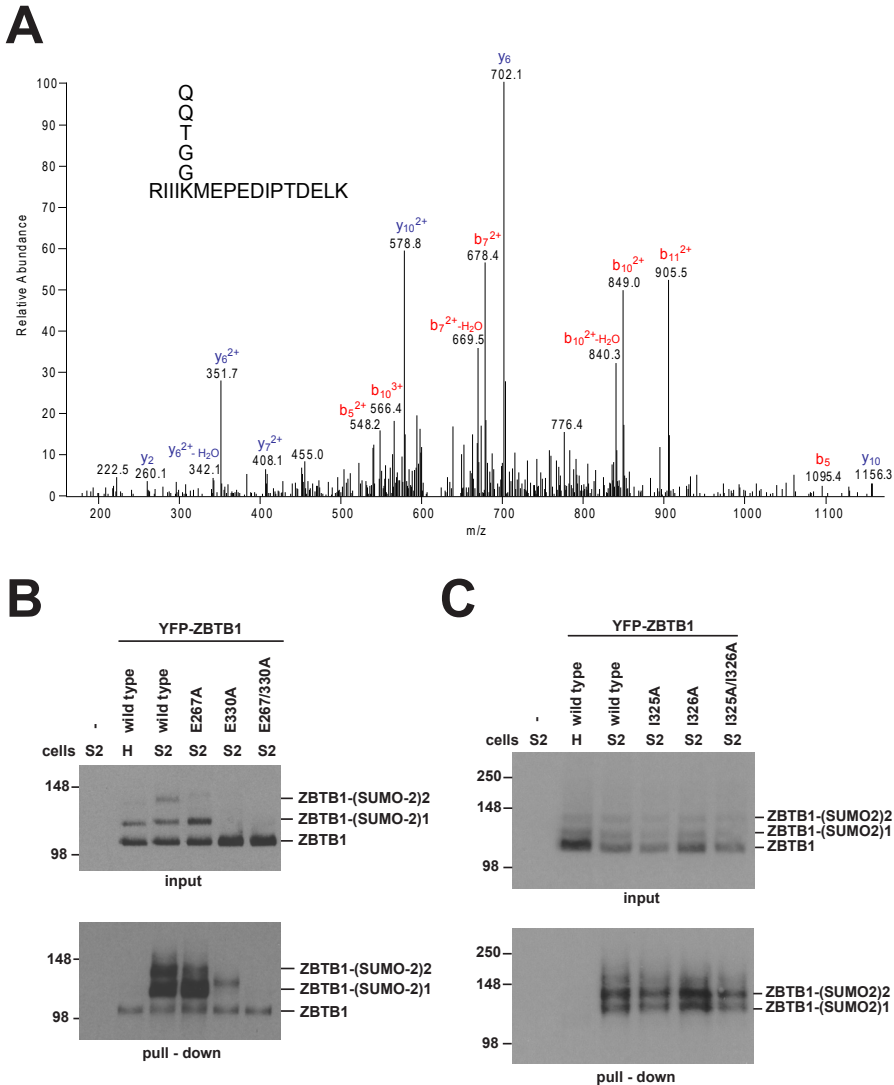


Figure S4 related to Figure 4. A. CID MS/MS spectrum showing the SUMOylation of ZBTB1 via lysine 328. B. SUMOylation analysis of YFP-ZBTB1 E267A, E330A single and double mutants. HeLa cells stably expressing His6-SUMO-2 (S2) and control HeLa (H) cells were transfected with expression constructs encoding YFP-ZBTB1 wild type, E267A, E330A single and double mutants. Cells were lysed 24 hours after transfection and His6-SUMO-2 conjugates were purified by IMAC. Total lysates (input) and purified fractions (pull down) were separated by SDS-PAGE, transferred to a membrane and probed using an antibody to detect YFP. C. The ZBTB1 K328 SUMOylation site does not consist of an integrated SUMO Interaction Motif (SIM) and a SUMOylation site. SUMO-SIM interactions are depending on large hydrophobic residues in the SIM. We mutated the isoleucines in ZBTB1 on positions 325 and 326 to alanines and compared the SUMOylation efficiencies of the mutants to the wild-type protein. No reduction in SUMOylation was observed for the mutants, indicating that the K328 SUMOylation site in ZBTB1 does not consist of an integrated SUMO Interaction Motif (SIM) and a SUMOylation site.

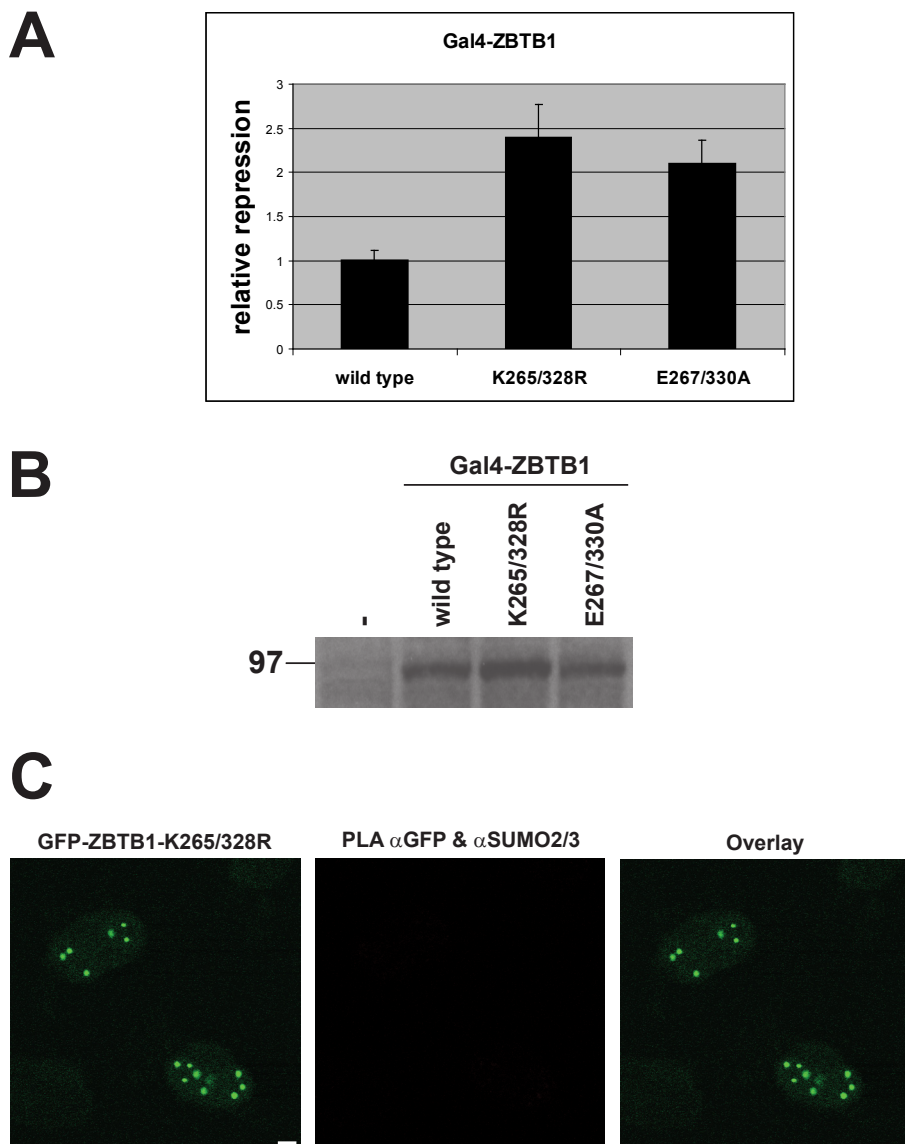


Figure S5 related to Figure 6. A and B. GAL4-ZBTB1- E267A-E330A luciferase activity and immunoblot. HeLa cells were grown on 24-well dishes and transfected with 500 ng of Gal4(DBD)-fusion expression plasmids and 500 ng of the reporter construct 5xGal4-Tk-Pgl3. Cells were lysed in reporter lysis buffer and luciferase activity was measured. (A) The transcriptional activities of Gal4-ZBTB1 wild type and SUMOylation mutants were determined. The error bars indicate one standard deviation from the average; results are representative of five independent experiments. (B) Transfection mixtures were split and one set of wells was lysed in LDS sample buffer to verify the expression levels of the Gal4-ZBTB1 proteins by immunoblotting using an antibody directed against Gal4. (C) GFP-ZBTB1-K265R-K328R PLA negative control. HeLa cells were transfected with an expression construct encoding GFP-ZBTB1-K265R-K328R, fixed and the PLA was performed using affinity purified peptide anti SUMO-2/3 antibodies and a monoclonal antibody directed against GFP. Secondary antibodies were labeled with specific oligonucleotides. Oligonucleotide hybridization, ligation, amplification and detection were performed.

Supplemental Table S1 Detailed list of the SUMOylation sites that were identified in our screen. Available online at: <http://www.sciencedirect.com/science/article/pii/S1097276510005733>

Supplementary Materials

Plasmids

Lysine-deficient SUMO-2 was previously described (11). Lysine-deficient SUMO2-Q87R was generated by QuickChange site-directed mutagenesis (Stratagene) using oligonucleotides 5'-CATCGACGTGTTCCGGCAGCAGACGGGAG-3' and 5'-CTCCCGTCTGCTGCCGGAACACGTCGATG-3' and lysine-deficient SUMO2-T90R was generated using oligonucleotides 5'-GTGTTCCAGCAGCAGAGGGGAGGTTAGGAATTCTG-3' and 5'-CAGAATTCCTAACCTCCCCTCTGCTGCTGGAACAC-3'

The cDNA encoding the ZBTB1 protein was obtained from the Mammalian Gene Collection (MGC code 60335; Image ID 6141266; supplied by MRC geneservice, Cambridge, UK) and amplified by a two-step PCR reaction using the following primers: 5'-AAAAAGCAGGCTATATGGCAAAGCCCAGCAC-3' and 5'-AGAAAGCTGGGTCTCAGTTCTTTCAAATGC-3' for the first reaction and 5'-GGGGACAAGTTTGTACAAAAAGCAGGCT-3' and 5'-GGGGACCACTTTGTACAAGAAAGCTGGGT-3' for the second reaction. The forward primer for the mutant lacking the BTB domain was 5'-AAAAAGCAGGCTATATGCAGGATGCAGATTGTTCC-3'. The cDNA was inserted into pDON207 employing standard Gateway technology (Invitrogen) and subsequently transferred to multiple different destination vectors to generate a T7-ZBTB1 expression construct and EYFP-, ECFP- EGFP- and GAL4(DBD)-tagged ZBTB1 expression plasmids. The fusions were made to the N-terminus of ZBTB1. EYFP-, ECFP- and EGFP-destination vectors were constructed by Dr. M. Posch (Wellcome Trust Biocentre, Dundee, UK). The Gal4(DBD)-destination vector was obtained by ligation of the Gateway cassette reading frame B (Invitrogen) into the *EcoRI* digested pCG4 plasmid (15), which was a kind gift of Dr. N.D. Perkins (Wellcome Trust Biocentre, Dundee, UK). T7-ZBTB1 was constructed using destination vector pDEST14 (Invitrogen).

To generate ZBTB1 SUMOylation site mutants, the consensus SUMOylation sites, lysine 265 and lysine 328, were mutated to arginine residues by QuickChange site-directed mutagenesis (Stratagene) using oligonucleotides 5'-GACAGTAACATCAGAGCTGAATTTGGTG-3' and 5'-CACCAAATTCAGCTCTGATGTTACTGTC-3' for the K265R mutation, 5'-GGATTATTATTAGGATGGAGCCAGAAG-3' and 5'-CTTCTGGCTCCATCCTAATAATAATCC-3' for the K328R mutation, 5'-GACAGTAACATCAAAGCTGCATTTGGTGAAAAAG-3 and 5'-CTTTTTCACCAAATGCAGCTTTGATGTTACTGTC-3' for the E267A mutation and 5'-GGATTATTATTAAGATGGCTCCAGAAGATATTCCTAC-3' and 5'-GTAGGAATATCTTCTGGAGCCATCTTAATAATAATCC-3' for the E330A mutation.

To generate mutations in the hydrophobic cluster preceding the SUMOylated lysine K328, we replaced isoleucines on positions 325 and 326 for the corresponding amino acids preceding the SUMOylated lysine 265, serine and asparagine respectively using oligonucleotides 5'-CTGAGAGGAAAAGGAGTATTATTAAGATGGAG-3' and 5'-CTCCATCTTAATAACTCCTTTTCTCTCAG-3' for the I325S mutation and oligonucleotides 5'-GAGAGGAAAAGGATTAATATTAAGATGGAGCC-3' and 5'-GGCTCATCTTAATTAATCCTTTTCTCTC-3' for the I326N mutation. The I325A mutation was generated using oligonucleotides 5'-CTGAGAGGAAAAGGGCTATTATTAAGATGGAG-3' and 5'-CTCCATCTTAATAAGCCCTTTTCTCTCAG-3'. The I326A mutation was generated using oligonucleotides 5'-GAGAG-

Chapter 4

GAAAAGGATTGCTATTAAGATGGAGCC-3' and 5'-GGCTCCATCTTAATAGCAATCCTTTTCCTCTC-3'. The BTB domain (aa1-141) of ZBTB1 was amplified using oligonucleotides 5'-ACAACGGATCCATGGCAAAGCCCAGCCAC-3' and 5'-GCCGCGGAATTCTTACCCAAATATCATTTTGCTG-3' and inserted into pGEX-2T.

Phosphorylation site mutants in NOP5/58-EGFP (a kind gift from Dr. Westman, Dundee, U.K.) were generated by site directed mutagenesis. The S502A mutant was generated using oligonucleotides 5'-GGAAGAACCACTTGCTGAGGAAGAACCA TG-3' and 5'-CATGGTTCTTCTCAGCAAGTGGTTCTTCC-3'. The S502D mutant was generated using oligonucleotides 5'-GGAAGAACCACTTGATGAGGAAGAACCATG-3' and 5'-CATGGTTCTTCTCATCAAGTGGTTCTTCC-3'.

The HA-RanGAP1 expression construct was a kind gift from Dr. Melchior (Heidelberg, Germany). The $\Delta 523_{524}$ mutant was generated using oligonucleotides 5'-GGCTCCTCGTGACATGCTCAAGAGTGAAGACAAG-3' and 5'-CTTGTCTTCACTCTTGAGCATGTGCACGAGGAGCC-3'. The G523H-L524H mutant was generated using oligonucleotides 5'-GGCTCCTCGTGACATGCATCACCTCAAGAGTGAAGACAAGG-3' and 5'-CCTTGTCTTCACTCTTGAGGTGATGCATGTGCACGAGGAGCC-3'. The G523N_L524N mutant was generated using oligonucleotides 5'-CAGGCTCCTCGTGACATGAATAACCTCAAGAGTGAAGACAAGG-3' and 5'-CCTTGTCTTCACTCTTGAGGTATTTCATGTGCACGAGAGCCTG-3'.

pCMX-SMRTe (16, 17) was a kind gift of Dr. E.J. Park and Dr. J.D. Chen (University of Massachusetts Medical School, Worcester, MA). The SMRT cDNA was amplified by PCR using pCMX-hSMRTe as template and oligonucleotides 5'-GGGGACAAGTTGTACAAAAAGCAGGCTCCATGTCGGGCTCCACACAGCCTGT-3' and 5'-GGGGACCACTTTGTACAAGAAAGCTGGGTGTCACTCGCTGTCGGAGAGTGTCTCGTA-3'. The amplified fragment was subsequently inserted into pDON207, and the EYFP-SMRT expression construct was obtained using standard Gateway technology. Constructs were verified by sequencing.

***In vivo* SUMO conjugation assays**

HeLa cells stably expressing His6-SUMO-2 and control HeLa cells were grown on 15cm culture dishes and transfected. Cells were isolated by trypsinization 24 hours after transfection, washed twice with ice-cold PBS and lysed in 1 ml lysis buffer containing 8 M urea, 100 mM $\text{Na}_2\text{HPO}_4/\text{NaH}_2\text{PO}_4$ and 10 mM Tris/HCl pH 7.0 at room temperature. After removal of DNA clumps, samples were sonicated 4x 5 secs on ice. Imidazole (5mM) was added where indicated and His6-SUMO-2 conjugates were purified on 50 μl Co^{2+} TALON beads (BD Biosciences) at room temperature. After washing the beads four times with 1 ml urea lysis buffer, SUMO-2 conjugates were eluted from the beads in 60 μl urea lysis buffer containing 200 mM imidazole. Alternatively, cells were solubilized in lysis buffer (6 M Guanidinium-HCl, 100 mM $\text{Na}_2\text{HPO}_4/\text{NaH}_2\text{PO}_4$, 10 mM Tris/HCl, pH 8.0, 20 mM Imidazole, 10 mM β mercapto-ethanol) and sonicated to reduce the viscosity. His6-SUMO conjugates were enriched on Ni-NTA Agarose beads (Qiagen) and washed using wash buffers A-D. (Buffer A: 6 M Guanidinium-HCl, 100 mM $\text{NaH}_2\text{PO}_4/\text{Na}_2\text{HPO}_4$, 10 mM Tris/HCl pH 8.0 and 0.2% Triton-X-100. Buffer B: 8 M Urea, 100 mM $\text{NaH}_2\text{PO}_4/\text{Na}_2\text{HPO}_4$, 10 mM Tris/HCl pH 8.0 and 0.2% Triton-X-100. Buffer C: 8 M Urea, 100 mM $\text{NaH}_2\text{PO}_4/\text{Na}_2\text{HPO}_4$, 10 mM Tris/HCl pH 6.3 and 0.2% Triton-X-100. Buffer D: 8 M Urea, 100 mM $\text{NaH}_2\text{PO}_4/\text{Na}_2\text{HPO}_4$, 10 mM Tris/HCl pH 6.3 and 0.1%

Triton-X-100). These wash buffers also contained 10 mM β mercapto-ethanol. Samples were eluted in 6.4 M Urea, 80 mM $\text{NaH}_2\text{PO}_4/\text{Na}_2\text{HPO}_4$, 8 mM Tris/HCl pH 7.0, 200 mM imidazole.

Electrophoresis and immunoblotting

Protein samples were size fractionated on Novex 4-12% Bis-Tris gradient gels using MOPS running buffer (Invitrogen) or on regular SDS-PAGE gels with a tris-glycine buffer. Note that these different methods cause slight differences in the running behavior of proteins (Invitrogen). Size fractionated proteins were subsequently transferred onto Hybond-C extra membranes (Amersham Biosciences) using a submarine system (Invitrogen). Blots were stained for total protein using Ponceau S (Sigma). After blocking with PBS containing 0.1% Tween-20 and 5% milk powder, the membranes were incubated with primary antibodies as indicated.

Electrophoresis, Coomassie Staining and In-gel digestion

The purified His6-SUMO-2 conjugates were separated by SDS-PAGE using Novex 4-12% gradient gels and MES SDS running buffer (Invitrogen), followed by staining with Colloidal Blue Kit (Invitrogen). Bands in the molecular range of 15-38 kDa were excised from the gel, cut into 2-mm³ cubes and in-gel digested with trypsin (Promega) essentially as described (18). The reduction and alkylation steps were performed before Lys-C digestion and therefore skipped during trypsin in-gel digestion. The peptides extracted from the gel after digestion were cleaned, desalted, concentrated and enriched on C₁₈ reverse phase StageTips (19). In-solution digested samples were analyzed on an LTQ-Orbitrap XL mass spectrometer whereas the analysis of in-gel digested samples was performed on an LTQ-Orbitrap Velos instrument (20).

Liquid Chromatography-Mass spectrometry

Mass spectrometric analysis was performed by nanoscale LC-MS/MS using LTQ-Orbitrap XL and LTQ-Orbitrap Velos instruments (Thermo Fisher Scientific, Germany) coupled to an EASY-nLC system (Proxeon Biosystems, Denmark) via a Proxeon nanoelectrospray interface. Peptides eluted from StageTips were separated on a 75 μm inner diameter reverse phase C₁₈ column packed in-house with 3 μm C18 beads (Dr. Maisch, Germany) with a 140 or 240 min gradient.

Data were acquired in data-dependent mode. In the case of the LTQ-Orbitrap XL, full scan spectra were acquired in the 300-1600 m/z range ($R = 60,000$ and target value of 1'000'000); 400-1000 m/z range was used in the 'single range' method; 'multiple ranges' experiments used mass regions m/z 300-500, m/z 450-650, m/z 600-900, m/z 850-1,250, m/z 1,200-1,800. Injection waveforms option was enabled in all survey scans to eject all ions outside of the specified mass range. For 'full range' and 'single range' orbitrap measurements the "lock mass" option was used to improve the mass accuracy of precursor ions (21). The ten most intense ions were fragmented by collision-induced dissociation (CID) with normalized collision energy of 35% and recorded in the linear ion trap (target value of 5,000) based on the survey scan and in parallel to the orbitrap detection of MS spectra.

In the case of the LTQ-Orbitrap Velos, survey scan acquisition was performed in the orbitrap with a resolution of 30,000 at m/z 400. Ten most intense ions were fragmented by higher-energy collisional dissociation (HCD) with normalized collision energy of 40% and recorded in the orbitrap with a resolution of

Chapter 4

7,500 at m/z 400 (target value of 50,000). The HCD experiments were performed in the 'full range' mode (300-1700 m/z : target value of 1'000'000) and 'multiple ranges' mode (mass ranges of 400-650 m/z , 600-900 m/z and 850-1300 m/z ; target value of 500'000). Survey and HCD fragment spectra were acquired in profile mode, whereas the acquisition of CID MS/MS spectra was done in centroid mode.

Data Processing and Analysis

Raw MS data files were processed with the MaxQuant software (version 1.0.14.3) (22) as previously described (23). Enzyme specificity was set to trypsin, allowing for cleavage N-terminal to proline residues and up to four missed cleavages. Cysteine carbamidomethylation was considered as a fixed modification, and methionine oxidation, protein N-acetylation and phosphorylation on serine, threonine and tyrosine residues were set as variable modifications in all experiments. In addition, mass addition of 114.0429 (GG signature tag derived from SUMO2-T90R) on lysine for the T90R experiment, and mass addition of 471.2078 (QQTGG signature tag remnant of SUMO2-Q87R) on lysine for the Q87R experiment, were considered as variable modifications. MS/MS peak list generated by MaxQuant were searched by the Mascot database search engine (Matrix Science, London, UK, version 2.1.04) against the human International Protein Index (IPI) database (version 3.37) (Kersey et al., 2004). The initial maximum allowed mass deviation was set to 7 ppm for peptide masses, 0.5 Da for low resolution CID fragment ions and 0.02 Da for high resolution HCD fragment ions.

4

Manual validation of Peptide Identifications

The best MS/MS spectra of all identified SUMOylated peptides were manually validated using the Viewer module of MaxQuant and Xcalibur Qual browser instruments (Thermo Fisher Scientific, Germany). The peptide matches were filtered by the following criteria: (i) maximum mass deviation smaller than 5 ppm; (ii) only peptides containing an internal SUMOylated lysine were accepted; (iii) reasonable coverage of b- and/or y- ions series; (iv) peptides containing prolines were required to show pronounced cleavage amino-terminal to the proline residue; (v) preferential cleavage C-terminally from aspartate and glutamate; (vi) presence of a_2/b_2 pairs. Additionally, Q87R HCD spectra were required to show QQTGG signature fragment ions in the low mass region: m/z 257.125 (QQ), m/z 240.097 (QQ with loss of ammonia) and m/z 239.114 (QQ with loss of water).

In vitro expression of proteins

In vitro transcription/translation of proteins was performed using 1 μ g of plasmid DNA (T7-ZBTB1) and a wheat germ-coupled transcription/translation system in 25 μ l reaction volumes according to the instructions provided by the manufacturer (Promega). [35 S]Methionine (17.5 μ Ci per labeling) (Amersham Biosciences) was used in the reactions to generate radiolabeled proteins.

In vitro SUMO conjugation assays

In vitro SUMO conjugation assays were performed in 10 μ l volumes containing 120 ng SAE1/2, 500 ng SUMO-2, 50 mM Tris/HCl pH 7.5, 5 mM $MgCl_2$, 2 mM ATP, 10 mM creatine phosphate, 3.5 U/ml creatine kinase, 0.6 U/ml inorganic pyrophosphatase, protease inhibitors and Ubc9 as indicated. SUMOylation

was carried out using 1 μ l of the *in vitro* transcribed and translated [³⁵S] labeled ZBTB1 or 30 μ M peptide. Reactions were incubated for 3 hours at 37°C. After termination of the reaction with LDS sample buffer (Invitrogen), reaction products were fractionated by SDS-PAGE using Novex 4-12% Bis-Tris gradient gels and MOPS running buffer (Invitrogen). Dried gels were exposed to X-Omat AR (XAR) autoradiography films (Kodak) to detect radiolabeled proteins.

Luciferase assays

HeLa cells were grown on 24-well tissue culture plates and transfected with 500 ng of Gal4-DBD or Gal4(DBD)-fusion expression plasmids and 500 ng of the reporter construct 5xGal4-Tk-Pgl3 (24). 24 hours after transfection, cells were washed with ice-cold PBS and lysed in 100 μ l reporter lysis buffer (Promega). As a control, the luciferase activity of the known transcriptional repressor thyroid hormone receptor (TR) was determined (25). Luciferase activity relative to Gal4-DBD was depicted. Equal expression of Gal4(DBD)-fusion plasmids was verified by immunoblotting. Transfection mixtures were split over two wells. Samples for immunoblotting were prepared in LDS sample buffer (Invitrogen).

Proximity Ligation Assay

Proximity Ligation was performed as previously described (26, 27). Cells were fixed for 15 minutes with 3.7% paraformaldehyde in PBS at 37°C and permeabilized for 15 minutes at room temperature with 0.1% Triton X-100 in TBS. After washing, cells were blocked for 10 minutes using 0.5% milk powder in TBST. Antibody incubations using monoclonal anti GFP antibody (Roche) and affinity purified rabbit anti SUMO-2/3 antibody (Eurogentec) were carried out overnight in blocking solution at room temperature. Subsequent steps were carried out at 37°C. Secondary antibodies were incubated for 1 hour. Hybridization was performed for 30 minutes in a humid chamber. This chamber was also used for ligation for 30 minutes, for amplification for 90 minutes and for detection for 30 minutes. Dot-like structures are an intrinsic characteristic of PLA signals and do not necessarily represent nuclear bodies.

Supplementary References

- Blomster, H. A., Hietakangas, V., Wu, J., Kouvonon, P., Hautaniemi, S., and Sistonen, L. (2009) Novel proteomics strategy brings insight into the prevalence of SUMO-2 target sites. *Mol. Cell Proteomics* 8, 1382-1390
- Ganesan, A. K., Kho, Y., Kim, S. C., Chen, Y., Zhao, Y., and White, M. A. (2007) Broad spectrum identification of SUMO substrates in melanoma cells. *Proteomics* 7, 2216-2221
- Gocke, C. B., Yu, H., and Kang, J. (2005) Systematic identification and analysis of mammalian small ubiquitin-like modifier substrates. *J. Biol. Chem.* 280, 5004-5012
- Golebiowski, F., Matic, I., Tatham, M. H., Cole, C., Yin, Y., Nakamura, A., Cox, J., Barton, G. J., Mann, M., and Hay, R. T. (2009) System-wide changes to SUMO modifications in response to heat shock. *Sci. Signal.* 2, ra24
- Li, T., Evdokimov, E., Shen, R. F., Chao, C. C., Tekle, E., Wang, T., Stadtman, E. R., Yang, D. C., and Chock, P. B. (2004) Sumoylation of heterogeneous nuclear ribonucleoproteins, zinc finger proteins, and nuclear pore complex proteins: a proteomic analysis. *Proc. Natl. Acad. Sci. U. S A* 101, 8551-8556
- Li, T., Santockyte, R., Shen, R. F., Tekle, E., Wang, G., Yang, D. C., and Chock, P. B. (2006) A general approach for investigating enzymatic pathways and substrates for ubiquitin-like modifiers. *Arch. Biochem. Biophys.* 453, 70-74
- Manza, L. L., Codreanu, S. G., Stamer, S. L., Smith, D. L., Wells, K. S., Roberts, R. L., and Liebler, D. C. (2004) Global shifts in protein sumoylation in response to electrophile and

- oxidative stress. *Chem. Res. Toxicol.* 17, 1706-1715
8. Matafora, V., D'Amato, A., Mori, S., Blasi, F., and Bachi, A. (2009) Proteomic analysis of nucleolar SUMO-1 target proteins upon proteasome inhibition. *Mol. Cell Proteomics*
 9. Pungaliya, P., Kulkarni, D., Park, H. J., Marshall, H., Zheng, H., Lackland, H., Saleem, A., and Rubin, E. H. (2007) TOPORS functions as a SUMO-1 E3 ligase for chromatin-modifying proteins. *J. Proteome Res.* 6, 3918-3923
 10. Rosas-Acosta, G., Russell, W. K., Deyrieux, A., Russell, D. H., and Wilson, V. G. (2005) A universal strategy for proteomic studies of SUMO and other ubiquitin-like modifiers. *Mol. Cell Proteomics* 4, 56-72
 11. Schimmel, J., Larsen, K. M., Matic, I., van Hagen, M., Cox, J., Mann, M., Andersen, J. S., and Vertegaal, A. C. (2008) The ubiquitin-proteasome system is a key component of the SUMO-2/3 cycle. *Mol. Cell Proteomics* 7, 2107-2122
 12. Vertegaal, A. C., Ogg, S. C., Jaffray, E., Rodriguez, M. S., Hay, R. T., Andersen, J. S., Mann, M., and Lamond, A. I. (2004) A proteomic study of SUMO-2 target proteins. *J. Biol. Chem.* 279, 33791-33798
 13. Vertegaal, A. C., Andersen, J. S., Ogg, S. C., Hay, R. T., Mann, M., and Lamond, A. I. (2006) Distinct and overlapping sets of SUMO-1 and SUMO-2 target proteins revealed by quantitative proteomics. *Mol. Cell Proteomics* 5, 2298-2310
 14. Zhao, Y., Kwon, S. W., Anselmo, A., Kaur, K., and White, M. A. (2004) Broad spectrum identification of cellular small ubiquitin-related modifier (SUMO) substrate proteins. *J. Biol. Chem.* 279, 20999-21002
 15. Chapman, N. R., and Perkins, N. D. (2000) Inhibition of the RelA(p65) NF-kappaB subunit by Egr-1. *J. Biol. Chem.* 275, 4719-4725
 16. Park, E. J., Schroen, D. J., Yang, M., Li, H., Li, L., and Chen, J. D. (1999) SMRTE, a silencing mediator for retinoid and thyroid hormone receptors-extended isoform that is more related to the nuclear receptor corepressor. *Proc. Natl. Acad. Sci. U. S. A.* 96, 3519-3524
 17. Wu, X., Li, H., Park, E. J., and Chen, J. D. (2001) SMRTE inhibits MEF2C transcriptional activation by targeting HDAC4 and 5 to nuclear domains. *J. Biol. Chem.* 276, 24177-24185
 18. Shevchenko, A., Tomas, H., Havlis, J., Olsen, J. V., and Mann, M. (2006) In-gel digestion for mass spectrometric characterization of proteins and proteomes. *Nat. Protoc.* 1, 2856-2860
 19. Rappsilber, J., Mann, M., and Ishihama, Y. (2007) Protocol for micro-purification, enrichment, pre-fractionation and storage of peptides for proteomics using StageTips. *Nat. Protoc.* 2, 1896-1906
 20. Olsen, J. V., Schwartz, J. C., Griep-Raming, J., Nielsen, M. L., Damoc, E., Denisov, E., Lange, O., Remes, P., Taylor, D., Splendore, M., Wouters, E. R., Senko, M., Makarov, A., Mann, M., and Horning, S. (2009) A dual pressure linear ion trap orbitrap instrument with very high sequencing speed. *Mol. Cell Proteomics* 8, 2759-2769
 21. Olsen, J. V., de Godoy, L. M., Li, G., Macek, B., Mortensen, P., Pesch, R., Makarov, A., Lange, O., Horning, S., and Mann, M. (2005) Parts per million mass accuracy on an Orbitrap mass spectrometer via lock mass injection into a C-trap. *Mol. Cell Proteomics* 4, 2010-2021
 22. Cox, J., and Mann, M. (2008) MaxQuant enables high peptide identification rates, individualized p.p.b.-range mass accuracies and proteome-wide protein quantification. *Nat. Biotechnol.* 26, 1367-1372
 23. Cox, J., Matic, I., Hilger, M., Nagaraj, N., Selbach, M., Olsen, J. V., and Mann, M. (2009) A practical guide to the MaxQuant computational platform for SILAC-based quantitative proteomics. *Nat. Protoc.* 4, 698-705
 24. Kalkhoven, E., Teunissen, H., Houweling, A., Verrijzer, C. P., and Zantema, A. (2002) The PHD type zinc finger is an integral part of the CBP acetyltransferase domain. *Mol. Cell Biol.* 22, 1961-1970
 25. Tone, Y., Collingwood, T. N., Adams, M., and Chatterjee, V. K. (1994) Functional analysis of a transactivation domain in the thyroid hormone beta receptor. *J. Biol. Chem.* 269, 31157-31161
 26. Soderberg, O., Leuchowius, K. J., Gullberg, M., Jarvius, M., Weibrecht, I., Larsson, L. G., and Landegren, U. (2008) Characterizing proteins and their interactions in cells and tissues using the in situ proximity ligation assay. *Methods* 45, 227-232
 27. Soderberg, O., Gullberg, M., Jarvius, M., Ridderstrale, K., Leuchowius, K. J., Jarvius, J., Wester, K., Hydring, P., Bahram, F., Larsson, L. G., and Landegren, U. (2006) Direct observation of individual endogenous protein complexes in situ by proximity ligation. *Nat. Methods* 3, 995-1000



**Uncovering SUMOylation
dynamics during cell
cycle progression reveals
FoxM1 as a key mitotic SUMO
target protein**

Joost Schimmel*, Karolin Eifler*, Jón Otti Sigurðsson*,
Sabine A.G. Cuijpers, Ivo A. Hendriks, Matty Verlaan – de
Vries, Christian D. Kelstrup, Chiara Francavilla, René H.
Medema, Jesper V. Olsen, Alfred C.O. Vertegaal

Molecular Cell 2014 53(6):1053-66

*These authors contributed equally to this work.

Supplemental data is available online at: <http://www.sciencedirect.com/science/article/pii/S1097276514001154>

Chapter 5. Uncovering SUMOylation dynamics during cell cycle progression reveals FoxM1 as a key mitotic SUMO target protein

Abstract

Loss of SUMO modification in mice causes genomic instability due to the missegregation of chromosomes. Currently, little is known about the identity of relevant SUMO target proteins that are involved in this process and about global SUMOylation dynamics during cell cycle progression. We performed a large-scale quantitative proteomics screen to address this and identified 593 proteins to be SUMO-2 modified, including the Forkhead transcription factor FoxM1, a key regulator of cell cycle progression and chromosome segregation. SUMOylation of FoxM1 peaks during G2 and M phase, when FoxM1 transcriptional activity is required. We found that a SUMOylation deficient FoxM1 mutant was less active compared to wild-type FoxM1, implicating that SUMOylation of the protein enhances its transcriptional activity. Mechanistically, SUMOylation blocks the dimerization of FoxM1, thereby relieving FoxM1 autorepression. Cells deficient for FoxM1 SUMOylation showed increased levels of polyploidy. Our findings contribute to understanding the role of SUMOylation during cell cycle progression.

5

Introduction

Cell cycle progression is extensively controlled via complex networks of reversible post-translational modifications (PTMs), including small chemical modifications like phosphorylation and modifications by ubiquitin and small ubiquitin-like proteins (1-3). Deregulation of these signaling cascades can result in uncontrolled cell cycle progression, causing genome instability and cancer (4-6). Cell cycle signal transducers represent major anti-cancer drug targets that are exploited to halt cell cycle progression in tumor cells (7).

More recently, mass spectrometry (MS)-based proteomics has enabled global analyses of different post-translational modification networks, including phosphorylation, ubiquitination and lysine acetylation (8). Interestingly, nuclear proteins and proteins involved in regulating metabolic processes showed significant cell cycle dynamics with notably high phosphorylation site occupancy in mitosis (9). Initial studies on the small ubiquitin-like modifier (SUMO) system revealed a key role for this modification in cell cycle progression (10-13). A failure to conjugate the single SUMO form in *S. cerevisiae*, Smt3, to target proteins due to a deletion of Ubc9 resulted in a G2/M block (14). Conversely, a failure to remove Smt3 from a subset of target proteins due to a deletion of the SUMO protease Ulp1 in *S. cerevisiae*

also resulted in a G2/M block (15) and Ulp2 is essential for spindle dynamics and cell cycle progression (16). Mice deficient for Ubc9 failed to progress through embryonic development and died at the early post-implantation stage due to DNA hypocondensation and genome instability (17).

Multiple SUMO target proteins were identified that play key roles during cell cycle progression including the trimeric replication clamp PCNA (18, 19), DNA topoisomerase II α (20), CENP-E (Zhang et al., 2008), CENP-I (21) and the chromosomal passenger complex subunit Borealin (22). Despite these interesting findings, we are lacking global insight in the regulation of cell cycle progression via SUMOylation. To address this, we have optimized the biochemical purification of SUMO target proteins and used a SILAC approach (23) to compare SUMOylation levels of these targets at different cell cycle stages. Follow-up experiments revealed that SUMOylation was needed for full transcriptional activation of the Forkhead box transcription factor FoxM1 and for counteracting polyploidy. Mechanistically, SUMOylation counteracts autorepression of FoxM1.

Results

Knockdown of UBA2 and Ubc9 in HeLa cells leads to decreased cell proliferation

To study the role of SUMOylation in cell cycle progression in a mammalian system, we infected HeLa and U2OS cells with lentiviruses encoding shRNAs against UBA2, Ubc9 or for a non-coding control shRNA. Western blot analysis confirmed that UBA2 and Ubc9 protein levels as well as the amount of SUMO conjugates were reduced but not abrogated after virus infection, whereas the pool of free SUMO was increased (Figure 1A). Colony formation of cells treated with UBA2 and Ubc9 knockdown viruses was compared to the control nine days after infection. Knockdown of UBA2 and Ubc9 limited colony formation to only about 1-2 % in HeLa cells and 4-22 % in U2OS compared to the control population (Figure 1B and Figure S1A). We further confirmed these findings by testing cell proliferation of Ubc9 depleted cells four days after infection. Ubc9 knockdown decreased proliferation by 24-45% both in HeLa and U2OS cells (Figure 1C and Figure S1B).

Surprisingly, flow cytometry on day four after virus infection did not reveal any significant differences between mock treated cells and cells treated with UBA2 and Ubc9 knockdown viruses (Figure 1D and Figure S1C) in contrast to the G2/M block observed in yeast cells lacking Ubc9 (14). From this we conclude that the decrease in colony formation after UBA2 and Ubc9 knockdown is neither caused by arresting the cells in a specific phase of the cell cycle nor by an increase in the apoptotic cell pool. These findings are consistent with recently reported results (24). Using BrdU pulse labeling, we could demonstrate a delay in cell cycle progression in response to inhibiting SUMOylation (Figure 1E and Figure S1D).

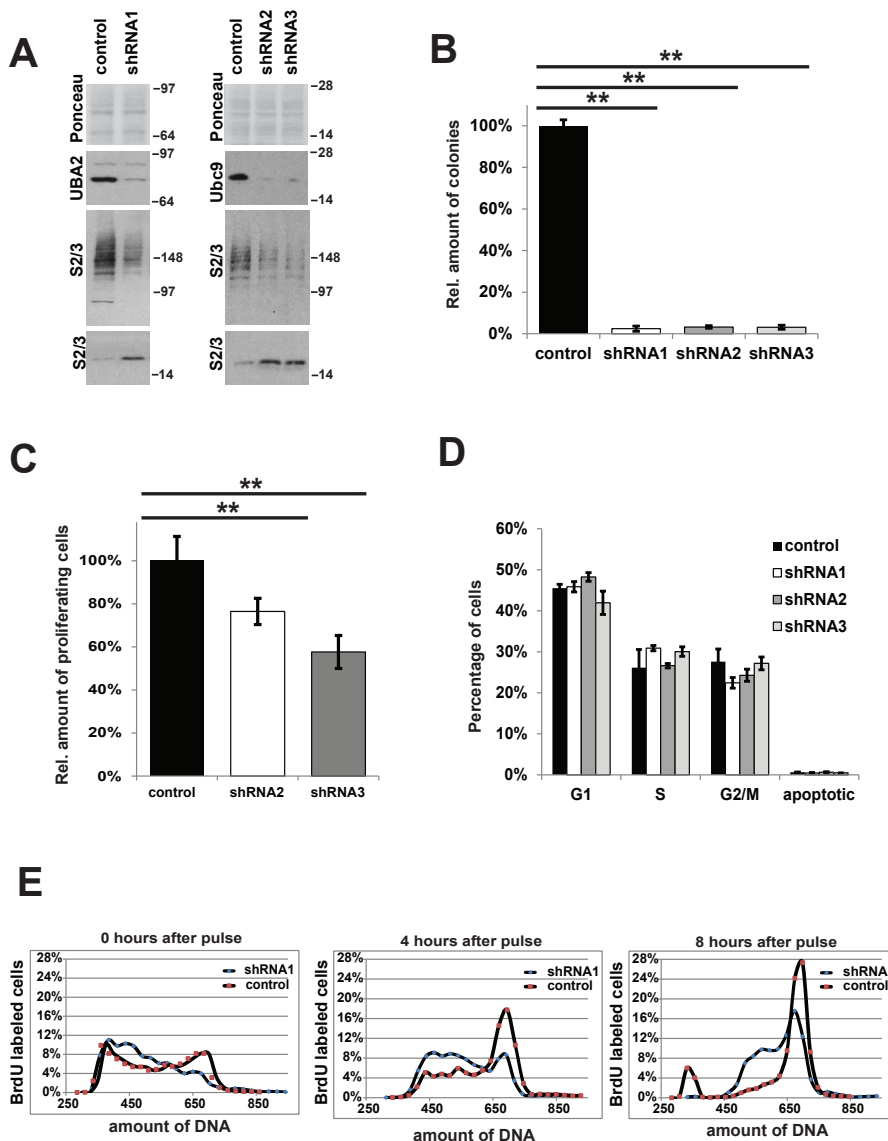


Figure 1. SUMOylation is required for cell proliferation A) HeLa cells were infected with lentiviruses expressing an shRNA against UBA2 (shRNA1) and two different shRNAs against Ubc9 (shRNA2 and shRNA3), or with a control virus respectively. A decrease in UBA2 and Ubc9 expression and SUMO conjugation levels and an increase in free SUMO was confirmed by immunoblotting four days after virus infection using antibodies against UBA2, Ubc9 and SUMO-2/3. B) Colony formation was determined nine days after infection by staining with Giemsa solution and counting colonies using the ImageJ Version 1.47v software. The values were normalized to the control. Error bars represent the standard deviation from the average obtained from three independent experiments. ** $p < 0.001$. C) The proliferation rate of cells treated with Ubc9 knockdown virus was compared to cells treated with control virus four days after infection by adding the cell metabolic activity reagent WST-1 to the growing cells and measuring the absorbance at 450 nm after two hours incubation. The values were normalized to the control and the standard error of the mean was determined from ten values obtained from three independent experiments.

** $p < 0.001$. D) The graph depicts the percentage of HeLa cells in each cell cycle phase measured by flow cytometry four days after virus infection. Error bars represent the standard deviation from the average obtained from three independent experiments. E) BrdU pulse chase experiments demonstrate a decelerated passage through the cell cycle for HeLa cells treated with shRNA1 for four days and released from the BrdU pulse for four hours or eight hours. See also Figure S1.

A quantitative proteomics approach to study global SUMOylation dynamics throughout the cell cycle

Subsequently, we were interested in identifying global SUMOylation dynamics during cell cycle progression using a quantitative proteomics approach. SUMOylation proteomics is challenging since SUMOylation levels of most proteins are low and SUMO proteases can rapidly cleave SUMOs from target proteins (25). To be able to purify SUMO targets from cells, we generated a HeLa cell line stably expressing Flag-tagged SUMO-2 bearing a Q87R mutation in order to shorten the peptide branch remaining after tryptic digestion to enable SUMO acceptor site mapping (26). SUMO-2 was chosen for these experiments since SUMO-2/3 are the most abundant SUMO family members (27), displaying cell cycle dynamics (28) and mature SUMO-2 and SUMO-3 are virtually identical. Moreover, these SUMO forms are able to form SUMO chains (29, 30) that play an important role in SUMOylation dynamics (31). Co-expression of GFP, linked to the Flag-SUMO-2 cDNA via an IRES, allowed sorting by flow cytometry of a homogeneous population of low expressing cells to avoid overexpression artifacts.

Analysis of the cells by confocal microscopy revealed that Flag-SUMO-2 was predominantly located in the nucleus as expected (Figure 2A). Immunoblotting analysis confirmed the relatively low expression of Flag-SUMO-2 compared to endogenous SUMO-2/3 levels in HeLa cells and the efficient enrichment of SUMO-2 conjugates by immunoprecipitation (IP) (Figure 2B).

For quantitative proteomic analysis, three different populations of HeLa cells expressing Flag-SUMO-2 were SILAC labeled with three distinct sets of isotopic variants of lysine and arginine. Cells were blocked with thymidine or the CDK1 inhibitor RO-3306 and either directly lysed or released from the blockage for different amounts of time as indicated in Figure 2C. Flow cytometry analysis confirmed the enrichment of synchronized cell populations at the respective cell cycle stages (Figure 2C). Cells released from the RO-3306 block for 8 hours were an exception due to the prolonged presence of G2/M arrested cells. Thus, G1 effects identified in this sample might be underestimated. For subsequent Flag-IP, lysates of synchronized cells were mixed with lysates obtained from asynchronous cells labeled with heavy amino acids as indicated in Figure 2C, resulting in three independent experiments (I.A, II.A and III.A). In addition, we obtained two different M phase-enriched samples (Figure 2D, 2F and S2B). Results obtained via flow cytometry confirmed enrichment of arrested cells in the respective cell cycle stage (Figure 2D). Asynchronous cells were heavy labeled and mixed with the mitotic samples, resulting in experiment IV.A.

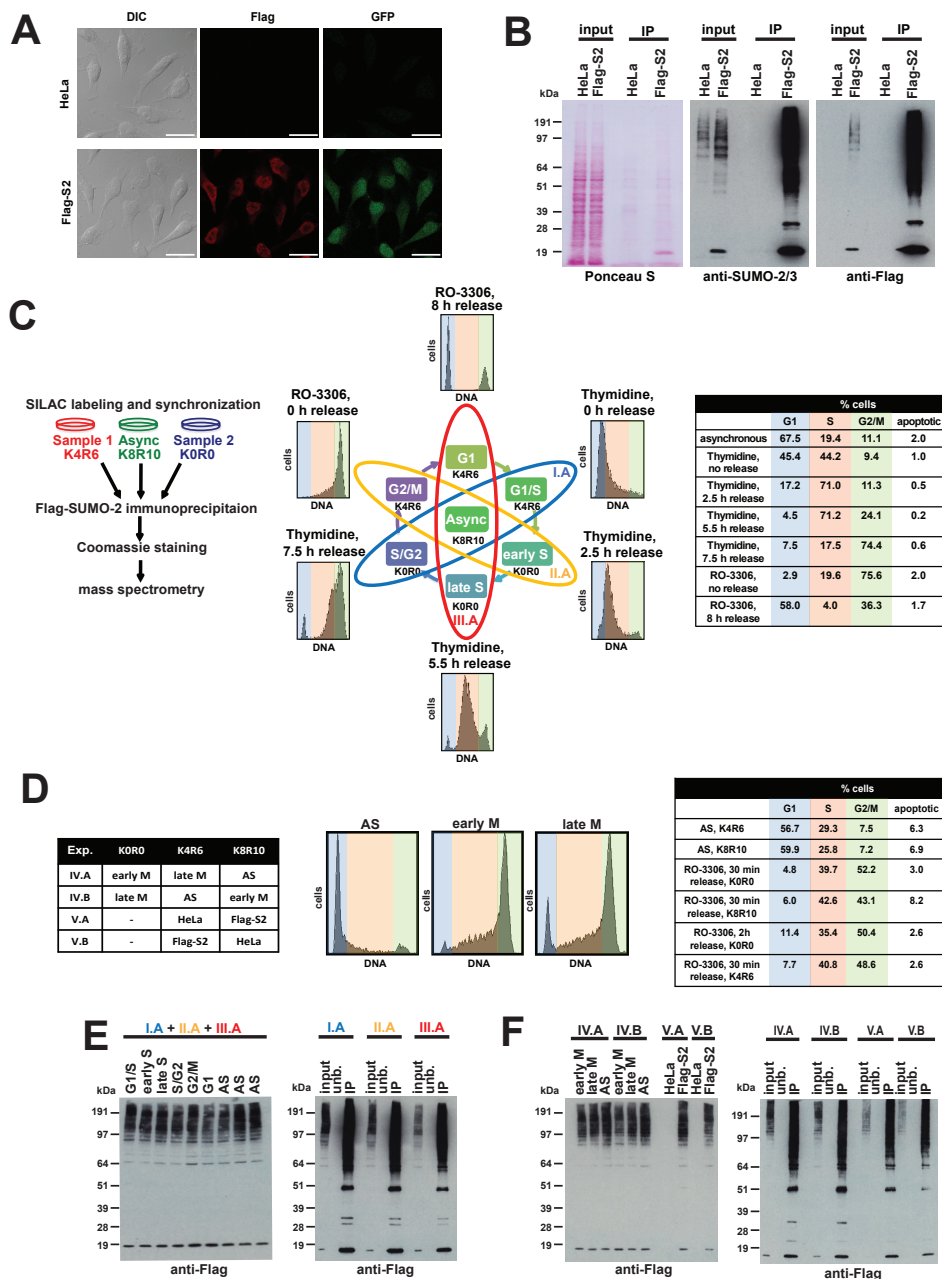


Figure 2. Global SUMO-2 conjugate dynamics during cell cycle progression A) HeLa cells were infected with a lentivirus encoding Flag-tagged SUMO-2-Q87R_IRES_GFP, and low expressing cells were sorted by flow cytometry. Flag-SUMO-2 was predominantly located in the nucleus. Scale bars are 25 μ m. B) Expression levels of total SUMO-2/3 and Flag-SUMO-2 conjugates in HeLa cells and Flag-SUMO-2 (Flag-S2) expressing stable cells were compared by immunoblotting. Flag-SUMO-2 conjugates were efficiently purified by IP. C) Strategy to identify SUMO-2 conjugates at different cell cycle stages using a quantitative proteomic approach. HeLa cells stably expressing Flag-SUMO-2 were SILAC-labeled with three different isotopic variants of lysine and arginine and treated as indicated to enrich cells in

different phases of the cell cycle. For the Flag-IP, equal amounts of a light labeled and a medium labeled synchronized lysate were mixed with a heavy labeled asynchronous sample resulting in three samples (I.A, II.A and III.A) comprising six different cell cycle stages. Cell cycle synchronization was confirmed by propidium iodide staining and flow cytometry and the percentage of cells in each cell cycle phase is depicted in the table. D) The left table depicts the combination of samples mixed for experiments IV and V: HeLa cells expressing Flag-SUMO-2 were SILAC-labeled and synchronized with RO-3306 in G2/M. Cells were released from the block for 30 minutes (early M-phase) and 2 hours (late M-phase), respectively. In addition, asynchronous HeLa cells and HeLa cells expressing Flag-SUMO-2 were SILAC-labeled and mixed as indicated in the table to obtain a parental control sample with the according label swap for mass spectrometric analysis. Synchronization of cells was confirmed via flow cytometry. The right table shows the percentage of apoptotic cells and of cells in G1, S and G2/M phase, respectively. E and F) Total cell lysates of the different synchronized cell pools and purification of Flag-SUMO-2 conjugates by IP were analyzed by immunoblotting using anti-Flag antibody. This was done for experiment I.A, II.A, III.A (E) and experiment IV.A, IV.B, V.A and V.B. (F). See also Figure S2.

To determine the amount of background binders obtained in this screen, we compared medium labeled asynchronous HeLa cells as a parental control to asynchronous heavy labeled HeLa cells expressing Flag-SUMO-2 (Figure 2D, 2F and S2B, experiment V.A). In addition, we performed a complete label-swap control for all samples (Figure 2F and Figure S2, experiment I.B-V.B), which corrects for experimental errors and false positive hits due to light labeled contaminants.

Flag-IP was performed for all ten experiments described and immunoblotting analysis was performed to determine total levels of Flag-SUMO-2 in each input fraction and to confirm highly efficient enrichment for SUMO-2 conjugates by IP (Figures 2E, 2F, S2D and S2E). Final eluted fractions of the Flag-IPs were separated by SDS-PAGE, stained with Coomassie, cut in ten gel slices and in-gel digested with trypsin. The Coomassie stained gel of Experiment I.B is shown as an example in Figure S2F. A total of 69,921 unique peptide variants covering 5180 proteins were identified by mass spectrometry at FDR<0.01 and their corresponding SILAC triplets were automatically quantified (Figure 3A, Table S1).

To deem a protein SUMOylated, we required a SILAC ratio of at least two between the FLAG-SUMO-2 HeLa cells and the parental control (Figure 3B, Table S2). Given the relatively low percentage of cells in G2/M in these control experiments we wanted to avoid excluding SUMO-2 target proteins that peak specifically in G2/M, therefore proteins with a SILAC ratio of at least two in G2/M enriched samples were also included in Table S2. A total of 249 proteins were significantly SUMO-2 up- or downregulated over the cell cycle, as well as 159 with a \log_2 dynamic range larger than 1.0 (Figure 3C, Figure S3A).

SUMOylation dynamics for a subset of the identified SUMO-2 target proteins might be explained by similar dynamics of non-modified forms of these proteins. Therefore, we have analyzed the dynamics of proteins at the total protein level. We have obtained quantitative information at the total protein level for 361 of the SUMO-2 target proteins, including 27 with a \log_2 dynamic range larger than 1.0 at the total protein level (Table S2).

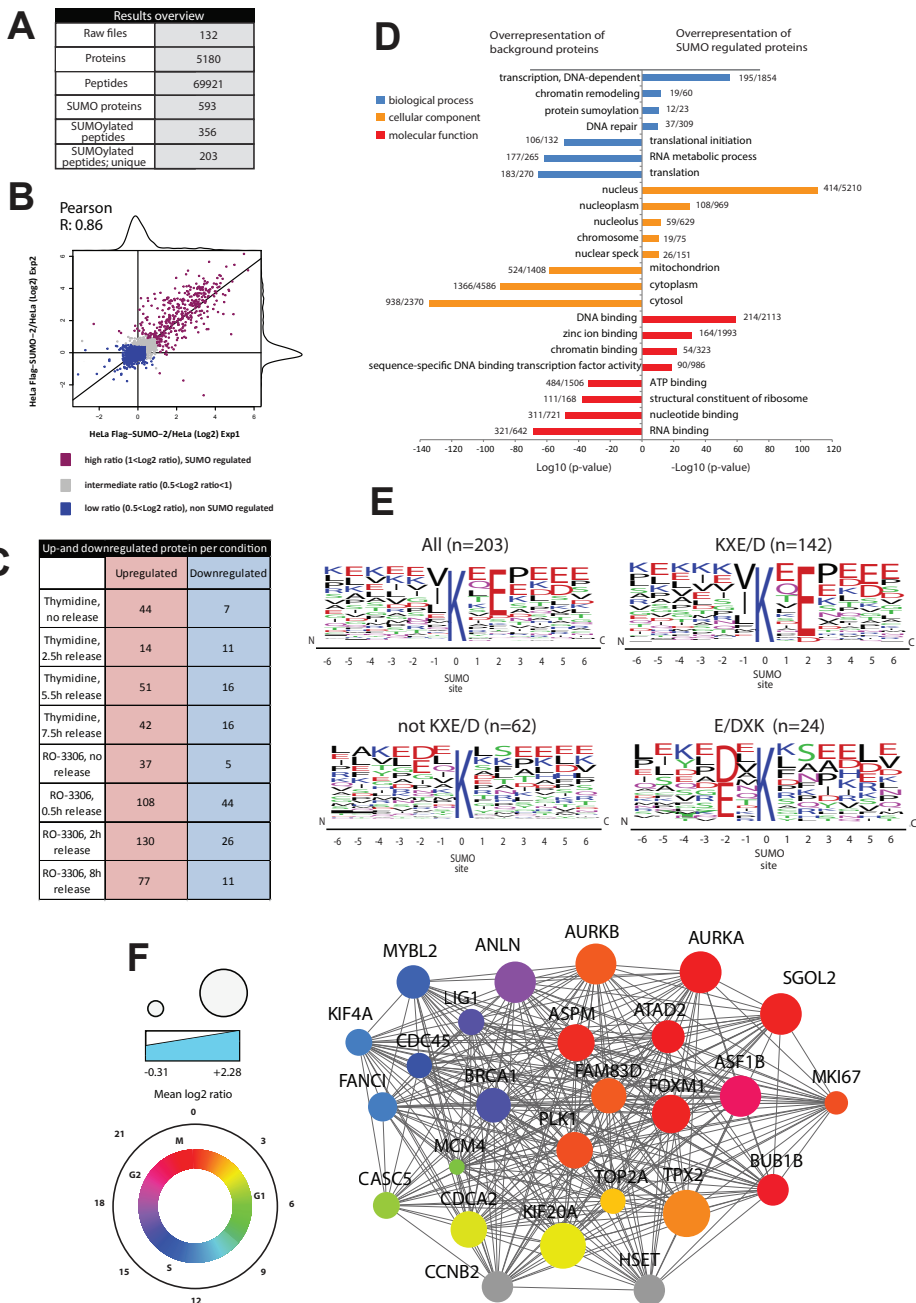


Figure 3. Global SUMOylation dynamics throughout the cell cycle; bioinformatics results

A) Overview of the proteomic experiments. Out of the 5180 proteins identified, 593 proteins were considered as SUMO targets based on SILAC filtering. A total of 356 peptides were identified carrying the QQTGG and/or pyroQQTGG modification, representing 203 unique SUMO-2 acceptor lysines. B) SILAC ratio reproducibility plot. Pearson correlation was calculated between both sets of experiments to determine the experimental reproducibility between biological replicates. The Flag-SUMO-2 HeLa cell line was compared to the parental HeLa cell line to determine which proteins were bona-fide SUMO

targets. SUMO target proteins with a \log_2 ratio >1 are indicated in purple, intermediate ratios between 0.5-1 are indicated in grey, whereas non-SUMOylated proteins with \log_2 ratio <0.5 are colored in dark blue. C) Overview of upregulated and downregulated SUMOylated proteins in each cell cycle condition. Proteins were filtered for presence in both label-swapped experiments and an average \log_2 ratio of >0.5 for upregulated targets and <-0.5 for downregulated targets. D) Gene Ontology (GO) enrichment analysis of SUMO modified proteins versus non-SUMOylated proteins. The bar plot shows the most significantly over-represented GO terms for biological process, cellular component and molecular function for SUMO regulated proteins (\log_2 ratio >1) and for non-SUMOylated proteins (\log_2 ratio <0.5). E) SUMO-2 acceptor lysine motif analysis. Weblogo visualization of the amino acid frequencies at each position ± 6 amino acids from the SUMO-2 acceptor site lysine residues. The size and sorting order of each amino acid indicates its specific frequency at each position and they are colored according to their chemical properties. F) Functional protein interaction network analysis based on the STRING database. The most significantly interconnected cluster within the total SUMO network visualized by Cytoscape. The cluster is found using the MCODE plug-in and has a MCODE score of 24.4. The functional interactions between proteins are displayed as edges between the proteins (nodes). The cluster has 26 proteins with a total of 305 interactions. The nodes are colored by their estimated cell-cycle peak-time according to the indicated color-scheme and their node size by their highest SILAC \log_2 ratio. See also Figure S3.

Gene ontology (GO) enrichment analysis of the SUMO-2 target proteins compared to a background of non-SUMOylated proteins from our dataset revealed a strong overrepresentation of nuclear proteins among the SUMO-2 targets. In particular SUMO modified proteins were highly enriched for sequence-specific DNA transcription factors (Figure 3D). Our dataset also contains 356 SUMO-2 modified peptides (Table S3) covering 203 unique SUMO acceptor sites (Table S4). Sequence motif analysis of the identified sites revealed a strong bias for the SUMO consensus motif $\Psi Kx E$ (142 sites, Figure 3E). We also found 24 sites situated in the previously described inverted SUMO consensus motif (26).

Functional protein interaction network analysis of the SUMO-2 regulated proteins based on the STRING database revealed a highly interconnected protein network (Figure S3B). The most significantly connected sub-clusters were identified using the MCODE plug-in for Cytoscape. The most significant cluster with an MCODE score of 24.4 contains 26 SUMO-2 regulated proteins that are color-coded according to their cell cycle peak-time (Figure 3F). SUMOylation of the different members of this network is predominantly peaking at that part of the cell cycle where they are functionally most active. For example, FANCI SUMOylation is peaking in S-phase where FANCI is involved in interstrand DNA crosslink repair during replication. ASPM, Aurora-A and -B, PLK1, BUB1B and FoxM1 are peaking in M-phase where they play roles in chromosome condensation and alignment, mitotic spindle formation, and segregation. Two additional functional protein clusters were highlighted by the MCODE analysis (Figures S3C and S3D). We demonstrate SUMOylation dynamics throughout the cell cycle by immunoblotting for eleven of the identified SUMO targets (Figure 4).

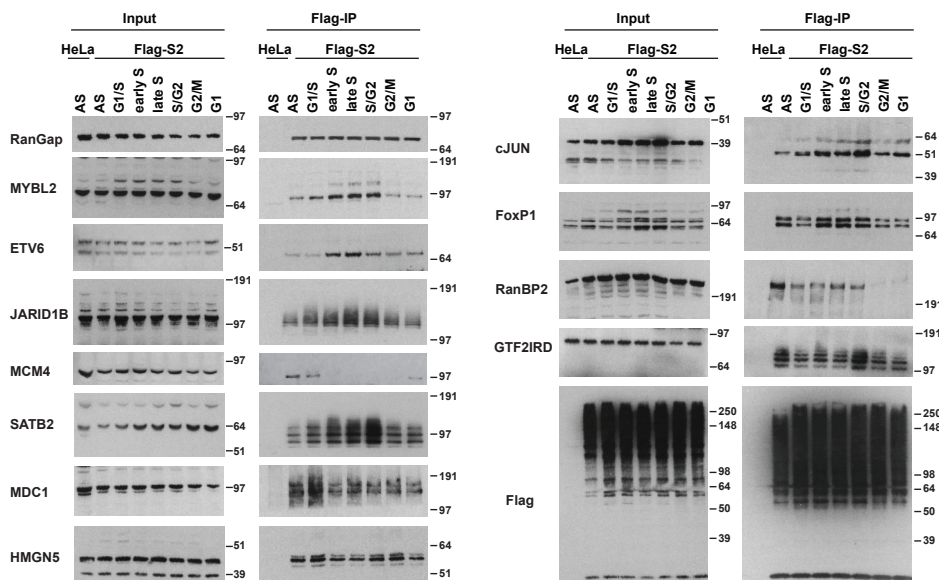


Figure 4. Confirmation of SUMO target proteins by immunoblotting HeLa cells stably expressing Flag-tagged SUMO-2 were synchronized at different stages of the cell cycle as described and Flag-SUMO-2 conjugates were purified via IP. Input samples and Flag-SUMO-2 purified fractions were analyzed by immunoblotting with antibodies as indicated. SUMOylation dynamics throughout the cell cycle was demonstrated for eleven different SUMO targets identified in the mass spectrometry screen and RanGAP1 was used as a control. Equal levels of SUMO conjugates in all samples were verified via immunoblotting using anti-Flag antibody. See also Figure S4.

FoxM1 is extensively SUMOylated

The Forkhead box transcription factor M1 (FoxM1) is essential for proper cell cycle progression by regulating a cluster of genes needed for the execution of mitosis (32). FoxM1 is essential for genome stability since FoxM1 deficiency resulted in aneuploidy. A related phenotype was also observed in a SUMOylation-deficient mouse model, however little is known about relevant SUMO target proteins (17). We selected FoxM1 for follow-up experiments to study the regulation of this important transcription factor by SUMOylation.

Interestingly, we found an increase in FoxM1 SUMOylation during M-phase in our proteomics project (Table S2). Immunoblotting analysis of Flag-SUMO-2 purified fractions showed that SUMOylation of FoxM1 strongly increased mainly in cells blocked at the G2/M border (Figure 5A). In asynchronous cells and eight hours after a release from the block, when most cells are in G1 phase (Figure 2C) we observed considerably lower FoxM1 SUMOylation levels. Increases in SUMOylation of FoxM1 can at least partly be explained by increases in total levels of FoxM1 upon synchronization. SUMOylation of FoxM1 was confirmed at the endogenous level (Figure S5A).

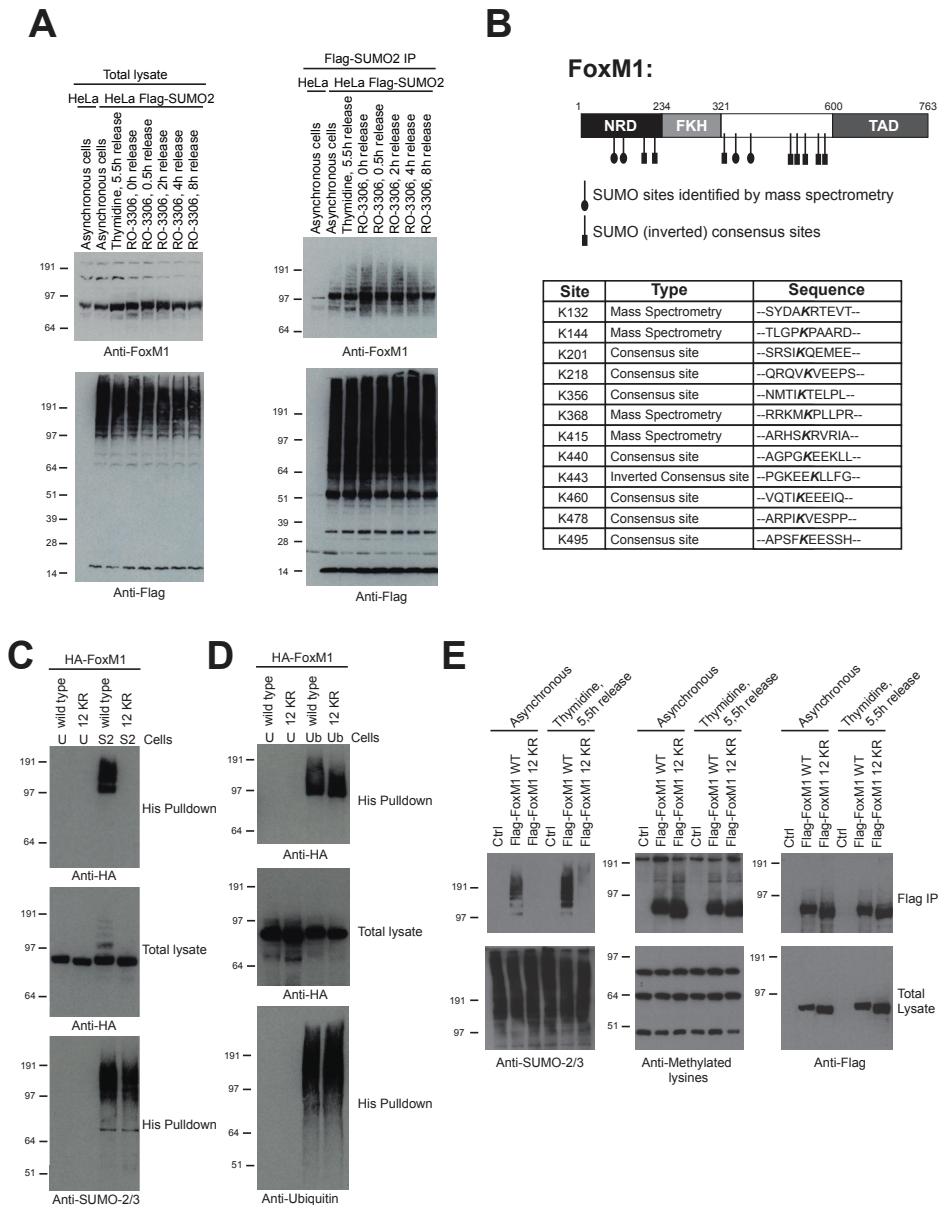


Figure 5. FoxM1 is extensively regulated via SUMOylation A) HeLa cells stably expressing Flag-SUMO-2 were synchronized with thymidine or RO-3306 and released for different time-points as depicted. Total lysates (left panel) or Flag-SUMO-2 enriched fractions (right panel) were separated by SDS-PAGE, transferred to a membrane, and probed using antibodies to detect FoxM1 or Flag. Asynchronous HeLa cells were used as a negative control for the Flag-SUMO-2 enrichment. B) Cartoon depicting Forkhead box protein M1 (FoxM1). FoxM1 is composed of 763 amino acids and harbors an N-terminal repressor domain (NRD), a Forkhead winged helix domain (FKH) and a C-terminal transactivation domain (TAD). FoxM1 contains 8 SUMOylation consensus sites and 4 additional SUMOylation sites identified by mass spectrometry. C) U2OS cells stably expressing His-SUMO-2 (S2) and control U2OS (U) cells were transfected with an expression construct encoding either HA-FoxM1 wild type or HA-FoxM1 lacking the SUMOylation sites (12KR). Cells were lysed 48 hours after transfection in 6 M Guanidine-HCL, and

Chapter 5

His-SUMO-2 conjugates were purified by IMAC. Total lysates and purified fractions (His pulldown) were separated by SDS-PAGE, transferred to a membrane, and probed using an antibody to detect HA. Total SUMO-2/3 levels in the purified fractions were detected with a SUMO-2/3 antibody. D) The experiment described in (C) was repeated in U2OS cells stably expressing His-Ubiquitin (Ub) and control U2OS (U) cells. Ubiquitination of HA-FoxM1 was detected using an antibody directed against the HA-tag. Total ubiquitin levels in the purified fractions were detected by probing immunoblots with an antibody directed against ubiquitin. E) U2OS cells were transfected with an empty vector (Ctrl), Flag-FoxM1 wild type (WT) or Flag-FoxM1 12KR. Asynchronous cells or cells released for 5.5 hours from a thymidine block were used for Flag-FoxM1 enrichment by Flag-IP. Total lysates (lower panels) and Flag-FoxM1 enriched fractions (upper panels) were separated by SDS-PAGE, transferred to a membrane, and probed using antibodies to detect SUMO-2/3, methylated lysines or Flag. See also Figure S5.

To study the functional relevance of FoxM1 SUMO modification, we have mapped the SUMO acceptor sites of this protein. FoxM1 has an N-terminal repressor domain (NRD), a Forkhead winged helix DNA binding domain (FKH) and a C-terminal transactivation domain (TAD) (Figure 5B). The protein contains seven lysines that are situated in the SUMOylation consensus motif Ψ KxE (lysines 201, 218, 356, 440, 460, 478 and 495) and one lysine that is situated in the inverted SUMOylation consensus motif E/DxK Ψ (lysine 443). Four additional SUMO acceptor sites that do not represent the classical consensus site were identified by mass-spectrometry analyses of SUMOylated recombinant FoxM1 proteins (Figure S5B).

To analyze the SUMOylation of FoxM1, a mutant was generated where these twelve lysines were mutated to arginines (12KR). Wild type and 12KR FoxM1 constructs were expressed in U2OS cells or in U2OS cells stably expressing a His tagged SUMO-2 construct. Analysis of the SUMO enriched fraction confirmed that SUMOylation of FoxM1 was abolished by these mutations (Figure 5C). Since FoxM1 is also regulated by ubiquitination (33), we demonstrated that ubiquitination of the 12KR mutant is similar to wild-type FoxM1 (Figure 5D).

Enrichment of Flag-FoxM1 wild type and Flag-FoxM1 12KR from U2OS cells showed the modification of FoxM1 wild type by endogenous SUMO-2/3 and the increase in SUMOylation of FoxM1 in thymidine released cells (Figure 5E). We did not observe modification of the FoxM1 12KR mutant by endogenous SUMO-2/3, further validating our SUMOylation deficient mutant. This experiment was used to confirm that in addition to ubiquitination, also methylation of FoxM1 is not affected by mutating these twelve lysines, by analyzing Flag-FoxM1 wild type and Flag-FoxM1 12KR enriched fractions by immunoblotting with an antibody directed against methylated-lysine. Nevertheless, some competition between the different PTMs could be observed (Table S5).

SUMOylation positively regulates FoxM1 transcriptional activity

To study the effect of SUMOylation on the function of FoxM1, we have compared the transcriptional activities of wild-type and SUMOylation-deficient (12KR) FoxM1. In our first approach we used two different luciferase constructs, one containing six

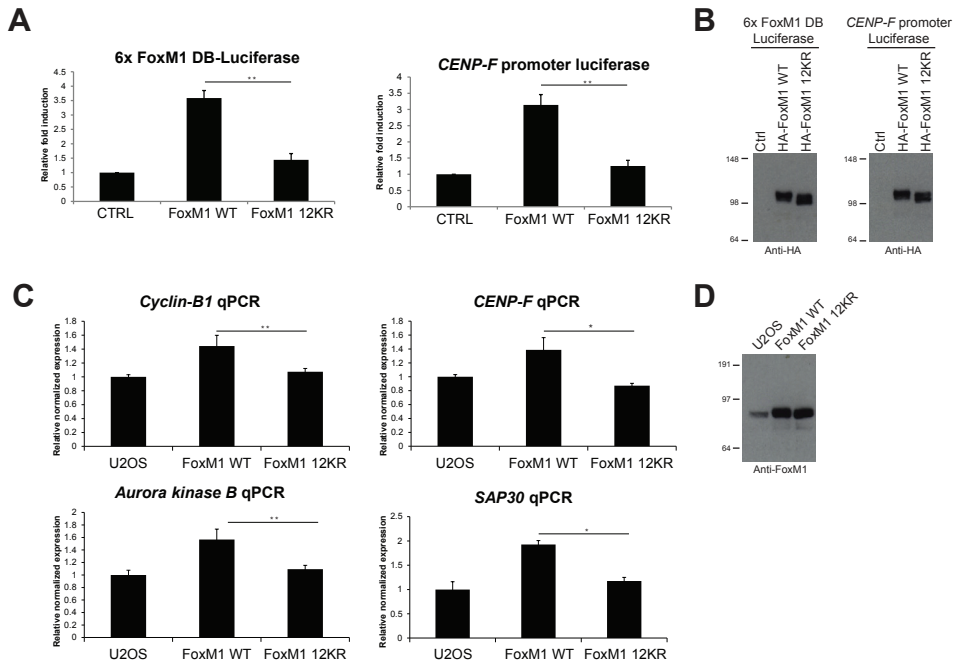


Figure 6. SUMOylation is required for FoxM1 transcriptional activity A) U2OS cells were (co) transfected with an empty vector, HA-FoxM1 wild type (WT) or HA-FoxM1 12KR, a luciferase reporter containing six FoxM1 DNA binding domains (6x FoxM1 DB-Luciferase, left panel) or a luciferase reporter containing the *CENP-F* promoter region (right panel) and a LacZ reporter. Cells were lysed in reporter lysis buffer 48 hours after transfection and luciferase activity and β -galactosidase activity (β -Gal) were measured. Results are representative of six independent experiments and corrected for transfection efficiency using β -Gal activity; the error bars indicate the standard deviation from the average. Results are shown as a relative fold induction compared to cells transfected with the empty vector. ** $p < 0.001$ B) Expression levels of HA-FoxM1 wild-type and HA-FoxM1 12KR proteins in the luciferase experiments were verified by immunoblotting using an antibody directed against the HA-tag. C) Quantitative PCRs were performed on U2OS cells, U2OS cells stably expressing Flag-FoxM1 wild type or U2OS cells stably expressing Flag-FoxM1 12KR. Primers for *Aurora kinase B*, *Cyclin-B1*, *CENP-F* and *SAP30* were used to quantify specific gene expression. The average expression levels of triplicates were normalized for the expression levels of the housekeeping gene *CAPNS1*. Results for the stable cell lines are shown as relative expression levels compared to U2OS cells (expression level set to 1). ** $p < 0.001$, * $p < 0.05$ D) The expression levels of HA-Flag-FoxM1 wild type and HA-Flag-FoxM1 12KR proteins in the quantitative PCR experiments were verified by immunoblotting using an antibody directed against FoxM1. See also Figure S6.

FoxM1 DNA binding sites (6x FoxM1 DB-luciferase) and one containing the promoter region of the known FoxM1 target gene *CENP-F* (32). We found that SUMOylation-deficient FoxM1 was less active compared to wild-type FoxM1, indicating that SUMOylation enhances FoxM1 transcriptional activity (Figures 6A and 6B). This observation was further supported by quantitative PCRs (qPCRs) on FoxM1 target genes. Relative mRNA expression levels for *Aurora kinase B*, *Cyclin-B1*, *CENP-F* and *SAP30* were lower in cells stably expressing Flag-FoxM1 12KR compared to cells stably expressing Flag-FoxM1 wild type at similar levels (Figure 6C and 6D).

Chapter 5

To analyze whether loss of SUMOylation on all twelve lysines of FoxM1 was needed for the reduced activity, we made domain specific FoxM1 SUMOylation mutants in the NRD domain (4KR) or in the undefined domain between the Forkhead and the TAD of FoxM1 (8KR). A small reduction in SUMOylation levels for both mutants indicated modification of both FoxM1 domains (Figure S6A and S6B). Consistently, a decreased FoxM1 activity was only observed in the 12KR mutant (Figure S6C and S6D). We conclude that FoxM1 is extensively SUMOylated, to increase its transcriptional activity.

Cells expressing SUMOylation-deficient FoxM1 are prone to develop polyploidy

Depletion of FoxM1 expression causes chromosome misalignment and malfunction of cytokinesis, giving rise to the accumulation of tetraploid and polyploid cells (32). To test whether SUMOylation of FoxM1 is functionally relevant, we set up knockdown and complementation experiments. The stable cell lines described in figure 6C and 6D were used for these assays. Silent mutations were introduced in the Flag-FoxM1 constructs to make them resistant to two independent FoxM1 shRNAs. Cells were infected with a non-targeting control shRNA or with one of the two FoxM1 shRNAs and analyzed three days after infection. Western blot analysis confirmed the efficient knockdown of endogenous FoxM1 in U2OS cells and stable expression of wild-type and SUMOylation-deficient Flag-FoxM1 (Figure 7A). Microscopy confirmed that both wild type and SUMOylation-deficient FoxM1 were localized in the nucleus (Figure S7A). A similar experiment was performed using GFP tagged FoxM1 to confirm that only endogenous FoxM1 was depleted in the stable cell lines without affecting exogenous FoxM1 (Figure S7C). These cells were however not suitable for rescue experiments due to interference of the large GFP tag with FoxM1 protein function. Cell cycle analysis of the different cell populations confirmed that FoxM1 knockdown resulted in increased populations of tetraploid and polyploid cells. Expression of both FoxM1 wild type and FoxM1 12KR could rescue the knockdown effects on the tetraploid cell population to a similar extent (Figure S7B). Also, no obvious differences were found in G1 phase and S phase cell populations when we compared FoxM1 wild type to the SUMOylation-deficient FoxM1 (Figure S7B). Interestingly, we observed a significant increase in polyploid cells when comparing cells expressing FoxM1 12KR to FoxM1 wild type cells (Figure 7B). Thus, cells deficient for FoxM1 SUMOylation were more sensitive to develop polyploidy.

SUMOylation inhibits the negative regulatory domain of FoxM1

Subsequently, we searched for a mechanistic explanation for the activation of FoxM1 by SUMOylation. In previous studies it was shown that FoxM1 is inhibited in G1 phase via direct interaction between the N-terminal repressor domain and the C-terminal transactivation domain (34, 35). To study the effects of FoxM1 SUMOylation on this

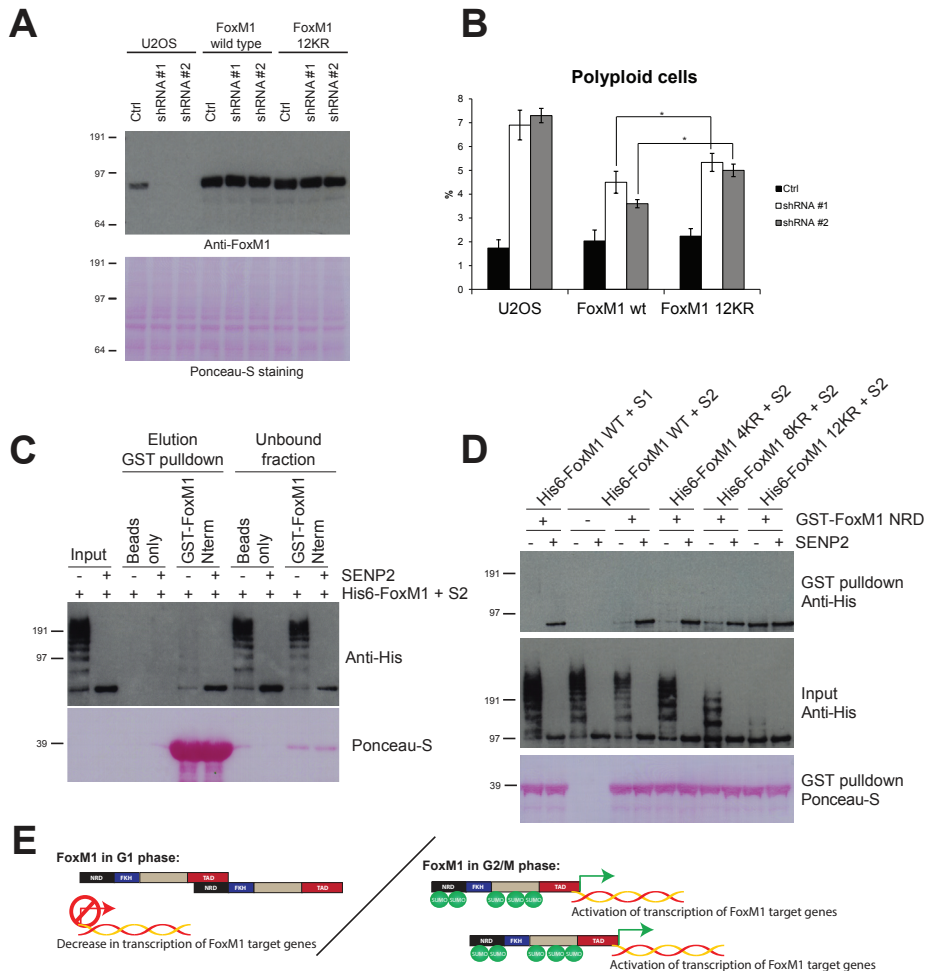


Figure 7. SUMOylation inhibits the negative regulatory domain of FoxM1 and is required to counteract polyploidy A and B) U2OS cells stably expressing Flag-FoxM1 wild type or Flag-FoxM1 12KR or parental U2OS cells were infected with two individual FoxM1 shRNA lentiviruses (shRNA #1 and shRNA #2) or a non-targeting shRNA (ctrl). Three days after infection cells were harvested for immunoblotting analysis with a FoxM1 antibody (A) and for propidium iodide staining and flow cytometry (B). Average values from three independent experiments are shown in percentages for the polyploid cell population. The error bars indicate the standard deviation from the average. * $p < 0.05$ C) Recombinant His-FoxM1 proteins were SUMOylated *in vitro* and SUMO-2 proteins were removed from His-FoxM1 by incubating the proteins with recombinant SENP2. Glutathione beads only or glutathione beads bound to a GST-FoxM1 N-terminal protein fragment (Nterm) were incubated with SUMOylated His-FoxM1 proteins or His-FoxM1 proteins treated with SENP2. Inputs, elution of the GST pulldown and the unbound fraction after the GST pulldown were analyzed by immunoblotting using an antibody directed against the His-tag. The amount of GST-FoxM1 proteins in the elution and the unbound fraction were verified by staining the membrane with Ponceau-S. D) The experiment described in (C) was repeated using His-FoxM1 wild type (WT) proteins SUMOylated *in vitro* with SUMO-1 and with 3 different His-FoxM1 mutants SUMOylated *in vitro* with SUMO-2; His-FoxM1 4KR, 8KR and 12KR. Inputs and elutions of the GST pulldown were analyzed by immunoblotting and compared to interaction levels of His-FoxM1 WT *in vitro* SUMOylated with SUMO-2. E) Our data indicate that SUMOylation of FoxM1 during G2 and M phase inhibits the formation of the inactive FoxM1 dimer. This contributes to the increased transcriptional activity of FoxM1 in these phases of the cell cycle. See also Figure S7.

Chapter 5

interaction, an *in vitro* interaction assay was performed. A GST tagged N-terminal FoxM1 protein fragment was coupled to glutathione beads and incubated with a mixture of unmodified and SUMOylated His-FoxM1 or unmodified His-FoxM1 proteins only. We observed that only unmodified full-length FoxM1 proteins interacted with the N-terminal part of FoxM1, while SUMOylated FoxM1 did not detectably interact with the protein (Figure 7C). By using the domain specific FoxM1 mutants previously described (4KR and 8KR) in this assay, we found that SUMOylation on both the NRD and on the undefined domain of FoxM1 blocks the interaction with the GST tagged NRD protein (Figure 7D). His-FoxM1 proteins SUMOylated with SUMO-1 were also unable to interact with the NRD, showing that extensive mono-SUMOylation on the twelve lysines is sufficient to block the interaction since SUMO-1 is impaired for polymerization (30). Interestingly, even a single modified form of FoxM1 no longer formed dimers. This leads us to propose a model where SUMOylation increases FoxM1 transcriptional activity by inhibiting the interaction between the repressor and activation domain of FoxM1 (Figure 7E).

Discussion

We have addressed the role of SUMOylation in cell cycle progression using a proteomics approach to purify and identify hundreds of SUMO target proteins. Co-regulation of these large sets of targets throughout the cell cycle enables orchestration of cell cycle progression via SUMOylation. All aspects of cell cycle progression are influenced by SUMOylation since these target proteins play roles in replication, DNA condensation, chromosome alignment and segregation and cytokinesis. We have also identified 203 SUMO-2 acceptor lysines. Functional analysis of the key mitotic SUMO target protein FoxM1 revealed a role for SUMO-modified FoxM1 in counteracting polyploidy.

Protein group modification

STRING analysis revealed complex interactions between the identified sets of SUMO-2 target proteins (Figures 3F and S3B). Half of the SUMOylated proteins depicted in Figure 3F have a known function in mitosis according to their GO biological process term. Interestingly, five of the proteins with SUMOylation peaking in G1/S are established players in the DNA replication pathway. The second most significant MCODE cluster (Figure S3C) consists of 11 SUMO-2 regulated proteins that are all involved in mRNA splicing via the spliceosome. The third significant MCODE cluster (Figure S3D) consists of 41 SUMOylated proteins of which 16 have transcriptional co-activator activity and seven of them are part of the MLL1 Histone-lysine N-methyltransferase complex.

These results are consistent with previous findings on the role of SUMOylation in yeast in response to DNA damage (36). In yeast, a set of interacting proteins

are SUMOylated and additionally contain SIMs for non-covalent interactions with SUMO. SUMOylation was proposed to act like a molecular glue to enhance group interaction. The networks identified in our screen could similarly be glued together by SUMOylation.

Regulation of FoxM1 via SUMOylation

The Forkhead box (Fox) transcription factor FoxM1 was selected for follow up experiments since this protein links the two major SUMO-regulated biological processes, transcription and the maintenance of genome stability. FoxM1 plays a key role in mitotic progression via transcriptional regulation of a network of genes including *Aurora kinase B*, *CENP-F*, *Cdc25B*, *Cyclin-B1* and *Survivin*. Deregulating the transcription of these genes by depleting FoxM1 expression resulted in a delay in G2 phase, reduced cell proliferation and defects in mitosis. Together these defects in FoxM1 depleted cells resulted in an increased population of cells with a $4n$ DNA content and the formation of aneuploid cells due to missegregation of chromosomes (32, 37). Previously, Ubc9 deficient cells were shown to have a related phenotype, but relevant SUMO target proteins were still missing (17). Our data indicate that FoxM1 is one of the SUMO target proteins relevant for explaining the phenotype of SUMOylation deficient cells.

SUMOylation of transcription factors frequently results in transcriptional inhibition with some exceptions (13, 38, 39). This is thought to occur via the recruitment of inhibitory complexes. In contrast, SUMOylation is required for activation of FoxM1 (Figure 6). Mechanistically, the bulky SUMO modifications prevent the negative regulatory domain from binding to the activation domain, blocking the formation of inactive dimers (Figure 7). Consequently, SUMOylated FoxM1 is thought to activate transcription in a monomeric form. Previously, phosphorylation of FoxM1 was proposed to counteract dimer formation (35), but the small size of this modification might be insufficient for full activation of the protein. Phosphorylation and SUMOylation could cooperate to activate FoxM1 via the phosphorylation-dependent SUMOylation motif (PDSM) $\Psi KxExxS$ (40), since downstream of K218 in FoxM1, a serine is located at position 223. However, phosphorylation of this serine has so far not been reported (35).

During the revision of our project, another paper was published on the regulation of FoxM1 by SUMOylation (41). In this paper, the authors claim that the mutation of five SUMOylation consensus motifs in FoxM1 abolished SUMOylation. Using our sensitive method to detect SUMOylation, we found that mutating SUMOylation consensus motifs in FoxM1 was not sufficient to abolish SUMOylation (Figure S5C). Whereas Myatt et al. found that SUMOylation inhibited FoxM1, we found that SUMOylation was required for full activity of FoxM1. This discrepancy could be due to the extensive use of a FoxM1-Ubc9 fusion protein by Myatt et al. that was

Chapter 5

employed to boost SUMOylation and was surprisingly located in the cytoplasm, which might explain its lower transcriptional activity. Furthermore, Myatt et al. enhanced SUMOylation of FoxM1 by transiently overexpressing Ubc9. Using a sensitive method to detect SUMOylation, there was no need for Ubc9 overexpression or the use of a FoxM1-Ubc9 fusion protein in our hands.

FoxM1 plays an important role in cancer and is thought to act as a classical oncogene (42, 43). Gene expression studies of primary tumors have revealed that FoxM1 is frequently upregulated in solid tumors. High expression levels of FoxM1 have been found in different types of solid tumors including lung, breast, colon, prostate and liver cancer (44, 45). These hallmarks of elevated FoxM1 expression established the idea that targeting FoxM1 in cancer may have therapeutic advantages (46, 47). Since SUMOylation of FoxM1 increases FoxM1 transcriptional activity, interfering with FoxM1 SUMOylation might be a potential interesting addition to FoxM1 based cancer therapies. However, currently little is known about the SUMOylation status of FoxM1 in cancer; this is a topic for future studies.

Conclusions and future perspective

Dynamic regulation of a large set of target proteins by SUMOylation plays an important role in cell cycle progression. In this study, we have identified hundreds of dynamically regulated SUMO-2 target proteins in all stages of the cell cycle using a quantitative proteomics approach and an optimized purification procedure that inactivates SUMO proteases and results in a high yield. The small Flag tag minimally impacts SUMO-2 and is expected not to interfere with SUMOylation dynamics, in contrast to large tags such as GFP that reduce the conjugation rate (48). Whereas valuable strategies to purify endogenous SUMOs are being developed (49), the yield of these methods is limited compared to the method that we have described here. Optimal yield is required to obtain global insight in SUMOylation dynamics.

Detailed functional analysis of SUMO targets requires the identification of the SUMO acceptor lysines in these proteins to create mutants deficient in SUMOylation. Currently, large-scale site-specific SUMOylation proteomics is still challenging (25, 26, 50). The set of SUMO acceptor lysines identified in this project is the largest set identified in a single study today, but is still modest and many SUMO-targeted lysines still need to be identified. The site-specific aspect of SUMOylation proteomics still needs further optimizing as it is clearly behind compared to phosphorylation and ubiquitination. Nevertheless, we believe that the dynamic set of SUMO target proteins identified in this study and the subset of SUMO acceptor sites represents a valuable resource for the scientific community.

Materials and methods

Cell lines, Cell culture, SILAC labeling and transfections

HeLa and U2OS cells were cultured in Dulbecco's modified Eagle's medium (Gibco Invitrogen Corporation, Grand Island, NY, USA) supplemented with 10% FCS (Gibco) and 100 U/ml penicillin and 100 µg/ml streptomycin (Gibco). For SILAC analysis, cells were essentially labeled as described before (23). Transfections were carried out using 2.5 µl polyethylenimine (PEI, 1 mg/ml, Alpha Aesar) per µg DNA.

SUMO target protein purification

Cells were lysed in four pellet volumes of lysis buffer (1% SDS, 0.5% NP-40 in PBS including phosphatase - and protease inhibitors). Chloroacetamide was added freshly at 70 mM and samples were sonicated and equalized. An equal volume of dilution buffer (2% Triton X-100, 0.5% sodium deoxycholate, 1% BSA in PBS including phosphatase - and protease inhibitors and freshly added 70 mM chloroacetamide) was added to the lysates and they were centrifuged for 45 minutes at 13.2 krpm at 4°C. The supernatants were mixed with Flag-M2 beads (Sigma). After 90 minutes incubation, the beads were washed 5 x with wash buffer (50 mM Tris, 150 mM NaCl, 70 mM chloroacetamide, 0.5% NP-40, phosphatase - and protease inhibitors) and bound proteins were eluted.

Mass spectrometry analysis

Purified proteins were size separated by SDS-PAGE, in-gel digested, extracted, desalted, concentrated and analyzed by mass spectrometry using an EASY-nLC system (Proxeon, Odense, Denmark) connected to the LTQ-Orbitrap Velos or to the Q-Exactive (both from Thermo Fisher Scientific, Germany) through a nano-electrospray ion source. Raw mass spectrometry (MS) files were processed with the MaxQuant software suite (version 1.4.0.3, Max Planck Institute of Biochemistry, Department of Proteomics and Signal Transduction, Munich, Germany).

Supplemental information

Supplemental information includes seven figures, five tables, supplemental experimental procedures and supplemental references.

Acknowledgments

We want to thank Drs. Lars Juhl Jensen and A.G. Jochemsen for advice and Sarah Sparks and Sharareh Sami Abolvardi for technical assistance. We thank Drs. Timmers, De Graaf, Meulmeester and Saitoh for plasmid constructs. This work was supported by the Netherlands Organization for Scientific Research (NWO) (A.C.O.V.). The NNF Center for Protein Research is supported by a generous donation from the Novo Nordisk Foundation. The work was furthermore supported by the Marie Curie Initial Training Networks program of the European Union (290257-UPStream to A.C.O.V. and J.V.O.), and the research career program FSS Sapere Aude (J.V.O.) from the Danish Research Council. None of the authors have a financial interest related to this work.

Chapter 5

Reference List

1. Fisher, D., Krasinska, L., Coudreuse, D., and Novak, B. (2012) Phosphorylation network dynamics in the control of cell cycle transitions. *J. Cell Sci.* 125, 4703-4711
2. Kirkin, V., and Dikic, I. (2007) Role of ubiquitin- and Ubl-binding proteins in cell signaling. *Curr. Opin. Cell Biol.* 19, 199-205
3. Wan, J., Subramonian, D., and Zhang, X. D. (2012) SUMOylation in control of accurate chromosome segregation during mitosis. *Curr. Protein Pept. Sci.* 13, 467-481
4. Kirkin, V., and Dikic, I. (2011) Ubiquitin networks in cancer. *Curr. Opin. Genet. Dev.* 21, 21-28
5. Lopez-Otin, C., and Hunter, T. (2010) The regulatory crosstalk between kinases and proteases in cancer. *Nat. Rev. Cancer* 10, 278-292
6. Bettermann, K., Benesch, M., Weis, S., and Haybaeck, J. (2012) SUMOylation in carcinogenesis. *Cancer Lett.* 316, 113-125
7. Zhang, J., Yang, P. L., and Gray, N. S. (2009) Targeting cancer with small molecule kinase inhibitors. *Nat. Rev. Cancer* 9, 28-39
8. Choudhary, C., and Mann, M. (2010) Decoding signalling networks by mass spectrometry-based proteomics. *Nat. Rev. Mol. Cell Biol.* 11, 427-439
9. Olsen, J. V., Vermeulen, M., Santamaria, A., Kumar, C., Miller, M. L., Jensen, L. J., Gnad, F., Cox, J., Jensen, T. S., Nigg, E. A., Brunak, S., and Mann, M. (2010) Quantitative phosphoproteomics reveals widespread full phosphorylation site occupancy during mitosis. *Sci. Signal.* 3, ra3
10. Gareau, J. R., and Lima, C. D. (2010) The SUMO pathway: emerging mechanisms that shape specificity, conjugation and recognition. *Nat. Rev. Mol. Cell Biol.* 11, 861-871
11. Hay, R. T. (2005) SUMO: a history of modification. *Mol. Cell* 18, 1-12
12. Geiss-Friedlander, R., and Melchior, F. (2007) Concepts in sumoylation: a decade on. *Nat. Rev. Mol. Cell Biol.* 8, 947-956
13. Flotho, A., and Melchior, F. (2013) Sumoylation: a regulatory protein modification in health and disease. *Annu. Rev. Biochem.* 82, 357-385
14. Seufert, W., Futcher, B., and Jentsch, S. (1995) Role of a ubiquitin-conjugating enzyme in degradation of S- and M-phase cyclins. *Nature* 373, 78-81
15. Li, S. J., and Hochstrasser, M. (1999) A new protease required for cell-cycle progression in yeast. *Nature* 398, 246-251
16. Schwartz, D. C., Felberbaum, R., and Hochstrasser, M. (2007) The Ulp2 SUMO protease is required for cell division following termination of the DNA damage checkpoint. *Mol. Cell Biol.* 27, 6948-6961
17. Nacerddine, K., Lehembre, F., Bhaumik, M., Artus, J., Cohen-Tannoudji, M., Babinet, C., Pandolfi, P. P., and Dejean, A. (2005) The SUMO pathway is essential for nuclear integrity and chromosome segregation in mice. *Dev. Cell* 9, 769-779
18. Ulrich, H. D. (2009) Regulating post-translational modifications of the eukaryotic replication clamp PCNA. *DNA Repair (Amst)* 8, 461-469
19. Armstrong, A. A., Mohideen, F., and Lima, C. D. (2012) Recognition of SUMO-modified PCNA requires tandem receptor motifs in Srs2. *Nature* 483, 59-63
20. Dawlaty, M. M., Malureanu, L., Jegathanan, K. B., Kao, E., Sustmann, C., Tahk, S., Shuai, K., Grosschedl, R., and van Deursen, J. M. (2008) Resolution of sister centromeres requires RanBP2-mediated SUMOylation of topoisomerase IIalpha. *Cell* 133, 103-115
21. Mukhopadhyay, D., Arnaoutov, A., and Dasso, M. (2010) The SUMO protease SENP6 is essential for inner kinetochore assembly. *J. Cell Biol.* 188, 681-692
22. Klein, U. R., Haindl, M., Nigg, E. A., and Muller, S. (2009) RanBP2 and SENP3 function in a mitotic SUMO2/3 conjugation-deconjugation cycle on Borealin. *Mol. Biol. Cell* 20, 410-418
23. Mann, M. (2006) Functional and quantitative proteomics using SILAC. *Nat. Rev. Mol. Cell Biol.* 7, 952-958
24. Neyret-Kahn, H., Benhamed, M., Ye, T., Le, G. S., Cossec, J. C., Lapaquette, P., Bischof, O., Ouspenskaia, M., Dasso, M., Seeler, J., Davidson, I., and Dejean, A. (2013) Sumoylation at chromatin governs coordinated repression of a transcriptional program essential for cell growth and proliferation. *Genome Res.* 23, 1563-1579
25. Vertegaal, A. C. (2011) Uncovering ubiquitin and ubiquitin-like signaling networks. *Chem. Rev.* 111, 7923-7940
26. Matic, I., Schimmel, J., Hendriks, I. A., van Santen, M. A., van de Rijke, F., van, D. H., Gnad, F., Mann, M., and Vertegaal, A. C. (2010) Site-specific identification of SUMO-2 targets in cells reveals an inverted SUMOylation motif and a hydrophobic cluster SUMOylation motif. *Mol. Cell* 39, 641-652
27. Saitoh, H., and Hinchev, J. (2000) Functional heterogeneity of small ubiquitin-related

- protein modifiers SUMO-1 versus SUMO-2/3. *J. Biol. Chem.* 275, 6252-6258
28. Zhang, X. D., Goeres, J., Zhang, H., Yen, T. J., Porter, A. C., and Matunis, M. J. (2008) SUMO-2/3 modification and binding regulate the association of CENP-E with kinetochores and progression through mitosis. *Mol. Cell* 29, 729-741
 29. Tatham, M. H., Jaffray, E., Vaughan, O. A., Desterro, J. M., Botting, C. H., Naismith, J. H., and Hay, R. T. (2001) Polymeric chains of SUMO-2 and SUMO-3 are conjugated to protein substrates by SAE1/SAE2 and Ubc9. *J. Biol. Chem.* 276, 35368-35374
 30. Matic, I., van, H. M., Schimmel, J., Macek, B., Ogg, S. C., Tatham, M. H., Hay, R. T., Lamond, A. I., Mann, M., and Vertegaal, A. C. (2008) In vivo identification of human small ubiquitin-like modifier polymerization sites by high accuracy mass spectrometry and an in vitro to in vivo strategy. *Mol. Cell Proteomics* 7, 132-144
 31. Tatham, M. H., Geoffroy, M. C., Shen, L., Plechanovova, A., Hattersley, N., Jaffray, E. G., Palvimo, J. J., and Hay, R. T. (2008) RNF4 is a poly-SUMO-specific E3 ubiquitin ligase required for arsenic-induced PML degradation. *Nat. Cell Biol.* 10, 538-546
 32. Laoukili, J., Kooistra, M. R., Bras, A., Kauw, J., Kerkhoven, R. M., Morrison, A., Clevers, H., and Medema, R. H. (2005) FoxM1 is required for execution of the mitotic programme and chromosome stability. *Nat. Cell Biol.* 7, 126-136
 33. Laoukili, J., Alvarez-Fernandez, M., Stahl, M., and Medema, R. H. (2008) FoxM1 is degraded at mitotic exit in a Cdh1-dependent manner. *Cell Cycle* 7, 2720-2726
 34. Park, H. J., Wang, Z., Costa, R. H., Tyner, A., Lau, L. F., and Raychaudhuri, P. (2008) An N-terminal inhibitory domain modulates activity of FoxM1 during cell cycle. *Oncogene* 27, 1696-1704
 35. Laoukili, J., Alvarez, M., Meijer, L. A., Stahl, M., Mohammed, S., Kleij, L., Heck, A. J., and Medema, R. H. (2008) Activation of FoxM1 during G2 requires cyclin A/Cdk-dependent relief of autorepression by the FoxM1 N-terminal domain. *Mol. Cell Biol.* 28, 3076-3087
 36. Psakhye, I., and Jentsch, S. (2012) Protein group modification and synergy in the SUMO pathway as exemplified in DNA repair. *Cell* 151, 807-820
 37. Wang, I. C., Chen, Y. J., Hughes, D., Petrovic, V., Major, M. L., Park, H. J., Tan, Y., Ackerson, T., and Costa, R. H. (2005) Forkhead box M1 regulates the transcriptional network of genes essential for mitotic progression and genes encoding the SCF (Skp2-Cks1) ubiquitin ligase. *Mol. Cell Biol.* 25, 10875-10894
 38. Ouyang, J., Valin, A., and Gill, G. (2009) Regulation of transcription factor activity by SUMO modification. *Methods Mol. Biol.* 497, 141-152
 39. Lyst, M. J., and Stancheva, I. (2007) A role for SUMO modification in transcriptional repression and activation. *Biochem. Soc. Trans.* 35, 1389-1392
 40. Hietakangas, V., Anckar, J., Blomster, H. A., Fujimoto, M., Palvimo, J. J., Nakai, A., and Sistonen, L. (2006) PDSM, a motif for phosphorylation-dependent SUMO modification. *Proc. Natl. Acad. Sci. U. S. A.* 103, 45-50
 41. Myatt, S. S., Kongsema, M., Man, C. W., Kelly, D. J., Gomes, A. R., Khongkow, P., Karunarathna, U., Zona, S., Langer, J. K., Dunsby, C. W., Coombes, R. C., French, P. M., Brosens, J. J., and Lam, E. W. (2013) SUMOylation inhibits FOXM1 activity and delays mitotic transition. *Oncogene*
 42. Zhao, F., and Lam, E. W. (2012) Role of the forkhead transcription factor FOXO-FOXM1 axis in cancer and drug resistance. *Front Med.* 6, 376-380
 43. Anders, L., Ke, N., Hydrbring, P., Choi, Y. J., Widlund, H. R., Chick, J. M., Zhai, H., Vidal, M., Gygi, S. P., Braun, P., and Sicinski, P. (2011) A systematic screen for CDK4/6 substrates links FOXM1 phosphorylation to senescence suppression in cancer cells. *Cancer Cell* 20, 620-634
 44. Koo, C. Y., Muir, K. W., and Lam, E. W. (2012) FOXM1: From cancer initiation to progression and treatment. *Biochim. Biophys. Acta* 1819, 28-37
 45. Wierstra, I. (2013) FOXM1 (Forkhead box M1) in tumorigenesis: overexpression in human cancer, implication in tumorigenesis, oncogenic functions, tumor-suppressive properties, and target of anticancer therapy. *Adv. Cancer Res.* 119, 191-419
 46. Radhakrishnan, S. K., Bhat, U. G., Hughes, D. E., Wang, I. C., Costa, R. H., and Gartel, A. L. (2006) Identification of a chemical inhibitor of the oncogenic transcription factor forkhead box M1. *Cancer Res.* 66, 9731-9735
 47. Halasi, M., and Gartel, A. L. (2013) Targeting FOXM1 in cancer. *Biochem. Pharmacol.* 85, 644-652
 48. Vertegaal, A. C., Ogg, S. C., Jaffray, E., Rodriguez, M. S., Hay, R. T., Andersen, J. S., Mann, M., and Lamond, A. I. (2004) A

Chapter 5

- proteomic study of SUMO-2 target proteins. 50. Hsiao, H. H., Meulmeester, E., Frank, B. T., Melchior, F., and Urlaub, H. (2009) "ChopNSpice," a mass spectrometric approach that allows identification of endogenous small ubiquitin-like modifier-conjugated peptides. *Mol. Cell Proteomics* 8, 2664-2675
49. Becker, J., Barysch, S. V., Karaca, S., Dittner, C., Hsiao, H. H., Berriel, D. M., Herzig, S., Urlaub, H., and Melchior, F. (2013) Detecting endogenous SUMO targets in mammalian cells and tissues. *Nat. Struct. Mol. Biol.* 20, 525-531

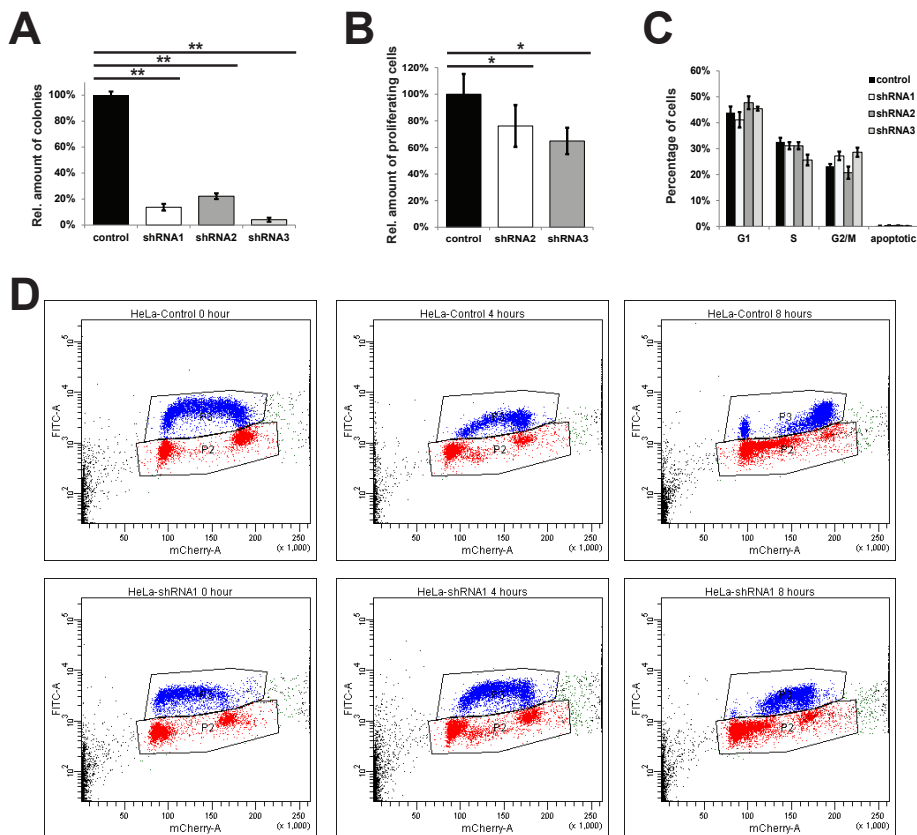


Figure S1 related to Figure 1: Cell cycle profile after UBA2 and Ubc9 knockdown. A) Colony formation of U2OS cells was determined nine days after infection with a control shRNA, shRNA1 (UBA2), shRNA2 or shRNA3 (both Ubc9) by staining with Giemsa solution and counting colonies using the ImageJ Version 1.47v software. The values were normalized to the control. Error bars represent the standard deviation from the average obtained from three independent experiments. ** $p < 0.001$. B) The proliferation rate of U2OS cells treated with Ubc9 knockdown virus was compared to cells treated with control virus four days after infection by adding the cell proliferation reagent WST-1 to the growing cells and measuring the absorbance at 450 nm after two hours incubation. The values were normalized to the control and the standard error of the mean was determined from ten values obtained from three independent experiments. * $p < 0.05$. C) Four days after infection with UBA2, Ubc9 and control viruses, U2OS cells were stained with propidium iodide and subjected to flow cytometry analysis. The graph depicts the percentage of cells in each cell cycle phase. Error bars represent the standard deviation from the average obtained from three independent experiments. D) HeLa cells treated with control shRNA and shRNA1 for four days were pulse-labeled with BrdU and released for four hours or eight hours before staining them with propidium iodide. The graphs depict the amount of DNA (mCherry-A) in BrdU labeled cells (blue) and non-labeled cells (red) at the respective time-points demonstrating a faster passage through the cell cycle for the control compared to cells with a reduced UBA2 expression.

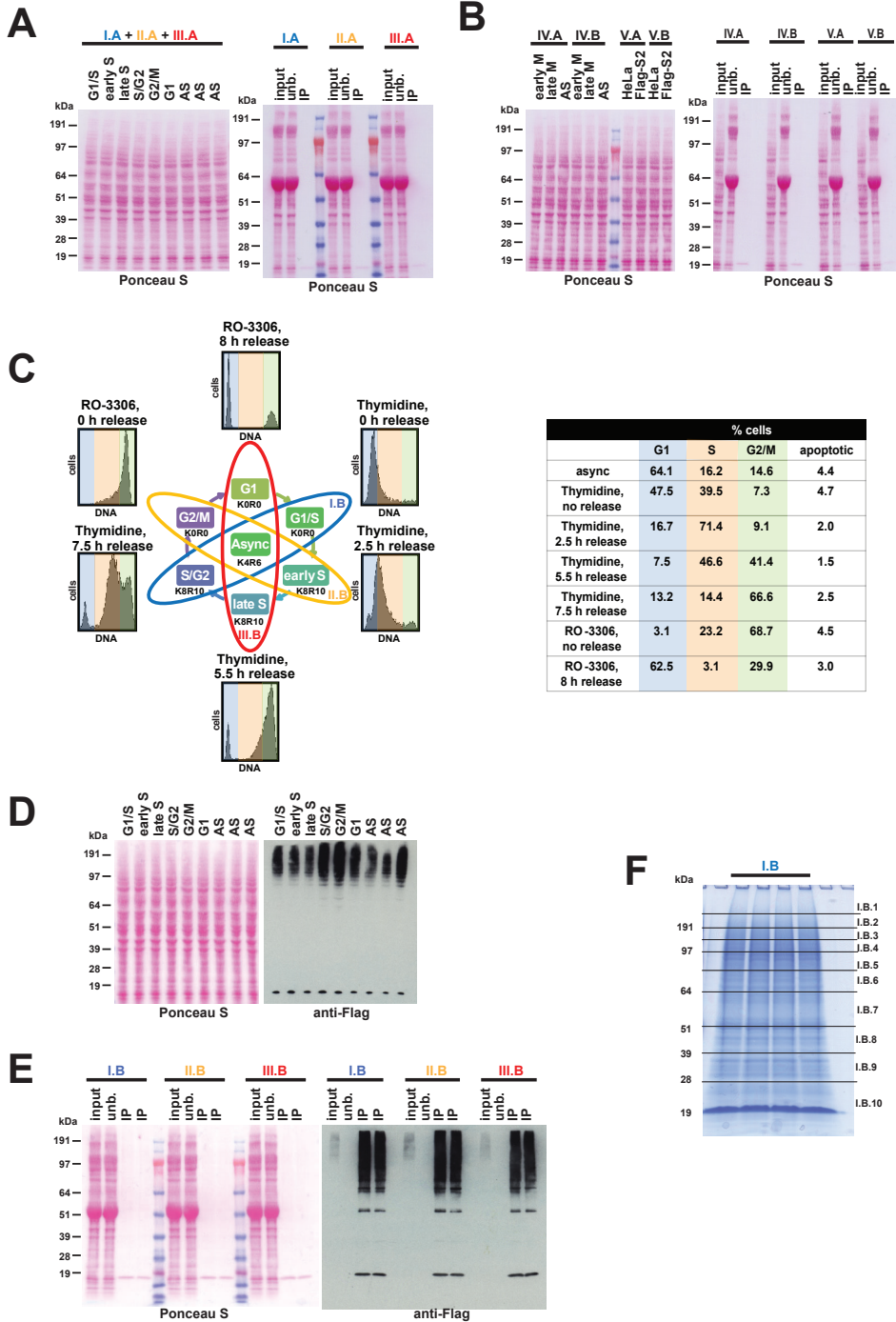


Figure S2. (legend on next page)

Chapter 5

Figure S2 related to Figure 2: Loading controls and label swap of SILAC-labeled cells synchronized in different cell cycle stages and purification of SUMO conjugates. A) HeLa cells stably expressing Flag-SUMO-2 were SILAC-labeled with three different isotopic variants of lysine and arginine. Three independent pools of light labeled (K0R0) cells and one pool of medium labeled (K4R6) cells were blocked with thymidine. Two pools of medium labeled cells were blocked with RO-3306. The light labeled cells were released from the thymidine block and lysed at three different time points (2.5 hours, 5.5 hours and 7.5 hours after release). Two pools of medium labeled cells were lysed directly after the thymidine block or the RO-3306 block. The third medium labeled pool was released from the RO-3306 block for eight hours and then lysed. Three pools of asynchronous cells were heavy labeled (K8R10) and served as an internal standard during the subsequent analysis. Total cell lysates of the different synchronized cell pools were size separated by SDS-PAGE and levels were analyzed by Ponceau S staining (left panel). For the Flag-immunoprecipitation, equal amounts of lysates from light-labeled and heavy-labeled synchronized cells were mixed with an equal amount of lysate from medium-labeled asynchronous cells, resulting in three samples (I.B, II.B and III.B) comprising six time points in cell cycle progression. Inputs, unbound fractions and immunoprecipitated samples were analyzed by Ponceau S staining (right panel). B) HeLa cells expressing Flag-SUMO-2 were SILAC-labeled and synchronized with RO-3306 in G2/M. Cells were released from the block for 30 minutes (early M-phase) and 2 hours (late M-phase), respectively (experiment IV.A and label swap experiment IV.B). In addition, asynchronous HeLa cells and asynchronous HeLa cells expressing Flag-SUMO-2 were SILAC-labeled and mixed to obtain a parental control sample for mass spectrometric analysis (experiment V.A and label swap experiment V.B). Total cell lysates of the different cell pools were size separated by SDS-PAGE and levels were analyzed by Ponceau S staining (left panel). Inputs, unbound fractions and immunoprecipitated samples were analyzed by Ponceau S staining (right panel). C) Label swap for the experiment described in (A). Cell cycle synchronization was confirmed by flow cytometry. Flow cytometry profiles are shown next to the respective samples and the percentage of cells in each cell cycle phase is depicted in the table. D) Lysates of the different synchronized cell pools from the experiment described in (C) were size-separated by SDS-PAGE and protein levels were analyzed by Ponceau S staining (left panel), levels of Flag-SUMO-2 conjugates were compared by immunoblotting using an antibody directed against the Flag epitope (right panel). E) Purification of Flag-SUMO-2 conjugates by immunoprecipitation in the experiment described in (C) was confirmed by immunoblotting for all three experiments. Inputs, unbound fractions and immunoprecipitated samples were size-separated by SDS-PAGE and levels were analyzed by Ponceau S staining (left panel). Levels of Flag-SUMO-2 conjugates were analyzed by immunoblotting using an antibody directed against the Flag epitope (right panel). F) The Flag-IP samples of all three experiments described in (C) were size separated by SDS-PAGE and stained with Coomassie. Each sample was divided into ten different gel slices according to the molecular weight of the purified proteins. These sections were further cut into small gel fragments, proteins were digested by trypsin, extracted and analyzed by mass spectrometry. The Coomassie stained gel for experiment I.B is shown as an example.

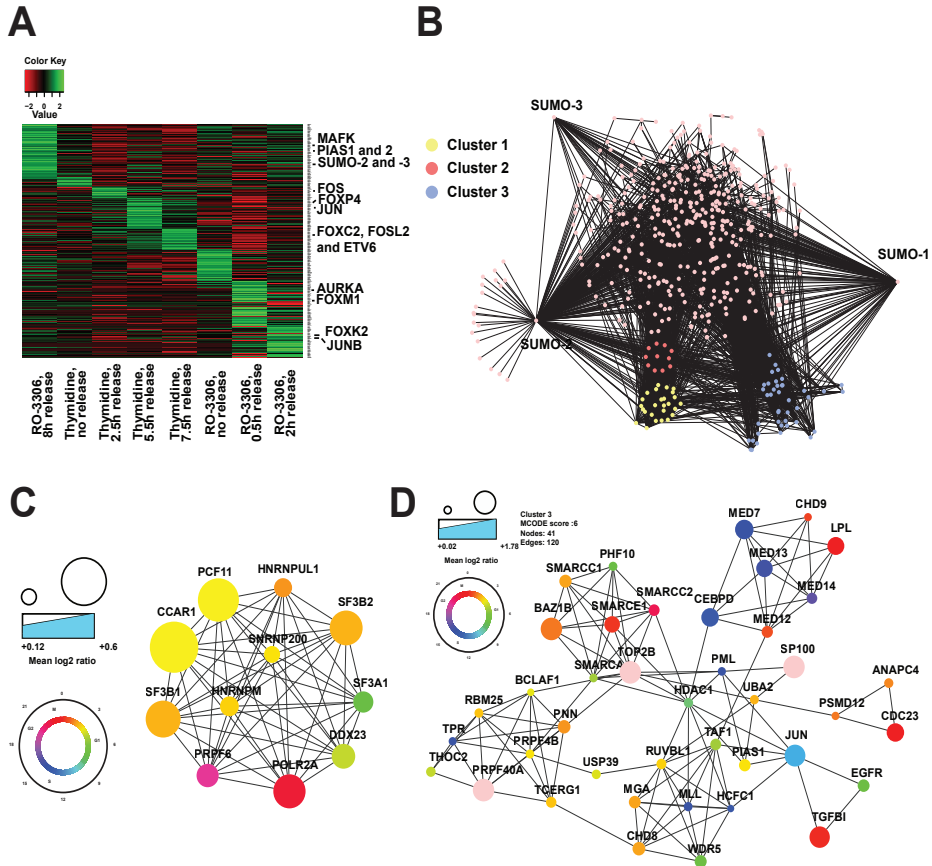


Figure S3, related to Figure 3. Global SUMOylation dynamics throughout the cell cycle.

A) A standardized heat map of SUMOylation proteins. Red indicates a low SILAC Log₂ ratio while green indicates a high SILAC Log₂ ratio of the SUMO target proteins at the different time points in the experiment. B) The total functional SUMO protein network. The STRING network including 474 nodes with 2538 edges was acquired and visualized in Cytoscape. The MCODE plugin for Cytoscape was used to find highly interconnected clusters within the network. The three most interconnected clusters in the total network are highlighted. C) The second most significantly interconnected cluster within the total SUMO network. The cluster contains 11 proteins with a total of 55 interactions. The nodes are colored by their estimated cell-cycle peak-time according to the indicated color-scheme and their node size by their highest SILAC log₂ ratio. D) The third most significantly interconnected cluster within the total SUMO network. The cluster contains 41 proteins with a total of 120 interactions. The nodes are colored by their estimated cell-cycle peak-time according to the indicated color-scheme and their node size by their highest SILAC log₂ ratio.

	% cells			
	G1	S	G2/M	apoptotic
asynchronous	55.8	20.8	23.0	0.4
Thymidine, no release	33.2	58.8	7.1	0.9
Thymidine, 2.5 h release	5.6	83.2	10.9	0.3
Thymidine, 5.5 h release	5.6	70.8	23.2	0.4
Thymidine, 7.5 h release	11.1	28.9	59.6	0.4
RO-3306, no release	1.2	21.5	75.3	2.0
RO-3306, 8 h release	62.2	5.5	29.4	2.9

Figure S4, related to Figure 4. Flow cytometry analysis of cell cycle synchronization. HeLa cells stably expressing Flag-SUMO-2 were synchronized in different stages of the cell cycle as previous described. Cell cycle synchronization was confirmed by flow cytometry, the percentage of cells in each cell cycle phase is depicted in the table.

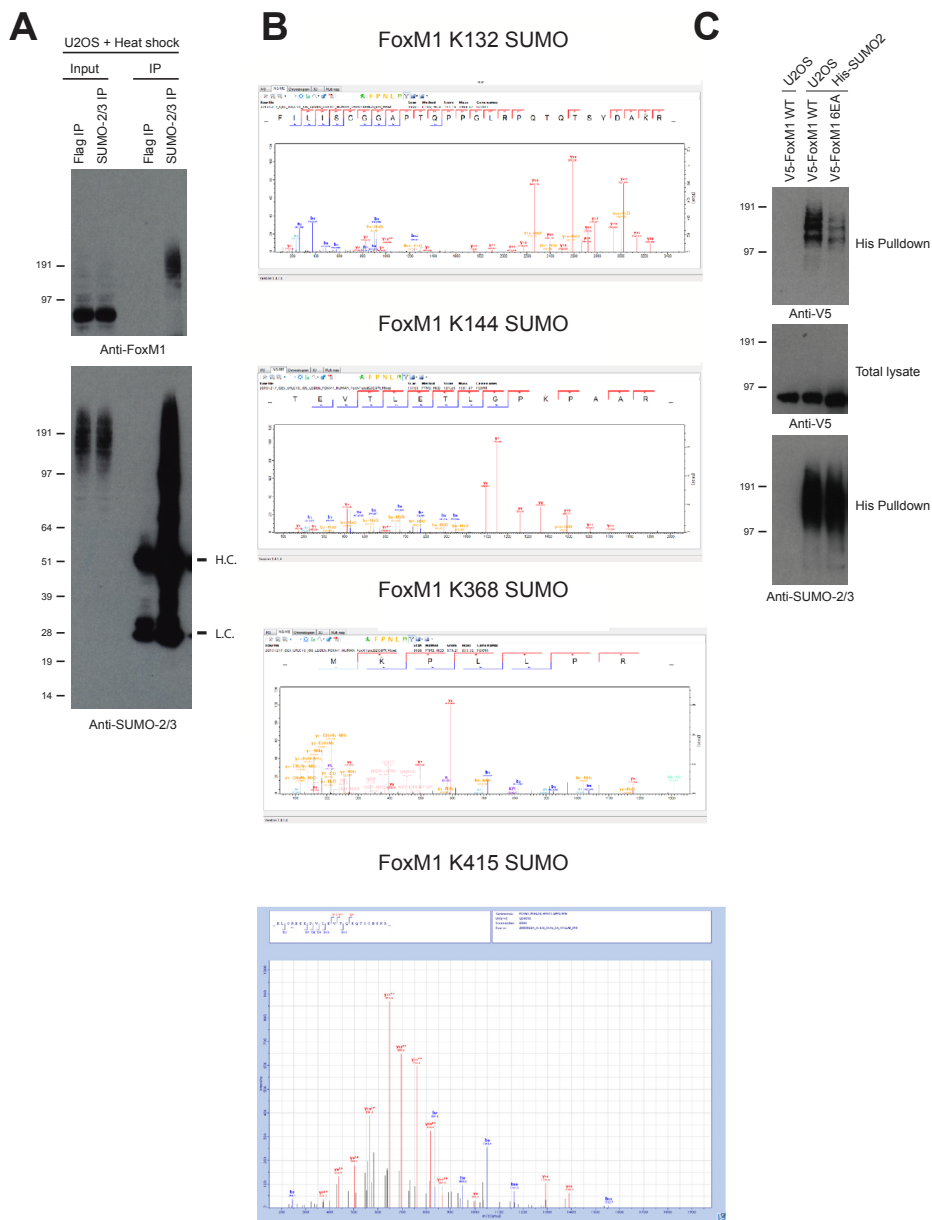


Figure S5. (legend on next page)

Figure S5, related to Figure 5. Endogenous FoxM1 SUMOylation and identification of SUMO-2 acceptor sites in FoxM1. A) U2OS cells were exposed to heat shock at 43°C for 1 hour to destabilize SUMO proteases and subsequently lysed for immunoprecipitation with a mouse monoclonal SUMO-2/3 antibody or a Flag antibody as a control. Input and IP samples were size separated by SDS-PAGE and analyzed by immunoblotting using FoxM1 antibody (upper panel) or SUMO-2/3 antibody (lower panel). Heavy Chains (H.C) and Light Chains (L.C) of the antibodies are indicated. B) MS/MS spectra for the SUMO acceptor sites in FoxM1. K132, K144 and K368 were found to be SUMO-2 modified in human FoxM1. Additionally K415 was found to be SUMO-1 modified in mouse FoxM1; this lysine is conserved in human FoxM1. C) U2OS cells stably expressing His-SUMO-2 were transfected with expression constructs encoding mouse V5-FoxM1 WT or V5-FoxM1 6EA (E201A, E218A, E356A, E461A, E479A and E496A). The six consensus sites mutated in this construct are conserved in human FoxM1. U2OS cells were transfected with a V5-FoxM1 WT construct as a control. Cells were lysed 48 hours after transfection in 6 M Guanidine-HCL, and His-SUMO-2 conjugates were purified by immobilized metal ion affinity chromatography. Total lysates and purified fractions (His pulldown) were separated by SDS-PAGE, transferred to a membrane, and probed using an antibody to detect V5. Total SUMO-2/3 levels in the purified fractions were detected with a SUMO-2/3 antibody.

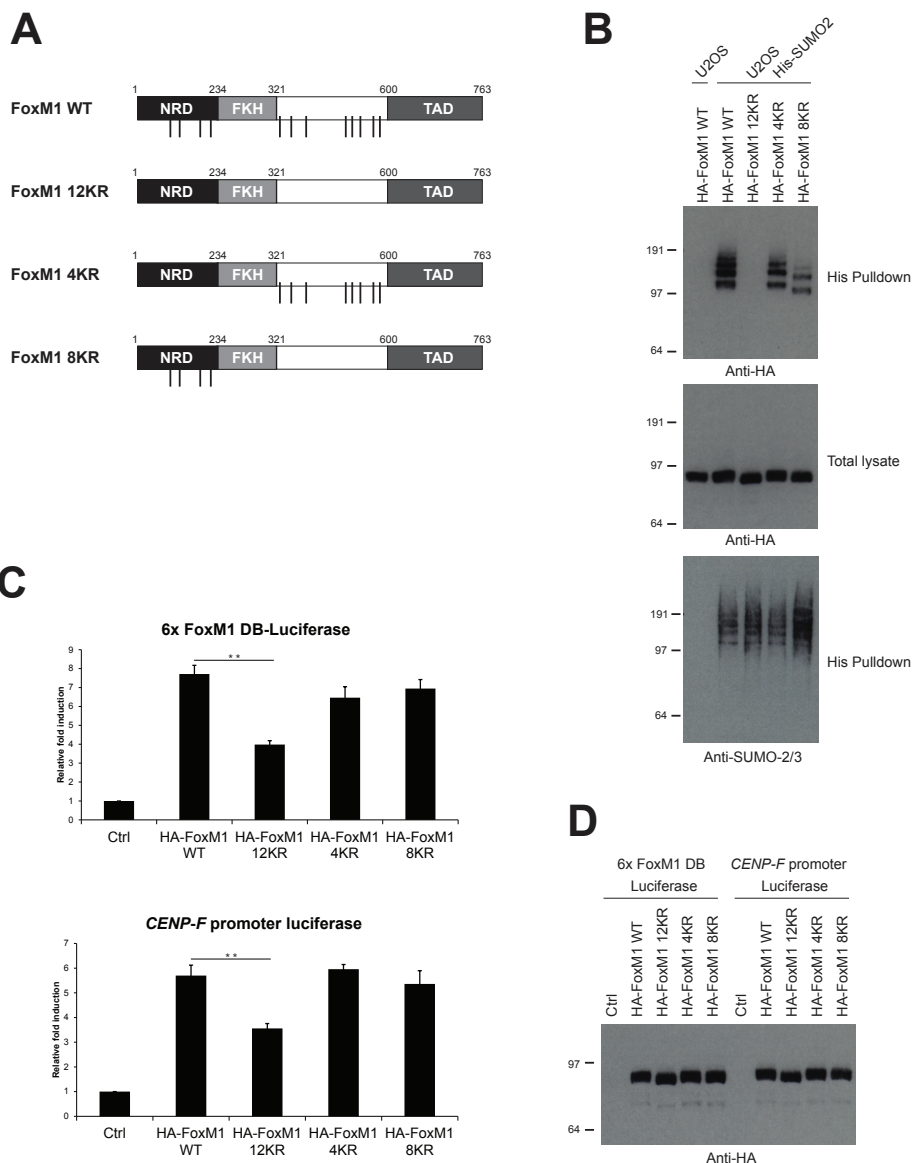


Figure S6, related to Figure 6. Analysis of domain specific FoxM1 SUMOylation mutants. A) Different FoxM1 mutants were generated. The four lysines in the N terminal repressor domain (4KR) or the eight lysines in the undefined domain between the Forkhead and the C terminal transactivation domain (8KR) were mutated to arginines. These mutants were compared to wild-type (WT) FoxM1 and the 12KR mutant of FoxM1. B) U2OS cells stably expressing His-SUMO-2 were transfected with expression constructs encoding HA-FoxM1 WT, HA-FoxM1 12KR, HA-FoxM1 4KR or HA-FoxM1 8KR. U2OS cells were transfected with HA-FoxM1 WT as a control. Cells were lysed 48 hours after transfection in 6 M Guanidine-HCL, and His-SUMO-2 conjugates were purified by immobilized metal ion affinity chromatography. Total lysates and purified fractions (His pulldown) were separated by SDS-PAGE, transferred to a membrane, and probed using an antibody to detect HA. Total SUMO-2/3 levels in the purified fractions were detected with an antibody directed against SUMO-2/3. C) U2OS cells were cotransfected with an empty vector, HA-FoxM1 WT, HA-FoxM1 12KR, HA-FoxM1 4KR or HA-FoxM1

8KR and a luciferase reporter containing six FoxM1 DNA binding domains (6x FoxM1 DB-Luciferase, upper panel) or a luciferase reporter containing the *CENP-F* promoter region (lower panel) and a LacZ reporter. Cells were lysed in reporter lysis buffer 48 hours after transfection and luciferase activity and β -gal activity were measured. Results are representative of four independent experiments and corrected for transfection efficiency using β -gal activity; the error bars indicate the standard deviation from the average. Results are shown as a relative fold induction compared to cells transfected with the empty vector. ** $p < 0.001$ D) Expression levels of the different HA-FoxM1 proteins in the luciferase experiments were verified by immunoblotting using an antibody directed against the HA-tag.

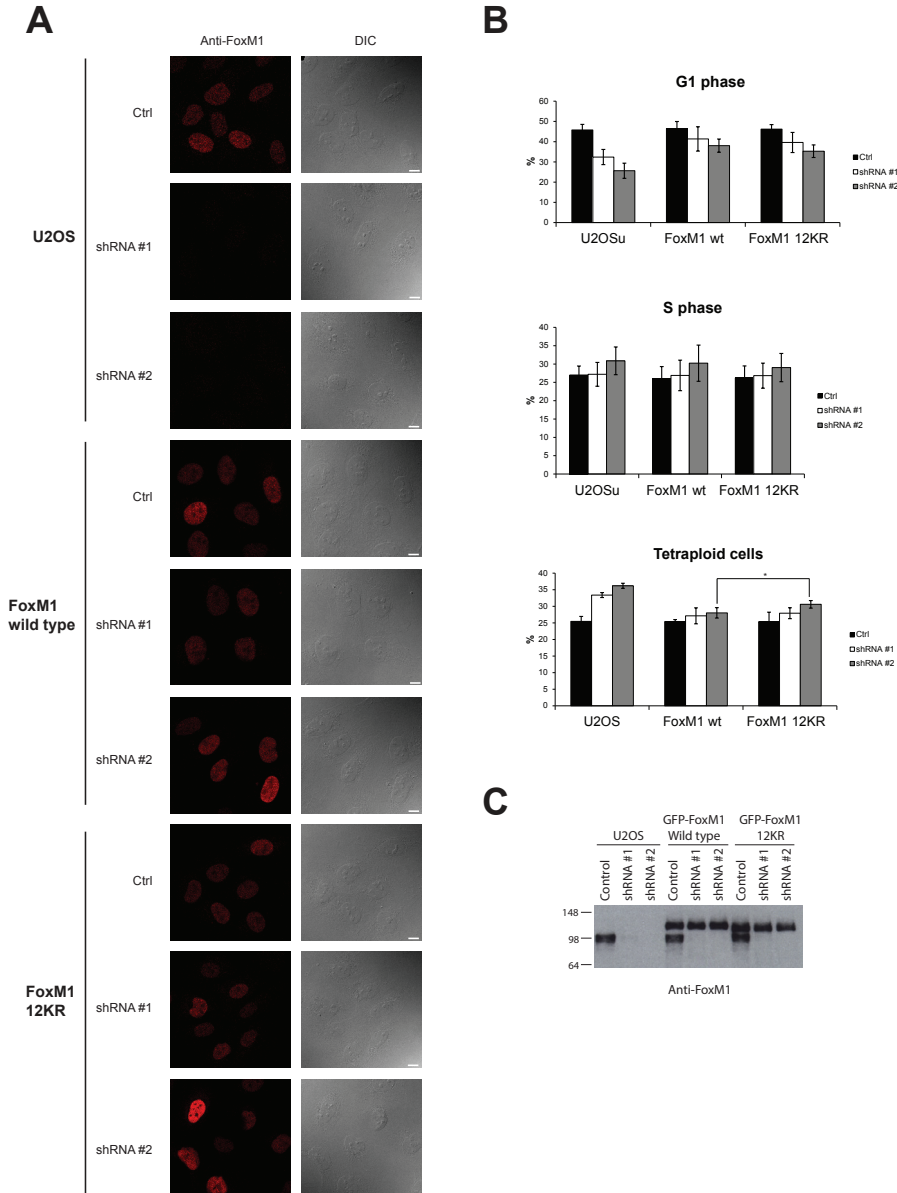


Figure S7. (legend on next page)

Chapter 5

Figure S7, related to Figure 7. FoxM1 knockdown and complementation experiments. A) U2OS cells, U2OS cells stably expressing Flag-FoxM1 wild type or Flag-FoxM1 12KR were infected with a non-targeting shRNA lentivirus, or two independent lentiviruses encoding FoxM1 shRNAs (shRNA #1 and #2). Cells were fixed three days after infection, stained with antibodies to detect FoxM1 and analyzed by confocal microscopy. Scale bars are 10 μ M. B) FACS analysis of G1 phase, S phase and tetraploid cells for the rescue experiment described in figures 7A and 7B. Average values from three independent experiments are shown in percentages; the error bars indicate the standard deviation from the average.

C) U2OS cells, U2OS cells stably expressing GFP-FoxM1 wild type or GFP-FoxM1 12KR were infected with a non-targeting shRNA lentivirus, or two independent lentiviruses encoding FoxM1 shRNAs (shRNA #1 and #2). Three days after infection cells were harvested for immunoblotting analysis with a FoxM1 antibody.

Supplemental Table Legends

- Table S1. List of all Identified Proteins in This Study, Related to Figures 2 and 3. This table lists all the proteins that were identified by mass-spectrometry in all the SILAC experiments described in this study.
- Table S2. List of all SUMO Targets, Related to Figures 2 and 3. This table contains all the proteins that have been classified as SUMO targets.
- Table S3. List of Identified SUMO-Acceptor Sites, Related to Figure 3. List of SUMO-modified peptides that have been identified in this study, carrying the QQTGG and/or pyroQQTGG modification.
- Table S4. List of Unique Identified SUMO-Acceptor Sites, Related to Figure 3. This table indicates the unique SUMO-modified sites that were identified in this study.
- Table S5. Post-Translational modification of FoxM1, Related to Figure 5. This table contains methylation, acetylation, ubiquitination and phosphorylation sites on FoxM1 identified by mass spectrometry.

Tables available online at: <http://www.sciencedirect.com/science/article/pii/S1097276514001154>

Supplementary Materials

Plasmids

The mature protein that we refer to as SUMO-2-Q87R has the following amino acid sequence: MSEEKP-KEGVKTENDHINLKVAGQDGSVVQFKIKRHTPLSKLMKAYCERQGLSMRQIRFRFDGQPINETDTPA-QLEMEDEDTIDVFRQQTGG (Tatham et al., 2001). The open reading frame of this protein was amplified with the following primers: 5'-TTACTGCAGATGGACTACAAGGACGACGATGACAAGACTAGTATGTCC-GAGGAGAAGCC-3' and 5'-AATCTCGAGCTAACCTCCCGTCTGCTGCCG-3' to introduce an N-terminal Flag-tag. This PCR product was cloned in between the *Pst*I and *Xho*I site of the plasmid pLV-CMV-IRES-eGFP (Vellinga et al., 2006) for lentiviral infection.

The cDNA encoding the human FoxM1 protein was obtained from the Mammalian Gene Collection (MGC code 9577; Image ID 3881055; supplied by Source Bioscience) and amplified by a two-step PCR reaction using the following primers: 5'-AAAAAGCAGGC TTAATGAAAAGTACCCCCGTCG-3' and 5'-A GAAAGCTGGGTTCTACTGTAGCTCA GGAATAAAC-3' for the first reaction and 5'-GGGACAAGTTG-TACAAAAAGCAGG CT-3' and 5'-GGGGACCACTTTGTACAAGAAAGCTGGGT-3' for the second reaction. The cDNA was inserted into pDON207 employing standard Gateway technology (Invitrogen). pDON207-FoxM1-12KR was generated by a gene synthesis service (GenScript). Silent mutations in both

pDON207-FoxM1 wild type and pDON207-FoxM1-12KR were introduced by QuickChange site-directed mutagenesis (Stratagene) using oligonucleotides 5'- CTAAGAGATCCCCTGCACAGCAAGAATC-CAACCAGGCAGAGG CCTCCAAG-3' and 5'-CTTGGAGGCCTCTGCCTGGTTGGATTCTTGCTGTGCAGGGG ATCTCTTAG-3' for resistance to FoxM1 shRNA #1 and 5'- GTTTCTGGCCTTGAGCA AACCGTCCCTAACTGAGGGCCTGGTCCTG-3' and 5'- CAGGACCAGGCCCTCAGT TAGGGAC-CGGTTTGCTGCAAGGCCAGAAAC-3' for resistance to FoxM1 shRNA #2. To generate pDON207-FoxM1-4KR and 8KR we have swapped regions of the wild type and 12KR constructs by restriction of these plasmids with *Bss*SI and *Xcm*I and subsequent ligation. These cDNAs were subsequently transferred to multiple different destination vectors to generate T7-6His-FoxM1 expression constructs, HA-tagged FoxM1 expression plasmids (pMT2-HA-Dest, a kind gift of Drs. Petra de Graaf and Marc Timmers, Utrecht, The Netherlands) or GFP- tagged FoxM1 (pBabe-GFP-puro-DEST, also a kind gift of Drs. Petra de Graaf and Marc Timmers, Utrecht, The Netherlands). cDNA of FoxM1 wild type and FoxM1-12KR was cloned into the *Spe*I and *Xho*I cloning sites of a pLV-Flag-IRES-GFP construct using the following primers: 5'- ttaactagtATGAAAAGTCCCGG-3' and 5'- aatctcgagCTACTGTAGCTCAG GAATAAAC-3' to generate Flag-tagged, GFP sortable FoxM1 constructs. All fusions were made to the N-terminus of FoxM1. The cDNA encoding the mouse FoxM1 protein was obtained from the Mammalian Gene Collection (Image ID 6417437; supplied by Source Bioscience) and amplified by a two-step PCR reaction using the following primers: 5'- AAAAAGCAGGCTCGATGAGAACCAGCCCCGCGG-3' and 5'- AGAAAG CTGGGTGCTAAGGGATGAACTGAGAC-3' for the first reaction and 5'-GGGGA-CAAGT TTGTACAAAAAGCAGGCT-3' and 5'-GGGACCACCTTTGTACAAGAAAGCTGGGT-3' for the second reaction. The cDNA was inserted into pDON207 employing standard Gateway technology (Invitrogen). Mutations were introduced by QuickChange site-directed mutagenesis using the following oligonucleotides: 5'-CAGCGTTAAGCAGGCA CTGGAAGAGAAG-3' and 5'- CTTCTCTCCAGTGCCT-GCTTAACGCTG-3' (E201A), 5'-CGGGTTAAGGTTGCGGAGCCCTCAGGAG-3' and 5'-CTCCTGAGGGCTCCGCAA CCTTAACCCG-3' (E218A), 5'-CCATCAA AACTGCAATCCCACTGGG-3' and 5'-CCCA GTGGGATTGCAGTTTTGATGG-3' (E356A), 5'-CCATTAAGGAAGCAGAAATGCAGC CTG-3' and 5'- CAGGCTGCATTCTGCTTCCCTTAATGG-3' (E461A), 5'-CCTATCAA GTGGCGAGCCCTCCCT TG-3' and 5'-CAAGGGAGGGCTCGCCACTTTGATAGG-3' (E479A), 5'-CGCTCAAAGAGGCGCTATC-CAACTC-3' and 5'-GAGTTGGATAGCGCT CTTTGAGCG -3' (E496A). Wild type and 6EA mouse FoxM1 cDNAs were subsequently transferred to the pcDNA3.1/nV5-DEST expression vector (Invitrogen). The 6x-FoxM1 DB-Luciferase, *CENP-F* promoter Luciferase and the GST tagged N terminal FoxM1 constructs were described previously (Laoukili et al., 2005; Laoukili et al., 2008). The CMV-LacZ reporter construct used in Luciferase assays was a kind gift of Dr. Erik Meulmeester. The SUMO-1 and SUMO-2 expressing constructs pE1E2S1 and pE1E2S2 were a kind gift of Dr. Hisato Saitoh (Uchimura et al., 2004).

Antibodies

The primary antibodies used were as followed: mouse anti-Ubc9 (BD Biosciences), mouse anti-UBA2 (Transduction Laboratories) mouse anti-Bromodeoxyuridine-Fluorescein (Roche Applied Science), mouse monoclonal anti-Flag M2, rabbit anti-HMGN5, mouse anti-polyHistidine Clone HIS-1 (All from Sigma), mouse monoclonal anti-SUMO-2/3 (Abcam), mouse anti-cJun and rabbit anti-ETV6 (kind gifts from Dr.

Chapter 5

D. Baker, Leiden, The Netherlands), rabbit anti-FoxP1 (Abcam), rabbit anti-FoxM1, mouse anti-Ubiquitin P4D1 (both from Santa Cruz Biotechnology), mouse monoclonal anti-HA.11 (Covance), mouse monoclonal anti-Methylated lysine (Abcam), mouse monoclonal anti-polyHistidine Clone HIS-1 (Sigma), rabbit anti-GTF21RD1, rabbit anti-JARID1B, rabbit anti-MDC1, rabbit anti-MYBL2, rabbit anti-SATB2, rabbit anti-RanBP2 (all from Bethyl laboratories), rabbit anti-MCM4 (Epitomics), mouse anti-RanGAP1 (Life Technologies), rabbit anti-V5 (Abcam), rabbit anti-SUMO-2/3 as previously described (Vertegaal et al., 2004).

SILAC labeling

For SILAC labeling, cells were grown in medium supplemented with [$^{12}\text{C}_6$, $^{14}\text{N}_4$]arginine (referred to as R0), [$^{13}\text{C}_6$, $^{14}\text{N}_4$]arginine (referred to as R6), [$^{13}\text{C}_6$, $^{15}\text{N}_4$]arginine (referred to as R10), [$^{12}\text{C}_6$, $^{14}\text{N}_2$]lysine (referred to as K0), [$^2\text{H}_4$, $^{12}\text{C}_6$, $^{14}\text{N}_2$]lysine (referred to as K4), or [$^{13}\text{C}_6$, $^{15}\text{N}_2$]lysine (referred to as K8) as indicated.

Lentiviral shRNA experiments

HeLa cells were infected at MOI 3 with lentivirus encoding shRNA TRCN0000007472 (shRNA1), shRNA TRCN0000007205 (shRNA2) or shRNA TRCN0000007206 (shRNA3). The medium was changed the next day and three days after infection, cells were transferred to different plates to proceed with FACS analysis, WST-1 analysis and colony formation assay. U2OS cells and U2OS cells stably expressing Flag-FoxM1 wild type or Flag-FoxM1 12KR were infected at MOI 2 with lentiviruses encoding shRNA TRCN0000015544 (shRNA #1) or shRNA TRCN0000015546 (shRNA #2) against FoxM1. Cells were split one day after infection and processed three days after infection for FACS analysis, immunoblotting and microscopy. In all shRNA experiments, a non-targeting shRNA SHC002 was used as a control virus. All shRNA constructs belong to the Mission shRNA library from Sigma-Aldrich.

WST-1 analysis

On day three after lentivirus infection, cells were transferred (three wells per lentivirus construct in the first and second experiment, four wells per construct in the third experiment) to a 96-well plate at a density of 3000 cells per well. After another 24 hours, the old medium was removed and 100 μl of medium mixed 10:1 with WST-1 cell metabolic activity reagent (Roche) was added to each well. The absorbance at 450 nm was measured two hours after addition of the reagent in a microplate reader Victor 3 (Perkin Elmer).

Colony formation assay

For the colony formation assay, cells were transferred to 10 cm dishes on day three after the lentivirus infection at a density of 10,000 cells per dish. Colonies were grown until day nine after the infection and fixed with methanol and acetic acid (3:1) for 15 minutes at room temperature. After drying the dishes, colonies were stained with Giemsa solution (Merck). Colony formation was quantified using ImageJ Version 1.47v software.

Synchronization of cells

Cells were blocked with 4 mM thymidine (Sigma) for 16 hours or 10 μM RO-3306 (Calbiochem) for 20 hours and released from this blockage by washing two times with PBS and adding fresh DMEM. A single round

of thymidine blocking was performed to limit DNA damage associated with this treatment. After the indicated time of release, cells were harvested by a mild trypsin treatment, one fifth of the sample was fixed for FACS analysis and the remaining sample was lysed in 4 pellet volumes of Flag-IP lysis buffer (1% SDS, 0.5% NP-40, 50 mM sodium fluoride, 1 mM sodium orthovanadate, 5 mM β -glycerol phosphate, 5 mM sodium pyrophosphate, 0.5 mM EGTA, 5 mM 1,10-phenanthroline, protease inhibitor including EDTA (Roche; 1 tablet per 10 ml buffer) in PBS). Lysates were frozen in liquid nitrogen and, if needed, stored at -80°C .

Immunoprecipitation

Flag-IP lysates described above were thawed at 30°C and 70 mM Chloroacetamide was added freshly. Samples were sonicated and incubated for 30 minutes at room temperature. Afterwards, samples were equalized using BCA and 30 μl of each lysate were kept as an input sample. An equal volume of dilution buffer (2% Triton X-100, 0.5% sodium deoxycholate, 1% BSA, freshly added 70 mM chloroacetamide, 5 mM sodium fluoride, 1 mM sodium orthovanadate, 5 mM β -glycerol phosphate, 5 mM sodium pyrophosphate, 0.5 mM EGTA, 5 mM 1,10-phenanthroline, protease inhibitor including EDTA (Roche; 1 tablet per 10 ml buffer) in 1x PBS) was added to the lysates and they were subsequently centrifuged for 45 minutes at 13.2 krpm at 4°C . The supernatant was mixed with prewashed Flag-M2 beads (Sigma; 30 μl beads per 1 ml of diluted sample) and incubated at 4°C for 90 minutes. Afterwards, the beads were washed 5 x with wash buffer (50 mM Tris, 150 mM NaCl, 70 mM chloroacetamide, 0.5% NP-40, 5 mM sodium fluoride, 1 mM sodium orthovanadate, 5 mM β -glycerol phosphate, 5 mM sodium pyrophosphate, 0.5 mM EGTA, 5 mM 1,10-phenanthroline, protease inhibitor including EDTA (Roche; 1 tablet per 10 ml buffer)) including three tube changes. Flag-SUMO-2 conjugates or Flag-FoxM1 proteins were eluted with one bead volume of 5% SDS and 1 mM Flag M2 epitope peptide in wash buffer. For SUMO-2/3 IPs, mouse monoclonal SUMO-2/3 antibodies were coupled to protein G sepharose (GE Healthcare). Cell lysis and the IP were performed as described above. SUMO-2/3 conjugates were eluted with one bead volume 1x Nupage LDS sample buffer (Invitrogen).

Fluorescence-activated cell sorting analysis and BrdU labeling

Cells were harvested by a mild trypsin treatment, washed two times with PBS and resuspended in 1.5 ml of PBS. Afterwards, 3.75 ml of 100% ethanol was added and the cells were fixed at 4°C at least overnight. On the day of flow cytometry analysis, the cells were first centrifuged at 1200 rpm for 2 minutes, the supernatant was removed and the cells were washed with PBS and 2% calf serum. Then, the cells were pelleted again and resuspended in 500 μl of PBS complemented with 2% calf serum, 25 $\mu\text{g}/\text{ml}$ propidium iodide (Sigma) and 100 $\mu\text{g}/\text{ml}$ RNase A (Sigma). Cellular DNA content was determined by flow cytometry with the BD LSRII system and BD FACS DIVA Software (BD Biosciences Clontech). Newly synthesized DNA was labeled by replacing the cell medium with medium containing 20 μM BrdU (Sigma). After 30 minutes of incorporation, the cells were released for 0, 4 or 8 hours. Cells were harvested by a mild trypsin treatment, washed once with PBS and resuspended in 0.5 ml of PBS. Subsequently, 5 ml of 70% ethanol was added and the cells were fixed at 4°C at least overnight. Next, the cells were washed with PBS and resuspended in 200 μl RNase A (0.5 mg/ml). After a 30 minute incubation at 37°C , the RNase A was removed by washing once with PBS. Afterwards, the cells were resuspended in 500 μl of solution A

Chapter 5

(5 M HCl and 0.5% Triton in MQ) and incubated for 20 minutes at room temperature. After neutralizing the solution by adding 10 ml of 1 M Tris pH 7.5, the cells were washed once with wash buffer 1 (0.5% Tween and 1% BSA in PBS). Subsequently, the cells were resuspended in FITC-conjugated anti-BrdU antibody (Roche) solution and incubated for 30 minutes at room temperature in the dark. Finally, the cells were washed twice with wash buffer 2 (0.5% Tween and 2% FCS in PBS), resuspended in PBS containing 20 µg/ml propidium iodide and analyzed by flow cytometry as described above.

Electrophoresis and immunoblotting

Protein samples were either separated via regular SDS-PAGE using a Tris-glycine buffer or on Novex 4-12% Bis-Tris gradient gels (Invitrogen) using MOPS buffer. Fractionated proteins were transferred onto Hybond-C extra membranes (Amersham Biosciences) using a submarine system (Invitrogen). Membranes were stained for total protein amounts with Ponceau S (Sigma) and blocked with PBS containing 5% milk powder and 0.1% Tween-20 before incubating with the primary antibodies as indicated.

Coomassie staining and in-gel digestion

Proteins were fractionated on Novex 4-12% gradient gels (Invitrogen) and stained with the Colloidal Blue Kit (Invitrogen) according to the manufacturer's protocol. Gel-lanes were divided into ten different slices as indicated and each slice was cut into 1 mm³ cubes. Gel slices were destained with 50% ethanol in 25 mM ammonium bicarbonate solution and dehydrated with absolute ethanol. Proteins were digested with sequencing-grade modified trypsin (Sigma) overnight. Trypsin activity was quenched by acidification with TFA and peptides were extracted from the gel plugs with increasing concentrations of acetonitrile in 0.5% acetic acid. Organic solvent was evaporated in a vacuum centrifuge (Lundby and Olsen, 2011).

Mass Spectrometry Analysis

The resulting peptides from in-gel digestion were desalted and concentrated on STAGE-tips with two C18 filters and eluted two times with 10 µl 40% acetonitrile in 0.5% acetic acid prior to online nanoflow liquid chromatography-tandem mass spectrometry (nano LC-MS/MS). All the experiments were performed on an EASY-nLC system (Proxeon, Odense, Denmark) connected to the LTQ-Orbitrap Velos or to the Q-Exactive (both from Thermo Fisher Scientific, Germany) through a nano-electrospray ion source. Peptides were separated in a 15 cm analytical column in-house packed with either 1,9 or 3 µm C18 beads (Reprosil-AQ, Pur, Dr. Manish, Ammerbuch-Entringen, Germany) with a 80 minutes gradient from 8% to 75% acetonitrile in 0.5% acetic acid at a flow rate of 250 nL/minute. The mass spectrometers were operated in data-dependent acquisition mode with a top 10 method. For Q-Exactive measurements, full-scan MS spectra were acquired at a target value of 1×10^6 and a resolution of 70,000, and the Higher-Collisional Dissociation (HCD) tandem mass spectra (MS/MS) were recorded at a target value of 1×10^6 and with a resolution of 35,000 with a normalized collision energy of 25%. For LTQ-Orbitrap Velos measurements, full-scan MS spectra were acquired at a target value of 1×10^6 and a resolution of 30,000, and the Higher-Collisional Dissociation (HCD) tandem mass spectra (MS/MS) were recorded at a target value of 5×10^4 and with a resolution of 7,500 with a normalized collision energy of 35%.

Peptide and protein identification

Raw mass spectrometric (MS) files were processed with the MaxQuant software suite (version 1.4.0.3, Max Planck Institute of Biochemistry, Department of Proteomics and Signal Transduction, Munich, Germany) by which the precursor MS signal intensities were determined and SILAC triplets were automatically quantified. HCD-MS/MS spectra were deisotoped and filtered such that only the 10 most abundant fragments for each 100 mass/charge ratio (m/z) range were retained (Cox et al., 2011). Proteins were identified by searching the HCD-MS/MS peak lists against a target/decoy version of the complete human Uniprot database supplemented with commonly observed contaminants such as porcine trypsin and bovine serum proteins. Tandem mass spectra were matched with an initial mass tolerance of 4.5 ppm on precursor masses and 20 ppm for fragment ions. Cysteine carbamidomethylation was searched as a fixed modification. Protein N-acetylation, N-pyroglutamine, oxidized methionine and SUMOylation (QQTGG) with monoisotopic mass of 471.20776 Da and pyroSUMOylation (pyroQQTGG) with monoisotopic mass of 454.18121 Da on lysine residues as variable modifications for the experiment. QQTGG and pyroQQTGG modified lysines were required to be located internally in the peptide sequence. Site localization probabilities were determined by MaxQuant using the PTM scoring algorithm (Cox and Mann, 2008; Olsen et al., 2006). The data set was filtered by posterior error probability to achieve a false discovery rate (FDR) below 1%. Only peptides with Andromeda score > 25 (unmodified and modified) were included in the total peptide list. Protein/peptides were considered as SUMOylated if they had a SILAC ratio > 2 between the Flag-SUMO-2 cell line and the parental control cells.

Bioinformatics analysis

Protein interaction network analysis was performed using interaction data from the STRING database version 9.05 (Szklarczyk et al., 2011). Only interactions with a STRING score above 0.4 are represented in the networks. Cytoscape (version 3.0.1) was used for visualization of protein interaction networks (Smoot et al., 2011). Clusters in that network were identified with MCODE (version 1.4.0 beta2) with MCODE score >6. MCODE is a Cytoscape plugin that finds clusters (highly interconnected regions) in a network. Clusters mean different things in different types of networks. For instance, clusters in a protein-protein interaction network are often protein complexes and parts of pathways, while clusters in a protein similarity network represent protein families (Bader and Hogue, 2003). Proteins in MCODE clusters were color-coded according to their cell-cycle peak-time using the cell-cycle color-scheme method previously described (Jensen et al., 2006). Significantly enriched Gene Ontology annotation terms were determined using Fisher's exact test from InnateDB (Lynn et al., 2008). P values were corrected for multiple hypotheses testing using the Benjamini and Hochberg FDR.

Purification of His-SUMO and His-Ubiquitin conjugates

U2OS cells expressing His-SUMO-2 or His-Ubiquitin were washed and collected in ice-cold PBS. Small aliquots of cells were lysed in 1x LDS for input samples. Guanidinium lysis buffer (6M guanidinium-HCl, 0.1 M $\text{Na}_2\text{HPO}_4/\text{NaH}_2\text{PO}_4$, 0.01 M Tris/HCl, pH 8.0 and competing imidazole) was added to the cell pellet to lyse the cells, after which the lysates were sonicated to reduce the viscosity. These lysates were used to determine the protein concentration using the BCA Protein Assay Reagent (Thermo Scientific); lysates

Chapter 5

were equalized and His-SUMO-2 or His-Ubiquitin conjugates were enriched on nickel-nitrilotriacetic acid-agarose beads (Qiagen) after which the beads were washed using wash buffers A to D. Wash buffer A: 6 M guanidinium-HCl, 0.1 M Na₂HPO₄/NaH₂PO₄, 0.01 M Tris/HCl, pH 8.0, 10 mM β-mercaptoethanol, 0.3% Triton X-100. Wash buffer B: 8 M urea, 0.1 M Na₂HPO₄/NaH₂PO₄, 0.01 M Tris/HCl, pH 8.0, 10 mM β-mercaptoethanol, 0.3% Triton X-100. Wash buffer C: 8 M urea, 0.1 M Na₂HPO₄/NaH₂PO₄, 0.01 M Tris/HCl, pH 6.3, 10 mM β-mercaptoethanol, 0.3% Triton X-100. Wash buffer D: 8 M urea, 0.1 M Na₂HPO₄/NaH₂PO₄, 0.01 M Tris/HCl, pH 6.3, 10 mM β-mercaptoethanol, 0.1% Triton X-100. Samples were eluted in 7 M urea, 0.1 M Na₂HPO₄/NaH₂PO₄, 0.01 M Tris/HCl, pH 7.0, 500 mM imidazole.

Luciferase assays

U2OS cells were grown on 24-well tissue culture plates and cotransfected with 100 ng of the luciferase reporter construct, 100 ng of the LacZ reporter construct and 300 ng expression plasmid as indicated. 48 hours after transfection, cells were washed with ice-cold PBS and lysed in 100 μl of Reporter Lysis Buffer (Promega) for luciferase activity measurement or in TNTBS (2% SDS, 1% NP-40, 150 mM NaCl, 50 mM Tris pH 7.5) for immunoblotting. Experiments were carried out in quadruplicate and all values were corrected for β-gal activity.

RNA isolation, RT-PCR and quantitative PCR

Total RNA was purified from 6 cm dishes using the SV total RNA isolation system (Promega) according to the manufacturer's protocol. Total RNA was amplified and converted into double-stranded cDNA by reverse transcription using ImProm-II Reverse Transcriptase (Promega) and Random Hexamers (Invitrogen). Real-time quantitative PCR was performed using a CFX384 Touch Real-Time PCR detection system (Bio-Rad) in which PCR reactions were performed in a 10 μl volume containing cDNA, FastStart Universal SYBR Green Master mix (Roche) and specific primers. The PCR was carried out with an initial denaturation at 95°C for 3 minutes, followed by 40 cycles of 95°C for 20 seconds, 55°C annealing for 20 seconds and 60°C elongation for 30 seconds. The following sense (S) and antisense (AS) primer sequences were used: *Aurora kinase B*, S 5'-ATTGCTGACTTCGGCTGGT-3', AS 5'-GTCCAGGGTGCCACACAT-3', *Cyclin-B1*, S 5'-TTTCGCCTGAGCCTATTTT-3', AS 5'-GCACATCCAGATGTTTCCATT-3', *CENP-F*, S 5'-GAGTCCTCAAACCAACAGC-3', AS 5'-TCCGCTGAGCAACTTTGAC-3', *SAP30*, S 5'-CGAGCTGGATAAGAGCGCAA-3', AS 5'-TGGTCTGGTTGGTAGCTTGA-3', *CAPNS1*, S 5'-ATGGTTTTGGCATTGACACATG-3', AS 5'-GCTTGCCTGTGGTGTGCGC-3'. Data were analyzed with the Bio-Rad CFX3 Manager software, average expression levels of triplicates were normalized for *CAPNS1* expression levels.

Recombinant proteins

His-FoxM1 recombinant proteins were purified essentially as described previously (Schimmel et al., 2010). Briefly, BL21 cells were cotransformed with a His-FoxM1 expression construct and the SUMO-2 expression vector pE1E2S2 or SUMO-1 expression vector pE1E2S1. Cells were grown to an OD₆₀₀ of 0.6. Cells were then grown overnight at 24°C in the presence of 0.1 mM isopropyl-β-D-thiogalactopyranoside (IPTG), 20 mM Hepes pH 7.5, 1 mM MgCl₂ and 0.05% Glucose. Lysates were prepared and SUMOylated

His-FoxM1 proteins were affinity-purified on Talon beads (BD Biosciences). 32 µg of SUMOylated His-FoxM1 protein was incubated with 0.7 µg of SENP2cd (BostonBiochem) at room temperature for 1 hour to remove the SUMO-2 moieties. GST tagged N-terminal FoxM1 was produced in *E. coli* and purified as described previously (Tatham et al., 2001).

***In vitro* interaction assay**

GST-Nterm-FoxM1 protein fragments bound to Glutathione Sepharose (GE Healthcare) or beads only were incubated with 5 µg of His-FoxM1 proteins for 1 hour at 4°C in NETN buffer (150 mM NaCl, 1 mM EDTA, 20 mM Tris pH 8.0, 0.5% NP-40). After incubation, beads were washed 5 times in NETN buffer. Beads were eluted in NETN buffer in the presence of 20 mM Glutathione (Sigma) at room temperature. The bound and unbound proteins were analyzed by immunoblotting.

Microscopy

Cells were grown on microscopy coverslips and fixed with 3.7% formaldehyde in PBS for 15 minutes at room temperature. Afterwards, cells were permeabilized with 1% Triton X-100 in PBS for 15 minutes and washed twice with PBS and once with PBS plus 0.05% Tween (PBS-T). Slides were blocked with 0.5% blocking reagent (Roche) in 0.1 M Tris, pH7.5 and 0.15 M NaCl for 10 minutes and the primary antibody was added for one hour. Coverslips were washed five times with PBS-T and incubated with the secondary antibody for one hour. Again, the coverslips were washed five times with PBS-T and dehydrated washing once with 70%, once with 90% and once with 100% ethanol. After drying the cells, the coverslips were mounted onto a microscopy slide using citifluor/DAPI solution (500 ng/ml) and samples were analyzed using a LEICA CTR6500 microscope.

Statistical Analysis

All the experiments have been performed at least in triplicate. Results shown are mean ± s.d and the p-value was calculated by Student's two tailed *t*-test.

Supplementary References

1. Tatham, M. H., Jaffray, E., Vaughan, O. A., Desterro, J. M., Botting, C. H., Naismith, J. H., and Hay, R. T. (2001) Polymeric chains of SUMO-2 and SUMO-3 are conjugated to protein substrates by SAE1/SAE2 and Ubc9. *J. Biol. Chem.* 276, 35368-35374
2. Vellinga, J., Uil, T. G., de, V. J., Rabelink, M. J., Lindholm, L., and Hoeben, R. C. (2006) A system for efficient generation of adenovirus protein IX-producing helper cell lines. *J. Gene Med.* 8, 147-154
3. Laoukili, J., Kooistra, M. R., Bras, A., Kauw, J., Kerkhoven, R. M., Morrison, A., Clevers, H., and Medema, R. H. (2005) FoxM1 is required for execution of the mitotic programme and chromosome stability. *Nat. Cell Biol.* 7, 126-136
4. Laoukili, J., Alvarez, M., Meijer, L. A., Stahl, M., Mohammed, S., Kleij, L., Heck, A. J., and Medema, R. H. (2008) Activation of FoxM1 during G2 requires cyclin A/Cdk-dependent relief of autorepression by the FoxM1 N-terminal domain. *Mol. Cell Biol.* 28, 3076-3087
5. Uchimura, Y., Nakamura, M., Sugawara, K., Nakao, M., and Saitoh, H. (2004) Overproduction of eukaryotic SUMO-1- and SUMO-2-conjugated proteins in *Escherichia coli*. *Anal. Biochem.* 331, 204-206
6. Vertegaal, A. C., Ogg, S. C., Jaffray, E., Rodriguez, M. S., Hay, R. T., Andersen, J. S., Mann, M., and Lamond, A. I. (2004) A proteomic study of SUMO-2 target proteins. *J. Biol. Chem.* 279, 33791-33798

7. Lundby, A., and Olsen, J. V. (2011) GeLCMS for in-depth protein characterization and advanced analysis of proteomes. *Methods Mol. Biol.* 753, 143-155
8. Cox, J., Neuhauser, N., Michalski, A., Scheltema, R. A., Olsen, J. V., and Mann, M. (2011) Andromeda: a peptide search engine integrated into the MaxQuant environment. *J. Proteome. Res.* 10, 1794-1805
9. Cox, J., and Mann, M. (2008) MaxQuant enables high peptide identification rates, individualized p.p.b.-range mass accuracies and proteome-wide protein quantification. *Nat. Biotechnol.* 26, 1367-1372
10. Olsen, J. V., Blagoev, B., Gnad, F., Macek, B., Kumar, C., Mortensen, P., and Mann, M. (2006) Global, in vivo, and site-specific phosphorylation dynamics in signaling networks. *Cell* 127, 635-648
11. Szklarczyk, D., Franceschini, A., Kuhn, M., Simonovic, M., Roth, A., Minguéz, P., Doerks, T., Stark, M., Müller, J., Bork, P., Jensen, L. J., and von, M. C. (2011) The STRING database in 2011: functional interaction networks of proteins, globally integrated and scored. *Nucleic Acids Res.* 39, D561-D568
12. Smoot, M. E., Ono, K., Ruscheinski, J., Wang, P. L., and Ideker, T. (2011) Cytoscape 2.8: new features for data integration and network visualization. *Bioinformatics.* 27, 431-432
13. Bader, G. D., and Hogue, C. W. (2003) An automated method for finding molecular complexes in large protein interaction networks. *BMC. Bioinformatics.* 4, 2
14. Jensen, L. J., Jensen, T. S., de, L. U., Brunak, S., and Bork, P. (2006) Co-evolution of transcriptional and post-translational cell-cycle regulation. *Nature* 443, 594-597
15. Lynn, D. J., Winsor, G. L., Chan, C., Richard, N., Laird, M. R., Barsky, A., Gardy, J. L., Roche, F. M., Chan, T. H., Shah, N., Lo, R., Naseer, M., Que, J., Yau, M., Acab, M., Tulpan, D., Whiteside, M. D., Chikatamarla, A., Mah, B., Munzner, T., Hokamp, K., Hancock, R. E., and Brinkman, F. S. (2008) InnateDB: facilitating systems-level analyses of the mammalian innate immune response. *Mol. Syst. Biol.* 4, 218
16. Schimmel, J., Balog, C. I., Deelder, A. M., Drijfhout, J. W., Hensbergen, P. J., and Vertegaal, A. C. (2010) Positively charged amino acids flanking a sumoylation consensus tetramer on the 110kDa tri-snRNP component SART1 enhance sumoylation efficiency. *J. Proteomics* 73, 1523-1534



The Cockayne Syndrome-B protein is SUMOylated upon UV induced DNA damage

Joost Schimmel, Mischa Vrouwe, Alex Pines,
Matty Verlaan – de Vries, Jesper V. Olsen, Leon H.F.
Mullenders, Alfred C.O. Vertegaal

Chapter 6. The Cockayne Syndrome-B protein is SUMOylated upon UV induced DNA damage

Abstract

Post translational modification of proteins by ubiquitin and Small Ubiquitin-Like Modifiers plays an essential role in various pathways of the DNA damage response. To get more insight in the involvement of SUMOylation in two of these pathways, we used a proteomics approach to identify regulated SUMO2 targets upon treatment with ultraviolet light (UV) or ionizing radiation (IR). The Cockayne Syndrome-B (CSB) protein was found to be SUMOylated specifically after UV induced DNA damage. CSB plays a key role during transcription coupled nucleotide excision repair (TC-NER) by recruiting a cluster of proteins essential for DNA repair. We found that CSB is SUMOylated on lysine 32 and lysine 205, this process is however not essential for cell survival after UV irradiation. Studying the dynamics of CSB SUMOylation revealed that this is an early response upon DNA damage. The recruitment of the Cockayne Syndrome-A (CSA) ubiquitin E3 ligase complex initiates the removal of SUMOylated CSB at a later stage in the DNA damage response. This can potentially be explained by the ubiquitination of the RNA polymerase II complex by CSA which leads to the dissociation of CSB from chromatin and subsequently to the loss of SUMOylation.

Introduction

The genetic code of cells is continuously under threat from exogenous and endogenous DNA-damaging agents such as ionizing radiation (IR), ultraviolet radiation (UV) and reactive oxygen species. To guarantee genomic stability, cells are equipped with a set of repair pathways that recognize and repair different kinds of DNA lesions. Deregulation of these DNA damage responses (DDRs) results in genomic instability which in turn often leads to the development of cancer, neurodegenerative diseases and many other syndromes (1, 2). During DDRs, DNA lesions are recognized by proteins, which induces a cascade of recruitment and activation of proteins that facilitate DNA repair.

Proteins involved in DNA repair are regulated upon DNA damage by posttranslational modifications such as ubiquitination and SUMOylation (3). Ubiquitin and Small Ubiquitin-like Modifiers (SUMOs) are covalently attached via an enzymatic cascade to lysines in target proteins to regulate the function of these proteins. Ubiquitin and SUMO specific proteases can reverse those modifications by catalytic cleavage, providing the cell with a highly dynamic and controllable system to react on different stimuli.

Since its discovery in the mid-1990s (4), SUMOylation has emerged as a regulator of many, mainly nuclear, cellular processes (5, 6). SUMOylation is regulating proteins in many ways; it can change the subcellular localization of proteins, induce complex formation and regulate the activity of enzymes. Furthermore, SUMOylation can have both positive and negative effects on protein stability, by either blocking ubiquitination of lysines or by targeting proteins for proteasomal degradation via the recruitment of SUMO targeted ubiquitin ligases (STUBLs) respectively (7, 8).

The first link between SUMOylation and DNA repair was revealed in studies on Base Excision Repair (BER), where SUMOylation induces a conformational change in the Thymine-DNA glycosylase protein and thereby stimulates the repair process (9, 10). Furthermore it has been shown that two SUMO specific E3 ligases, PIAS1 and PIAS4, accumulate at sites of double strand breaks (DSBs). At DSBs, these E3 ligases SUMOylate BRCA1 to induce its activity and SUMOylation is required for the accumulation of repair proteins to facilitate repair of DSBs (11).

SUMO and ubiquitin also act together during the DDR, best exemplified by the modification of the homotrimeric, ring shaped protein Proliferating Cell Nuclear Antigen (PCNA). PCNA encircles DNA where it acts as a processing factor for DNA polymerases and as an interaction platform for proteins involved in DNA metabolism. Monoubiquitination of PCNA on lysine 164 upon DNA damage induces the recruitment of polymerases needed for translesion synthesis, whereas SUMOylation on the same lysine inhibits recombination during DNA synthesis by recruiting the anti-recombinogenic helicase Srs2 (12, 13). The role of SUMO and ubiquitin crosstalk in DNA repair was further emphasized by the observation that the SUMO-dependent recruitment of RNF4, a well-studied STUBL, to DSBs induces an ubiquitination signal that is essential for efficient repair of DSBs (14, 15).

Here we have identified the Cockayne Syndrome-B (CSB) protein as a novel SUMO2 target protein. Cockayne syndrome is a severe autosomal-recessive disease caused by mutations in either the CSB or CSA gene. Patients suffer from UV sensitivity, premature aging and neurodevelopmental abnormalities; these phenotypes are partly explained by a defect in transcription-coupled nucleotide excision repair (TC-NER) (16). The CSB protein plays a key role in TC-NER. A DNA lesion in the actively transcribed strand of a gene causes the stalling of the elongating RNA polymerase machinery. This stalling induces the strong interaction between RNA polymerase II (RNAPII) and CSB; subsequently CSB initiates the recruitment of NER specific proteins that facilitate the proper repair of the DNA lesion (17). Using a SILAC based proteomic approach we found that CSB is specifically SUMOylated upon DNA damage induced by UV irradiation. We show that SUMOylation of CSB on two lysines is an early response to DNA damage and that the recruitment of the Cockayne-Syndrome-A (CSA) ubiquitin E3 ligase complex results in the destabilization of SUMOylated CSB.

Chapter 6

Results

A quantitative proteomics approach to study SUMOylation dynamics in response to UV and IR treatment

It has been well established that SUMOylation of proteins plays an important role in the DNA Damage Responses (DDR) in cells (3). We were interested to analyze the global changes in SUMOylation in two different sub pathways of this response. We choose to use Ultraviolet C (UV-C) irradiation which is known to induce thymine dimers and 6,4-photoproducts. These types of DNA damage are repaired by Nucleotide Excision Repair (NER). For the second type of DNA damage we used Ionizing Radiation (IR). IR mainly results in double strand breaks in DNA, which are repaired by either Non Homologous End Joining (NHEJ) or Homologous Recombination (HR) (18).

To be able to quantify changes in SUMOylation patterns after these types of DNA damage we used a SILAC (Stable Isotope Labeling by Amino acids in Culture) approach to label three different populations of U2OS cells expressing Flag-SUMO2 with three distinct sets of isotopic variants of lysine and arginine (Figure 1A). These cells were either treated with 4 gray (GY) (IR, Heavy labeled), 20 J/m² UV (Medium labeled) or left untreated (Light labeled). Cells were allowed to grow for an additional hour after the induction of DNA damage, subsequently cells were lysed and mixed before enrichment of SUMOylated proteins by a Flag-SUMO2 immunoprecipitation (IP) (Figure 1B). In addition we performed a duplicate with swapped SILAC labels to correct for experimental errors and false positive hits. Eluted fractions of the Flag-IPs were separated by SDS-PAGE, stained with Coomassie, cut in ten gel slices and in-gel digested with trypsin. These tryptic digests were analyzed by nano-scale reversed phase liquid chromatography combined with high-resolution mass spectrometry.

A summary of the results can be found in Figure 1C. Western blot analysis confirmed the UV specific increase in SUMOylation of CSB and XPC, while SUMOylation of Senataxin and MDC1 was increased after both UV and IR treatment. SUMOylation of RanGap1 and SART1 was not affected by the two types of DNA damage (Figure 1D). Total SUMO levels in the same experiment were analyzed by an anti-SUMO-2/3 Western (Figure 1E). CSB and XPC seem to be very efficient SUMO target proteins after UV treatment since the modified forms are already visible on Westerns for total lysates. Visualizing SUMOylated forms of a protein without any pre-enrichment of SUMOs is quite rare due to the low stoichiometry of SUMO modification on proteins (19).

The Cockayne Syndrome-B protein is extensively SUMOylated on lysine 32 and lysine 205 after UV treatment

Because of its emerging role in TC-NER, we decided to further analyze the SUMOylation on CSB upon UV induced DNA damage. CSB has an acidic domain, several ATPase motifs clustered in the middle of the protein (20) and a C-terminal

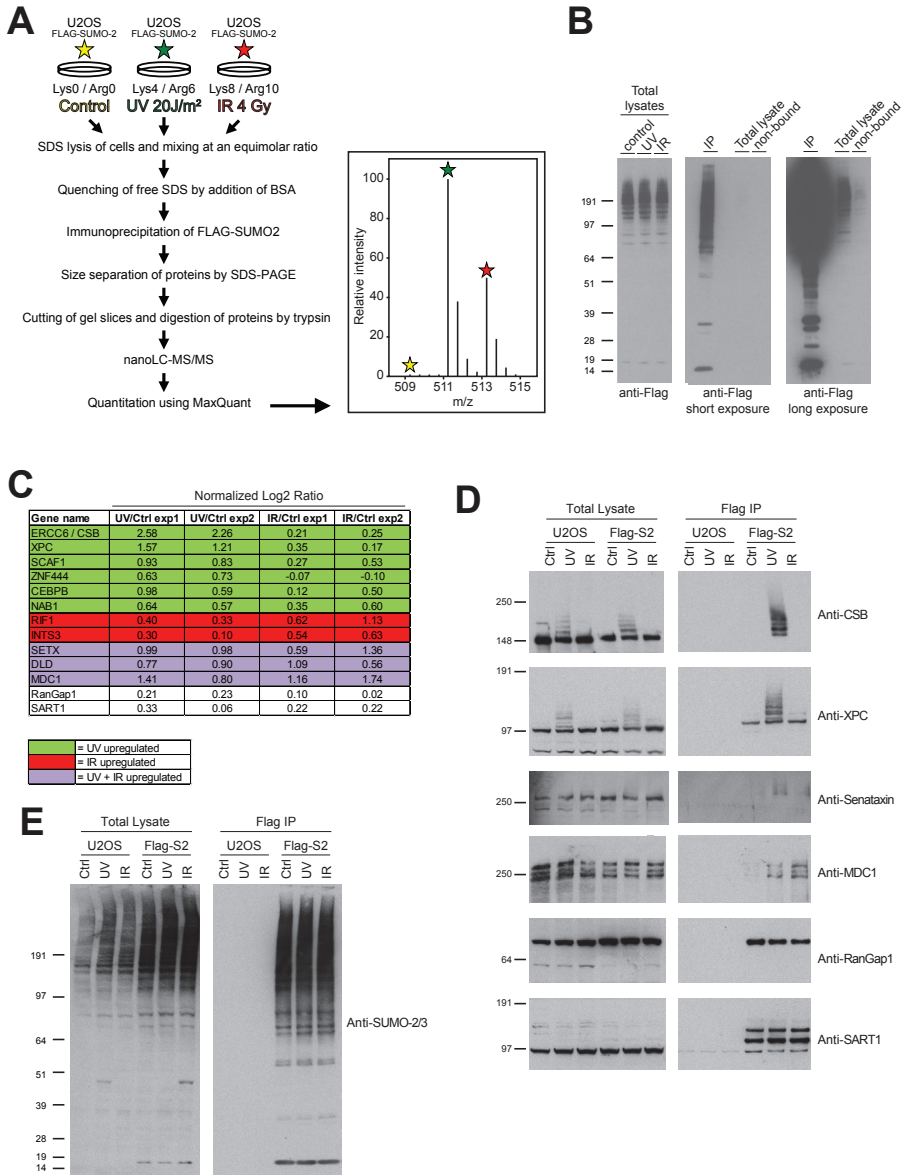


Figure 1. SUMOylation dynamics in response to UV and IR treatment A) Strategy to identify SUMO-2 conjugates in response to UV and IR using a quantitative proteomic approach. U2OS cells stably expressing Flag-SUMO-2 were SILAC-labeled with three different isotopic variants of lysine and arginine and treated as indicated. For the Flag-IP, equal amounts of the three different lysates were mixed and SUMO2 conjugates were enriched using a Flag IP. B) Total cell lysates of the three cell populations Flag-SUMO2 conjugates were analyzed by immunoblotting using anti-Flag antibody. C) Table summarizing the results from the mass spectrometry analysis. The normalized log₂ ratio is shown for 13 targets, experiment 1 (exp1) and experiment (exp2) refers to the label swap. D) U2OS cells or U2OS cells stably expressing Flag-SUMO2 were treated as in (A) and Flag-SUMO2 conjugates were purified via IP. Total lysates and Flag-SUMO-2 (Flag-IP) purified fractions were analyzed by immunoblotting with antibodies as indicated. E) Total levels of SUMO-2 in the experiment described in (D) were analyzed immunoblotting using anti SUMO-2/3 antibody.

Chapter 6

ubiquitin binding domain (UBD) (21). Analysis of the amino acid sequence revealed that five lysines of CSB are situated in the SUMOylation consensus motif Ψ KxE (Lysines 32, 205, 481, 1359 and 1489) (Figure 2A).

To analyze whether these lysines are used for SUMOylation lysine to arginine mutations were made for all five consensus sites (5KR). U2OS or U2OS Flag-SUMO2 cells stably expressing GFP tagged wild type (WT) or 5KR CSB were generated and SUMOylation of these proteins in untreated or UV treated (20 J/m²) cells were analyzed. Flag-SUMO2 enrichment confirmed the UV dependent SUMOylation of WT-CSB, and similar to endogenous CSB we could detect the modified CSB bands also on total lysate samples. SUMOylation of CSB is completely abolished in the 5KR mutant, thus CSB is indeed SUMOylated on the SUMO consensus sites (Figure 2B).

Next we wanted to know whether all five consensus sites are used for SUMOylation. To analyze this we made a lysine 1489 (1KR), a lysine 1489, 1359 (2KR), a lysine 1489, 1359, 481 (3KR) and a lysine 1489, 1359, 481, 205 (4KR) mutant and compared SUMOylation levels of these different proteins. Interestingly, no reduction in SUMOylation was observed in the first three mutants, suggesting that SUMOylation mainly takes place on the two N-terminal SUMO consensus sites. Indeed adding lysine 205 to the 3KR mutant decreased SUMOylation of CSB (Figure 1C) and mutating only lysine 32 and 205 (2KR) seem to be sufficient to abolish SUMOylation (Figure 1D). Western blots for SUMO-2/3 or XPC were included to confirm efficient and equal purification of SUMOylated proteins in all Flag-SUMO2 IPs.

Previously, it has been shown that CSB accumulates at local UV-damaged subnuclear areas (22). We analyzed and compared the subcellular localization of WT and the SUMO deficient 5KR CSB proteins in U2OS cells stably expressing GFP tagged CSB proteins. Local UV lesions were induced by using a porous UV-blocking membrane (23). 1 hour after UV irradiation cells were fixed and analyzed for GFP expression. Cells were stained with a XPC antibody to visualize the damaged areas in the nucleus. Both wild type and the SUMO deficient CSB proteins accumulated at the locally damaged areas in the cell together with XPC (Figure 2E). Thus, SUMOylation of CSB does not affect the localization of the protein at sites of DNA damage.

SUMOylation of CSB is not essential for cell survival after UV

To study the functional relevance of SUMOylation of CSB upon DNA damage we made use of a CSB-deficient cell line derived from a Cockayne syndrome patient (CS1AN) (24). These cells are hypersensitive to UV irradiation (25, 26) and fail to recover RNA synthesis after UV irradiation (27, 28).

CS1ANsv cells were infected with lentiviruses expressing either WT- or 5KR-

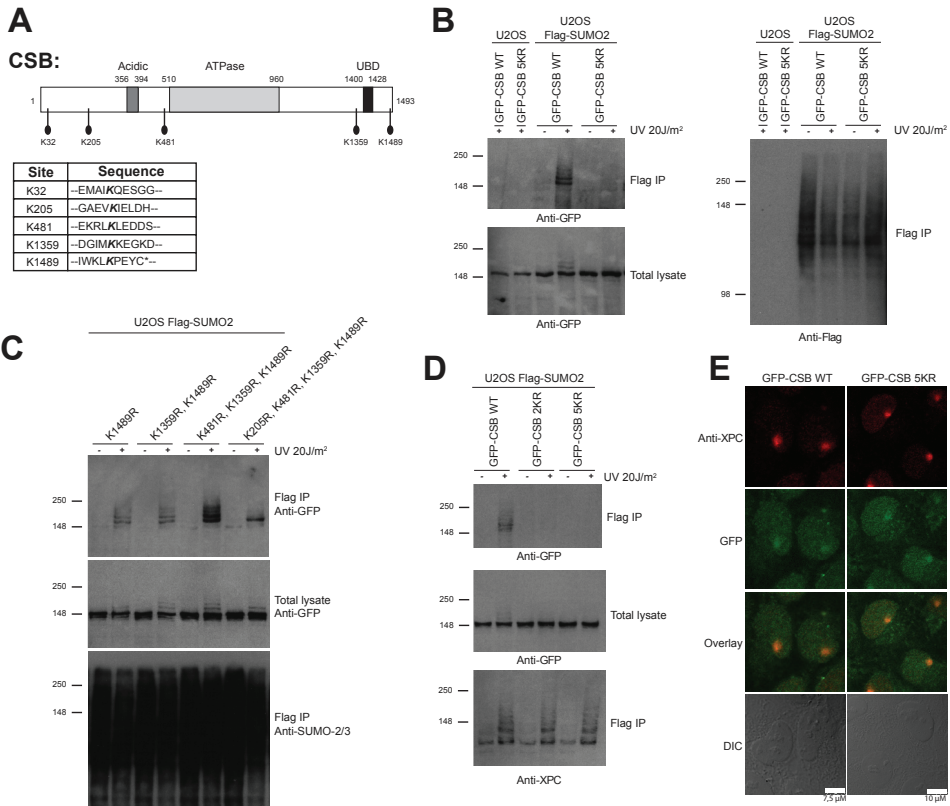


Figure 2. CSB is SUMOylated on lysine 32 and lysine 205 after UV treatment A) Cartoon depicting Cockayne Syndrome-B (CSB). CSB is composed of 1493 amino acids and harbors an acidic region, multiple ATPase motifs and an Ubiquitin binding domain (UBD). CSB contains 5 SUMOylation consensus sites. B) U2OS cells and U2OS cells stably expressing Flag-SUMO-2 were infected with retroviruses encoding either GFP-CSB wild type (WT) or GFP-CSB lacking the SUMOylation consensus sites (5KR). Cells were either treated with 20 J/m² of UV or left untreated and cultured for an additional hour. Cells were lysed and SUMO2 conjugates were enriched by Flag IP. Total lysates and Flag purified fractions were analyzed by immunoblotting using anti-GFP antibody (left panel) or anti-Flag antibody (right panel, Flag-IP only). C) The experiment described in (B) was repeated with GFP-CSB mutants as indicated. Total lysates and Flag purified fractions were analyzed by immunoblotting using anti-GFP antibody or anti-XPC antibody. D) The experiment described in (B) was repeated with GFP-CSB WT, a GFP-CSB mutant lacking lysine 32 and lysine 205 (2KR) and GFP-CSB 5KR. E) U2OS cells expressing either GFP-CSB WT or GFP-CSB 5KR were locally irradiated with 100 J/m² UV and allowed to recover for one hour. Cells were fixed and stained using anti-XPC antibody. GFP and XPC expression was analyzed by confocal fluorescent microscopy. Differential interference contrast (DIC) was used to visualize the nuclei.

CSB to generate stable cell lines. The relative UV sensitivity of WT-CSB and 5KR-CSB was determined by exposing the cells to different doses of UV and quantifying the clonal survival of these cells on day 14 after treatment. As published, CS1ANsv cells were very sensitive to UV irradiation, whereas normal human fibroblasts (VH10) showed significant resistance towards UV treatment. CS1ANsv cells expressing WT- or 5KR-CSB rescued the UV sensitivity of CS1ANsv cells to a similar extent (Figure 3A and 3B).

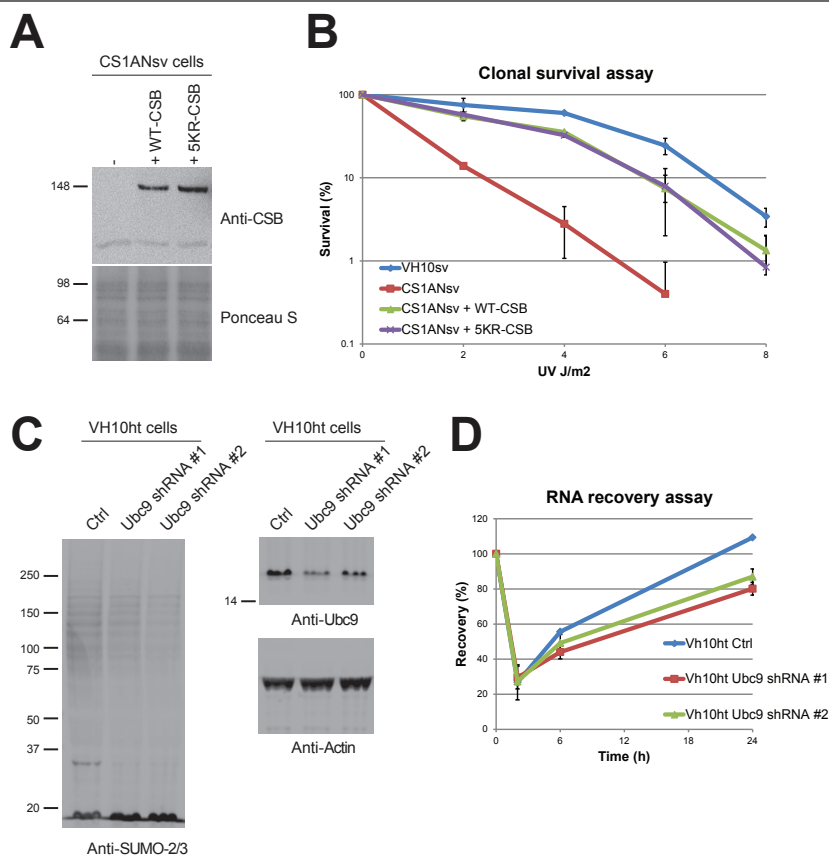


Figure 3. Clonal survival and RNA recovery assays (A) CS1ANsv cell lines stably expressing WT- or 5KR-CSB were generated, expression levels of CSB were analyzed by immunoblotting using anti-CSB antibody. (B) The CS1ANsv stable cell lines and VH10sv cells were treated with different doses of UV as indicated. 14 days after UV treatment, cell survival was analyzed by counting colonies. Cell survival of untreated cells (0 J/m²) was set at 100% for each cell type. The error bars indicate the SD from the average. (C) VH10ht cells were infected with lentiviruses expressing either a non-targeting control shRNA (Ctrl) or two individual Ubc9 shRNAs (Ubc9 shRNA #1 or #2). Total SUMO-2/3 and Ubc9 levels were analyzed by immunoblotting with anti-SUMO-2/3 and anti-Ubc9 antibodies respectively. Equal protein levels were analyzed by immuno-blotting with anti-Actin. (D) Two days after lentiviral infection, cells were treated with 10 J/m² UV. The RNA recovery was analyzed at 2, 6 and 24 hours after UV treatment. RNA synthesis in untreated cells was set at 100%; the error bars indicate the SD from the average.

Interestingly, knocking down the single known SUMO E2 enzyme Ubc9 with two independent shRNAs did significantly reduce RNA synthesis recovery after UV treatment in VH10 cells (Figure 3C and 3D). Preliminary results suggest that the transcriptional recovery is not affected in the SUMO deficient CSB cell line (data not shown); however this remains to be confirmed with additional experiments. Taken together, these results demonstrate that SUMOylation of CSB upon UV treatment is not essential for the cells to survive after DNA damage. However, global SUMOylation after DNA damage does seem to contribute to the efficient restart of transcription when the lesions are repaired.

CSB SUMOylation dynamics reveals a novel link between the two complementation groups in Cockayne Syndrome

Since SUMOylation is a highly dynamic and reversible process, we wanted to investigate the timing and stability of CSB SUMOylation upon UV treatment. To establish this, we have set up an Elisa assay to be able to quantify the amount of CSB SUMOylation at different time-points after UV treatment. Anti-Flag coated well plates were incubated with lysates from U2OS Flag-SUMO2 cells. After extensive washing, the plates were incubated with SUMO-2 or CSB antibodies. The binding of these antibodies was detected by incubating with a secondary antibody coupled to Biotin. Biotin binding was detected by incubating with Streptavidin coupled to HRP, which in turn was visualized and quantified by incubating with peroxidase.

To validate this assay, CSB and SUMO-2 detection was analyzed in untreated or UV treated (20 J/m^2) cell lysates prepared 1 hour after treatment. For CSB we observed an increase in signal after UV treatment, representing SUMOylated CSB, whereas the SUMO-2 signal is unchanged (Figure 4A). Next, U2OS Flag-SUMO2 cells were treated with 20 J/m^2 of UV and lysates were made at different time-points after treatment. The procedure described above was repeated and the CSB signal was quantified. We found that SUMOylation of CSB after induced DNA damage is an early event already visible after 15 minutes and peaking after 30 minutes. After 30 minutes CSB SUMOylation slowly disappears again to almost undetectable levels after 24 hours (Figure 4B).

Removal of SUMOylated proteins is regulated by SUMO specific proteases (29) or by the activity of STUBLs (8). Upon DNA damage, CSB recruits the Cockayne Syndrome-A (CSA) protein as part of a Cullin-like E3 ligase complex for ubiquitin (30). We were interested to see whether the recruitment of this CSA-E3 complex is involved in the processing of SUMOylated CSB. Therefore we used a CSA deficient cell line derived from a Cockayne Syndrome patient (CS3BEsv) (25, 31). CS3BEsv cells and its derivative expressing His tagged CSA were used to make cell lines expressing Flag-SUMO2. These cells were treated with 20 J/m^2 UV alone or in combination with proteasome inhibition by adding MG132 for 3 hours, subsequently SUMOylated proteins were enriched 1 hour after UV treatment using a Flag-IP. Efficient SUMOylation of CSB was observed in CS3BEsv cell, while complementing these cells with His-CSA strongly reduced the amount of SUMOylated CSB. This difference can be nullified by blocking proteasomal degradation with MG132 (Figure 4C), indicating that the activity of the CSA-E3 ligase complex is needed for the removal of SUMOylated CSB. Because CSB SUMOylation is increasing the first 30 minutes after UV (Figure 4B), we expected that CSA would not play a role in destabilizing SUMOylated CSB in this time frame. Indeed when we compared SUMOylation of CSB in cell lysates made at different time-points after UV treatment, an effect on the stability was observed in the complement cell line from 1 hour on (Figure 4D).

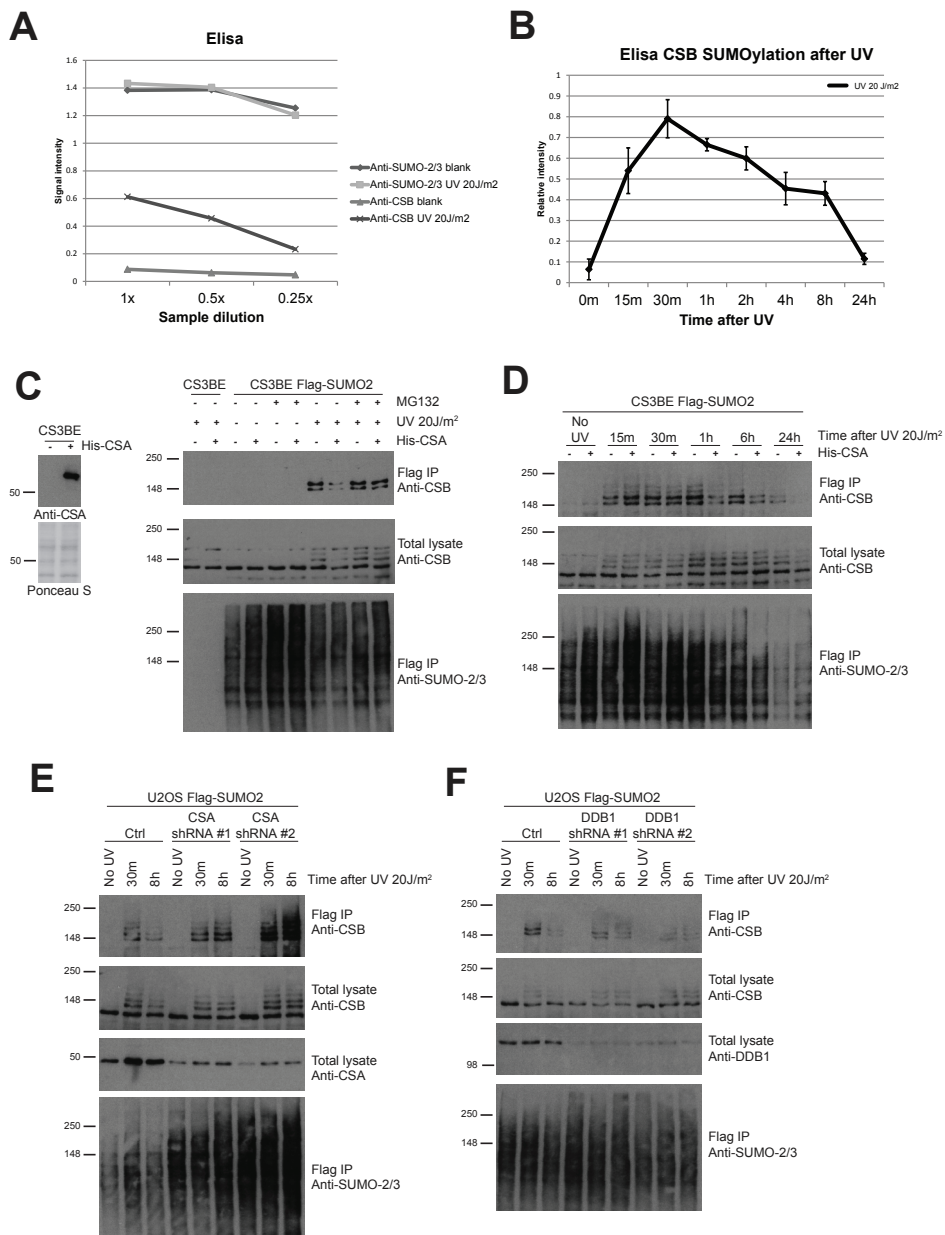


Figure 4. CSB SUMOylation dynamics after UV treatment A) Anti-Flag coated well plates were incubated with different diluted lysates of U2OS Flag-SUMO2 cells that recovered for one hour after irradiation with 20 J/m² or lysates of untreated U2OS Flag-SUMO2 cells (blank). Plates were then incubated with anti-SUMO-2/3 or anti-CSB antibody and the intensity of these signals was detected by Elisa. B) Anti-Flag coated well plates were incubated with lysates of U2OS Flag-SUMO2 cells that were allowed to recover for the indicated time-points after irradiation with 20 J/m² UV. Plates were then incubated with anti-CSB antibody to detect SUMOylated CSB; the intensity of this signal was detected by Elisa. The error bars indicate the SD from the average. C) The CSA deficient cell line CS3BE was complemented by stable expression of His-CSA. CSA expression was analyzed by immunoblotting with anti-CSA antibody (left panel). These cells were infected with lentiviruses encoding Flag-SUMO2. Cells were either treated with

20 J/m² of UV or left untreated and cultured for an additional hour. Another set of cells was treated in the same way in combination with MG132 treatment for 3 hours. Cells were lysed and SUMO2 conjugates were enriched by Flag IP. Total lysates and Flag purified fractions were analyzed by immunoblotting using anti-CSB antibody or anti-Flag antibody (Flag IP only). D) Cells described in (C) were allowed to recover for the indicated time-points after irradiation with 20 J/m² UV. Cells were lysed and SUMO2 conjugates were enriched by Flag IP. Total lysates and Flag purified fractions were analyzed by immunoblotting using anti-CSB antibody (left panel) or anti-Flag antibody (Flag IP only). E and F) U2OS cells stably expressing Flag-SUMO2 were infected with lentiviruses expressing a non-targeting control shRNA (Ctrl), two independent shRNAs against CSA (E) or two independent shRNAs against DDB1 (F). Untreated cells or cells that were allowed to recover for 30 minutes or 8 hours after irradiation with 20 J/m² UV were lysed and SUMO2 conjugates were enriched by Flag IP. Total lysates and Flag purified fractions were analyzed by immunoblotting using anti-CSB antibody (left panel) or anti-Flag antibody (Flag IP only). Knockdown of CSA and DDB1 was confirmed by immunoblotting using anti-CSA antibody (E) and anti-DDB1 antibody (F) on total lysates.

Strikingly, while we still observed CSB SUMOylation after 24 hours in the CS3BEsv cell line, SUMOylation completely disappeared in the His-CSA complement cell line. The role of the CSA-E3 ligase complex in CSB SUMOylation stability was further confirmed by knock-down studies on CSA and DDB1. DDB1 is an adapter protein for Cullin-like ligases and directly interacts with CSA (32). Expression of both proteins was knocked-down by two independent shRNAs in U2OS Flag-SUMO2 cells. Cells were left untreated or were treated with UV and harvested after either 30 minutes or 8 hours, SUMOylation of CSB in cells with CSA or DDB1 knockdown was compared to cells treated with a non-targeting control shRNA (Ctrl). While the SUMOylation of CSB was strongly reduced after 8 hours in the Ctrl treated cells, we observed a stabilizing effect on CSB SUMOylation with both CSA knockdown (Figure 4E) and DDB1 knockdown (Figure 4F). Interestingly, knocking down CSA seems to have an overall effect on total SUMOylation levels in this experiment (Figure 4E). This data shows that the recruitment of the CSA-E3 ligase complex after DNA damage regulates the stability of SUMOylated CSB.

CSA, a potential STUBL for SUMOylated CSB?

Because of its effect on SUMOylated CSB, we wondered whether the CSA-E3 ligase could act as a STUBL. One of the features of a STUBL is the strong affinity for SUMOylated proteins (33). As CSA is specifically recruited by CSB bound to chromatin (34), a cellular fractionation assay (35) was used to enrich for chromatin associated proteins. UV induced DNA damage results in the strong binding of CSB to RNAPII on chromatin and in the SUMOylation of CSB, therefore we hypothesized that CSB SUMOylation is exclusive for the chromatin bound fraction. Using the fractionation assay we indeed found that modified CSB bands are only observed after UV treatment in total lysates and the chromatin enriched fraction, but not in the cytosolic fraction and soluble nucleus in U2OS cells (Figure 5A).

The previously described CSB deficient cell line CS1AN and the WT-CSB or 5KR-CSB complement lines were used to analyze the CSA recruitment by CSB.

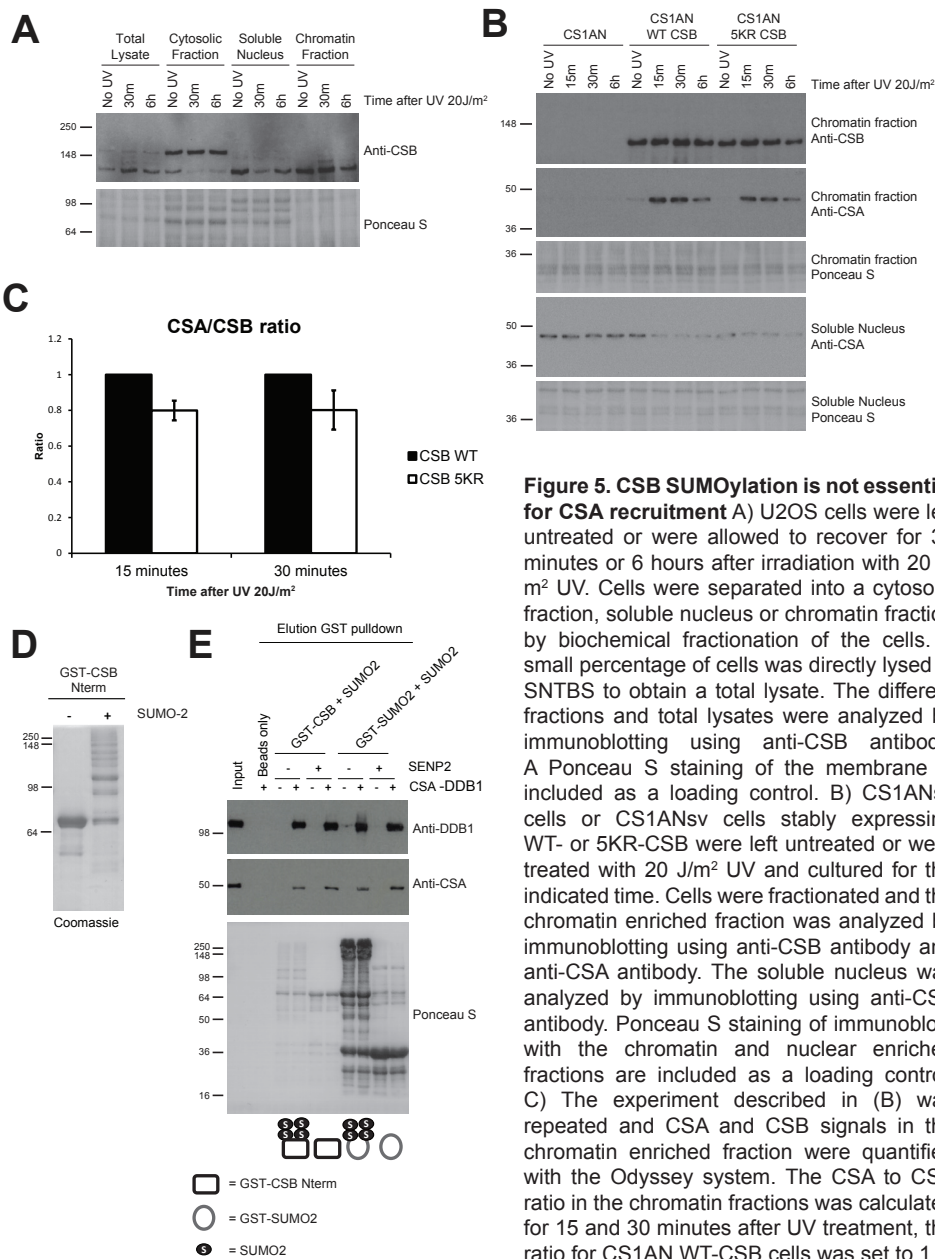


Figure 5. CSB SUMOylation is not essential for CSA recruitment A) U2OS cells were left untreated or were allowed to recover for 30 minutes or 6 hours after irradiation with 20 J/m² UV. Cells were separated into a cytosolic fraction, soluble nucleus or chromatin fraction by biochemical fractionation of the cells. A small percentage of cells was directly lysed in SNTBS to obtain a total lysate. The different fractions and total lysates were analyzed by immunoblotting using anti-CSB antibody. A Ponceau S staining of the membrane is included as a loading control. B) CS1ANsv cells or CS1ANsv cells stably expressing WT- or 5KR-CSB were left untreated or were treated with 20 J/m² UV and cultured for the indicated time. Cells were fractionated and the chromatin enriched fraction was analyzed by immunoblotting using anti-CSB antibody and anti-CSA antibody. The soluble nucleus was analyzed by immunoblotting using anti-CSA antibody. Ponceau S staining of immunoblots with the chromatin and nuclear enriched fractions are included as a loading control. C) The experiment described in (B) was repeated and CSA and CSB signals in the chromatin enriched fraction were quantified with the Odyssey system. The CSA to CSB ratio in the chromatin fractions was calculated for 15 and 30 minutes after UV treatment, the ratio for CS1AN WT-CSB cells was set to 1.0.

The error bars indicate the SD from the average. D) Recombinant GST tagged N-terminal CSB protein fragments (GST-CSB Nterm) were *in vitro* SUMOylated with SUMO2. SUMOylated and unmodified GST-CSB protein fragments were size-separated by SDS-PAGE and detected by Coomassie staining of the gel. E) Recombinant GST-CSB protein fragments and GST-SUMO2 proteins were SUMOylated *in vitro* and coupled to glutathione beads. SUMO2 conjugates were removed by incubating these proteins with recombinant SENP2. Glutathione beads only or beads bound to the described proteins were incubated with recombinant CSA-DDB1 protein complex. Input and elution of the GST pull-down were analyzed by immunoblotting using anti-DDB1 and anti-CSA antibodies. Ponceau S staining of the membrane is included to visualize the recombinant GST tagged proteins.

These cells were left untreated or were treated with 20 J/m² of UV and harvested at different time-points. Analysis of the chromatin fraction confirmed that CSA recruitment depends on CSB, no recruitment was observed in the CS1AN cell line; instead CSA remained in the soluble nucleus upon UV treatment. CSA is specifically recruited to the chromatin after UV treatment in both the WT-CSB and the 5KR-CSB cell line (Figure 5B). To quantify the CSA recruitment in WT-CSB and 5KR-CSB cell lines, this experiment was repeated and the CSA/CSB ratio was calculated for both experiments. Although CSA recruitment might be slightly reduced in the 5KR-CSB cells in chromatin fractions 15 minutes after UV treatment, the effects are quite modest and probably lose significance after 30 minutes (Figure 5C).

Furthermore, no difference in interaction between the CSA-DDB1 complex and unmodified or SUMOylated CSB proteins was observed *in vitro*. In this experiment GST tagged N-terminal CSB protein fragments were SUMOylated *in vitro* (Figure 5D) and SUMOs were removed by adding SENP2 to obtain unmodified N-terminal CSB fragments. These proteins were incubated with recombinant CSA-DDB1 complexes and subsequently purified using glutathione beads. Although the CSA-DDB1 complex strongly interacts with CSB, no difference was observed between SUMO modified and unmodified CSB (Figure 5E). Interestingly, we did observe a strong interaction between the CSA-DDB1 complex and both mono-SUMO2 as well as SUMO2 chains (Figure 5E). The GST-SUMO2 levels in this experiment were significantly higher than the GST-CSB levels. The interaction between the CSA-DDB1 complex and SUMO2 might thus be overestimated compared to the interaction with the N-terminal CSB protein fragments. We conclude that the CSA-E3 ligase complex does not act as a classical STUBL towards the binding of SUMOylated CSB.

To see whether the CSA-E3 ligase complex can ubiquitinate CSB, we repeated the experiment described in Figure 4C and replaced Flag-SUMO2 expression for Flag-Ubiquitin expression. Enrichment for ubiquitinated proteins with a Flag IP revealed that adding back His-CSA into CS3BE cells does induce CSB ubiquitination in untreated cells. However, ubiquitination of CSB was reduced after UV treatment and surprisingly even further reduced in combination with MG132 treatment (Figure 6). The destabilization of SUMOylated CSB can therefore not be explained by the ubiquitination and proteasomal degradation via the CSA-E3 ligase complex.

Identification of targets for CSA mediated ubiquitination

To identify other targets for CSA dependent ubiquitination, we set up another SILAC screen. For this experiment, the previously described CS3BE cell line and the complemented CS3BE cell line expressing CSA-Flag were used. A His-ubiquitin expression vector was introduced in these cell lines to enable the purification of ubiquitinated proteins. Four differently treated sets of medium and heavy labeled cells were mixed, His-Ubiquitin conjugates were purified and analyzed by mass

Chapter 6

spectrometry (Figure 7A). Interestingly, we found an increase in ubiquitination of RNAPII subunit RPB1 in the CSA-Flag cell line in two experiments. An increased heavy/medium (CS3BE + CSA-Flag / CS3BE) ratio was found for RPB1 in cells that were treated with UV and either allowed to recover for 1 hour or for 6 hours in combination with MG132 (Figure 7A). By using an antibody for the active RNAPII subunit RPB1 (anti-phospho-RPB1), we confirmed that ubiquitination of this protein is increased in the CSA-Flag complement cell line after UV induced DNA damage (Figure 7B). We conclude that RNAPII is a target for CSA-dependent ubiquitination and degradation upon UV induced DNA damage. Potentially, this could lead to the dissociation of CSB from chromatin, leading to deSUMOylation of CSB in the nucleus (Figure 8).

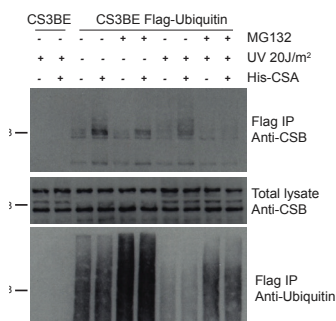


Figure 6. CSA dependent ubiquitination of CSB is reduced after UV treatment. CS3BE cells or CS3BE cells stably expressing His-CSA were infected with lentiviruses encoding Flag-ubiquitin. Cells were either treated with 20 J/m² of UV or left untreated and cultured for an additional hour, another set of cells was treated in the same way in combination with MG132 treatment for 3 hours. Cells were lysed and ubiquitin conjugates were enriched by Flag IP. Total lysates and Flag purified fractions were analyzed by immunoblotting using anti-CSB antibody or anti-Flag antibody (Flag IP only).

6

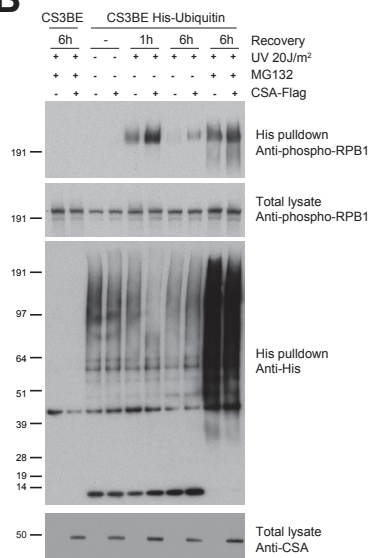
A

Experiment	Medium labeled	Heavy labeled	UV	Recovery	MG132
1	CS3BE	CS3BE + CSA-Flag	No UV	-	-
2	CS3BE	CS3BE + CSA-Flag	20 J/m ²	1 hour	-
3	CS3BE	CS3BE + CSA-Flag	20 J/m ²	6 hours	-
4	CS3BE	CS3BE + CSA-Flag	20 J/m ²	6 hours	+

RNA polymerase II, subunit RPB1	Normalized Log ₂ Ratio			
	Exp1	Exp2	Exp3	Exp4
	0	0.64	0	0.6

Figure 7. Identification of targets for CSA mediated ubiquitination (A) Setup of SILAC experiment. CS3BE cells or CS3BE + CSA-Flag cells stably expressing His-ubiquitin were SILAC labeled and treated as indicated, His-ubiquitin conjugates were purified by IMAC and analyzed by mass spectrometry. The normalized log₂ ratios in each experiment are depicted for the RNAPII subunit RPB1. **(B)** The experiment described in (A) was repeated, total lysates and His-ubiquitin purified fractions were analyzed by immunoblotting using anti-phospho-RPB1 antibody or anti-His antibody (His pulldown only). CSA expression in total lysates was analyzed by immunoblotting using anti-CSA antibody

B



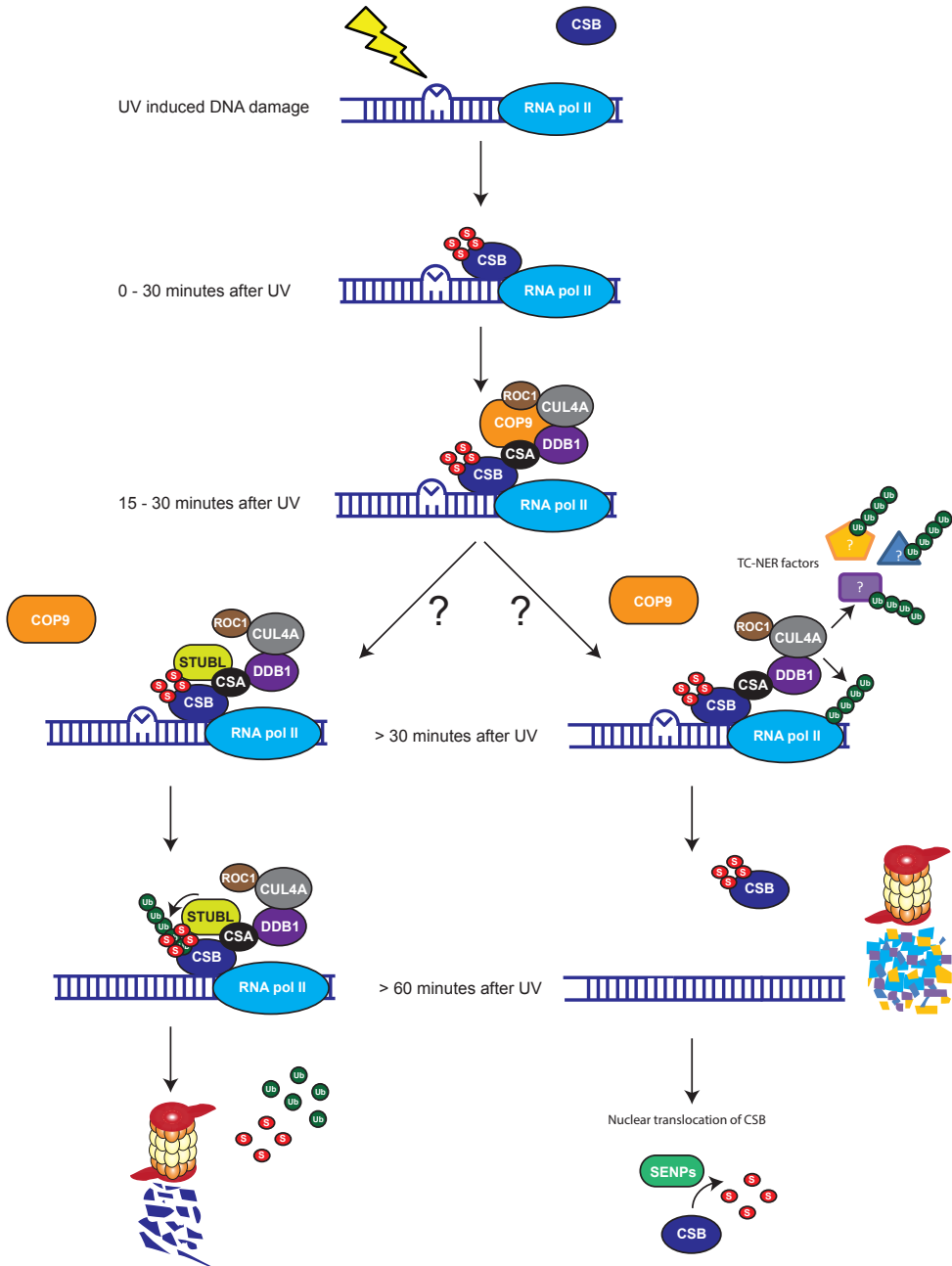


Figure 8. Model During transcription, CSB interacts dynamically with RNAPII. UV induced DNA damage causes stalling of the RNAPII complex and this initiates a more stable interaction between CSB and RNAPII. CSB SUMOylation is an early event upon UV induced DNA damage. The recruitment of the CSA E3 ligase complex initiates the destabilization of SUMOylated CSB at later time points after DNA damage. The exact mechanism behind this destabilization is currently unknown; the recruitment of a STUBL or the ubiquitination of RNA polymerase II by the CSA complex could potentially play a role. See main text for more details

Chapter 6

Discussion

CSB is a novel SUMO2 target protein

We have studied the SUMOylation of the TC-NER factor CSB upon UV induced DNA damage. This protein was identified as a novel SUMO2 target protein in a SILAC based proteomics screen for SUMO2 targets upon UV and IR treatment. In addition to CSB, the previously published SUMO target XPC (36) was also identified as a 'UV-dependent' SUMO target. XPC is another component of the TC-NER pathway (30) showing that at least two proteins that are essential for TC-NER are modified by SUMO2 upon DNA damage. This screen also showed that some targets are only SUMOylated upon the activation of specific DNA repair pathway (UV or IR specific), while other proteins are targets for SUMOylation in two separate repair pathways (UV + IR upregulated). Due to the harsh filtering of targets by using a label swap experiment, it is most likely that there are many more SUMO2 regulated targets in these DNA repair pathways that remain to be identified.

CSB is SUMOylated on two lysines located in the N-terminus of the protein

SUMOylation often occurs on lysines located in the so called 'SUMO consensus motif' ψ KxE, however SUMOylation of lysines not located in this motif is frequently reported (37). CSB has 5 lysines located in the SUMO consensus motif and mutational analysis of the CSB protein revealed that SUMOylation of CSB mainly takes place on lysine 32 and lysine 205. SUMOylation on these two lysines is exclusively and abundantly happening after DNA damage induced by UV irradiation, which raises the question what mechanism is responsible for this specificity?

Several studies revealed a strong link between chromatin and SUMOylation activity. It has been shown that SUMO proteins and components of the SUMOylation machinery often colocalizes and interacts with chromatin (38). In addition, it was recently found that active promoters of genes are areas with a high SUMOylation activity (39). Thus, chromatin seem to be contents of the nucleus that display an increased SUMOylation activity. Since CSB strongly binds to stalled RNAPII on chromatin (34) upon UV induced DNA damage, we wondered whether this translocation could explain the increase in SUMOylation. Indeed, we found that SUMOylation of CSB predominantly takes place in chromatin enriched fractions after UV treatment (Figure 5A), potentially explaining the UV specific SUMOylation.

Intriguingly, an ATP dependent conformational change in CSB is essential for stable CSB-chromatin association after UV irradiation (40). In this study, the authors suggest that a stable CSB-chromatin interaction under normal conditions is prevented by the N-terminal region of CSB that blocks the DNA interaction surface of the protein. In the presence of a lesion-stalled transcription, this autorepression is released by an ATPase induced conformational change of CSB. Since CSB is SUMOylated on the N-terminus upon DNA damage, it would be interesting to study if

this conformational change is needed to induce CSB SUMOylation. Future research is also needed to investigate whether SUMOylation has an effect on the induction, stability and duration of the conformational change in CSB upon DNA damage.

Furthermore, it would be interesting to study the involvement of a specific SUMO E3 ligase in CSB SUMOylation. Potential candidates are PIAS1 and PIAS4; previously it was found that these E3 ligases are recruited to sites of DNA damage (41). Another interesting E3 ligase to study is CBX4, a family member of the chromatin-associated PcG proteins. CBX4 mediated SUMOylation of the polycomb complex protein BMI1 regulates its accumulation at sites of DNA damage (42).

CSB SUMOylation is dispensable for UV survival of cells

Clonal survival assays showed that SUMOylation of CSB is not essential for long term survival of cells after UV irradiation. Although it has been shown that interfering with global SUMOylation leads to serious cellular defects (43) (44), abolishing SUMOylation on single protein level often lacks notable phenotypes. Therefore it has been proposed that SUMOylation regulates cellular processes by modifying protein groups involved in a particular process (45). We found at least one other UV specific SUMO target that is involved in TC-NER, XPC, and it is most likely that SUMO modifies a whole set of proteins that are regulating the repair of UV induced lesions.

The role of SUMOylation in TC-NER could thus also be explained by group modification; indeed it has been published that two PIAS SUMO E3 ligases play an essential role in promoting NER in yeast (46). In agreement with this data, we found that knocking down the SUMO E2 enzyme Ubc9 significantly decreased the recovery in RNA synthesis after a UV induced block in transcription. Recovery of RNA synthesis by RNAPII depends on the efficient repair of a DNA lesion and is therefore a good readout for efficient DNA repair (47, 48). Whether SUMOylation of CSB has a direct effect on the transcriptional restart after UV induced DNA damage should be addressed by future research. In addition, the recent developed method to measure the kinetics of nucleotide excision repair (49) is an interesting tool to study the involvement of CSB SUMOylation in efficient repair of lesions.

Link between SUMOylated CSB and CSA recruitment

In Cockayne Syndrome there are two genetic complementation groups: CS-A and CS-B (50). Mutations in either CSA or CSB lead to similar phenotypes in CS patients and both proteins play key roles in TC-NER. Despite these similarities, the exact link between CSA and CSB and their cooperative function in DNA repair remains to be elucidated (51). Binding of CSB to stalled RNAPII upon DNA damage is essential for the recruitment of CSA. Subsequently, CSA is required for the recruitment of HMG1, XAB2 and TFIIIS but dispensable for the attraction of core NER factors (30). CSA is recruited to sites of DNA damage as part of a Cullin-like ubiquitin E3 ligase

Chapter 6

complex further consisting of DDB1, Cullin 4A and Roc1. At an early stage after UV irradiation, this E3 ligase is inactive due to the binding of the COP9 signalosome (CSN) to the complex which leads to the deneddylation of Cullin 4A. The CSN complex dissociates from the E3 ligase complex at later time points after UV and this potentially releases ubiquitination activity of the E3 ligase (52).

So far, it is unclear what the targets are for CSA dependent ubiquitination at sites of DNA damage. CSB has been suggested as a UV-specific target for CSA mediated ubiquitination and subsequent proteasomal degradation (32). Although we observed an increase in CSB ubiquitination in CSA complemented cell-lines, this was strongly reduced after UV treatment and even further reduced in combination with inactivation of the proteasome. It is important to note that the usage of tagged-ubiquitin constructs excludes the detection of potential linear ubiquitin chains on CSB. Nevertheless, in our hands it does not look like CSB is a target for UV-dependent degradation via the CSA E3 ligase complex. However, we did find that the recruitment of this complex is responsible for the destabilization of SUMOylated CSB at later time-points after UV. This observation provides a novel link between CSB and CSA but raises the question how CSA is regulating the destabilization of SUMOylated CSB. As mentioned above CSA does most likely not act as a STUBL, but potentially CSA could still recruit a STUBL to sites of DNA damage to ubiquitinate SUMOylated CSB. Recently, RNF111 was identified as a STUBL that facilitates the DNA damage response by recognizing SUMOylated XPC (53). It would be interesting to study the effect of RNF111 on SUMOylated CSB, since both CSB and XPC are SUMO targets in the TC-NER pathway.

Another explanation for the destabilization of SUMOylated CSB by the CSA complex is the ubiquitination of TC-NER factors by this complex. Ubiquitination of RNAPII (and other TC-NER proteins) by the CSA complex could potentially induce the dissociation of CSB from chromatin and translocation to the nucleoplasm. Since CSB is exclusively SUMOylated on chromatin, this translocation could lead to the deSUMOylation of CSB in the nucleus by SUMO specific proteases (Figure 8). Intriguingly, RNA polymerase II ubiquitination and degradation is believed to be a 'last-resort' response to DNA damage in yeast. In this model, Cdc48 disassembles ubiquitinated RNAPII from chromatin resulting in its proteasomal degradation (54). It would be interesting to see whether the mammalian Cdc48 homolog, VCP/p97 has similar effects on human RNAPII. If this is the case, one could study the effect on SUMOylated CSB after repression of VCP/p97 expression to see whether the stability of SUMOylated CSB is indeed linked to the degradation of RNAPII. Furthermore, it was recently found that Cdc48 and its cofactor acts as a SUMO-targeted segregase towards SUMOylated Rad52 during DNA double-strand break repair (55). Therefore it would be very interesting to see if VCP/p97 is also recruited by the TC-NER machinery and whether this is dependent on the SUMOylation of CSB.

Materials and methods

Cell culture, SILAC labeling and generation of cell lines

U2OS, CS3BEsv, CS1ANsv and VH10ht cells were cultured in Dulbecco's modified Eagle's medium (Gibco Invitrogen Corporation, Grand Island, NY, USA) supplemented with 10% FCS (Gibco) and 100 U/ml penicillin and 100 µg/ml streptomycin (Gibco). For SILAC analysis, cells were essentially labeled as described before (56). Briefly, cells were grown in medium supplemented with [$^{12}\text{C}_6$, $^{14}\text{N}_4$]arginine (referred to as Arg0), [$^{13}\text{C}_6$, $^{14}\text{N}_4$]arginine (referred to as Arg6), [$^{13}\text{C}_6$, $^{15}\text{N}_4$]arginine (referred to as Arg10), [$^{12}\text{C}_6$, $^{14}\text{N}_2$]lysine (referred to as Lys0), [$^2\text{H}_4$, $^{12}\text{C}_6$, $^{14}\text{N}_2$]lysine (referred to as Lys4), or [$^{13}\text{C}_6$, $^{15}\text{N}_2$]lysine (referred to as Lys8) as indicated. U2OS cells stably expressing Flag-SUMO2 were previously described (57). U2OS cells stably expressing GFP-CSB proteins were generated by infecting cells with retroviruses encoding different GFP-CSB constructs and the Puromycin resistant gene. After infection, cells were selected for GFP-CSB expression by culturing in medium supplemented with 1 µg/ml of Puromycin (Calbiochem). CS1ANsv cells stably expressing WT- or 5KR-CSB were generated by infecting cells with lentiviruses encoding CSB and the Blastidicin resistant gene. After infection, cells were selected for CSB expression by culturing in medium supplemented with 400 µg/ml G418 (Roche). CS3BE cells stably expressing His-CSA or CSA-Flag were generated by infecting cells with lentiviruses encoding CSA and the Blastidicin resistant gene. After infection, cells were selected for CSB expression by culturing in medium supplemented with either 5 µg/ml Blastidicin (Invitrogen) (His-CSA) or 100 µg/ml G418 (CSA-Flag). All cells were cultured in CELLSTAR flasks (175cm²) and petri dishes (145 x 20 mm) (both from Greiner Bio-One).

Plasmids

The pLV-CMV-Flag-SUMO2-IRES-eGFP plasmid was previously described (57). Ubiquitin cDNA was cloned into pLV-CMV-Flag-IRES-eGFP vector. Wild type CSB cDNA was cloned into pDON207 (Invitrogen). This construct was used to make lysine to arginine mutations using the following primers: 5'-GAAGAAATGGCAATCAGGCAAGAAAGTGGTG-3' and 5'-CACCACCTTCTTGCTGATTGCATTTCTTC-3' (K32R), 5'-GAGGAGCAGAGGTGAGAATTGAACTAGATCAC-3' and 5'-GTGATCTAGTTCAATTC TCACCTCTGCTCCTC-3' (K205R), 5'-CAAAGAGAAACGTCTGAGGCTGGAGGACGA TTC-3' and 5'-GAATCGTCTCCAGCCTCAGACGTTTCTCTTTG-3' (K481R), 5'-CAG GATGGCATCATGAGAAAGGAGGGAAAAG-3' and 5'-CTTTTCCCTCTTTCTCATGA TGCCATCCTG-3' (K1359R), 5'-GAATTTGGAAACTCAGGCCAGAATACTGC-3' and 5'-GCAGTATTCTGGCCTGAGTTTCCAAATTC-3' (K1489R). The different CSB constructs were subsequently transferred to pBabe-puro-GFP-Dest (a kind gift of Petra de Graaf and Marc Timmers, Utrecht, The Netherlands) or pLenti-NEO-Dest (Addgene, number 17392) employing standard Gateway technology (Invitrogen). To create N-terminal CSB protein fragments, cDNA encoding amino acid 1 until 341 of CSB was cloned into pDON207. Subsequently, this cDNA was transferred to pDEST15 (T7-GST-Dest, Invitrogen) using standard Gateway technology. Synthetic oligos encoding either the 6His-StrepII-tag or the Flag-tag were inserted into pENTR4 (Invitrogen). Wild type CSA cDNA was subsequently cloned into these vectors and transferred to pLenti6.3 V5-DEST (Invitrogen) to obtain lentiviral vectors expressing His- or Flag-tagged CSA. The pGEX-2T-SUMO2gg vector was a kind gift of Prof. Dr. Ron Hay (58). The SUMO-2 encoding construct pE1E2S2 was a kind gift of Prof. H. Saitoh (59). The CSA-DDB1 encoding construct was a kind gift of Dr. E. Meulenbroek (60).

Chapter 6

Antibodies

The primary antibodies used were as followed: mouse monoclonal anti-Flag M2, mouse anti-His, rabbit anti-Actin (all from Sigma), mouse monoclonal anti-SUMO-2/3, rabbit monoclonal anti-Ercc8 (CSA), goat anti-DDB1 (all from Abcam), mouse anti-Ubiquitin P4D1 (Santa Cruz Biotechnology), rabbit anti-MDC1, rabbit anti-CSB, rabbit anti-XPC, rabbit anti-Senataxin (all from Bethyl laboratories), mouse anti-RanGap1 (Life Technologies), rabbit anti-SUMO-2/3 and rabbit anti-SART1 were previously described (61, 62), mouse anti-GFP (Roche), mouse anti-Ubc9 (BD biosciences), rabbit anti-Phospho-Rpb1 CTD (Ser2/Ser5) (Cell signaling).

Flag-SUMO2 and Flag-Ubiquitin immunoprecipitation

Flag-SUMO2 and Flag-Ubiquitin conjugates were enriched with a Flag immunoprecipitation as described before (57).

Electrophoresis and immunoblotting

Protein samples were either separated via regular SDS-PAGE using a Tris-glycine buffer or on Novex 4-12% Bis-Tris gradient gels (Invitrogen) using MOPS buffer. Fractionated proteins were transferred onto Hybond-C extra membranes (Amersham Biosciences) using a submarine system (Invitrogen). Membranes were stained for total protein amounts with Ponceau S (Sigma) and blocked with PBS containing 5% milk powder and 0.1% Tween-20 before incubating with the primary antibodies as indicated.

Coomassie staining, in-gel digestion and Mass Spectrometry analysis

This was essentially done as previously described (57). Briefly, Coomassie stained gel slices were destained with 50% ethanol in 25 mM ammonium bicarbonate solution and dehydrated. Resulting peptides from in-gel digestion were desalted and concentrated on STAGE-tips with two C18 filters; eluted peptides were analyzed on an EASY-nLC system (Proxeon) connected to the Q-Exactive (Thermo Fisher Scientific).

Global and local UV irradiation

UV irradiation of cell was essentially performed as described before (63). Briefly, cells were rinsed with phosphate-buffered saline (PBS) and exposed to UV-C (254 nm; TUV lamp; Philips). After irradiation cells were cultured in their original medium for time-points as indicated. For local irradiation PBS washed cells were covered with a micro-porous polycarbonate filter containing 5 μm pores (Millipore) and irradiated with 100 J/m^2 UV. After irradiation cells were cultured in their original medium for one hour.

Microscopy

Cells were fixed, stained and analyzed as described before (57).

UV survival

Survival of cells was determined essentially as described before (64). Briefly, cells were exposed to UV (2, 4, 6 or 8 J/m^2) and left to grow for 14 days. Cells were fixed and stained with methylene blue, colonies

were counted and the amount of colonies was compared to untreated cells (0 J/m²) which was set to 100 % survival.

RNA recovery assay

48 hours after infection, VH10ht cells were plated on 96-well plates and UVC-irradiated (10J/m²), and subsequently cultured in their original medium for different time-periods (0–24 h) to allow RNA synthesis recovery. Cells were then incubated for 1 h in medium supplemented with 1mM of EU (Invitrogen) to detect global RNA transcription. Image acquisition and data processing are automated. Typical RNA synthesis images were captured by the BD pathway 855 and analyzed by Cell profiler software.

Elisa assay

Anti-Flag-M2 coated well plates (Sigma) were prewashed with PBS-T (0.05 % Tween-20 in PBS). Wells were incubated with lysates diluted in dilution buffer, according to the Flag immunoprecipitation procedure (57) for 1,5 hours at 4°C. Wells were washed with PBS-T (3 times) and incubated with rabbit anti-CSB or rabbit anti-SUMO-2/3 antibodies for 1,5 hours at 4°C and washed again with PBS-T (3 times). Subsequently, wells were incubated with swine anti-rabbit biotinylated antibody (DAKO) for 1,5 hours at 4°C and washed three times with PBS-T. Next, wells were incubated with Streptavidin-HRP (R&D systems) and incubate for 20 minutes at room temperature after which the plates were washed with PBS-T (3 times). HRP was detected by incubating with the Substrate Reagent Pack (R&D systems) for 20 minutes at room temperature; reactions were stopped by adding 1M H₂SO₄. Signal intensity was measured at 450 nm using a platereader.

Lentiviral shRNA experiments

U2OS cells were infected at MOI 3 with lentivirus encoding shRNA TRCN0000003720 (CSA shRNA #1), shRNA TRCN0000 003721 (CSA shRNA #2), shRNA TRCN0000082853 (DDB1 shRNA #1), shRNA TRCN0000082857 (DDB1 shRNA #2) or non-targeting shRNA SHC002 (Ctrl). The medium was changed the next day and four days after infection, cells were harvested. For the RNA recovery assay, VH10ht cells were infected at MOI 3 with lentivirus encoding shRNA TRCN0000007205 (Ubc9 shRNA #1) or shRNA TRCN0000007206 (Ubc9 shRNA #2) or non-targeting shRNA SHC002 (Ctrl).

Biochemical fractionation of cells

Cellular fractionation assays were essentially performed as described previously (35).

Recombinant proteins

The GST tagged N-terminal CSB fragment and GST tagged SUMO2 were produced in *E. coli* and purified as described previously (58). 10His-CSA-6His-DDB1 protein complex were essentially produced and purified as described previously (60). Briefly, Sf9 cell pellets expressing 10His-CSA-6His-DDB1 were lysed in lysis buffer (50 mM Tris pH 8.0, 20 mM Imidazole, 200 mM NaCl, 0.1 % Triton X-100, 5 mM β-mercaptoethanol, protease inhibitor minus EDTA (Roche)). Cell lysates were sonicated and centrifuged for 30 minutes at 9000 RPM at 4°C. The supernatant was incubated with NiNTA agarose (Qiagen) for 3

Chapter 6

hours at 4°C. Subsequently, the beads were washed 4 times with lysis buffer supplemented with 30 mM Imidazole. Proteins were eluted with an Imidazole gradient (50 mM Imidazole to 500 mM Imidazole) for 15 minutes at 4°C each elution. The 10His-CSA-6His-DDB1 complex from the elution with 300 mM Imidazole was used for the interaction experiments.

***In vitro* interaction experiment**

Recombinant GST tagged proteins bound to Glutathione Sepharose (GE Healthcare) were left untreated or were incubated with 5 µg SENP2cd (BostonBiochem) at 4°C for 2 hours. Beads were washed twice with 0.5 M NaCl, 1 mM PMSF, protease inhibitor cocktail (Roche) in 1X PBS and three times with NETN buffer (150 mM NaCl, 1 mM EDTA, 20 mM Tris pH 8.0, 0.5% NP-40). These beads or beads only were incubated with 5 µg of 10His-CSA-6His-DDB1 protein complexes for 2 hours at 4°C in NETN buffer. After incubation, beads were washed 5 times in NETN buffer. Beads were eluted in NETN buffer in the presence of 20 mM Glutathione (Sigma) at room temperature for 15 minutes.

Purification of His-Ubiquitin conjugates

His-Ubiquitin conjugates were purified as described previously (57).

Reference List

1. Hoeijmakers, J. H. (2001) Genome maintenance mechanisms for preventing cancer. *Nature* 411, 366-374
2. Jackson, S. P., and Bartek, J. (2009) The DNA-damage response in human biology and disease. *Nature* 461, 1071-1078
3. Jackson, S. P., and Durocher, D. (2013) Regulation of DNA damage responses by ubiquitin and SUMO. *Mol. Cell* 49, 795-807
4. Mahajan, R., Delphin, C., Guan, T., Gerace, L., and Melchior, F. (1997) A small ubiquitin-related polypeptide involved in targeting RanGAP1 to nuclear pore complex protein RanBP2. *Cell* 88, 97-107
5. Flotho, A., and Melchior, F. (2013) Sumoylation: a regulatory protein modification in health and disease. *Annu. Rev. Biochem.* 82, 357-385
6. Geiss-Friedlander, R., and Melchior, F. (2007) Concepts in sumoylation: a decade on. *Nat. Rev. Mol. Cell Biol.* 8, 947-956
7. Gill, G. (2004) SUMO and ubiquitin in the nucleus: different functions, similar mechanisms? *Genes Dev.* 18, 2046-2059
8. Perry, J. J., Tainer, J. A., and Boddy, M. N. (2008) A SIM-ultaneous role for SUMO and ubiquitin. *Trends Biochem. Sci.* 33, 201-208
9. Baba, D., Maita, N., Jee, J. G., Uchimura, Y., Saitoh, H., Sugasawa, K., Hanaoka, F., Tochio, H., Hiroaki, H., and Shirakawa, M. (2005) Crystal structure of thymine DNA glycosylase conjugated to SUMO-1. *Nature* 435, 979-982
10. Steinacher, R., and Schar, P. (2005) Functionality of human thymine DNA glycosylase requires SUMO-regulated changes in protein conformation. *Curr. Biol.* 15, 616-623
11. Morris, J. R., Boutell, C., Keppler, M., Densham, R., Weekes, D., Alamshah, A., Butler, L., Galanty, Y., Pangon, L., Kiuchi, T., Ng, T., and Solomon, E. (2009) The SUMO modification pathway is involved in the BRCA1 response to genotoxic stress. *Nature* 462, 886-890
12. Hoegge, C., Pfander, B., Moldovan, G. L., Pyrowolakis, G., and Jentsch, S. (2002) RAD6-dependent DNA repair is linked to modification of PCNA by ubiquitin and SUMO. *Nature* 419, 135-141
13. Bergink, S., and Jentsch, S. (2009) Principles of ubiquitin and SUMO modifications in DNA repair. *Nature* 458, 461-467
14. Galanty, Y., Belotserkovskaya, R., Coates, J., and Jackson, S. P. (2012) RNF4, a SUMO-targeted ubiquitin E3 ligase, promotes DNA double-strand break repair. *Genes Dev.* 26, 1179-1195
15. Yin, Y., Seifert, A., Chua, J. S., Maure, J. F., Golebiowski, F., and Hay, R. T. (2012) SUMO-targeted ubiquitin E3 ligase RNF4 is required for the response of human cells to DNA damage. *Genes Dev.* 26, 1196-1208

16. Cleaver, J. E., Bezrookove, V., Revet, I., and Huang, E. J. (2013) Conceptual developments in the causes of Cockayne syndrome. *Mech. Ageing Dev.* 134, 284-290
17. Lagerwerf, S., Vrouwe, M. G., Overmeer, R. M., Fouteri, M. I., and Mullenders, L. H. (2011) DNA damage response and transcription. *DNA Repair (Amst)* 10, 743-750
18. Blanpain, C., Mohrin, M., Sotiropoulou, P. A., and Passegue, E. (2011) DNA-damage response in tissue-specific and cancer stem cells. *Cell Stem Cell* 8, 16-29
19. Johnson, E. S. (2004) Protein modification by SUMO. *Annu. Rev. Biochem.* 73, 355-382
20. Cleaver, J. E., Lam, E. T., and Revet, I. (2009) Disorders of nucleotide excision repair: the genetic and molecular basis of heterogeneity. *Nat. Rev. Genet.* 10, 756-768
21. Anindya, R., Mari, P. O., Kristensen, U., Kool, H., Giglia-Mari, G., Mullenders, L. H., Fouteri, M., Vermeulen, W., Egly, J. M., and Svejstrup, J. Q. (2010) A ubiquitin-binding domain in Cockayne syndrome B required for transcription-coupled nucleotide excision repair. *Mol. Cell* 38, 637-648
22. van, d. B., V, Citterio, E., Hoogstraten, D., Zotter, A., Egly, J. M., van Cappellen, W. A., Hoeijmakers, J. H., Houtsmuller, A. B., and Vermeulen, W. (2004) DNA damage stabilizes interaction of CSB with the transcription elongation machinery. *J. Cell Biol.* 166, 27-36
23. Volker, M., Mone, M. J., Karmakar, P., van, H. A., Schul, W., Vermeulen, W., Hoeijmakers, J. H., van, D. R., van Zeeland, A. A., and Mullenders, L. H. (2001) Sequential assembly of the nucleotide excision repair factors in vivo. *Mol. Cell* 8, 213-224
24. Schmickel, R. D., Chu, E. H., Trosko, J. E., and Chang, C. C. (1977) Cockayne syndrome: a cellular sensitivity to ultraviolet light. *Pediatrics* 60, 135-139
25. Mayne, L. V., Priestley, A., James, M. R., and Burke, J. F. (1986) Efficient immortalization and morphological transformation of human fibroblasts by transfection with SV40 DNA linked to a dominant marker. *Exp. Cell Res.* 162, 530-538
26. Venema, J., Mullenders, L. H., Natarajan, A. T., van Zeeland, A. A., and Mayne, L. V. (1990) The genetic defect in Cockayne syndrome is associated with a defect in repair of UV-induced DNA damage in transcriptionally active DNA. *Proc. Natl. Acad. Sci. U. S. A* 87, 4707-4711
27. Mayne, L. V., and Lehmann, A. R. (1982) Failure of RNA synthesis to recover after UV irradiation: an early defect in cells from individuals with Cockayne's syndrome and xeroderma pigmentosum. *Cancer Res.* 42, 1473-1478
28. Troelstra, C., van, G. A., de, W. J., Vermeulen, W., Bootsma, D., and Hoeijmakers, J. H. (1992) ERCC6, a member of a subfamily of putative helicases, is involved in Cockayne's syndrome and preferential repair of active genes. *Cell* 71, 939-953
29. Drag, M., and Salvesen, G. S. (2008) DeSUMOylating enzymes--SENPs. *IUBMB. Life* 60, 734-742
30. Fouteri, M., and Mullenders, L. H. (2008) Transcription-coupled nucleotide excision repair in mammalian cells: molecular mechanisms and biological effects. *Cell Res.* 18, 73-84
31. Brumback, R. A., Yoder, F. W., Andrews, A. D., Peck, G. L., and Robbins, J. H. (1978) Normal pressure hydrocephalus. Recognition and relationship to neurological abnormalities in Cockayne's syndrome. *Arch. Neurol.* 35, 337-345
32. Groisman, R., Kuraoka, I., Chevallier, O., Gaye, N., Magnaldo, T., Tanaka, K., Kisselev, A. F., Harel-Bellan, A., and Nakatani, Y. (2006) CSA-dependent degradation of CSB by the ubiquitin-proteasome pathway establishes a link between complementation factors of the Cockayne syndrome. *Genes Dev.* 20, 1429-1434
33. Prudden, J., Pebernard, S., Raffa, G., Slavin, D. A., Perry, J. J., Tainer, J. A., McGowan, C. H., and Boddy, M. N. (2007) SUMO-targeted ubiquitin ligases in genome stability. *EMBO J.* 26, 4089-4101
34. Fouteri, M., Vermeulen, W., van Zeeland, A. A., and Mullenders, L. H. (2006) Cockayne syndrome A and B proteins differentially regulate recruitment of chromatin remodeling and repair factors to stalled RNA polymerase II in vivo. *Mol. Cell* 23, 471-482
35. Wysocka, J., Reilly, P. T., and Herr, W. (2001) Loss of HCF-1-chromatin association precedes temperature-induced growth arrest of tsBN67 cells. *Mol. Cell Biol.* 21, 3820-3829
36. Wang, Q. E., Zhu, Q., Wani, G., El-Mahdy, M. A., Li, J., and Wani, A. A. (2005) DNA repair factor XPC is modified by SUMO-1 and ubiquitin following UV irradiation. *Nucleic Acids Res.* 33, 4023-4034
37. Matic, I., Schimmel, J., Hendriks, I. A., van Santen, M. A., van de Rijke, F., van, D. H., Gnad, F., Mann, M., and Vertegaal, A. C. (2010) Site-specific identification of SUMO-2 targets in cells reveals an inverted

- SUMOylation motif and a hydrophobic cluster SUMOylation motif. *Mol. Cell* 39, 641-652
38. Cubenas-Potts, C., and Matunis, M. J. (2013) SUMO: a multifaceted modifier of chromatin structure and function. *Dev. Cell* 24, 1-12
 39. Neyret-Kahn, H., Benhamed, M., Ye, T., Le, G. S., Cossec, J. C., Lapaquette, P., Bischof, O., Ouspenskaia, M., Dasso, M., Seeler, J., Davidson, I., and Dejean, A. (2013) Sumoylation at chromatin governs coordinated repression of a transcriptional program essential for cell growth and proliferation. *Genome Res.*
 40. Lake, R. J., Geyko, A., Hemashettar, G., Zhao, Y., and Fan, H. Y. (2010) UV-induced association of the CSB remodeling protein with chromatin requires ATP-dependent relief of N-terminal autorepression. *Mol. Cell* 37, 235-246
 41. Galanty, Y., Belotserkovskaya, R., Coates, J., Polo, S., Miller, K. M., and Jackson, S. P. (2009) Mammalian SUMO E3-ligases PIAS1 and PIAS4 promote responses to DNA double-strand breaks. *Nature* 462, 935-939
 42. Ismail, I. H., Gagne, J. P., Caron, M. C., McDonald, D., Xu, Z., Masson, J. Y., Poirier, G. G., and Hendzel, M. J. (2012) CBX4-mediated SUMO modification regulates BMI1 recruitment at sites of DNA damage. *Nucleic Acids Res.* 40, 5497-5510
 43. Nacerddine, K., Lehembre, F., Bhaumik, M., Artus, J., Cohen-Tannoudji, M., Babinet, C., Pandolfi, P. P., and Dejean, A. (2005) The SUMO pathway is essential for nuclear integrity and chromosome segregation in mice. *Dev. Cell* 9, 769-779
 44. Seufert, W., Fitcher, B., and Jentsch, S. (1995) Role of a ubiquitin-conjugating enzyme in degradation of S- and M-phase cyclins. *Nature* 373, 78-81
 45. Psakhye, I., and Jentsch, S. (2012) Protein group modification and synergy in the SUMO pathway as exemplified in DNA repair. *Cell* 151, 807-820
 46. Silver, H. R., Nissley, J. A., Reed, S. H., Hou, Y. M., and Johnson, E. S. (2011) A role for SUMO in nucleotide excision repair. *DNA Repair (Amst)* 10, 1243-1251
 47. Cheung, A. C., and Cramer, P. (2011) Structural basis of RNA polymerase II backtracking, arrest and reactivation. *Nature* 471, 249-253
 48. Gaillard, H., and Aguilera, A. (2013) Transcription coupled repair at the interface between transcription elongation and mRNP biogenesis. *Biochim. Biophys. Acta* 1829, 141-150
 49. Choi, J. H., Gaddameedhi, S., Kim, S. Y., Hu, J., Kemp, M. G., and Sancar, A. (2013) Highly specific and sensitive method for measuring nucleotide excision repair kinetics of ultraviolet photoproducts in human cells. *Nucleic Acids Res.*
 50. Tanaka, K., Kawai, K., Kumahara, Y., Ikenaga, M., and Okada, Y. (1981) Genetic complementation groups in cockayne syndrome. *Somatic. Cell Genet.* 7, 445-455
 51. Saijo, M. (2013) The role of Cockayne syndrome group A (CSA) protein in transcription-coupled nucleotide excision repair. *Mech. Ageing Dev.* 134, 196-201
 52. Groisman, R., Polanowska, J., Kuraoka, I., Sawada, J., Saijo, M., Drapkin, R., Kisselev, A. F., Tanaka, K., and Nakatani, Y. (2003) The ubiquitin ligase activity in the DDB2 and CSA complexes is differentially regulated by the COP9 signalosome in response to DNA damage. *Cell* 113, 357-367
 53. Poulsen, S. L., Hansen, R. K., Wagner, S. A., van, C. L., van Belle, G. J., Streicher, W., Wikstrom, M., Choudhary, C., Houtsmuller, A. B., Martejijn, J. A., Bekker-Jensen, S., and Mailand, N. (2013) RNF111/Arkadia is a SUMO-targeted ubiquitin ligase that facilitates the DNA damage response. *J. Cell Biol.* 201, 797-807
 54. Wilson, M. D., Harreman, M., and Svejstrup, J. Q. (2013) Ubiquitylation and degradation of elongating RNA polymerase II: the last resort. *Biochim. Biophys. Acta* 1829, 151-157
 55. Bergink, S., Ammon, T., Kern, M., Schermelleh, L., Leonhardt, H., and Jentsch, S. (2013) Role of Cdc48/p97 as a SUMO-targeted segregase curbing Rad51-Rad52 interaction. *Nat. Cell Biol.* 15, 526-532
 56. Mann, M. (2006) Functional and quantitative proteomics using SILAC. *Nat. Rev. Mol. Cell Biol.* 7, 952-958
 57. Schimmel, J., Eifler, K., Sigurethsson, J. O., Cuijpers, S. A., Hendriks, I. A., Verlaan-de, V. M., Kelstrup, C. D., Francavilla, C., Medema, R. H., Olsen, J. V., and Vertegaal, A. C. (2014) Uncovering SUMOylation Dynamics during Cell-Cycle Progression Reveals FoxM1 as a Key Mitotic SUMO Target Protein. *Mol. Cell*
 58. Tatham, M. H., Jaffray, E., Vaughan, O. A., Desterro, J. M., Botting, C. H., Naismith, J. H., and Hay, R. T. (2001) Polymeric chains of SUMO-2 and SUMO-3 are conjugated to protein substrates by SAE1/SAE2 and Ubc9. *J. Biol. Chem.* 276, 35368-35374
 59. Uchimura, Y., Nakamura, M., Sugawara, K., Nakao, M., and Saitoh, H. (2004) Overproduction of eukaryotic SUMO-1- and

- SUMO-2-conjugated proteins in *Escherichia coli*. *Anal. Biochem.* 331, 204-206
60. Meulenbroek, E. M., and Pannu, N. S. (2012) Overproduction, purification, crystallization and preliminary X-ray diffraction analysis of Cockayne syndrome protein A in complex with DNA damage-binding protein 1. *Acta Crystallogr. Sect. F. Struct. Biol. Cryst. Commun.* 68, 45-48
 61. Vertegaal, A. C., Ogg, S. C., Jaffray, E., Rodriguez, M. S., Hay, R. T., Andersen, J. S., Mann, M., and Lamond, A. I. (2004) A proteomic study of SUMO-2 target proteins. *J. Biol. Chem.* 279, 33791-33798
 62. Vertegaal, A. C., Andersen, J. S., Ogg, S. C., Hay, R. T., Mann, M., and Lamond, A. I. (2006) Distinct and overlapping sets of SUMO-1 and SUMO-2 target proteins revealed by quantitative proteomics. *Mol. Cell Proteomics.* 5, 2298-2310
 63. Overmeer, R. M., Gourdin, A. M., Gigliamari, A., Kool, H., Houtsmuller, A. B., Siegal, G., Fousteri, M. I., Mullenders, L. H., and Vermeulen, W. (2010) Replication factor C recruits DNA polymerase delta to sites of nucleotide excision repair but is not required for PCNA recruitment. *Mol. Cell Biol.* 30, 4828-4839
 64. Pines, A., Vrouwe, M. G., Martejn, J. A., Typas, D., Luijsterburg, M. S., Cansoy, M., Hensbergen, P., Deelder, A., de, G. A., Matsumoto, S., Sugawara, K., Thoma, N., Vermeulen, W., Vrieling, H., and Mullenders, L. (2012) PARP1 promotes nucleotide excision repair through DDB2 stabilization and recruitment of ALC1. *J. Cell Biol.* 199, 235-249



Summary and Discussion

Chapter 7. Summary and Discussion

Post translational modifications (PTMs) are orchestrated by highly active and reversible enzymatic systems to regulate the functional diversity of proteins. Because of their dynamic nature, PTMs are used by the cell as a controllable system to regulate a wide variety of processes (1). Studying modifications of proteins will give us more insight in how the cell uses PTMs to regulate cellular processes and how different PTMs act together to adjust the function of proteins. The research described in this thesis focuses one of these PTMs, the Small ubiquitin-Like Modifier (SUMO). SUMOs are proteins that are covalently attached to lysines in target proteins. These studies have uncovered hundreds of SUMO target proteins and acceptor sites and revealed a role for SUMOylation in protein degradation, cell cycle progression and DNA repair. The results from the different studies presented in this thesis are summarized and discussed in this chapter.

7.1 Crosstalk between SUMO and ubiquitin

Proteasome regulated SUMO-2 target proteins

In chapter 2 we reported on the cooperation between SUMOylation and ubiquitination in the regulation of a subset of SUMO-2 target proteins. Abolishing proteasomal degradation by blocking the proteasome resulted in the increase in SUMOylation of 73 proteins. This increase seemed to be independent of the total levels of these proteins, suggesting that only the SUMOylated forms are subjected to proteasomal degradation. So far, SUMOylation on its own has never directly been linked to the proteasomal degradation of proteins, this seems to be exclusive for proteins modified with ubiquitin chains (2, 3). The degradation of these SUMOylated proteins can therefore only be explained by a system where SUMO marks these proteins for subsequent ubiquitination and degradation.

In the same period as we published these findings, several reports came out on the identification of the so called 'SUMO targeted ubiquitin ligases' (STUBLs) SLX5/SLX8 in yeast and RNF4 in mammals (4-7). These studies provided mechanistic insight in how SUMOylated proteins are targeted for proteasomal degradation. STUBLs can bind non-covalently to SUMO via multiple SUMO interacting motifs (SIMs) in these ubiquitin E3 ligases, resulting in the ubiquitination and degradation of the SUMOylated proteins they bind. Interestingly, Tatham and coworkers found that RNF4 preferentially binds to polySUMO-chains *in vitro* through four SIMs in the N-terminus of the protein. We observed an increase in SUMO chains upon proteasomal degradation, supporting this model of recognition. Surprisingly, abolishing SUMO chain formation by making a lysine deficient SUMO-2 construct

did not change the processing of SUMO-2 targets by the proteasome and had no effect on the co-purification of ubiquitin. Future research should point out whether monoSUMOylation on several lysines in a protein can also be recognized by RNF4 and thus functionally replace polySUMOylation on single lysines.

We also found direct evidence for the ubiquitination of SUMO-2/3 proteins. Currently, it is unclear whether crosstalk between SUMO and ubiquitin is regulated by the ubiquitination of SUMO or by the ubiquitination of adjacent lysines in target proteins. It would also be interesting to study whether unanchored SUMO proteins and SUMO chains are subjected to direct proteasomal degradation via ubiquitination. In our study we concluded that conjugated SUMOs are recycled by the proteasome since blocking the proteasome resulted in a lack of 'free' SUMO needed for the SUMOylation of another set of targets. It is unclear exactly how these SUMO proteins are recycled by the proteasome; future research should show whether this is regulated by the activity of SUMO specific proteases located at proteasomes or if proteasomes cannot distinguish between SUMO and ubiquitin and process both proteins in a similar way (8, 9). Ubiquitin polymers are recycled via deubiquitinating enzymes associated with the regulatory particle of the proteasome.

The identification of another STUBL, RNF111, revealed that crosstalk between SUMO and ubiquitin is not limited to proteasomal degradation. RNF111 recognizes SUMOylated proteins and mainly induces lysine-63 linked ubiquitin chain formation; these types of chains are not processed by the proteasome and are mainly linked to a role in endocytosis and DNA repair (10-12). It is thus very likely that more STUBLs and other forms of crosstalk between SUMO and ubiquitin will be discovered in the near future.

Identification of USP11 as a SUMO-targeted ubiquitin protease

In chapter 3 we found evidence that the RNF4 mediated ubiquitination of SUMOylated proteins is reversible via the activity of the ubiquitin specific protease USP11. By performing RNF4 purifications from cells we found an interaction between RNF4 and USP11, the nature of this interaction remains to be elucidated. Preliminary *in vitro* data suggest that RNF4 and USP11 do not interact directly; several Importin proteins co-purifying with RNF4 could potentially play a role in facilitating the interaction (data not shown).

Interplay between ubiquitin E3 ligases and ubiquitin specific proteases are reported more often and are necessary to achieve a balanced system. This is best exemplified by studies on the deubiquitinating enzyme USP7. USP7 regulates several components of the ubiquitin machinery, including the E2 enzyme Ube2E1 and the E3 enzyme Hdm2 (13, 14). In these cases, USP7 protects these E3 enzymes from proteasomal degradation by regulating their deubiquitination. Although we did not study the direct effect of USP11 on RNF4 ubiquitination so far, we did not observe

Chapter 7

an effect on RNF4 protein stability after USP11 knockdown, suggesting that USP11 is not involved in regulating RNF4 protein levels.

Mechanistically, we showed that USP11 can counteract RNF4 activity towards the ubiquitination of SUMO-2 chains. In *in vitro* assays, USP11 can deubiquitinate hybrid SUMO2-ubiquitin chains that were produced by RNF4. Interaction studies revealed that USP11 has a low affinity for binding to SUMO2-ubiquitin chains as compared to RNF4; we did observe a strong interaction between USP11 and unanchored ubiquitin chains. Surprisingly, mutating four potential SIMs in USP11 did significantly reduce its deubiquitination activity towards SUMO2-ubiquitin. Therefore it is plausible that USP11 binds to SUMO2-ubiquitin chains through sequential interaction with ubiquitin, SUMO2 and perhaps also RNF4.

In line with recent findings (15) we found that USP11 regulates the stability of PML nuclear bodies. RNF4 ubiquitinates SUMOylated PML, resulting in the destabilization of PML nuclear bodies; USP11 can counteract this by stabilizing SUMOylated PML. PML is a tumour suppressor and is often found to be downregulated in various types of cancer; this is potentially regulated by proteasomal degradation of PML (16, 17). Blocking PML degradation with the help of USP11 would therefore be a potential interesting approach in cancer treatment. Indeed Wu and coworkers found that USP11-mediated regulation of PML stability plays an important role in brain tumour pathogenesis (15). In addition, USP11 has been linked to DNA damage repair where it regulates DNA repair proteins including BRCA2 and p53. (18). It has been shown that interfering with USP11 levels reduces survival of cancer cells upon different drug treatments (19, 20). Whether this is linked to USP11's deubiquitination activity towards SUMOylated proteins would be an interesting addition to future research on USP11. So far, we only observed an effect of USP11 on PML SUMOylation; USP11 knockdown studies in combination with a SILAC approach could be useful to identify novel SUMO target proteins that are regulated by USP11.

7

7.2 Identification of SUMOylation sites

Although SUMOylation often takes place on the so called 'SUMO consensus motif' ψ KxE/D (where ψ is a big hydrophobic amino acid and x can be any amino acid), not all of these motifs are necessarily used and SUMOylation often occurs on lysines situated in non-consensus motifs. Research on the effects of SUMOylation on individual targets is therefore often hampered by struggles to identify the acceptor lysines.

To be able to identify SUMO acceptor lysines in proteins, we have developed a method which is described in chapter 4. By introducing an arginine close to the C-terminus of SUMO-2, we were able to identify 103 SUMOylation sites by tryptic digestion and mass spectrometry analysis. We found a huge overrepresentation

of SUMO consensus motifs among the identified sites (+/- 70%), showing that the SUMO machinery has a high preference for this motif. This preference lays in the direct binding of the SUMO E2 enzyme Ubc9 to the consensus motif, which positions the catalytic site of Ubc9 towards the lysine that is subsequently SUMOylated (21, 22).

Apparently, the consensus site alone is in some cases not sufficient for efficient Ubc9 binding; several other features can induce the interaction with Ubc9 and thereby initiate SUMOylation. The identification of the so called 'phosphorylation-dependent SUMOylation motif' (PDSM) and the 'negatively charged amino acid-dependent SUMOylation motif' (NDSM) showed that site specificity can be regulated at additional levels (23-25). These studies showed that phosphorylation or negatively charged amino acids downstream of SUMO consensus sites results in a stronger interaction with Ubc9 and therefore induces SUMOylation. In our study we found the first direct evidence for PDSM regulated SUMOylation by identifying peptides for four proteins that were both SUMOylated and also phosphorylated downstream of the acceptor lysine. We also found a new additional type of extended SUMOylation motif, where the consensus motif is preceded by at least two more hydrophobic amino acids (the HCSM). The efficient SUMOylation of these kind of sites can probably also be explained by an enhanced binding of Ubc9, this was published before for the SUMO target protein RanGAP1 (22).

Surprisingly, we also identified an inverted SUMO consensus motif, suggesting that Ubc9 can bind to these sites in two directions. So far, no studies have been reported on the significance of this inverted consensus motif.

Finally, we also mapped SUMO acceptor lysines that did not fit to any form of SUMO consensus site; the question remains how specificity for these lysines is regulated. One potential explanation could be that these lysines are located in a 'SUMOylation motif' only in the structured protein but not in the unstructured peptide surrounding the lysine. In line with this hypothesis, it was previously found that the ubiquitin conjugating enzyme E2-25K was SUMOylated on a non-consensus site only in the context of a folded protein; in unstructured peptides this site was not used for SUMOylation (26). Another explanation for the SUMOylation of non-consensus sites is the non-covalent interaction between the Ubc9-SUMO thioester and a SUMO interacting motif close to the modified lysine. This mechanism of SUMOylation was previously shown for the ubiquitin-specific protease 25 (27). A third option is the binding of a SUMO E3 ligase to non-consensus motifs to induce SUMOylation; PCNA SUMOylation on lysine 164 for example depends on binding of the E3 ligase Siz1 (28). Analysis of the surrounding sequence in the identified non-consensus sites and analysis of their location in the structured protein could provide more insight into the mechanism of SUMOylation.

7.3 SUMOylation in genome stability

DNA damage and disorganization of chromosome segregation are two important sources of genome instability, an evolving hallmark of cancer (29). In chapter 5 and 6 of this thesis we have focused on a potential role for SUMOylation in maintaining genome stability.

FoxM1 SUMOylation is important for cell cycle progression

In chapter 5 we performed a large-scale proteomics screen to analyze global SUMOylation dynamics during cell-cycle progression. Among the 593 identified SUMO2 targets, we found a G2 and M phase specific increase in SUMOylation of the transcription factor FoxM1. Currently we lack insight in how this increase in SUMOylation is regulated. Potentially, it could just simply reflect the increase in total expression levels for FoxM1; this has been published to occur during S phase (30). Another explanation could be the increased binding of FoxM1 to DNA during these phases of the cell cycle; recently it was found that active promoters of genes are areas with a high SUMOylation activity (31). Interestingly, crystal structure analysis showed that the DNA-binding domain of FoxM1 has a relative low affinity for its consensus promoter sequence (32). Since SUMOylation can have both positive as well as negative effects on the binding of transcription factors to DNA, it would be interesting to study the effects of FoxM1 SUMOylation on its DNA binding abilities (33, 34). A third possibility for the observed increase in FoxM1 SUMOylation during G2 and M phase is the subcellular localization of the SUMO machinery. Colocalization of FoxM1 and either SUMO E3 ligases or SUMO specific proteases during a specific phase of the cell cycle could potentially regulate SUMOylation levels of FoxM1 (35).

Follow-up experiments brought to light that SUMOylation of FoxM1 during G2 and M phase induces its transcriptional activity by blocking the auto-inhibitory interaction between the N-terminus and the C-terminus of the protein. SUMOylation on either the N-terminal repressor domain of FoxM1 alone or on the domain separating the Forkhead part from the transcriptional activation part of the protein was sufficient to block the inhibitory interaction *in vitro*. However, mutating SUMOylation sites in either domain separately had no effect on the transcriptional activity of FoxM1, suggesting that you need to block SUMOylation completely to release autorepression. Solving the crystal structure for the folded FoxM1 protein could provide more insight in how SUMOylation is blocking the interaction between two FoxM1 molecules.

FoxM1 transcriptional activity is essential for proper cell cycle progression by regulating a set of genes that are needed for the execution of mitosis. Previously, it was shown that deregulation of FoxM1 activity induces missegregation of chromosomes, resulting in aneuploidy and thus genomic instability (36). In line with these findings, we found that decreasing FoxM1 activity by abolishing its SUMOylation induced the formation of polyploid cells. This correlates with the phenotype found in mouse

embryonic fibroblasts lacking Ubc9 expression (37) and can thus partly explain the observed defects in cells where overall SUMOylation is abolished. However, it is very unlikely that restoring FoxM1 SUMOylation alone would be sufficient to counteract these defects, since we found that SUMOylation modifies whole protein groups during cell cycle progression.

In general, SUMOylation of transcription factors inhibits their activity; FoxM1 is thus one of the exceptions to the rule (38). Inhibition of transcription factors by SUMOylation is often linked to complex formation through non-covalent interactions with SIM containing repressor complexes. The fact that FoxM1 acts as its own repressor and the observation that FoxM1 does not contain classical SIM motifs contributes to our conclusions that SUMOylation prevents the dimerization of FoxM1 proteins. A somewhat similar mechanism was previously published for the transcription factor Ikaros; SUMOylation of Ikaros induces its activity by preventing the interaction with a repressor complex (39). Interestingly, the p19ARF protein was previously identified as a negative regulator of FoxM1 activity. Binding of p19ARF to the C-terminus of FoxM1 results in inhibition of its activity by targeting FoxM1 to the nucleolus (40). It would be interesting to see whether FoxM1 SUMOylation can not only induce the relief of autorepression but also block the interaction with p19ARF.

Because of its emerging role during cell cycle progression, FoxM1 is an important subject in cancer treatment studies. Although cells need a certain level of FoxM1 activity to properly divide, high FoxM1 expression levels are often linked to many forms of human cancer (41). It is thus evident that cells need to balance FoxM1 activity to maintain genome stability. This balance is mainly kept by regulating the expression levels and by post translational modifications of FoxM1. Quickly after execution of mitosis, FoxM1 is inactivated by dephosphorylation and FoxM1 protein levels are decreased by ubiquitination and proteasomal degradation (42, 43). Intriguingly, we also identified FoxM1 as a proteasome regulated SUMO2 target in chapter 2. Since SUMOylation of FoxM1 peaks during mitosis, it would be interesting to see whether SUMOylation of FoxM1 targets the protein for ubiquitination and degradation during G1 phase. Unpublished data indeed showed that RNF4 can specifically bind to and ubiquitinate SUMOylated FoxM1 proteins *in vitro*. Knocking down RNF4 expression in cells did however not have any effect on the SUMOylation of FoxM1, suggesting a role for other, yet unknown, STUBLs. Surprisingly, FoxM1 was identified as a potential target for anticancer therapies with proteasome inhibitors. Treatment of cells with proteasome inhibitors such as MG132 decreased FoxM1 transcriptional activity and FoxM1 expression. It is unlikely that this effect is linked to the increased SUMOylation of FoxM1, since we found that this induces FoxM1 activity. The inhibitory effect of proteasome inhibition of FoxM1 can potentially be explained by the stabilization of transcriptional regulators and repressors of FoxM1 (44).

A lot of other anticancer therapies have been described that target FoxM1

Chapter 7

function, mainly on expression levels (45). However, there are still a lot of challenges in FoxM1 targeting when it comes to the delivery of inhibitors to tumours and their specificity. Interfering with FoxM1 SUMOylation could provide a high level of specificity and result in the decrease of FoxM1 transcriptional activity in tumours. Future research could focus on analyzing SUMOylation levels of FoxM1 in various cancers and should point out if it is possible to specifically target FoxM1 SUMOylation in these cancers. So far, no technique has been described to interfere with SUMOylation of individual endogenous SUMO target proteins; this is a main challenge for the scientific SUMO community.

DNA damage triggers the SUMOylation of CSB

Over the last years it became evident that SUMOylation of DNA repair proteins is an important process in the DNA damage response (46). Therefore we wanted to identify target proteins that are SUMOylated in two subpathways of the DNA damage response. In chapter 6 we have used a proteomics approach to identify proteins that are regulated by SUMO2 upon treatment with IR or UV. One of the most interesting findings in this screen, in our opinion, was the UV specific SUMOylation of CSB; this protein was therefore chosen for follow-up experiments. CSB belongs to the SWI2/SNF2 family of DNA-dependent ATPases and plays an essential role in transcription coupled nucleotide excision repair (TC-NER). Stalling of the RNA polymerase II complex (RNAPII) upon encountering a lesion in the transcribed strand initiates the strong interaction between CSB and RNAPII on the chromatin. Subsequently, CSB facilitates the recruitment of proteins that regulate the repair of the lesion and the transcriptional restart after repair (47). Mutations in either the CSA or CSB gene results in the severe autosomal recessive disorder, Cockayne syndrome (CS). CS is at least partly caused by a defect in TC-NER; CS cells fail to quickly repair lesions in the transcribed strand of active genes and fail to resume RNA synthesis after UV induced DNA damage (48).

By making point mutations in the SUMO consensus sites in CSB, we found that CSB is SUMOylated on two lysines in the N-terminus of the protein upon UV induced DNA damage. The UV-specificity of this modifications lies most likely in the increased recruitment of CSB to chromatin upon DNA damage, since chromatin are contents of the nucleus that display increased SUMOylation activity (49). Indeed, we only observed CSB SUMOylation in chromatin enriched fractions from cells exposed to UV and not in the soluble nucleus. It is important to note that a substantial fraction of the total CSB protein was already observed in the chromatin fraction in untreated cells. The increase in CSB levels in the chromatin fraction after UV treatment were modest; however, we did observe a strong depletion of CSB in the soluble nucleus shortly after UV treatment. Nevertheless, it is possible that other mechanisms are involved in the UV-specific SUMOylation of CSB, since we did not observe

SUMOylation of CSB in untreated cells. The colocalization with specific SUMO E3 ligases or conformational changes in CSB upon UV induced DNA damage are therefore interesting subjects for future research.

So far, we lack insight in the role that CSB SUMOylation plays during DNA repair; follow up experiments are needed to unravel the downstream consequences. Interestingly, it was previously published that CSB undergoes a conformational change to release its N-terminal autorepression and enable the stable CSB-chromatin interaction after UV irradiation (50). Since SUMOylation of CSB takes place on the N-terminus after UV treatment, it would be interesting to see if SUMO is involved in this conformational change; potentially SUMO could have similar effects on CSB as we found for FoxM1 in chapter 5. Several proteins have been shown to interact with the N-terminus of CSB (51): the N-terminus of CSB stimulates the incision activity of NEIL1, thereby enhancing base excision repair (52); PARP1 binding to the N-terminus of CSB results in the poly(ADP-ribosyl)ation of CSB which inhibits its ATPase activity (53) and binding of the c-Abl kinase to the N-terminus of CSB upon oxidative stress initiates the phosphorylation of CSB (54). Since SUMOylation often enhances interactions through SIMs or blocks interactions by shielding binding domains, it would be interesting to see if SUMOylation of CSB has an effect on these or other interactions. Furthermore it would be interesting to analyze the effects of CSB SUMOylation on the RNAPII complex. In general it is believed that the assembly and binding of the NER complex does not need the displacement of RNAPII per se; backtracking and/or a conformational change of the complex might be sufficient to facilitate DNA repair (47). Future research should point out if SUMOylation of CSB is somehow involved in the regulation of the RNAPII complex upon DNA damage.

Complement studies with wild type and SUMO deficient CSB in the Cockayne syndrome cell line CS1AN showed that SUMOylation of CSB is not essential for the long term survival of cells after UV irradiation. It is important to note that this cell line still expresses the N-terminal part of CSB (amino acids 1-336) and the CSB-PGBD3 fusion protein (which contains the first 465 amino acids of CSB) (55, 56). It is currently unclear whether SUMOylation of these proteins in CS1AN cells can functionally complement the SUMOylation of full-length SUMO deficient CSB in this experiment. Long term survival of cells after DNA damage only reflects their ability to adapt to stress stimuli and does not give information on efficiency and timing of DNA repair. Additional experiments are therefore essential to see whether CSB SUMOylation plays a role in the quality and quantity of DNA repair and other cellular processes. First of all, the recovery of RNA synthesis after UV treatment should be compared between cells expressing wild type or SUMO deficient CSB; a fast and efficient transcriptional restart is a feature of proper DNA repair. We found that reducing overall SUMOylation by knocking down Ubc9 does slow down RNA synthesis recovery, showing that global SUMOylation of proteins after DNA damage

Chapter 7

is important for efficient repair. Furthermore we should investigate the effect of SUMOylation on CSBs ATPase activity, *in vitro* experiments have been developed in the past to address this (57). By using a method to measure nucleotide excision repair kinetics we could analyze and quantify the efficiency of repair between wild type and SUMO deficient CSB expressing cells (58). Besides its emerging role in TC-NER, CSB has also been implicated in general transcription regulation upon stress stimuli (48). Because SUMOylation is particularly important in regulating transcription, it would be interesting to perform transcriptome analysis in cells expressing wild type or SUMO deficient CSB.

Crosstalk between SUMOylation and ubiquitination could potentially also play an important role in TC-NER. Analysis of CSB SUMOylation dynamics revealed that this is an early event after UV treatment and that the recruitment of the CSA ubiquitin E3 ligase complex initiates the destabilization of SUMOylated CSB. In contrast to a previously published paper (59), we think that the CSA complex is not regulating the direct ubiquitination of CSB after UV but induces the ubiquitination and degradation of the RNAPII complex. This results in the dissociation of CSB from chromatin, which potentially induces the deSUMOylation of CSB in the nucleus by SUMO specific proteases. These results are in conflict with a previous published project where researchers stated that RNAPII is ubiquitinated by Nedd4 but not by CSA upon DNA damage (60). Interestingly, BRCA1 has been linked to CSB ubiquitination and BRCA1 was identified as a SUMO regulated ubiquitin ligase (61, 62). Whether SUMOylation of CSB is important for its ubiquitination by BRCA1 remains to be elucidated.

Recently, it was found that another NER factor, XPC, is SUMOylated in response to DNA damage and that XPC SUMOylation initiates the recruitment of the STUBL RNF111 (10). Potentially, CSB SUMOylation could also recruit a STUBL to induce (auto)ubiquitination at sites of DNA damage. Ubiquitination of CSB upon UV induced DNA damage can be antagonized by the recruitment of the UVSSA-USP7 complex (63-65). Future research should point out whether CSB SUMOylation is involved in and/or affected by the recruitment of this complex.

Concluding remarks

The results presented in this thesis showed that SUMOylation, sometimes in coordination with other PTMs, plays an important role in protein stability, cell cycle progression and DNA repair. Regulation of proteins by a coordinated SUMOylation / deSUMOylation system is thus essential to maintain genome stability; deregulation of this balance has been linked to the development of several human cancers (66). Restoring this balance in these cancer types is therefore an attractive entry point for therapeutic interventions and could provide a high level of specificity.

In line with previous findings (67), we found that the role of SUMOylation in

cellular processes can sometimes only be explained by the simultaneous modification of groups of proteins involved in a process. Improvement of mass spectrometry based research in the near future should give a complete coverage of the SUMO landscape in different cellular processes. In addition, site specific identification of SUMO target proteins will facilitate the studies on individual SUMOylated proteins. This will help us understand whether SUMOylation of individual proteins can have clear and significant downstream consequences; in a lot of cases it is more likely that individual modifications only add up to the adequate regulation of a particular process. A combination of mass spectrometry based research and follow up experiments on identified SUMOylated proteins will help us to understand the emerging role of SUMOylation in eukaryotic life.

Reference List

- Walsh, C. T., Garneau-Tsodikova, S., and Gatto, G. J., Jr. (2005) Protein posttranslational modifications: the chemistry of proteome diversifications. *Angew. Chem. Int. Ed Engl.* 44, 7342-7372
- Glickman, M. H., and Ciechanover, A. (2002) The ubiquitin-proteasome proteolytic pathway: destruction for the sake of construction. *Physiol Rev.* 82, 373-428
- Xu, P., Duong, D. M., Seyfried, N. T., Cheng, D., Xie, Y., Robert, J., Rush, J., Hochstrasser, M., Finley, D., and Peng, J. (2009) Quantitative proteomics reveals the function of unconventional ubiquitin chains in proteasomal degradation. *Cell* 137, 133-145
- Prudden, J., Pebernard, S., Raffa, G., Slavin, D. A., Perry, J. J., Tainer, J. A., McGowan, C. H., and Boddy, M. N. (2007) SUMO-targeted ubiquitin ligases in genome stability. *EMBO J.* 26, 4089-4101
- Sun, H., Levenson, J. D., and Hunter, T. (2007) Conserved function of RNF4 family proteins in eukaryotes: targeting a ubiquitin ligase to SUMOylated proteins. *EMBO J.* 26, 4102-4112
- Tatham, M. H., Geoffroy, M. C., Shen, L., Plechanovova, A., Hattersley, N., Jaffray, E. G., Palvimo, J. J., and Hay, R. T. (2008) RNF4 is a poly-SUMO-specific E3 ubiquitin ligase required for arsenic-induced PML degradation. *Nat. Cell Biol.* 10, 538-546
- Lallemand-Breitenbach, V., Jeanne, M., Benhenda, S., Nasr, R., Lei, M., Peres, L., Zhou, J., Zhu, J., Raught, B., and De, T. H. (2008) Arsenic degrades PML or PML-RAR α through a SUMO-triggered RNF4/ubiquitin-mediated pathway. *Nat. Cell Biol.* 10, 547-555
- Hickey, C. M., Wilson, N. R., and Hochstrasser, M. (2012) Function and regulation of SUMO proteases. *Nat. Rev. Mol. Cell Biol.* 13, 755-766
- Ciechanover, A., and Schwartz, A. L. (1998) The ubiquitin-proteasome pathway: the complexity and myriad functions of proteins death. *Proc. Natl. Acad. Sci. U. S. A.* 95, 2727-2730
- Poulsen, S. L., Hansen, R. K., Wagner, S. A., van, C. L., van Belle, G. J., Streicher, W., Wikstrom, M., Choudhary, C., Houtsmuller, A. B., Marteijn, J. A., Bekker-Jensen, S., and Mailand, N. (2013) RNF111/Arkadia is a SUMO-targeted ubiquitin ligase that facilitates the DNA damage response. *J. Cell Biol.* 201, 797-807
- Sun, H., and Hunter, T. (2012) Poly-small ubiquitin-like modifier (PolySUMO)-binding proteins identified through a string search. *J. Biol. Chem.* 287, 42071-42083
- Weissman, A. M. (2001) Themes and variations on ubiquitylation. *Nat. Rev. Mol. Cell Biol.* 2, 169-178
- Sarkari, F., Wheaton, K., La, D. A., Mohamed, M., Shaikh, F., Khatun, R., Arrowsmith, C. H., Frappier, L., Saridakis, V., and Sheng, Y. (2013) Ubiquitin-specific protease 7 is a regulator of ubiquitin-conjugating enzyme UbE2E1. *J. Biol. Chem.* 288, 16975-16985
- Cummins, J. M., and Vogelstein, B. (2004) HAUSP is required for p53 destabilization. *Cell Cycle* 3, 689-692
- Wu, H. C., Lin, Y. C., Liu, C. H., Chung, H. C., Wang, Y. T., Lin, Y. W., Ma, H. I., Tu, P. H., Lawler, S. E., and Chen, R. H. (2014) USP11 regulates PML stability to control Notch-induced malignancy in brain tumours. *Nat. Commun.* 5, 3214
- Gurrieri, C., Capodiecì, P., Bernardi, R., Scaglioni, P. P., Nafa, K., Rush, L. J., Verbel, D. A., Cordon-Cardo, C., and Pandolfi, P. P.

- (2004) Loss of the tumor suppressor PML in human cancers of multiple histologic origins. *J. Natl. Cancer Inst.* 96, 269-279
17. Chen, R. H., Lee, Y. R., and Yuan, W. C. (2012) The role of PML ubiquitination in human malignancies. *J. Biomed. Sci.* 19, 81
 18. Reyes-Turcu, F. E., Ventii, K. H., and Wilkinson, K. D. (2009) Regulation and cellular roles of ubiquitin-specific deubiquitinating enzymes. *Annu. Rev. Biochem.* 78, 363-397
 19. Schoenfeld, A. R., Apgar, S., Dolios, G., Wang, R., and Aaronson, S. A. (2004) BRCA2 is ubiquitinated in vivo and interacts with USP11, a deubiquitinating enzyme that exhibits prosurvival function in the cellular response to DNA damage. *Mol. Cell Biol.* 24, 7444-7455
 20. Burkhart, R. A., Peng, Y., Norris, Z. A., Tholey, R. M., Talbott, V. A., Liang, Q., Ai, Y., Miller, K., Lal, S., Cozzitorto, J. A., Witkiewicz, A. K., Yeo, C. J., Gehrman, M., Napper, A., Winter, J. M., Sawicki, J. A., Zhuang, Z., and Brody, J. R. (2013) Mitoxantrone Targets Human Ubiquitin-Specific Peptidase 11 (USP11) and Is a Potent Inhibitor of Pancreatic Cancer Cell Survival. *Mol. Cancer Res.* 11, 901-911
 21. Rodriguez, M. S., Dargemont, C., and Hay, R. T. (2001) SUMO-1 conjugation in vivo requires both a consensus modification motif and nuclear targeting. *J. Biol. Chem.* 276, 12654-12659
 22. Bernier-Villamor, V., Sampson, D. A., Matunis, M. J., and Lima, C. D. (2002) Structural basis for E2-mediated SUMO conjugation revealed by a complex between ubiquitin-conjugating enzyme Ubc9 and RanGAP1. *Cell* 108, 345-356
 23. Hietakangas, V., Anckar, J., Blomster, H. A., Fujimoto, M., Palvimo, J. J., Nakai, A., and Sistonen, L. (2006) PDSM, a motif for phosphorylation-dependent SUMO modification. *Proc. Natl. Acad. Sci. U. S. A.* 103, 45-50
 24. Yang, S. H., Galanis, A., Witty, J., and Sharrocks, A. D. (2006) An extended consensus motif enhances the specificity of substrate modification by SUMO. *EMBO J.* 25, 5083-5093
 25. Anckar, J., and Sistonen, L. (2007) SUMO: getting it on. *Biochem. Soc. Trans.* 35, 1409-1413
 26. Pichler, A., Knipscheer, P., Oberhofer, E., van Dijk, W. J., Korner, R., Olsen, J. V., Jentsch, S., Melchior, F., and Sixma, T. K. (2005) SUMO modification of the ubiquitin-conjugating enzyme E2-25K. *Nat. Struct. Mol. Biol.* 12, 264-269
 27. Meulmeester, E., Kunze, M., Hsiao, H. H., Urlaub, H., and Melchior, F. (2008) Mechanism and consequences for paralog-specific sumoylation of ubiquitin-specific protease 25. *Mol. Cell* 30, 610-619
 28. Yunus, A. A., and Lima, C. D. (2009) Structure of the Siz/PIAS SUMO E3 ligase Siz1 and determinants required for SUMO modification of PCNA. *Mol. Cell* 35, 669-682
 29. Hanahan, D., and Weinberg, R. A. (2011) Hallmarks of cancer: the next generation. *Cell* 144, 646-674
 30. Korver, W., Roose, J., and Clevers, H. (1997) The winged-helix transcription factor Trident is expressed in cycling cells. *Nucleic Acids Res.* 25, 1715-1719
 31. Neyret-Kahn, H., Benhamed, M., Ye, T., Le, G. S., Cossec, J. C., Lapaquette, P., Bischof, O., Ouspenskaia, M., Dasso, M., Seeler, J., Davidson, I., and Dejean, A. (2013) Sumoylation at chromatin governs coordinated repression of a transcriptional program essential for cell growth and proliferation. *Genome Res.*
 32. Littler, D. R., Alvarez-Fernandez, M., Stein, A., Hibbert, R. G., Heidebrecht, T., Aloy, P., Medema, R. H., and Perrakis, A. (2010) Structure of the FoxM1 DNA-recognition domain bound to a promoter sequence. *Nucleic Acids Res.* 38, 4527-4538
 33. Goodson, M. L., Hong, Y., Rogers, R., Matunis, M. J., Park-Sarge, O. K., and Sarge, K. D. (2001) Sumo-1 modification regulates the DNA binding activity of heat shock transcription factor 2, a promyelocytic leukemia nuclear body associated transcription factor. *J. Biol. Chem.* 276, 18513-18518
 34. Ross, S., Best, J. L., Zon, L. I., and Gill, G. (2002) SUMO-1 modification represses Sp3 transcriptional activation and modulates its subnuclear localization. *Mol. Cell* 10, 831-842
 35. Gill, G. (2004) SUMO and ubiquitin in the nucleus: different functions, similar mechanisms? *Genes Dev.* 18, 2046-2059
 36. Laoukili, J., Kooistra, M. R., Bras, A., Kauw, J., Kerkhoven, R. M., Morrison, A., Clevers, H., and Medema, R. H. (2005) FoxM1 is required for execution of the mitotic programme and chromosome stability. *Nat. Cell Biol.* 7, 126-136
 37. Nacerddine, K., Lehembre, F., Bhaumik, M., Artus, J., Cohen-Tannoudji, M., Babinet, C., Pandolfi, P. P., and Dejean, A. (2005) The SUMO pathway is essential for nuclear integrity and chromosome segregation in mice. *Dev. Cell* 9, 769-779

38. Lyst, M. J., and Stancheva, I. (2007) A role for SUMO modification in transcriptional repression and activation. *Biochem. Soc. Trans.* 35, 1389-1392
39. Gomez-del, A. P., Koipally, J., and Georgopoulos, K. (2005) Ikaros SUMOylation: switching out of repression. *Mol. Cell Biol.* 25, 2688-2697
40. Kalinichenko, V. V., Major, M. L., Wang, X., Petrovic, V., Kuechle, J., Yoder, H. M., Dennewitz, M. B., Shin, B., Datta, A., Raychaudhuri, P., and Costa, R. H. (2004) Foxm1b transcription factor is essential for development of hepatocellular carcinomas and is negatively regulated by the p19ARF tumor suppressor. *Genes Dev.* 18, 830-850
41. Wierstra, I. (2013) FOXM1 (Forkhead box M1) in tumorigenesis: overexpression in human cancer, implication in tumorigenesis, oncogenic functions, tumor-suppressive properties, and target of anticancer therapy. *Adv. Cancer Res.* 119, 191-419
42. Laoukili, J., Alvarez-Fernandez, M., Stahl, M., and Medema, R. H. (2008) FoxM1 is degraded at mitotic exit in a Cdh1-dependent manner. *Cell Cycle* 7, 2720-2726
43. Chen, Y. J., Dominguez-Brauer, C., Wang, Z., Asara, J. M., Costa, R. H., Tyner, A. L., Lau, L. F., and Raychaudhuri, P. (2009) A conserved phosphorylation site within the forkhead domain of FoxM1B is required for its activation by cyclin-CDK1. *J. Biol. Chem.* 284, 30695-30707
44. Bhat, U. G., Halasi, M., and Gartel, A. L. (2009) FoxM1 is a general target for proteasome inhibitors. *PLoS. One.* 4, e6593
45. Halasi, M., and Gartel, A. L. (2013) Targeting FOXM1 in cancer. *Biochem. Pharmacol.* 85, 644-652
46. Jackson, S. P., and Durocher, D. (2013) Regulation of DNA damage responses by ubiquitin and SUMO. *Mol. Cell* 49, 795-807
47. Foustari, M., and Mullenders, L. H. (2008) Transcription-coupled nucleotide excision repair in mammalian cells: molecular mechanisms and biological effects. *Cell Res.* 18, 73-84
48. Velez-Cruz, R., and Egly, J. M. (2013) Cockayne syndrome group B (CSB) protein: at the crossroads of transcriptional networks. *Mech. Ageing Dev.* 134, 234-242
49. Cubenas-Potts, C., and Matunis, M. J. (2013) SUMO: a multifaceted modifier of chromatin structure and function. *Dev. Cell* 24, 1-12
50. Lake, R. J., Geyko, A., Hemashettar, G., Zhao, Y., and Fan, H. Y. (2010) UV-induced association of the CSB remodeling protein with chromatin requires ATP-dependent relief of N-terminal autorepression. *Mol. Cell* 37, 235-246
51. Aamann, M. D., Muftuoglu, M., Bohr, V. A., and Stevnsner, T. (2013) Multiple interaction partners for Cockayne syndrome proteins: implications for genome and transcriptome maintenance. *Mech. Ageing Dev.* 134, 212-224
52. Muftuoglu, M., de Souza-Pinto, N. C., Dogan, A., Aamann, M., Stevnsner, T., Rybanska, I., Kirkali, G., Dizdaroglu, M., and Bohr, V. A. (2009) Cockayne syndrome group B protein stimulates repair of formamidopyrimidines by NEIL1 DNA glycosylase. *J. Biol. Chem.* 284, 9270-9279
53. Thorslund, T., von, K. C., Harrigan, J. A., Indig, F. E., Christiansen, M., Stevnsner, T., and Bohr, V. A. (2005) Cooperation of the Cockayne syndrome group B protein and poly(ADP-ribose) polymerase 1 in the response to oxidative stress. *Mol. Cell Biol.* 25, 7625-7636
54. Imam, S. Z., Indig, F. E., Cheng, W. H., Saxena, S. P., Stevnsner, T., Kufe, D., and Bohr, V. A. (2007) Cockayne syndrome protein B interacts with and is phosphorylated by c-Abl tyrosine kinase. *Nucleic Acids Res.* 35, 4941-4951
55. Weiner, A. M., and Gray, L. T. (2013) What role (if any) does the highly conserved CSB-PGBD3 fusion protein play in Cockayne syndrome? *Mech. Ageing Dev.* 134, 225-233
56. Troelstra, C., van, G. A., de, W. J., Vermeulen, W., Bootsma, D., and Hoeijmakers, J. H. (1992) ERCC6, a member of a subfamily of putative helicases, is involved in Cockayne's syndrome and preferential repair of active genes. *Cell* 71, 939-953
57. Citterio, E., Rademakers, S., van der Horst, G. T., van Gool, A. J., Hoeijmakers, J. H., and Vermeulen, W. (1998) Biochemical and biological characterization of wild-type and ATPase-deficient Cockayne syndrome B repair protein. *J. Biol. Chem.* 273, 11844-11851
58. Choi, J. H., Gaddameedhi, S., Kim, S. Y., Hu, J., Kemp, M. G., and Sancar, A. (2013) Highly specific and sensitive method for measuring nucleotide excision repair kinetics of ultraviolet photoproducts in human cells. *Nucleic Acids Res.*
59. Groisman, R., Kuraoka, I., Chevallier, O., Gaye, N., Magnaldo, T., Tanaka, K., Kisselev, A. F., Harel-Bellan, A., and Nakatani, Y. (2006) CSA-dependent degradation of CSB by the ubiquitin-proteasome pathway establishes a link between complementation factors of the Cockayne syndrome. *Genes*

- Dev. 20, 1429-1434
60. Anindya, R., Aygun, O., and Svejstrup, J. Q. (2007) Damage-induced ubiquitylation of human RNA polymerase II by the ubiquitin ligase Nedd4, but not Cockayne syndrome proteins or BRCA1. *Mol. Cell* 28, 386-397
 61. Wei, L., Lan, L., Yasui, A., Tanaka, K., Saijo, M., Matsuzawa, A., Kashiwagi, R., Maseki, E., Hu, Y., Parvin, J. D., Ishioka, C., and Chiba, N. (2011) BRCA1 contributes to transcription-coupled repair of DNA damage through polyubiquitination and degradation of Cockayne syndrome B protein. *Cancer Sci.* 102, 1840-1847
 62. Morris, J. R., Boutell, C., Keppler, M., Densham, R., Weekes, D., Alamshah, A., Butler, L., Galanty, Y., Pangon, L., Kiuchi, T., Ng, T., and Solomon, E. (2009) The SUMO modification pathway is involved in the BRCA1 response to genotoxic stress. *Nature* 462, 886-890
 63. Nakazawa, Y., Sasaki, K., Mitsutake, N., Matsuse, M., Shimada, M., Nardo, T., Takahashi, Y., Ohyama, K., Ito, K., Mishima, H., Nomura, M., Kinoshita, A., Ono, S., Takenaka, K., Masuyama, R., Kudo, T., Slor, H., Utani, A., Tateishi, S., Yamashita, S., Stefanini, M., Lehmann, A. R., Yoshiura, K., and Ogi, T. (2012) Mutations in UVSSA cause UV-sensitive syndrome and impair RNA polymerase II processing in transcription-coupled nucleotide-excision repair. *Nat. Genet.* 44, 586-592
 64. Schwertman, P., Lagarou, A., Dekkers, D. H., Raams, A., van der Hoek, A. C., Laffeber, C., Hoeijmakers, J. H., Demmers, J. A., Fousteri, M., Vermeulen, W., and Marteijn, J. A. (2012) UV-sensitive syndrome protein UVSSA recruits USP7 to regulate transcription-coupled repair. *Nat. Genet.* 44, 598-602
 65. Zhang, X., Horibata, K., Saijo, M., Ishigami, C., Ukai, A., Kanno, S., Tahara, H., Neilan, E. G., Honma, M., Nohmi, T., Yasui, A., and Tanaka, K. (2012) Mutations in UVSSA cause UV-sensitive syndrome and destabilize ERCC6 in transcription-coupled DNA repair. *Nat. Genet.* 44, 593-597
 66. Bettermann, K., Benesch, M., Weis, S., and Haybaeck, J. (2012) SUMOylation in carcinogenesis. *Cancer Lett.* 316, 113-125
 67. Psakhye, I., and Jentsch, S. (2012) Protein group modification and synergy in the SUMO pathway as exemplified in DNA repair. *Cell* 151, 807-820



Nederlandse samenvatting

Chapter 8. Nederlandse samenvatting

Cellen worden beschouwd als de basale bouwstenen van het leven. Celdeling zorgt ervoor dat één enkele cel uiteindelijk uitgroeit tot een compleet organisme. Door cel specialisatie ontstaan groepen cellen met een specifieke structuur die uiteindelijk vorm geven aan verschillende weefsels en organen. Alle cellen bevatten de erfelijke informatie die nodig is voor het uitvoeren van celdeling en specialisatie, deze informatie is opgeslagen in de vorm van DNA gelegen in chromosomen. DNA bestaat uit twee lange strengen van vier verschillende nucleotiden, de erfelijke informatie ligt besloten in de specifieke volgorde van deze nucleotiden. Een gen is zo'n specifiek stuk DNA, hiervan wordt een kopie gemaakt in de vorm van RNA, een proces dat we kennen als transcriptie. De code op het RNA wordt vervolgens vertaald in eiwitten (translatie) door een specifieke volgorde van aminozuren aan elkaar te koppelen; drie aaneensluitende nucleotiden in het RNA coderen voor één van de twintig bestaande aminozuren. De gevormde eiwitten reguleren allerlei biologische processen in de cel die nodig zijn voor een efficiënte celdeling en specialisatie.

Het menselijk genoom bevat tussen de 20.000 en 25.000 genen; theoretisch gezien zou dit dus resulteren in dezelfde hoeveelheid eiwitten die in een cel gemaakt kunnen worden. Er zijn echter verschillende processen in de cel die ervoor zorgen dat één gen kan resulteren in verschillende varianten RNA transcripten. De totale set van eiwitten die gemaakt wordt in de cel, het proteoom, is dus velen malen groter dan de hoeveelheid genen. De functionele diversiteit van het proteoom wordt verder uitgebreid door post-translationele modificaties (PTMs) van eiwitten; PTMs bestaan uit kleine chemische veranderingen, of de binding van kleine eiwitten aan aminozuren. Modificaties van eiwitten worden gereguleerd door een set enzymen. PTMs kunnen worden gekoppeld aan aminozuren in eiwitten door enzymen die we ligases noemen, een andere set enzymen (proteases) kunnen deze modificaties weer verwijderen. Deze dynamische modificaties worden door de cel gebruikt om de functie van eiwitten te veranderen om zo cellulaire processen te reguleren.

Het onderzoek in dit proefschrift is gericht op één van deze PTMs, een eiwit genaamd Small Ubiquitin-like Modifier (SUMO). SUMOs behoren tot de familie van ubiquitine-achtige eiwitten, deze eiwitten binden aan één specifiek soort aminozuur (lysines) in andere eiwitten. Het proces waarin SUMO bindt aan een lysine in een ander eiwit noemen we SUMOylering. Voorafgaand onderzoek heeft aangetoond dat SUMOylering essentieel is voor de ontwikkeling en levensvatbaarheid van organismen. Desondanks hebben we nog maar weinig inzicht in welke eiwitten worden geSUMOyleerd onder bepaalde omstandigheden en wat de functionele consequentie is van deze modificatie. Daarom hebben we in dit proefschrift een techniek gebruikt waarmee we eiwitten kunnen identificeren die geSUMOyleerd

worden, deze techniek heet massa spectrometrie (MS). Met opvolgende experimenten op enkele geïdentificeerde eiwitten hebben we geprobeerd meer inzicht te krijgen in de rol die SUMO speelt in verschillende cellulaire processen.

Binding van ubiquitine aan andere eiwitten resulteert in veel gevallen in de degradatie van dat eiwit door een eiwitcomplex genaamd het proteasoom. Lange tijd werd gedacht dat SUMOylering en ubiquitineren twee onafhankelijke processen zijn en dat SUMOylering niet leidt tot eiwitafbraak. In hoofdstuk 2 tonen we echter aan dat SUMO en ubiquitine op sommige eiwitten samenwerken. Door de activiteit van het proteasoom te remmen, waren we in staat om met behulp van MS drieënzeventig eiwitten te identificeren waarop SUMO en ubiquitine samenwerken. Voor deze eiwitten werkt de SUMOylering als een signaal om vervolgens geubiquitineerd en afgebroken te worden. Andere publicaties betreffende dit onderwerp lieten zien dat dit onder andere gereguleerd wordt door het eiwit RNF4, een ligase die specifiek bindt aan geSUMOyleerde eiwitten om vervolgens deze eiwitten te ubiquitineren. Verder toonden we in dit hoofdstuk aan dat het proteasoom een belangrijke rol speelt bij het recyclen van niet-gebonden 'beschikbare' SUMO eiwitten die gebruikt kunnen worden voor de SUMOylering van een andere set eiwitten.

In hoofdstuk 3 zijn we opzoek gegaan naar eiwitten die interacteren met RNF4 om zo meer te weten te komen over de samenwerking tussen SUMO en ubiquitine. Eén van de eiwitten die we hebben geïdentificeerd als bindingspartner van RNF4 is de ubiquitine specifieke protease USP11. Met proeven in reageerbuizen toonden we aan dat RNF4 in staat is om ubiquitine eiwitten te koppelen aan SUMO eiwitten en dat USP11 deze ubiquitine eiwitten weer kan verwijderen. Waar RNF4 dus de ubiquitineren en daarbij de afbraak van geSUMOyleerde eiwitten initieert, kan USP11 dit tegenwerken door de ubiquitine eiwitten weer te verwijderen. Eén van de eiwitten waarop dit proces plaats vindt in cellen is PML. Dit eiwit vormt kleine complexen in de kern van een cel, zogenaamde kernlichaampjes. We ontdekten dat USP11 deze PML kernlichaampjes beschermt voor RNF4 geïnduceerde afbraak in respons op DNA schade.

SUMOylering vindt vaak plaats op een lysine die zich bevindt in een zogenaamde SUMO 'consensus' sequentie van vier specifieke aminozuren op een rij. Lang niet alle bestaande SUMO consensus sequenties worden echter gebruikt voor SUMOylering en SUMO kan ook aan lysines binden die zich niet bevinden in deze sequentie. Wetenschappelijk onderzoek naar SUMOylering wordt daardoor vaak bemoeilijkt door een gebrek aan kennis over de exacte plekken in een eiwit waar SUMO kan binden. Daarom hebben we in hoofdstuk 4 een techniek ontworpen waarmee we op grote schaal SUMO-bindingsplekken kunnen identificeren. Door een mutatie aan te brengen in het SUMO eiwit werd het makkelijker om met behulp van massa spectrometrie SUMO-bindingsplekken te identificeren. In totaal hebben we 103 lysines geïdentificeerd in 82 verschillende eiwitten waaraan SUMO

Chapter 8

bindt. Analyse van de aminozuren rondom de geïdentificeerde lysines liet zien dat SUMOylering inderdaad vaak plaats vindt op de SUMO consensus sequentie (76 van de 103). Bovendien ontdekten we dat de SUMO consensus sequentie in sommige gevallen ook gebruikt wordt voor SUMOylering wanneer deze een omgekeerde volgorde heeft in het eiwit. Verder toonden we aan dat een cluster van zogenaamde hydrofobe aminozuren rondom de SUMO consensus sequentie kunnen bijdragen aan efficiënte SUMOylering. Ook hebben we enkele eiwitten geïdentificeerd waarbij de SUMOylering wordt gereguleerd door de fosforylering (een andere PTM) van een aminozuur in de buurt van de gemodificeerde lysine.

Voorafgaand onderzoek heeft aangetoond dat SUMOylering een essentiële rol speelt bij de levenscyclus van de cel, de celcyclus. Tijdens de celcyclus vinden er een opeenvolgende reeks processen plaats in een cel (verdeeld in verschillende fases) die leiden tot groei en de deling in twee nieuwe dochtercellen die elk weer hetzelfde proces ondergaan. Ondanks dat we weten dat SUMO een belangrijke rol speelt tijdens deze processen, hebben we nog maar weinig inzicht in welke eiwitten worden gereguleerd door SUMOylering tijdens de celcyclus. Daarom hebben we in hoofdstuk 5 met behulp van chemische stoffen cellen gesynchroniseerd in een aantal verschillende fases van de celcyclus. Vervolgens hebben we in deze verschillende celpopulaties geSUMOyleerde eiwitten geïdentificeerd en gekwantificeerd. In totaal hebben we 593 geSUMOyleerde eiwitten kunnen identificeren, van 249 van deze eiwitten veranderde de SUMOylering tijdens verschillende fases van de celcyclus. Bovendien hebben we met deze methode 203 lysines geïdentificeerd waar SUMO aan bindt. In het resterende deel van dit hoofdstuk hebben we ingezoomd op één door SUMO gereguleerd eiwit: FoxM1.

FoxM1 is een zogenaamde transcriptiefactor die de expressie van genen reguleert die essentieel zijn voor de deling van een cel. We zagen dat de SUMOylering van FoxM1 toenam in die fases van de celcyclus waar een verhoogde FoxM1 activiteit nodig is. Door de lysines waaraan SUMO bindt in FoxM1 te muteren vonden we dat SUMOylering belangrijk is voor de activatie van FoxM1. Mechanistisch gezien voorkomt SUMOylering de interactie tussen twee FoxM1 eiwitten; deze zogenaamde dimerisatie van FoxM1 heeft een remmende werking op zijn eigen activiteit. Functioneel gezien vonden we dat de activatie van FoxM1 door SUMO belangrijk is voor een goede celdeling. Cellen die de FoxM1 mutant tot expressie brengen die niet langer geSUMOyleerd kan worden, bevatten vaker meerdere sets chromosomen, wat erop duidt dat er in deze cellen iets mis gaat bij de deling.

Een andere belangrijke rol voor SUMOylering is de regulatie van processen die betrokken zijn bij het herstellen van beschadigd DNA. Ook hierbij is er een gebrek aan inzicht in welke eiwitten daarbij door SUMO gemodificeerd en gereguleerd worden. In hoofdstuk 6 hebben we geSUMOyleerde eiwitten geïdentificeerd in cellen waar DNA schade is toegebracht door behandeling met ultraviolet licht (UV)

of ioniserende straling (IR). We kwamen tot de ontdekking dat voor verschillende eiwitten SUMOylering alleen plaatsvindt na UV en/of IR behandeling. Tijdens het vervolg onderzoek hebben we ons gericht op de SUMOylering van het Cockayne Syndroom-B (CSB) eiwit, die specifiek plaatsvindt na UV geïnduceerde DNA schade.

Het CSB eiwit speelt een essentiële rol bij een specifiek DNA-herstelmechanisme, namelijk Transcriptie-gekoppeld DNA herstel (TCR). Dit herstelmechanisme wordt geactiveerd wanneer de transcriptie van een gen door een polymerase geblokkeerd wordt door de aanwezigheid van DNA schade. CSB bindt hierbij aan de polymerase en is verantwoordelijk voor het rekruteren van eiwitten die de schade kunnen detecteren en herstellen. Patiënten met Cockayne Syndroom (CS) hebben een mutatie in het CSA of CSB gen waardoor het TCR mechanisme niet meer werkt. Cellen afkomstig van een CS patiënt vertonen daarom een overgevoeligheid voor UV-licht en falen in het herstarten van transcriptie na UV geïnduceerde DNA schade.

We toonden aan dat de SUMOylering van CSB na UV geïnduceerde DNA schade zeer efficiënt is en voornamelijk plaats vindt op twee SUMO consensus sequenties in het eiwit. De overgevoeligheid van CS patiëntcellen voor UV kon worden teruggebracht door de expressie van zowel het originele CSB eiwit evenals het CSB eiwit dat niet langer geSUMOyleerd kan worden. Dit laat zien dat de SUMOylering van CSB niet essentieel is voor cellen om te overleven na UV geïnduceerde DNA schade. Vervolg experimenten zijn echter nog nodig om te kijken of de SUMOylering van CSB belangrijk is voor de kwaliteit en kwantiteit van DNA herstel.

Tevens zagen we dat de SUMOylering van CSB zeer snel na UV geïnduceerde DNA schade plaatsvindt en daarna weer afneemt. We toonden aan dat het rekruteren van CSA door CSB een rol speelt bij deze afname in geSUMOyleerd CSB. CSA is onderdeel van een ubiquitine E3 ligase complex; potentieel zou CSA dus kunnen werken als een SUMO specifieke ubiquitine E3 ligase op CSB. Dit bleek echter niet het geval te zijn en we denken nu dat CSA nodig is om de polymerase waar CSB aan bindt na UV behandeling te ubiquitineren. Dit zou kunnen leiden tot de dissociatie van CSB van het beschadigde DNA, waarna de SUMO eiwitten van CSB worden verwijderd door SUMO specifieke proteases in de nucleus.

Afsluitende opmerking

De resultaten in dit proefschrift tonen aan dat SUMOylering, soms in samenwerking met andere PTMs, een belangrijke rol speelt in eiwit stabiliteit, de celcyclus en DNA herstelmechanismen. De regulatie van eiwitten door een gebalanceerd SUMOylering / deSUMOylering systeem is dus essentieel om het genoom intact te houden; in verschillende humane kanker types is gevonden dat deze balans verstoord is. Het herstellen van deze balans is daarom een interessant onderwerp voor toekomstig onderzoek en een potentiële invalshoek voor de behandeling van deze vormen van kanker.

Chapter 8

In lijn met wat andere onderzoeksgroepen hebben gepubliceerd, ontdekten we dat de rol van SUMOylering in cellulaire processen in sommige gevallen alleen verklaard kan worden door de modificatie van groepen eiwitten. Door de ontwikkeling van de massa spectrometrie techniek zou het in de toekomst mogelijk moeten zijn om het complete 'SUMO landschap' tijdens verschillende cellulaire processen in kaart te brengen. Daarbij kan de techniek die we ontwikkeld hebben om de plekken in een eiwit waar SUMO bindt te identificeren bijdragen aan het onderzoek naar individuele geSUMOyleerde eiwitten. Bovendien kunnen we daardoor analyseren of de SUMOylering van individuele eiwitten grote gevolgen heeft; in veel gevallen is het waarschijnlijker dat dit alleen een kleine bijdrage heeft aan de regulatie van een cellulair proces. Een combinatie van massa spectrometrie en vervolgonderzoek naar de geïdentificeerde geSUMOyleerde eiwitten zal ons uiteindelijk meer inzicht geven in de belangrijke rol die SUMOylering speelt in het leven.

List of abbreviations

53BP1	Tumor suppressor p53-binding protein 1
Aos1	Activation of Smt3
APC/C	anaphase-promoting complex/cyclosome
ATG12	Autophagy-Related Protein 12
ATG8	Autophagy-Related Protein 8
ATP	Adenosine triphosphate
BCA	Bicinchoninic acid assay
BER	Base Excision Repair
BRCA1	Breast Cancer Type 1 Susceptibility Protein
BRCA2	Breast Cancer Type 2 Susceptibility Protein
BrdU	5-bromo-2'-deoxyuridine
BTB	Broad-Complex, Tramtrack and Bric-a-brac
BubR1	Budding uninhibited by benzimidazoles 1 beta
BZEL	Zinc finger and BTB-containing protein 46
C-Abl	Abelson tyrosine-protein kinase 1
CBX4	Chromobox Protein Homolog 4
Cdc48	Cell division control protein 48
CDK1	Cyclin-Dependent Kinase 1
cDNA	Circular DNA
CENP	Centromere protein
CFP	Cyan Fluorescent Protein
CID	Collision-induced dissociation
CMV	Cytomegalovirus
CPC	Chromosomal passenger complex
CPT	Camptothecin
CS	Cockayne Syndrome
CSA	Cockayne syndrome A
CSB	Cockayne syndrome B
CSN	COP9 signalosome
DAPI	4',6-diamidino-2-phenylindole
Daxx	Death Domain-Associated Protein 6
DDB1	DNA damage-binding protein 1
DDR	DNA damage response
DeSI	Desumoylating isopeptidase
DIC	Differential Interference Contrast
DMEM	Dulbecco's Modified Eagle's Medium
DNA	Deoxyribonucleic acid
DNMT1	DNA (cytosine-5)-methyltransferase 1
DSB	Double Strand Break
DTT	Dithiothreitol
DUB	Deubiquitinating enzyme
DUSP	Domain present in Ubiquitin-Specific Proteases
Elisa	Enzyme-Linked Immunosorbent Assay
Elk-1	E26 transformation-specific domain-containing protein 1
FACS	Fluorescence-Activated Cell Sorting

List of abbreviations

FAT10	HLA-F adjacent transcript 10
FBS	Fetal Bovine Serum
FKH	Forkhead winged helix DNA binding domain
FoxM1	Forkhead box protein M1
GATA-1	GATA-binding factor 1
GFP	Green Fluorescent Protein
GO	Gene Ontology
GST	Glutathione S-transferase
HA	Hemagglutinin
HCD	Higher-Collisional Dissociation
HCSM	Hydrophobic Cluster SUMOylation Motif
HDAC	Histone deacetylase
HEK293	Human Embryonic Kidney 293
HER2C	Human epidermal growth factor receptor 2c
HIF-1 α	Hypoxia-inducible factor 1-alpha
His-tag	Polyhistidine-tag
hnRNP M	Heterogeneous nuclear ribonucleoprotein M
HR	Homologous recombination
HRP	Horseradish peroxidase
HU	Hydroxyurea
HUB1	Histone monoubiquitination 1
I κ B α	NF- κ B inhibitor alpha
IKK γ	Inhibitor of NF- κ B kinase subunit gamma
IMAC	Immobilized metal affinity chromatography
IP	Immunoprecipitation
IPTG	Isopropyl- β -D-thiogalactopyranoside
IR	Ionizing Radiation
IRES	Internal Ribosome Entry Site
ISG15	Interferon-stimulated gene 15
LC	Liquid Chromatography
LDS	Lithium Dodecyl Sulphate
LFQ	Label-Free Quantification
LTQ	Linear Ion Trap Mass Spectrometer
LV	Lentivirus
LysC	Lysyl Endopeptidase
m/z	Mass/charge ratio
MBP	Maltose-Binding Protein
MCF-7	Michigan Cancer Foundation-7
MCODE	Molecular Complex Detection
MDC1	Mediator of DNA damage checkpoint protein 1
MEF	Mouse embryonic fibroblast
MES	2-(N-morpholino)ethanesulfonic acid
MMS	Methylmethane sulfonate
Mms2	Methyl methanesulfonate sensitive 2
MOPS	3-(N-morpholino)propanesulfonic acid
mRNA	Messenger RNA
MS	Mass spectrometry

List of abbreviations

MS/MS	Tandem mass spectrometry
NB	Nuclear body
NDSM	Negatively charged amino acid-Dependent SUMOylation Motif
Nedd	Neural precursor cell expressed developmentally down-regulated
NEIL-1	Nei-like protein 1
NEMO	NF-kappa-B essential modulator
NER	Nucleotide excision repair
NF-kB	Nuclear factor NF-kappa-Beta
NHEJ	Non-homologous end joining
Ni-NTA	Nickel - Nitrilotriacetic acid
NOP58	Nucleolar Protein 58
NPC	Nuclear pore complex
NRD	N-terminal repressor domain
NSE2	Non-structural maintenance of chromosomes element 2 homolog
NuRD	Nucleosome Remodeling Deacetylase
p53	Cellular Tumor Antigen p53
PAGE	Polyacrylamide gel electrophoresis
PARI	PCNA-interacting partner
PARP	Poly ADP Ribose Polymerase
PBS	Phosphate buffered saline
PBST	Phosphate Buffered Saline containing Tween-20
PcG	Polycomb group
PCNA	Proliferating cell nuclear antigen
PCR	Polymerase Chain Reaction
PDSM	Phosphorylation-dependent sumoylation motif
PEI	Polyethylenimine
PEP	Posterior error probability
PGBD3	PiggyBac transposable element-derived protein 3
PHYRE2	Protein Homology/analogy Recognition Engine V2.0
PIAS	Protein inhibitor of activated STAT
PLA	Proximity Ligation Assay
PML	Promyelocytic leukemia protein
PML-RAR α	PML-retinoic acid receptor alpha
Pol	Polymerase
ppm	Parts per million
PTM	Post translational modification
RAD51	Radiation sensitive 51
RanBP2	Ran-binding protein 2
RanGAP1	Ran GTPase-activating protein
Rap1	Repressor/activator site-binding protein 1
RAP80	Receptor-associated protein 80
RCF	Relative Centrifugal Force
Rfp	RING finger protein
RING	Really interesting new gene
RNA	Ribonucleic acid
RNAPII	RNA polymerase II
RNF	RING finger protein

List of abbreviations

RPA	Replication protein A
RPB1	DNA-directed RNA polymerase III largest subunit
RPM	Rounds per minute
SAE	SUMO-activating enzyme subunit
SART1	Squamous cell carcinoma antigen recognized by T-cells 1
SD	Standard Deviation
SDS	Sodium dodecyl sulphate
SEM	Standard error of the mean
SENP	Sentrin-specific protease
shRNA	Short hairpin RNA
SILAC	Stable Isotope Labeling by Amino acids in Cell culture
SIM	SUMO interacting motif
Siz	SAP and Miz-finger domain-containing protein
SLX5/8	Synthetic lethal of unknown function protein 5 and 8
SMC5/6	Structural maintenance of chromosomes protein 5 and 6
SMRT	Silencing mediator of retinoic acid and thyroid hormone receptor
Smt3	Suppressor of mitochondrial initiation factor two 3
Sp100	Speckled 100 kDa protien
STAT	Signal transducer and activator of transcription
STRING	Search Tool for the Retrieval of Interacting Genes/Proteins
STUBL	SUMO targeted ubiquitin ligase
SUMO	Small Ubiquitin-like Modifier
SWI2/SNF2	SWItch 2/Sucrose NonFermentable 2
TAD	Transactivation domain
TAP	Tandem Affinity Purification
TC-NER	Transcription Coupled NER
TDG	Thymine-DNA glycosylase
Topo II α	Topoisomerase II α
TOPORS	Topoisomerase I-binding RING finger protein
U2OS	U-2 Osteosarcoma
Ub	Ubiquitin
Uba2	Ubiquitin Activating enzyme E1-like
Ubc13	Ubiquitin-conjugating enzyme 13
Ubc9	Ubiquitin carrier protein 9
Ubch5a	Ubiquitin-Conjugating Enzyme E2 D1
UBD	Ubiquitin binding domain
UBE1	Ubiquitin-Like Modifier-Activating Enzyme 1
UBL	Ubiquitin like
UBL5	Ubiquitin-Like Protein 5
UCH	Ubiquitin Carboxyl-terminal Hydrolase
Ulp	Ubiquitin-like-specific protease
Uls1	Ubiquitin ligase for SUMO conjugates protein 1
URM1	Ubiquitin-related modifier 1
USP11	Ubiquitin-specific-processing protease 11
USP25	Ubiquitin carboxyl-terminal hydrolase 25
USP7	Ubiquitin carboxyl-terminal hydrolase 7
USPL1	Ubiquitin-specific peptidase-like protein 1

List of abbreviations

UV	Ultraviolet
UVSSA	UV-stimulated scaffold protein A
VCP/p97	Valosin-containing protein
WST-1	Water-soluble tetrazolium salt-1
WT	Wild-type
XPC	Xeroderma pigmentosum group C-complementing protein
YFP	Yellow Fluorescent Protein
ZBTB1	Zinc Finger and BTB Domain-Containing Protein 1
β -Gal	Beta-galactosidase

Curriculum Vitae

Joost Schimmel was born on the 17th of April 1984 in Lopik, the Netherlands. In 2001 he received his HAVO diploma at the CSG Willem de Zwijger in Schoonhoven. After that he attended the HLO in Utrecht studying Molecular Biology, as part of this study he performed an internship at the Hubrecht Institute in the lab of Prof. dr. L de Windt. Under supervision of Dr. R.J. van Oort he studied the role of the transcription factor MEF2 in heart failure. After the successful completion of the HLO he started as a research technician at the department of Molecular and Cellular Biology at the Leiden University Medical Center in the lab of Dr. A.C.O. Vertegaal. In this research group, he started his PhD training in January 2010, studying the role of SUMOylation in several cellular processes. Since April 2014 he is working as a postdoc in the lab of Dr. M. Tijsterman at the department of Toxicogenetics at the Leiden University Medical Center.

List of publications

1. Hendriks, I.A.*, **Schimmel, J.***, Olsen, J.V. and Vertegaal, A.C. (2014) USP11 Counteracts RNF4 and Stabilizes PML Nuclear Bodies. *Submitted*
2. **Schimmel, J.***, Eifler, K.*, Sigurethsson, J. O.*, Cuijpers, S. A., Hendriks, I. A., Verlaan-de, V. M., Kelstrup, C. D., Francavilla, C., Medema, R. H., Olsen, J. V., and Vertegaal, A. C. (2014) Uncovering SUMOylation Dynamics during Cell-Cycle Progression Reveals FoxM1 as a Key Mitotic SUMO Target Protein. *Mol. Cell* 53, 1053-1066
3. Zhang, L., Huang, H., Zhou, F., **Schimmel, J.**, Pardo, C. G., Zhang, T., Barakat, T. S., Sheppard, K. A., Mickanin, C., Porter, J. A., Vertegaal, A. C., van, D. H., Gribnau, J., Lu, C. X., and ten, D. P. (2012) RNF12 controls embryonic stem cell fate and morphogenesis in zebrafish embryos by targeting Smad7 for degradation. *Mol. Cell* 46, 650-661
4. Matic, I.*, **Schimmel, J.***, Hendriks, I. A.*, van Santen, M. A.*, van de Rijke, F., van, D. H., Gnad, F., Mann, M., and Vertegaal, A. C. (2010) Site-specific identification of SUMO-2 targets in cells reveals an inverted SUMOylation motif and a hydrophobic cluster SUMOylation motif. *Mol. Cell* 39, 641-652
5. **Schimmel, J.**, Balog, C. I., Deelder, A. M., Drijfhout, J. W., Hensbergen, P. J., and Vertegaal, A. C. (2010) Positively charged amino acids flanking a sumoylation consensus tetramer on the 110kDa tri-snRNP component SART1 enhance sumoylation efficiency. *J. Proteomics*. 73, 1523-1534
6. Brouwer, A. K., **Schimmel, J.**, Wiegant, J. C., Vertegaal, A. C., Tanke, H. J., and Dirks, R. W. (2009) Telomeric DNA mediates de novo PML body formation. *Mol. Biol. Cell* 20, 4804-4815
7. **Schimmel, J.***, Larsen, K. M.*, Matic, I.*, van, H. M., Cox, J., Mann, M., Andersen, J. S., and Vertegaal, A. C. (2008) The ubiquitin-proteasome system is a key component of the SUMO-2/3 cycle. *Mol. Cell Proteomics*. 7, 2107-2122
8. Matic, I., van, H. M., **Schimmel, J.**, Macek, B., Ogg, S. C., Tatham, M. H., Hay, R. T., Lamond, A. I., Mann, M., and Vertegaal, A. C. (2008) In vivo identification of human small ubiquitin-like modifier polymerization sites by high accuracy mass spectrometry and an in vitro to in vivo strategy. *Mol. Cell Proteomics*. 7, 132-144
9. van Oort, R. J., van, R. E., Bourajjaj, M., **Schimmel, J.**, Jansen, M. A., van der Nagel, R., Doevendans, P. A., Schneider, M. D., van Echteld, C. J., and De Windt, L. J. (2006) MEF2 activates a genetic program promoting chamber dilation and contractile dysfunction in calcineurin-induced heart failure. *Circulation* 114, 298-308

*, Equal author contributions

